

University of Southampton Research Repository ePrints Soton

Copyright © and Moral Rights for this thesis are retained by the author and/or other copyright owners. A copy can be downloaded for personal non-commercial research or study, without prior permission or charge. This thesis cannot be reproduced or quoted extensively from without first obtaining permission in writing from the copyright holder/s. The content must not be changed in any way or sold commercially in any format or medium without the formal permission of the copyright holders.

When referring to this work, full bibliographic details including the author, title, awarding institution and date of the thesis must be given e.g.

AUTHOR (year of submission) "Full thesis title", University of Southampton, name of the University School or Department, PhD Thesis, pagination

UNIVERSITY OF SOUTHAMPTON

School of Ocean and Earth Sciences

Biofouling of Natural and Artificial Surfaces in the Marine Environment and Possible Antifouling Strategies for Long-Term, In Situ Deployment by

Alexandra Meier

Thesis for the degree of Doctor of Philosophy

September 2013

ABSTRACT

Biofouling is a major problem for long-term deployment of sensors in marine environments. The aim of this project is to find a practical and effective strategy to prevent the biofilm formation on sensors; especially in the marine environment. This requires understanding of: 1) variability in the nature and severity of fouling as a function of the deployment location. For this purpose the planktonic and biofilm microbial community structure of the Mid-Cayman ridge were examined. 2) The effect of biofouling the material from which the surface is manufactured. 3) Efficacy of antifouling strategies that could be applied.

Experiments, deploying on a variety of artificial materials deployed for 10 days and 23 months at 4,700 m in the Cayman Trough, showed that significant biofilm formation occurred. Biofilm surface coverage was used as a biomass indicator. The results demonstrate microfouling might turn out to be a major problem for long-term deployment in this type of extreme environment and therefore the potential need for mitigation strategies for any kind of long-term deployments of remote sensors in marine environments.

Possible antifouling techniques might be surface modification. Cyclic Olefin Copolymer (COC), COC embedded with copper, copper(I) oxide, and copper(II) oxide respectively were examined. In order to test the effectives of copper and copper oxides embedded, samples were exposed to an eutrophic environment, the Solent, for 14 day. These showed a significant variance in the live cell number between all materials (p = 1.14E-8). COC embedded with copper also showed a reduction in the Total cell number and the ratio of live to total cells. For the community analysis a denaturing gradient of 30-50% and 30-80% were determined to be sufficient for the separation of eukaryotic and archaean/bacterial.

Another approach to increase the fouling resistance of materials is to change their surface characteristics. As example regarding this approach micro-/nano-structuring and plasma treatment to create hydrophobic and hyper-hydrophobic surfaces were examined in a laboratory experiment. In this study examined example significant reduction of biofilm formation at an intermediary wettability of the surface.

The electrolysis of seawater for the production of chlorine is currently used in a variety of fields e.g. on ship hull surfaces or in pipelines, but the huge power consumption prohibited the use for remote sensors until now. The examined sensor electrode with included seawater electrolysis demonstrated significant fouling reduction of over 50% on sensor electrode deployed for 20 days using an incorporated cleaning waveform.

The main conclusions of this project is that there is still need to investigate long-term effects of biofouling on artificial surfaces, especially in the deep sea environment, as well as that there is still need to investigate further mitigation strategies.

Contents

Chapter 1 Introduction	18
1.1 Aim of the study	18
1.2 The Marine Environment	20
1.2.1 Deep Sea Environment	21
1.2.2 Hydrothermal Vents - A special case of deep-sea environment	22
1.2.3 Biogeography	23
1.3 Biofouling and Biofilms	25
1.3.1 What exactly is biofouling?-	25
1.3.2 Micro-fouling and Biofilms – The first stage of Biofouling	26
1.3.3 Biofilm development	27
1.3.4 Extracellular polymers	30
1.3.5 Quorum Sensing	30
1.3.6 Implications and Impact of Fouling	31
1.4 Methods for the Analysis of Biofilms	32
1.4.1 Biofilm Structure and Biomass Determination	32
1.4.2 Biofilm community composition	34
Chapter 2: Method Development and Optimisation	38
2.1 Chemicals, Materials and Solutions	38
2.1.1 Chemicals and Materials	38
2.1.2 Solutions	40
2.2 Microscope Techniques	41
2.2.1 EDIC/EF Microscopy	41
2.2.2 Laser Scanning Confocal Microscopy	42
2.2.3 Environmental Scanning Electron Microscopy	42
2.2.4 Staining Protocol using fluorescent Dyes	42
2.2.5 Quantification using fluorescent images	43
2.3 Contamination of surfaces with Pseudomonas fluorescens	43
2.4 Molecular Techniques	43
2.4.1 Quantification of DNA extracts	44
2.4.2 Biofilm Removal and DNA extraction optimisation	45
2.4.3 Testing DNA Extraction Techniques	47
2.4.4 Polymerase Chain Reaction	50
2.4.5 Quantitative PCR	51
2.4.6 DGGE	51
2.5 Problems with the re-amplification of DGGE extracts	52
2.5.1 Testing DNA concentrations	52
2.5.2 Test Cell extraction Methods	53

2.5.3 Gel-extraction and re-amplification using <i>Pseudomonas fluorescens</i>	56
Chapter 3: Microbial Community Structure of the Mid-Cayman Ridge	59
3.1 Introduction	59
3.1.1 The Mid-Cayman Ridge	60
3.2 Methods and Materials	61
3.2.1 Sample Acquisitioning and Treatment	61
3.2.2 DGGE	62
3.2.3 Sequencing	63
3.3 Results & Discussion	63
3.3.1 Planktonic DNA concentrations in various depths at the Mid Cayman	Rise
	63
3.3.2 Microbial Hydrothermal Vent Community of the Mid-Cayman Rise	69
Chapter 4: Development of biofilms on artificial surfaces	74
4.1 General Introduction	74
4.2 Biofouling on Seaglider after 110 day deployment in the North Atlantic	74
4.2.1 Methods and material	75
4.2.2 Results and Discussion	76
4.3 Development of hyper-baric biofilms on engineering surfaces in the Deep	o-Sea
	81
4.3.1 Methods and Materials	81
4.3.2 Results for Mooring I: Biofouling after 10 day deployment in the deep	p-sea
	84
4.3.3 Results for mooring II and III: Biofouling after 23 month deployment	
the deep-sea	95
4.4 Discussion Biofouling in the Deep-Sea	113
4.4.1 Microscopic Analysis	113
4.4.2 Molecular Analysis	115
Chapter 5: Antifouling strategies	118
5.1 Passive Antifouling Strategies	118
5.2 Surface Modification	120
5.2.1 COC with embedded Copper, Copper(I) oxide, and Copper(II) oxide	120
5.2.2 Surface modification via plasma treatment and micro-/nanostructuri	าg
	128
5.3 Active Antifouling Strategies	133
5.4 Antifouling for a sensor electrode via electrolysis of seawater	134
5.4.1 Method and Materials	134
5.4.2 Results and Discussion	136
Chapter 6 Conclusions	145
6.1 Microbial Community Structure of the Mid-Cayman Ridge	146

6.2 Development of biofilms on artificial surfaces	147
6.3 Antifouling Strategies	148
Chapter 7 References	151
Appendix I: Code of Matlab program for pixel counter	166
Written by Xi Huang	166
Appendix II: Denaturing Gradient Gel Electrophoresis (DGGE) Protocol	169
Solutions & Chemicals	169
Preparation of the Denaturing Gradient Gel	170
Gel Plate Preparation & Assembly	170
Gel Pouring	171
Running the Gel	173
Developing and Viewing the Gel	173
Excising DNA bands	174
Appendix III: Creation of copper embedded COC samples	175
Creation of COC/cyclohexane solution	175
Creation of copper/COC mixtures	175
Coating COC wafers	175
Flattening the coated wafer surfaces	175
Exposing the copper particles	176

List of figures

	Figure 1.1: Overview of temporal settlement of fouling organisms	. 25
	Figure 1.2: Overview of the biofilm development	. 28
	Figure 2.1: Flow Chart of the analysis of microbial community	. 44
	Figure 2.2: Standard curve of Pico Green assay	. 45
	Figure 2.3: Analysis of DNA extract from biofilm removal experiments	. 47
	Figure 2.4: Analysis of DNA extracts form DNA extraction experiments	. 49
	Figure 2.5: Comparison of gel-electrophoresis images of PCR products before DC	GE
an	d re-amplification products	. 53
	Figure 2.6: Horizontal 8 % acrylamide gel without denaturant gradient	. 54
	Figure 2.7: Gel-electrophoresis image of the gel-extractsl	. 55
	Figure 2.8: Gel-electrophoresis image of re-amplified gel-extracts	. 56
	Figure 2.9: Gel-electrophoresis image of inital PCR products	. 57
	Figure 2.10: Re-amplification results after gel-extraction from 8% acrylamide gel	. 58
	Figure 3.1: Geographical positions of the Beebe Vent Field at a depth of 4,960 m	١,
an	d Von Damm vent field at a depth of 2,300 m	. 60
	Figure 3.2: Diagram of tow-yo'ing CTD to locate hydrothermal vent sites	.61
	Figure 3.3: Image of the old hydrothermal vent chimney from the Beebe vent field	d
at	a depth of 4,960 m	. 62
	Figure 3.4: Analysis of DNA extracts from seawater filtrates using Muyer primer s	set
		. 65
	Figure 3.5: DNA extracts using Crenarcheota primer set	. 67
	Figure 3.6: Analysis of DNA extracts from natural biofilm samples	. 70
	Figure 3.7: Overview of geographical positions of sample site and sources of	
clo	sest found alignment match	. 72
	Figure 4.1: Photographs of the seaglider on recovery after 110 day deployment in	n
the	North Atlantic	. 75
	Figure 4.2: Overlay images of SYTO©9 stained seaglider samples taken with	
EV	OS_fl microscope in three different fluorescent filters	. 77
	Figure 4.3: Laser Scanning Confocal Microscopy image of biofouling section on	
sea	aglider after 110 day deployment in the North Atlantic	. 78
	Figure 4.4: Image of DGGE gel of DNA extracts from seaglider	. 79
	Figure 4.5: Scheme of the position of the moorings in relation to the Hydrotherm	ıal
Ve	nts and geographical positions	. 82
	Figure 4.6: Mooring setup of the biofouling experiment	. 83
	Figure 4.7: Microscope images of Biofilm formation on plain glass slide deployed	d at
4.7	700 m for 10 days	. 85

Figure 4.8: Microscopic images of biofouling on artificial surfaces after 10 day
deployment at 4,700 m86
Figure 4.9: Scanning electro-micrographs of engineering surfaces deployed for 10
days at 4,700 m 87
Figure 4.10: Biofilm surface coverage as indicator for biomass on engineering
surface deployed for 10 days at 4,700 m
Figure 4.11: Bioanalyzer results for PCR products of extracted DNA from different
engineering surfaces after 10 day deployment at 4,700 m
Figure 4.12: Pie Charts of PCR product quantification using a Bioanalyzer92
Figure 4.13: Image of DGGE gel for extracted DNA from different engineering
surface after 10 day deployment at 4,700 m93
Figure 4.14: Brightfield microscopic image of glass surface deployed on mooring II
for 23 months using the EVOSfl (AMG, USA), scale bar 1000 μm
Figure 4.15: Microscopic images of unstained glass surface simulating sensor
exterior after 23 month at 4,700 m
Figure 4.16: 3D image of auto-fluorescence detected on glass surface deployed on
mooring III for 23 months in the vicinity of the Beebe vent field
Figure 4.17: SEM images of glass surface deployed on mooring III for 23 months in
the vicinity of the Beebe vent field
Figure 4.18: Microscopic images of biofouling on artificial surfaces after 23 month
deployment on mooring II at 4,700 m in the biofouling tube simulating interior of
sensor
Figure 4.19: Microscopic images of biofouling on artificial surfaces after 23 month
deployment on mooring II at 4,700 m in the biofouling box simulating exterior of
sensor
Figure 4.20: Microscopic images of biofouling on artificial surfaces after 23 month
deployment on mooring III at 4,700 m in the in the vicinity of the BeeBe vent field 101
Figure 4.21: Scanning electro-micrographs of engineering surfaces deployed on
mooring II for 23 month at 4,700 m
Figure 4.22: Scanning electro-micrographs of engineering surfaces deployed on
mooring III for 23 month at 4,700 m within the vicinity of the BeeBe vent field 103
Figure 4.23: Biofilm surface coverage as indicator for biomass on engineering
surface deployed for 23 months at 4,700 m (Mooring II)
Figure 4.24: Biofilm surface coverage as indicator for biomass on engineering
surface deployed for 23 months at 4,700 m in the vicinity of the Beebe bent field
(Mooring III)
Figure 4.25: Image of DGGE gel from extracted DNA from different engineering
surface 23 month deployment at 4,700 m
Figure 5.1: Images of COC and copper coated COC

List of tables

Table 2.1: Chemicals and Materials used	38
Table 2.2: Solutions for DNA extractrion using Chelex	40
Table 2.3: Solutions for DNeasy extraction Kit	40
Table 2.4: Solutions for DGGE	41
Table 2.5: List of primers used in the project	50
Table 2.6: Primer sequences for specific for P. fluorescens 16S rDNA (Tsaloglo	u et
al 2012)	57
Table 3.1: DNA concentration of filter extracts; direct measurement without re	<u>3</u> -
calculation	64
Table 3.2: 16S rDNA sequence similarities to closest alignment match of extra	ıcted
DGGE bands from seawater filtration	68
Table 3.3: 16S rDNA sequence similarities to closest alignment match of extra	icted
DGGE bands from the Beebe Vent Field	71
Table 4.1: Closest alignment match to 16SrDNA sequence of extracted DGGE	bands
of the seaglider samples	80
Table 4.2: Single-factor ANOVA with subsequent post-hoc comparison results	of the
biofilm coverage determined by the quantification of the fluorescence microscopy	/
images	89
Table 4.3: Results for PCR amplification using High Sensitive DNA Assay	
(Bioanalyser,Agilent)	90
Table 4.4: closest alignment match to 16S rDNA sequence of extracted DGGE	bands
from short-term mooring	94
Table 4.5: Single factor ANOVA with subsequent post hoc comparison results	of the
biofilm coverage determined by the quantification of fluorescence images of surfa	aces
	105
Table 4.6: Comparison of surface coverage and biofilm thickness of short-terr	n and
long-term mooring samples	108
Table 4.7: Concentrations [ng/µl] of DNA extracts using Pico Green Assay	108
Table 4.8: Results for PCR amplification using DNA 7500 Assay (Bioanalyzer,	
Agilent)	109
Table 4.9: Closest alignment match to 16S rDNA sequence of extracted DGGE	
bands from long-term moorings	111
Table 5.1: Alive cell to total biofilm coverage ratio of the biofilm coverage	
determined by the quantification of the fluorescence microscopy images and	125
Table 5.2: Single-factor ANOVA with subsequent post hoc comparison results	of the
biofilm coverage determined by the quantification of the fluorescence microscopy	/
images	125

Table 5.3: closest alignment matches to 16S rDNA sequence of extracted DGGE	
bands from COC surfaces exposed to the Solent127	
Table 5.4: Biofilm surface coverage in regard to structure ration and plasma	
treatment132	
Table 5.5: Closest alignment match to 18S rDNA of extracted DGGE bands from	
sensor electrodes deployed in the Solent	

DECLARATION OF AUTHORSHIP

I, Alexandra Meier declare that the thesis entitled

Biofouling of Natural and Artificial Surfaces in the Marine Environment and Possible Antifouling Strategies for Long-Term, In Situ Deployment

and the work presented in the thesis are both my own, and have been generated by me as the result of my own original research. I confirm that:

- this work was done wholly or mainly while in candidature for a research degree at this University;
- where any part of this thesis has previously been submitted for a degree or any other qualification at this University or any other institution, this has been clearly stated;
- where I have consulted the published work of others, this is always clearly attributed;
- where I have quoted from the work of others, the source is always given. With the
 exception of such quotations, this thesis is entirely my own work;
- I have acknowledged all main sources of help;
- where the thesis is based on work done by myself jointly with others, I have made clear exactly what was done by others and what I have contributed myself; parts of this work have been published as: Meier, A., Tsaloglou, N. M., Mowlem, M. C., Keevil, C. W., & Connelly, D. P. (2013). Hyperbaric biofilms on engineering surfaces formed in the deep sea. *Biofouling*, 29(9), 1029-1042.

Signed			 	 		
Date:	.09.08.20) 5	 	 	 	

Acknowledgements

First I would like to thank my supervisors Dr. Doug Connelly, Dr. Maria-Nefeli Tsaloglou, Prof. Dr. William Keevil and Dr. Matt Mowlem for allowing me to work on this interesting and diversified topic.

A special thanks goes to the people of the sensor development group at the NOC for their moral support and advice.

I would like to thank the Master and ship's company of the *RRS James Cook*, and UK National Marine Facilities staff, for their assistance in *RRS James Cook* Voyage 44; and of the RRS discovery during the cruise D374. Katrin Linse, Katrin Zwirglmaier, and David Pearce from the British Antarctic Survey, for the use of their equipment aboard the *RRS James Cook*.

I would also like to thank Rob Brown from the Workshop at the NOC, Southampton for his help and the design of the Biofouling Tube.

A very special thanks goes to SENSEnet, a Marie Curie Initial Training Network (ITN) funded by the European Commission Seventh Framework Programme, for the money without which nothing would have been possible.

At last I would like to thank my family and friends for their support and encouragement.

Definitions and abbreviations

AHL N-Acyl-Homoserine

ATP Adenosin Triphosphate

ChEss Chemosynthetic Ecosystem Science

CNI Close Neighbour Interchange

COC Cyclic Olefin Copolymer

COI Cytochrome Oxidase Subunit I

COP Cyclic Olefin Polymer

CTC 5-Cyano-2,3-Ditolyltertrazolium Chloride

CTD Conductivity Temperature Depth

Cu Copper

DAPI 4',6'-Diamidin-2-Phenylindole Dichloride

DGGE Denaturing Gradient Gel Electrophoresis

DLVO Derjaguin-Landau-Verwey-Overbeek

dNTP's Deoxynucleotides

EDIC Episcopic Differential Interference Contrast

EF Epifluorescence

EPS Extracellular Polymeric Substances

FISH Fluorescence On Situ Hybridization

HMC Hoffman Modulation Contrast Microscope

ITS Internal Transcribed Spacer

LSCM Laser Scanning Confocal Microscopy

MCL Maximum Composite Likelihood

ME Minimum Evolution

MEGA5 Molecular Evolutionary Genetics Analysis

mRNA Messenger RNA

OMZ Oxygen Minimum Zone

PCR Polymerase Chain Reaction

PMMA Polymethyl Methacrylate

qPCR Quantitative Polymerase Chain Reaction

RFLP Restriction Length Polymorphism

SEM Scanning Electron Microscopy

SST Sea Surface Temperature

TEM Transmission electron microscopy

TRFPL Terminal Restriction Length Polymorphism

VBNC Viable But Not Culturable

Chapter 1 Introduction

Long term monitoring of the environment is essential for understanding and assessing environmental change and global processes such as global warming; this includes understanding underlying processes, feedbacks and prediction of future trends. *In situ* sensor technology promises to deliver a paradigm shift in the spatial and temporal resolution of data availability, particularly for biogeochemical parameters (Prien, 2007). In the marine environment the collection of these data is made more difficult due to the process of biofouling of the monitoring equipment.

Biofouling or biological fouling has been identified in many areas of the modern world, such as the commercial and health industries, and even in private households (Dang and Lovell, 2000). As mentioned it is also a major problem in environmental monitoring and the *in situ* sensing of aquatic systems. In the absence of a mitigation strategy biofouling occurs after only a short deployment in the marine environment, since regardless of the sensor, the interface surface between the instrument and the environment is modified by the formation of a biofilm almost as soon as it is deployed (Kerr, 1998). The effects range from measurement drift, which can be compensated, to blockage of channels, which render the sensor inoperative (Kerr, 1998).

The development of anti-fouling strategies for in situ sensors is critical for their functionality and requires a multidisciplinary approach.

1.1 Aim of the study

In order to develop anti-fouling strategies, we need to understand the processes of fouling and identify targets for research efforts. This includes developing an understanding of differences in the severity of fouling in relation to environment and material of the sensors. Therefore the aim of this project was the assessment of the efficiency of active and passive antifouling methods for exposed marine sensor surfaces. The mitigation strategies tested were seawater-electrolysis for chlorine production, surface modification via COC with embedded Copper, Copper(I) oxide, and Copper(II) oxide, plasma treatment and micro-/nano-structuring.

For the successful assessment of these antifouling techniques the following existing microscopy and molecular techniques were extended and combined to create a workflow:

- Microscopy:
 - four different microscopy techniques were used for analysing the samples: EDIC, which allows the microscopic examination of opaque surfaces ((Keevil, 2003)), epi-fluorescence microscopy, LSCM and environmental SEM.Imaging techniques

• Biomass determination using: surface coverage by epifluorescence microscopy through the development of a new protocol for quantification and to distinguish between live and dead cells by using a combination of fluorescent stains in marine biofilms; nucleic acids stains: used for enumeration of total cells attached to a surface; and functional electron transport systems stain: used for enumeration of actively respiring/live cells

- Molecular biology: Microbial community analysis:
 - Polymerase chain reaction (PCR) representing the three kingdoms
 Archea, Bacteria, and Eukarya
 - Optimization of denaturing gradient gel electrophoresis (DGGE)

Previous research concentrated on the eutrophic and euphotic zones of the oceans neglecting the deep-sea. Of special interest is the relation between the microbial community composition and the severity of fouling. Therefore, biofilms from the deep sea and planktonic microbial community from different depth have been collected at the Mid Cayman Ridge and analysed and their differences examined in order to further the understanding the effect of depth and geographic location on biofilm formation and mitigation of biofilms.

Investigate the susceptibility of sensor materials to biofilm formation in different marine environments on different artificial substrates, especially the deep-sea, is essential for the assessment of the need for antifouling strategies. For this purpose biofouling samples of a seaglider after 110 day deployment in the Mid-Atlantic were collected and analysed as example of the problem of biofouling during actual deployment. A selection of material deployed in the Mid-Cayman Ridge at a depth of 4,700 m for 10 days and 23 months respectively were also analysed in order to determine if there is an actual requirement of antifouling strategies in the deep sea.

Part of this thesis will also consider the planktonic and sessile microbial community of the Mid Cayman Ridge as both are the source of any possible biofouling developed on the material samples deployed in this region. It might also enable the assessment if there is alteration of biofilm composition between natural and artificial substrates.

Describing the development of biofilms on artificial surfaces and analysing its composition could lead to a better understanding of the process itself as well as give an insight to which mitigation technique might be the most promising.

In the final part of this thesis efficiency of the selected mitigation strategies are assessed using both laboratory as well as in situ experiments.

But first a short overview over different fields connected to this multidisciplinary project follows.

1.2 The Marine Environment

Oceans cover over 70% of the Earth's surface with the deepest point, the Challenger Deep in the Mariana Trench, close to 11000 m (Canganella and Kato, 2001).

Sunlight is essential to life in the sea, as its penetration into the water controls the maximal depth distribution of plants and photosynthic primary production (Snelgrove, 2001). The majority of the marine environment lies in perpetual darkness, although most animal life (with the exception of chemoautotrophic environments (Van Dover, 2000) is either directly or indirectly dependent on the primary production near the surface. Sunlight also controls ocean temperature via predominantly infrared light of which 98% is absorbed within one metre of the surface. Variations in the radiation intensity are limited at the Equator to 50°N, but more significant, particularly seasonally, in latitudes higher than 50°N where there is also a lower light intensity (Lalli and Parsons, 1997a).

Thus sea surface temperature (SST) can range from 30°C in the Tropics to -1.9°C in Polar Regions. The variation in SST is used to determine these zones in the oceans (Lalli and Parsons, 1997b):

- Tropical (SST above 25°C)
- Subtropical (SST: 25°C to 15°C),
- Temperate (lower SST boundary: 5°C northern limit, 2°C southern limit),
- Polar (<0 2°C or5°C)

The temperate zones are characterized by a mixture of polar and subtropical water, in these zones the maximal annual temperature range occur.

The greatest environmental fluctuations occur at or near the surface, where interaction with the atmosphere results in an exchange of gases, produces variations in temperature and salinity, and creates water turbulence from winds.

There is also a vertical temperature distribution (Lalli and Parsons, 1997b, J.D. and P.A., 1991). Starting from the surface the mixed layer has an almost uniform temperature to 200 m. In the open ocean between 200/300 m and 1000 m the temperature decreases. This layer is also called the permanent thermocline and temperature difference can be as large as 20°C. Below this the temperature continues to decrease more slowly and in most oceans the temperature at 2000/3000 m never rises above 4°C. At greater depths the temperature lies between 0 – 3°C.

Another common division of the water column uses light penetration and photosynthesis. Here the water column is divided into three zones: the euphotic zone, the disphotic zone, and the aphotic zone (Lalli and Parsons, 1997b).

Ecology is also being used to differentiate between depth zones (Gage J.D., 1991):

- I. Sublittoral or subtidal: low watermark to 0-2 km
- II. Bathyal or archibenthal: 0.2 km 2 km
- III. Abyssal: 2 km 6 km

IV. Hadal: >6 km

In the marine environment ecology also distinguishes between two basic environments: the pelagic, which is the water column, and the benthic, the bottom (Snelgrove, 2001).

The geographic distribution of species is further influenced by physical properties and adaptations. For example the geographic range of cold-stenothermic (restricted to a narrow temperature limits) species may be very wide as some species that can be found at the shallow depth in the Arctic are also present at depth of 2000-3000 m in Equatorial areas where similar cold temperatures prevail (Lalli and Parsons, 1997b).

1.2.1 Deep Sea Environment

The deep-sea is the world's largest single ecosystem with 50% of the earth's surface covered by oceans more than 3000 m deep with an average ocean depth of 3800 m. It is regarded as the most remote, seemingly difficult environment for life on Earth, and it is also the least understood environment (Gage J.D., 1991)

The modern study in the deep-sea started in the middle of the 19th century with Forbes 'azoic hypothesis' 1844 stating; only little or no life existed below 600 m depth. This was soon contradicted by Sars, 1864, 1868 and Thomson1873.

In the 1960s and '70s the unexpectedly high species diversity were discovered and changed the view of the deep-sea from being 'deserts' to 'tropical rainforests' in comparison with terrestrial environments (Deming, 1998).

During the 1970s and '80s the deep-sea research saw the discovery of seasonality in reproduction and respiration in response to seasonal surface production (Lightfoot et al., 1979, Tyler and Gage, 1984) and the discovery of rich 'oasis' of life depending on sulphur oxidizing and methanotrophic bacterial primary production (Hydrothermal Vents and cold Seeps) independent of the surface production. Many of the invertebrates found in "seep communities" are taxonomically similar to those found at hydrothermal vent sites indicating they are cognate (Van Dover, 2000).

The deep-sea is generally seen as a physically stable environment (Sanders, 1968), where salinity below 2 km depth is relative constant at 34.8 % \pm 0.3 % and declining to 34.65 % at the deepest levels (Svedrup et al., 1942, Sanders et al., 1965). Oxygen levels in the deep-sea are near saturation exception to this are areas where the oxygen minimum layer impinges on the upper continental slope, in enclosed basins and so called oxygen minimum zones (OMZ). OMZ are regions with ultra-low O_2 concentrations and have been increasing in the last decades (Stramma et al., 2008, Stramma et al., 2012). The most extreme parameter in the deep-sea is the hydrostatic pressure. The effects of increased pressure especially in relation to the low temperature can most clearly be seen in the adaptation of key enzymes in deep-sea organisms (Somero et al., 1983, Jannasch and Taylor, 1984). For example microbial activity in deep-sea

sediments can be one to three orders of magnitude slower than in shallow water (Van Dover, 2000).

As all food in the non-chemosynthetic regions of the deep-sea are derived from the primary production on the surface of which only 1 to 5 % reaches the sea-floor, this is a "food-limited" environment (Van Dover, 2002, Lalli and Parsons, 1997c). As such indigenous barophilic micro-flora in deep-sea sediment adapted to rapidly respond to sudden enrichments in the environment (Deming and Colwell, 1985, Turley et al., 1988, Alongi, 1990) resulting in variety in the biological process rates (growth) within spatially and temporally dynamic habitats found in the deep-sea environment.

1.2.2 Hydrothermal Vents - A special case of deep-sea environment

Deep sea hydrothermal vents were first discovered on the Galapagos Rift in 1977 (Corliss et al., 1979).

They were the first biological systems entirely reliant on chemoautotrophic primary production (Van Dover, 2000), with a bacterial population as the base of the food chain (Jannasch, 1995). Hydrothermal vents, unlike the general deep-sea environment, are considered to be independent from the surface production of the overlying ocean.

But hydrothermal vents are not the only environments where chemosynthesis occurs, it is also known in coastal waters and sediments.

In the marine environment organic material is partially oxidised by sulphatereducing bacteria under anaerobic conditions:

$$SO_{a}^{2} + 2 [CH_{3}O] \rightarrow S^{2} + 2 CO_{3} + H_{3}O$$

Here sulphide (S², H₃S, HS³) is a primary product.

In the upper layers of sediment or at the interface with seawater in the presence of O_3 , sulphate is subject to microbial oxidation:

$$S^{2-} + CO_1 + O_2 + H_2O \longrightarrow SO_4^{2-} + [CH_2O]$$

This describes the sulphur cycle in seawater, but there occurs no net gain of organic material as sulphide is produced from organic material. In contrast in the hydrothermal vent environments the sulphide originates from geochemical interactions between the ocean crust and the seawater allowing the generation of new organic material (Van Dover, 2000).

The spacing and longevity of hydrothermal-vent habitats is determined by the underlying geology, and to be more precise, the character of the underlying magma of hydrothermal vents. They can only occur wherever heat and porosity is sufficient to drive hydrothermal convection. The diffuse, warm-water flows with its rich sulphide contents form the basis for the chemosynthetic food chain (Van Dover, 2000).

Mixing and dilution of the hot vent fluids, at approximately 110°C with the ambient water results in a biological zonation of hydrothermal systems and short-term variability of low-temperature vent fluids (between 1 °C s⁻¹ and 5-10 °C over 10s intervals (Johnson et al., 1988b). This variability is extremely important for organisms

requiring simultaneous delivery of O₃ rich seawater for aerobic respiration and sulphide-rich fluids for support of microbial primary production (Johnson et al., 1988a).

Another important aspect of vent systems are hydrothermal plumes which are buoyant (due to temperature and content) which eventually reach a level of neutral buoyancy whilst spreading horizontally and are subsequently advected further by deep ocean currents (Van Dover, 2000). These can be very helpful in finding new vent sites. They are also zones of chemical reactions between vent fluid and seawater and important as habitats and resource for microorganisms and zooplankton. The plume advection also enables chemical flux and dispersal of vent biota (Van Dover, 2000)

Free-living microorganisms play an important role in the vent ecosystems as producers of organic carbon and sinks for reduced compounds e.g. inorganic sulphur (Van Dover, 2000). Free-living microbes are generally metabolically diverse and are able to inhabit a wide range of environments, including wide thermal and chemical extremes. In the natural environment, chemoautotrophic free-living microbial communities at vent sites might be generally mixotrophic. However, due to limitations of the techniques used for testing chemoautotrophy these organisms might appear autotrophic in the laboratory (Karl, 1995).

Extremely successful symbiotic associations are another important aspect of deepsea vent ecosystems. The success of these associations distinguishes them from their shallow water counterparts (Tarasov et al., 2005). Chemoautotrophic microorganisms can be associated with their invertebrate hosts either as endo- or as epi-symbionts (Van Dover, 2002). The association between invertebrates and chemoautotrophic microorganism was first suggested by Lonsdale (1977) (Lonsdale, 1977) and later confirmed by microscopic evidence of bacterial chemoautotrophic endo-symbionts in giant tubeworms (Cavanaugh, 1983).

1.2.3 Biogeography

Studies the deep-sea, especially the chemosynthetic environments, are often associated with the term biogeography. Biogeography is the study of the geographical distribution of organisms and biological communities, and understanding vent endemic species, the regions that they are limited to, and how the organisms move between vents has been subjected of much debate (German, 2011, Moalic et al., 2011). Though we have some understanding of the patterns in the global distribution of vent fauna, we still lack fundamental knowledge about how connected and/or unique these environments are (Flores et al., 2011).

Since their first discovery the descriptions of more than 700 new species, has made vent sites a major source of newly described species (German, 2011) and indicates a high degree of endemicity in vent species (Van Dover, 1995, Gebruk et al., 1997). The

biological communities at the macroinvertebrate level show distinct groupings and assemblages that has led to the recognition of six distinct biogeographic provinces (Van Dover, 2002). At the microbial level this provincial distinction has not been explored to any great extent.

Answering the question of the past and present dispersal mechanisms of vent species between vent systems has become a main focus in the understanding of these complex biological communities (Van Dover, 2002). The development of molecular tools in addition to taxonomic and physiological tools can aid in our understanding of vent species and their community structures (Flores et al., 2011, Black et al., 1998). Some animals show evidence of a "stepping stone" mechanism, effectively leaping from one chemosynthetic environment to another, others appear to be influenced by the ridge topography and some do not show any indication for either dispersal mechanism model (Vrijenhoek, 1997). Vent habitats and other chemosynthetic environments are generally viewed as "islands" or "oases" in the deep-sea ecosystem. Tunicliffe and colleagues (1995) propose that vent fauna dispersal might be linked to the temporal stability and spatial patterns of these vent habitats; these distributions in time and space are considered to be dependent on the underlying geology (Tunnicliffe et al., 1998).

Our understanding of the current connectivity between different biogeographic provinces and functioning deep-sea ecosystems may be enhanced by the determination of the historical linkages between vent sites, and their geological and hydrographical connections. To that aim the ChEss (Chemosynthetic Ecosystem Science) program, as part of the Census of Marine Life project, identified areas to look at evidence for past linkages between hydrothermal systems (e.g. Cayman Trough) and those areas that may represent crossroads between the biogeographic provinces (e.g. Scotia Sea, S. Atlantic) (German, 2011).

Identification of relationships between biogeographic regions plays an essential part in the designation of Marine Protected Areas with the increasing interest in the exploitation of the deep sea ecosystem resources.

The solution of the interactions of biogeographically interactions may lie in the study of macrofauna, but study of microbial communities and their distribution might also play a role in defining the connectivity of these environments.

1.3 Biofouling and Biofilms

1.3.1 What exactly is biofouling?-

In the marine environment biofouling has been known since ancient times, when mostly macro-organisms were noted to be responsible for the deterioration of ship performance e.g. the shipworm (Yebra, 2004).

Biofouling or biological fouling can be defined the `undesirable accumulation of microorganisms, plants, and animals on surfaces immersed in water '(Yebra, 2004). In the 1930's Zobell and colleagues noted that bacteria and other microorganisms are the primary colonizers in the fouling process ((Zobell and Allen, 1935)

Fouling is generally divided into four maturation stages (Figure 1.1) (Yebra, 2004, Abarzua and Jakubowski, 1995):

- 1. Formation of a conditioning film consisting of dissolved polysaccharides, proteins and proteoglycans
- 2. Formation of a microbial biofilm
- 3. Transformation from microbial biofilm to a complex community containing multicellular organisms
- 4. Settlement and growth of macro-algae

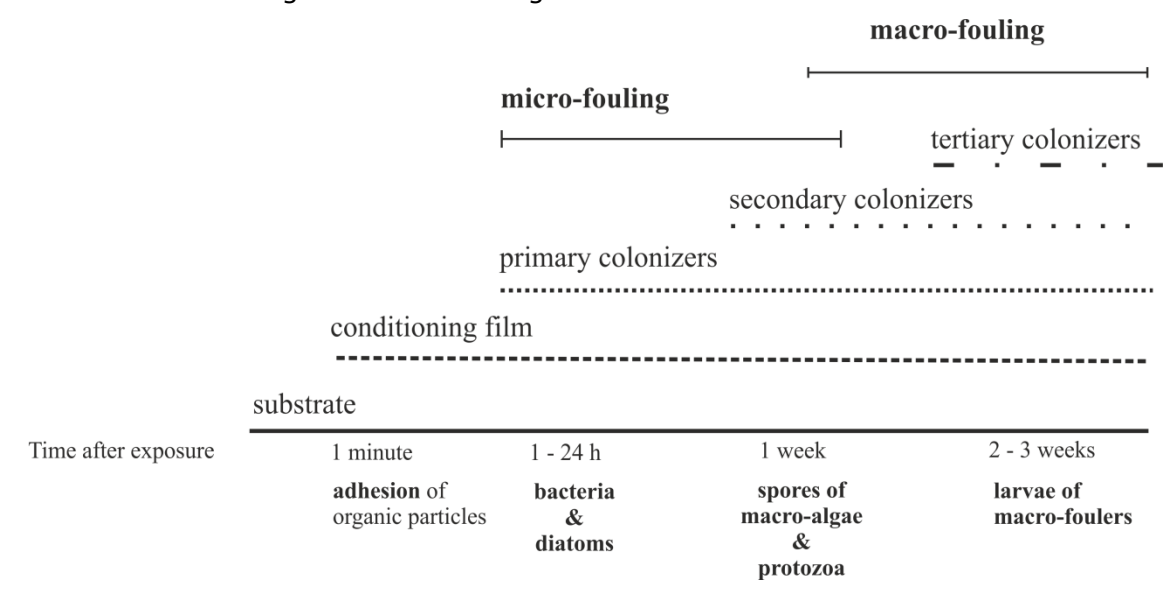


Figure 1.1: Overview of temporal settlement of fouling organisms (Abarzua and Jakubowski, 1995)

In the literature (Chambers et al., 2006, Gardella, 1997) only two main stages are distinguished, micro-fouling and macro-fouling. Microfouling; occurs first and is caused by microorganisms developing on the surface. Macro-fouling usually occurs after microfouling and results from the settlement of algae spores (Holmstrom, 2002), larvae of Hydroides e.g. *Hydroides elegans* or Barnacles e.g. *Balanus amphitrite* (Hung et al., 2005a, Hung et al., 2005b) and macro-algae onto a pre-existing fouling layer.

This fouling layer changes the surface characteristics facilitating an easier attachment (see

1.3.3 Biofilm development). There are rare cases where this settlement is not necessarily preceded by micro-fouling (Kristensen, 2008), which means that an effective antifouling strategy against microorganisms might not be 100 % effective in preventing macro-fouling.

Micro-fouling communities are bacterial-algal films also called biofilms dominated by diatoms and bacteria (up to 99.9 % of the adherent organic material (Railkin, 2004)). Some of the most widely distributed bacteria associated with fouling, in both marine and freshwater environments, belong to the genera Pseudomonas, Vibrio, Micrococcus, Achromobacter, and Flavobacterium (Railkin, 2004).

Studies have shown a succession within the population of the microbial community, from primary colonizers and early succession species, which create conditions favourable for the late-succession species. Among the first colonisers are bacteria and diatoms which are then followed by autotrophic and heterotrophic protozoa such as flagellates, amoebae, heliozoans and ciliates (Caron and Sieburth, 1981, Railkin, 2004, Dang and Lovell, 2000).

The speed of fouling as well as its severity is dependent on several environmental parameters such as temperature, pH and salinity (Yebra, 2006). For example biofilms form within a fortnight in boreal-arctic waters during the warm season whereas in subtropical waters they only take a week to form (Railkin, 2004).

In environmental sensors the preservation of the quality of the measurements and low maintenance are prerequisites for long-term deployment. In order to achieve this one major aspect is the prevention or delay of the first stages of biofouling (Cowling, 2000). Therefore, the focus of this project is the study and prevention of micro-fouling and biofilm formation respectively. For the successful development of a strategy for protection against biofouling the key processes involved in the fouling of a surface must first be identified and the subsequent primary succession understood (Railkin, 2004).

1.3.2 Micro-fouling and Biofilms - The first stage of Biofouling

Biofilm formation is recognised as the first stage and as such the major cause of biofouling (Godwin Wesley, 2009). Therefore it is important to understand the development of biofilms in general.

Already studies in the 1930's and 40' observed the effect of solid surfaces on bacterial activity and that most marine bacteria appeared to be found associated with solid surfaces (Zobel (Zobell, 1943, Zobell and Allen, 1935, Zobell and Anderson, 1936)l) Recent studies have shown that biofilms are ubiquitous and let to the theory that biofilms are probably the dominant mode of microbial growth in nature (McLean, 2002, Costerton, 1995). Growth inside a biofilm provides several advantages over

planktonic growth; these include increased access to nutrients, protection against toxins, e.g. antibiotics, and dynamic environments, and shelter from predation (Dang and Lovell, 2000, Garrett et al., 2008). Most of these advantages are a result of the extracellular matrix that is one of the defining aspects of a biofilm. The function of this matrix will be reviewed in detail later.

Although some biofilms have beneficial uses as they are used in wastewater treatment plants or help with food digestion, they can be the cause of major problems in medicine, healthcare, and industry, where their undesired formation can lead to major health issues and biodegradation of materials (Jenkinson, 2001, Keevil, 2002).

A biofilm consists of microbial colonies enclosed in an adhesive, usually polysaccharide material, attached to a surface (Brock, 1994), bacteria and diatoms are considered to be the main constituents of a biofilm (Godwin Wesley, 2009).

1.3.3 Biofilm development

Most studies generally divide biofilm development into four or five main stages, as can be seen in Figure 1.2:

Formation of a conditioning film on any surface exposed to an aquatic environment (not shown in the diagram)

- 1. Reversible adhesion or settlement of microorganisms
- 2. Irreversible attachment of microorganisms; extracellular polymeric substances (EPS) production
- 3. Growth and development of the microbial community
- 4. Maturation of the biofilm; development of 3D-structures e.g.: waterchanels
- 5. Detachment of microorganisms from the biofilm

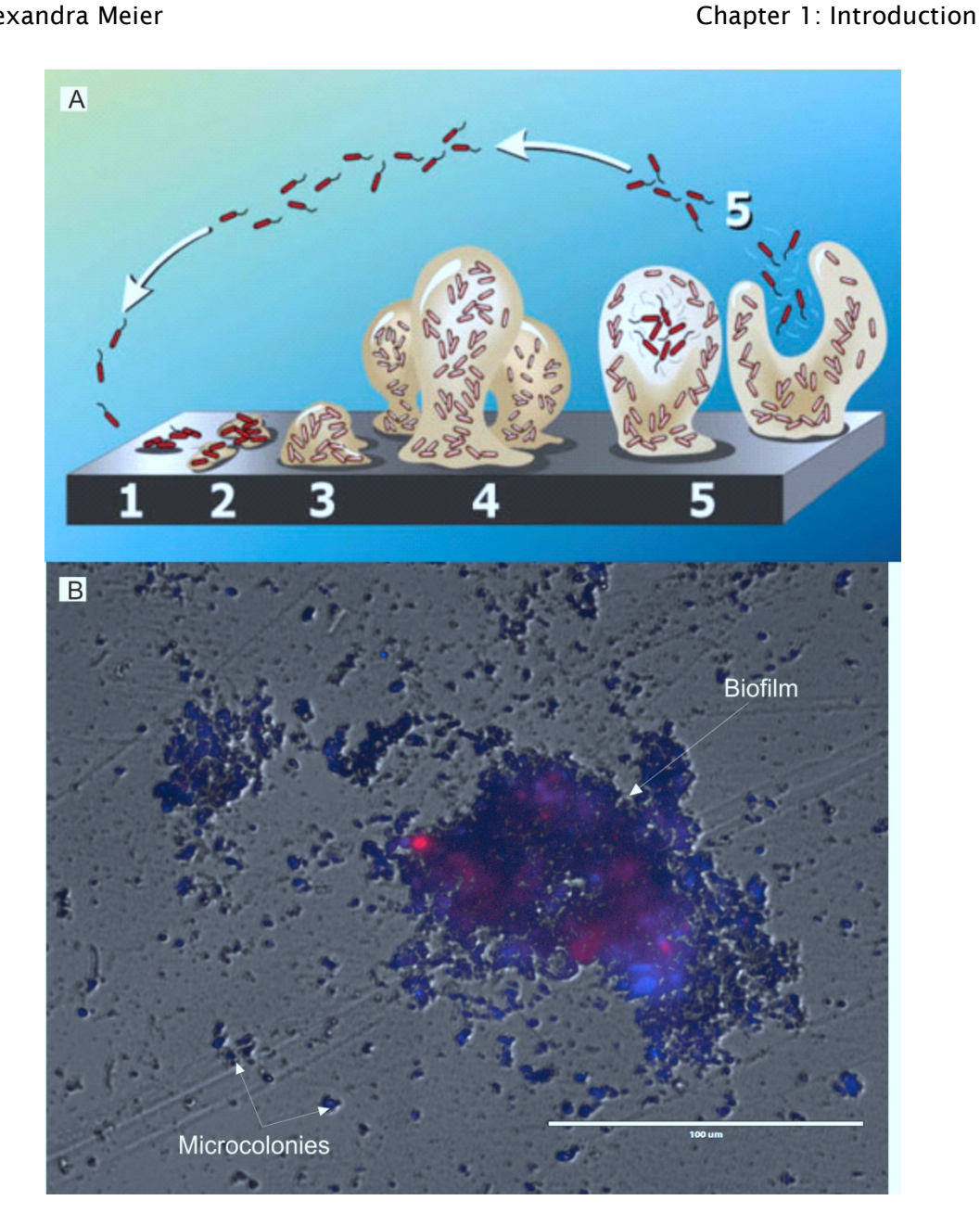


Figure 1.2: Overview of the biofilm development; (A) schematic of biofilm formation starting with the attachment of the cells and finishing with the dispersal/detachment of the cells from the biofilm (Figure adapted from www.erc.montana.edu) (B) Overlay of Bright

Although some researchers do not include the formation of the conditioning film as a separate step (Characklis, 1990), others see this as a prerequisite of a biofilm formation (Garrett et al., 2008). A conditioning film is formed by the adsorption of ions and other dissolved substances e.g. sugars, amino acids, proteins, fatty and humic acids. This physical process starts immediately when a surface is submerged and saturation concentrations of adsorbed substances are reached within tens of minutes (Railkin, 2004, Whelan and Regan, 2006). This layer of dissolved inorganic and organic materials modifies surface properties. The adsorption of these compounds produces a more negatively charged surface and increases the wettability of the exposed materials

(Loeb and Neihof, 1975, Marszalek et al., 1979). These changes in the characteristics of the surface properties make it more accessible to the primary colonizers (Garrett et al., 2008).

The next stage in the biofilm development, the reversible adhesion of the planktonic microbes to the substrate, is mainly influenced by physical forces such as van der Waals forces, steric interactions and electrostatic interactions (Fang et al., 2000). The interplay of these forces are described by the classical Derjaguin-Landau-Verwey-Overbeek (DLVO) theory (Hermansson, 1999, Ellwood et al., 1982), which states that the total energy of a system consisting of two closely positioned surfaces is the sum of energies of their electrostatic and dispersive interactions (Railkin, 2004). An extended DLVO theory also takes hydrophobic/hydrophilic and osmotic interactions between the surface molecules of the substrate and the bacterial membrane into account (Garrett et al., 2008). This stage of the biofilm development is rapid, generally within 15 to 30 minutes (Railkin, 2004).

In contrast irreversible attachment of the microorganism is much slower and generally takes between 9 and 12 hours, or sometimes longer depending on the species involved (Railkin, 2004). This step is characterised by the secretion of extracellular polymers and the irreversible attachment of the bacteria to a surface via this extracellular matrix (Railkin, 2004, Flemming, 2008). Here the biological factors like cell wall properties and composition of the extracellular matrix are involved in the attachment become the main influence (Flemming, 2008).

The fourth stage can be summarised as the maturation of the biofilm, during which biofilms develop a distinct structure and are heterogeneous with respect to the cell density, there are clusters of microorganisms, called microcolonies, and regions of low cell density, thought to be water channels (McLean, 2002). These water channels are thought to enable an improved nutrient flow and the disposal of waste products within the biofilm (Mathee, 2002). This 3D structure also allows the development of unique microenvironments within the biofilm. An example is the generation of micro-aerobic regions within the biofilm, allowing the growth of micro-aerophilic organisms (McLean, 2002, Robinson, 1995). Another aspect is the reaching of a dynamic equilibrium of cells entering and leaving the biofilm is reached (Jenkinson, 2001).

When the cell density reaches a certain level or other environmental triggers occur parts of the biofilm are detached, the so called sloughing off. This characterises the last stage in the biofilm development, although this process and its triggers are not yet fully understood (Kristensen, 2008).

Since most studies on biofilm formation and development were done on monocultures, especially *Pseudomonas aeruginosa* (Peeters, 2008, Mueller et al., 1992, Gu et al., 1998, Bakke, 2001, Wirtanen et al., 2001), regarded as a model organism in the study of biofilms, not all findings may be transferrable to multi-species natural

biofilms. However, when natural biofilms were compared with the data derived from monoculture biofilms similarities were observed (Flemming, 2008). For example studies have shown that biofilm development in the stages described above (cross ref here) is seen in both cultured and natural biofilms, as is the production of an extracellular matrix (Sauer et al., 2002). However the temporal and spatial variation as well as the extent of the EPS production seem to be influenced by the community composition and environmental factors and are not yet fully understood (Baker, 1998).

In the natural environment bacteria are generally considered the initial colonizers with diatoms settling afterwards (Landoulsi et al., 2011, Dobretsov et al., 2006), but in the absence of bacteria diatoms have demonstrated the ability to attach to clean substrates (Cooksey and Cooksey, 1988).

1.3.4 Extracellular polymers

One of the main characteristics of biofilm formation is the synthesis of extracellular polymers and their association with the irreversible attachment of microorganisms. This matrix of Extracellular Polymeric Substances (EPS) (Flemming, 2008) has several important functions, it is responsible for the adhesion of the bacteria to each other and to the surface. But the EPS's are also important in the creation of the biofilm architecture and are the predominant means by which the 3D-structure of the biofilm is created and maintained during the maturation of the biofilm (McLean, 2002).

Another important feature of EPS matrix is the ability to trap nutrients from the surrounding waters and concentrate them within the biofilm (Godwin Wesley, 2009). This together with the influence of EPS's on porosity, density, water content, charge, sorption properties, hydrophobicity and mechanical stability determines the immediate living conditions in this environment (Flemming, 2008).

It is also hypothesised that the composition of the EPS matrix, which varies in respect to local environmental factors like heavy metal concentration and toxins, has an influence on the digestibility of the biofilm by predators as well as the stability of the biofilm against environmental conditions (Decho and Lopez, 1993).

The EPS matrix can also contain extracellular DNA (e-DNA), this could have a structural role in supporting the biofilm (Flemming, 2008).

1.3.5 Quorum Sensing

An important characteristic of biofilms is the intercellular communication between individual microorganisms; this is generally known as quorum sensing (Bassler, 1999, Bassler, 2002). This communication is used by individuals of the community to control their phenotype, to change their behaviour and even to coordinate a regulation of behaviour (Holden, 2007). Quorum sensing is promoted by small signalling molecules, which sometimes are called auto-inducers (Flemming, 2008). This system consists of

three components: the signal molecule, signal synthesis and signal (Brackman, 2009). Three classes of signalling molecules have been identified: oligo-peptides predominantly in Gram-positive bacteria, N-acyl-homoserine lactones (AHLs) mostly in Gram-negative bacteria and LuxS/autoinducers-2class found in both Gram-negative and Gram-positive bacteria (Brackman, 2009, Flemming, 2008).

Probably the best known example for quorum sensing is in the case of *Vibrio fischeri*. This species can exist as a free-living bacterium in the marine environment as well as a symbiont, colonizing light organs of some fish and squid species (Holden, 2007). These light organs provide the bacteria with a favourable environment. Only as a symbiont, and only when the cell density inside the light organ exceeds a certain level, do they emit light (Holden, 2007). But quorum sensing is not limited to occurrence between the same species; it can also take place between different bacterial species occupying the same ecological niche, e.g. a biofilm (Holden, 2007).

In some species the quorum sensing system regulates virulence and as such the study of how to inhibit it has become an attractive target for the development of novel therapeutic agents (Holden, 2007). The use of quorum sensing for antifouling strategies is being studied (Brackman, 2009).

1.3.6 Implications and Impact of Fouling

The accumulation of microorganisms, plants and animals on submersed surfaces compromises the functionality of structures and can also sometimes result in the degradation or corrosion of the surface the organisms settle on, a process known as bio-deterioration (Surman et al., 1996). This deterioration can include a wide variety of substances such as metals, polymers and concrete (Fang et al., 2002).

Structures suffering from biofouling include pipelines, cables, fishing nets, pillars of bridges and platforms (Kristensen, 2008). But it is not only large structures that are susceptible also small devices such as environmental sensors. Sensors are especially vulnerable to micro-fouling because the biofilm formation impedes the performance of the sensors very quickly regardless of the type of sensor (Kerr, 1998). It does not matter if it is a membrane such as those of pH or oxygen sensors or the optical window in sensors for turbidity and chlorophyll, in every case the function of the sensors are degraded (Whelan and Regan, 2006). Its effects range from measurement drift, for which one can compensate in some circumstances (e.g. if in situ calibration is feasible), to the blockage of channels, which renders the sensor inoperative. For example in sensors, where the measurement is based on the specimen diffusing through a membrane as in some pH or oxygen sensors, the pathway may simply be physically blocked by the biofilm formation (Pichette et al., 2007). Whereas optical sensors, e.g. turbidity (Mitchell et al., 2003) or chlorophyll (Klevenz et al., 2011), are affected in two distinct ways: one the light is scattered by material obstructing the

pathway and secondly by adsorption of light. To a certain degree it is possible to compensate for the light scattering as it occurs evenly for the whole spectrum resulting in a general drop in the light intensity. As for the absorption of light, biofilms typical cause temporal variations in the absorption spectrum, rendering compensation more challenging, this is mostly due to photosynthetic organisms (Kerr, 1998).

Another aspect is the corrosion and degradation of the materials used in the sensors which might not affect the measurements directly but has an effect on the integrity of the sensor (Hiromoto et al., 2005, Fang et al., 2002). An interaction between bacterial surface molecules and release of metal ions at a metal/liquid interface has also been proposed and a direct involvement of EPS production in the deterioration of stainless steel and copper has been proven (Beech, 2004, Beech and Sunner, 2004). In general it can be said, the longer the deployment period the more severe the effects of biofouling.

1.4 Methods for the Analysis of Biofilms

1.4.1 Biofilm Structure and Biomass Determination

Microscopic Techniques

Many microscopic methods have been developed and adapted for the analysis of biofilms (Brackman, 2009, Brown, 1998, Fang et al., 2000, Keevil, 2003). Microscopic examination of biofilms allows the analysis of spatial structures within biofilms, the heterogeneity of the distribution, the stages in biofilm development and the impact of biofilms on the substrate surface (Mansfeld et al., 1994, Li et al.). Combined with fluorescent stains, microscopy is also used for quantification of the biomass.

Microscopy methods include transmission electron microscopy (TEM), scanning electron microscopy (SEM), episcopic differential interference contrast microscopy (EDIC), fluorescence microscopy, and Laser scanning confocal microscopy (LSCM) (Surman et al., 1996). The advantages and disadvantages afforded by these methods are discussed below. The methods can be divided into two distinct groups: electron microscopy and contrast/confocal laser microscopy.

The great advantage of the electron microscopy technique is the high magnification allowing detailed examination of the biofilm, the material surface and its degradation as a result of the biofilm formation (Wen et al., 2009, Yi et al., 2009, Yuan et al., 2007). The TEM transmits a focused high energy electron beam through the sample producing a detailed internal cross-section, with a possible resolution down to 50 pm (Brown, 1998). For the SEM the resolution is about an order of magnitude lower as a low energy electron beam is used to raster scan the surface of a specimen, allowing to map the topography (Landoulsi et al., 2011, Li et al., 2010).

TEM and standard (as opposed to environmental) SEM have large disadvantages since there is a shrinking effect of the biofilm due to dehydration during the preparation, but they can be used to map a topography of complex shapes (Surman et al., 1996). With the environmental SEM no such dehydration is needed, allowing the analysis of the biofilm structures without shrinking artefacts (Surman et al., 1996).

The LSCM relays on a laser scanning and exciting the fluorescence of a sample, obtaining optical images at various depth which can be used to generated 3D images (Walker et al., 1998). The use of fluorescent marker with the LSCM also allows the differentiation and mapping of marked microorganisms inside a biofilm (Brown, 1998, Doiron et al., 2012).

EDIC/EF microscopy has been proven to be useful in the examination of biofilm formation on opaque surfaces such as metals, plastics, tissue surfaces and in vivo medical devices (Keevil, 2003). EDIC is based on conventional light microscopy technique with the polarizer placed above the sample generating a real-time pseud-3D image. The placement of the polarizer allows for the examination of opaque samples (Keevil, 2003). As EDIC/EF does not require the use of a cover slip, so the biofilm is not compressed and it allows a detailed study of the surface topography. If used in conjunction with fluorescence stains or markers this method allows the distinction between viable and non-viable bacteria (Surman et al., 1996) or even the distribution of microorganisms (Giao et al., 2009, Wilks et al., 2005, Wilks et al., 2006). The measurement of the biofilm thickness and/or coverage can be used as proxy for biomass.

Quantitative staining techniques

Crystal violet (C₂₅H₃₀ClN₃) staining is frequently used to quantify biofilms by measuring the absorption of the bound Crystal violet (Peeters, 2008). It is typically used as a part of the classical microbiological identification scheme to distinguish between gram positive and gram negative bacteria, but it can be used as an indiscriminate cationic stain which binds to the negatively charged structures in the cell membrane (Brock, 1994). The measurement of the absorbance of the crystal violet bound in a biofilm can give an indication of the biomass (Christensen et al., 1985). The absorbance of the bound stain can either be done while still bound to the cells (e.g. if the biofilm is grown in a microtitre plate (Peeters, 2008) or after the stain is redissolved in acetic acid (Peeters, 2008). However, the results need to be carefully evaluated in respect to biomass quantification since the stain may also bind to negatively charged structures within the EPS matrix and on the surface of the substratum.

The biomass can also be determined by the use of **fluorescent stains**, binding to DNA such as SYTO®9 (Brackman, 2009) and 4′,6′-diamidin-2-phenylindole dichloride (DAPI) (Ishii et al., 2004), or fluorescently labelled probes (Lo Giudice et al., 2012) in

association with epifluorescence and laser scanning confocal microscopy (LSCM) (see 0)(Lawrence, 1998, Honraet, 2006). DNA fluorescent stains not associated with specific DNA probes bind indiscriminately to all DNA molecules present in the sample. Although some stains are not able to penetrate an intact cell membrane due to their physical properties (Wilks et al., 2005, Wilks et al., 2006). These different staining capabilities can be used for the determination of the ratio between dead and life cells. Another technique to distinguish live cells is the use of fluorescent stains linked to metabolic reactions of live cells. One such stain is 5-cyano-2,3-ditolytetrazolium chloride (CTC) (Rodriguez et al., 1992). This stain is reduced through electron transport in respiring cells resulting in a red fluorescence (Weaver et al., 2008). The combination of this stain with a nucleic acid stain such as DAPI (Wirtanen et al., 2001) or Syto9 allows one to distinguish between and quantify live and total cell numbers. In contrast hybridising nucleic acid probes bind to specific nucleic acid sequences. They can be labelled with fluorescent stains and can detect species or genes of interest if their sequence is known a priori (Robinson et al., 1995). Probes can also be designed to bind to specific surface proteins of the cell membranes (Keevil, 2003). One of the most used nucleic acid probe techniques is Fluorescence In Situ Hybridization (FISH) (Robinson, 1995, Surman et al., 1996). FISH uses fluorescent labelled nucleic acid probes complimentary to specific genes or mRNA that bind in situ with minimal disturbance to the cell or structure being studied (Huber et al., 2004). Specific probes are useful if the presence, distribution or absence of a specific species is analysed. But for the quantification of samples with unknown community composition non-specific fluorescent stains are better suited as no knowledge of the microorganisms is need. The determination of biomass by microscopy with the help of stains and probes has the advantage that it can also give information about the structure of the biofilm such as the spatial distribution of the cells or certain species inside the biofilm. Whereas the staining with crystal violet can only provide an absolute measurement of the biomass, with no information about spatial distribution inside the biofilm or the ratio of dead to live cells, but it is a fast and easy method.

1.4.2 Biofilm community composition

Molecular Techniques

In recent years several **molecular assays** for quantification of live and total cell numbers have been developed to support and enhance existing methods. Two important state of the art techniques are the luciferase assay for the quantification of viable cells (Maukonen et al., 2000, Cooksey et al., 1993, Venkateswaran et al., 2003) and the quantitative polymerase chain reaction (qPCR) for DNA quantification (Petersen et al., 2011, Thompson et al., 2005, Thompson et al., 2004). The Luciferase assay measures the amount of ATP present by determining the light emission resulting from

the reaction of luciferin with ATP. The luciferase is the enzyme catalysing this reaction of luciferin to luciferin adenylate and the subsequent oxidation of this compound produces the light emission (Cooksey et al., 1993, Venkateswaran et al., 2003). The amount of ATP gives an indication of the number of viable cells, but because the ATP concentration within a cell may vary with species, cell size and health of the cells, it is difficult to extrapolate the exact cell number (Eigenbrode et al., 2009, Venkateswaran et al., 2003). Because of this the method is only semi-quantative it needs to be supported by other assays. Another disadvantage is that the luciferase assay cannot distinguish between microorganisms.

The second technique qPCR is more versatile. qPCR is a variant of the polymerase chain reaction (PCR) where the amount of amplified material (amplicon) is measured at certain points during the assay (real-time measurement) in contrast to a normal PCR where the amplicon can only be measured after the assay is finished (end-point measurement). A characteristic time history of amplicon amount vs. the number of thermal / amplification cycles can be calibrated to give a quantitative measurement of the initial amount of target present in the sample. Detection of DNA while it is amplified is typically via a fluorescent reporter molecule. These reporter molecules can either be generic markers like SYBR®Green, a fluorescent DNA stain, or more specific markers like fluorescent labelled probes for Bacteria and Archaea (Petersen et al., 2011).

Examination of the Community Composition

The examination of the community composition is an important aspect of the assessment of the impact of environmental factors and antifouling strategies on the development of a biofilm and the subsequent fouling.

Before the advance of molecular methods only cultivable microorganisms could be identified. But the concept of a viable but not culturable state (VBNC) (Bloomfield et al., 1998) in microbiology, is also encountered in environmental samples. The application of new methods showed that up to 99% of microorganisms found in the environment, and in natural biofilms specifically, cannot be grown in the laboratory (Brock, 1987). Other advantages of the molecular methods are that when compared to classical identification they are fast. Molecular assays needed to achieve this can be divided into two main groups, those for DNA extraction and purification, and those which perform the analysis of DNA sequences.

In addition to the older phenol/chloroform extraction and purification of DNA (Bahattab et al., 2011), several other methods have been developed over the years (Martín-Platero et al., Price, 2009). The phenol/chloroform extraction uses an aqueous and an organic solvent phase to separate the DNA from the proteins respectively. The proteins are denatured in the organic phase, while the DNA is contained in the

aqueous phase (Price, 2009). The phenol/chloroform extraction was later improved by stabilizing the DNA and gave rise to the commercial Trizol extraction (Haimov-Kochman et al., 2006). Other commercially available extraction kits were developed using solid phase extractions (Price, 2009). Here the DNA is separated from proteins and other cell constituents by binding in the presence of chaotropic salts to a solid phase containing silica particles (Boom, 1990). The chaotropic salts disrupt the weak electrostatic repulsion between the DNA and the silica allowing formation of hydrogen bonds and the adsorption of the DNA to the silica (Melzak et al., 1996)

A wide variety of molecular techniques have been used for the study of microbial communities ranging from Restriction Fragment Length Polymorphism (RFLP) analysis with subsequent sequencing (Haddad et al., 1995), the generation of clone libraries (Polz and Cavanaugh, 1995, Auguet et al., 2009), Denaturing Gradient Gel Electrophoresis (DGGE) (Muyzer et al., 1995) through to pyrosequencing (Huber et al., 2007). The target sites for these analyses range from the whole to partial 16S rRNA gene or enzyme-specific genes, eg the mitochondrial cytochrome oxidase subunit I (COI) gene, for a more specific approach (Black et al., 1997). The 16S RNA gene as a region in the DNA with the correct ration between conserved areas, allowing primer binding, and areas able to tolerate mutation in its sequence, has been used to explore microbial communities and identify dominant organisms in a number of environments (Biddle et al., 2006, Flores et al., 2011, Lenk et al., 2011, Wilson, 2009, Huse et al., 2008).

Culture-independent technique e.g. Terminal Restriction Fragment Length Polymorphisms (T-RFLP) has been used in a variety of studies in the deep-sea environment (Moeseneder et al., 2001b, Moeseneder et al., 2001a, Luna et al., 2009). The amplified DNA is digested using restriction enzymes and the resulting fragments are separated by electrophoresis on a polyacrylamide gel (Pozos et al., 2004, Liu et al., 1997). A change in DNA sequence can result in the deletion or creation of recognition sites for the enzymes, which creates a variation in fragment sizes and a characteristic band pattern which allows for the identification of known species.

Another culture-independent technique to analyse community diversity is DGGE. The method is based on DGGE analysis of polymerase chain reaction (PCR) amplified 16S DNA, allowing rapid analysis of both community diversity and differences between sample types (Muyzer et al., 1995, Muyzer et al., 1993, Cleary et al., 2012). By using the dependence of the chemical melting points of the DNA double strand to its GC-content and sequence of nucleic acids, it is possible to separate equal length PCR fragments of mixed communities (Muyzer et al., 1993) to determine differences in the community composition. Additionally such separated DNA bands can be extracted and used for sequencing to identify specific bacteria, by using internet databases such as

DNAblast. These sequences can also be used to generate phylogenetic trees (Dang and Lovell, 2000).

Another method to analyse bacterial communities of multispecies biofilms is DNA fingerprinting. Here the internal transcribed spacer (ITS) region of 16S-23S genes, which is non-functional, is amplified using PCR (Boyer et al., 2001). This region is easy to amplified and has a high variability even between closely related species. The amplified DNA is digested using restriction enzymes, specific to certain DNA sequences, and the resulting fragments are separated by electrophoresis on a polyacrylamide gel (Pozos et al., 2004, Liu et al., 1997). A change in DNA sequence can result in the deletion or creation of recognition site for the enzymes. This creates a variation in fragment sizes and a characteristic band pattern which allows for the identification of known species.

A similar but slightly different approach is use of the Restriction Fragment Length Polymorphism (RFLP). In this method the 16S rDNA is amplified and fluorescent labelled using PCR. The amplicons are then digested with a restriction enzyme and separated by gel electrophoresis. This again results in a species specific band pattern which can be used for the identification of known species (Hung et al., 2005b).

However, both of these methods are of only limited use in identifying unknown species.

Optimisation

Chapter 2: Method Development and Optimisation

In order to assess the efficiency of any given antifouling strategy an array of different techniques is necessary, as the process of biofouling occurs in a series of stages and identifying key processes by understanding the development of biofilms may provide methods for the prevention of biofouling (Railkin, 2004).

Measuring the overall biomass of the accumulated biofilm is one aspect and in order to get an accurate overview the use of more than one microscopic method is essential as sample preparation and or the imaging process might influence the results between techniques (Surman et al., 1996). Further understanding of the microbial community is needed, since the population composition has a major impact on the degree of the fouling. The reason for this is that corrosion rate as well as amount of EPS secreted is influenced by which microorganisms make up the biofilm. Molecular biology techniques involving the 16S rRNA genes have been proven to be highly successful in the description of complex microbial communities (Amann et al., 1995).

Also the 3D-structure and community composition of a biofilm is indicative of the development stage of the biofilm.

This chapter gives an overview of methods and materials used as well as their optimisation. This was necessary in order to generate a work flow with control mechanisms (Figure 2.1) for the analysis of microbial community composition to be able to compare results of the analysed samples treatment used in the project.

2.1 Chemicals, Materials and Solutions

2.1.1 Chemicals and Materials

The chemicals and materials used in this study are listed below in Table 2.1.

Table 2.1: Chemicals and Materials used

Chemical / Material	Source / Supplier
100bp DNA Ladder	New Englad Biolabs, UK
1kb DNA Ladder	New Englad Biolabs, UK
4',6'-diamidin-2-phenylindole dichloride (DAPI)	Invitrogen, UK
40% Acrylamide/Bis solution (37.5:1)	Biorad, UK
5-cyano-2,3-ditolyltertrazolium chloride (CTC)	Invitrogen, UK
Agarose	Fisher Scientific, UK
Agilent DNA 12K Kit	Agilent Technologies
Agilent High Sensitivity DNA Kit	Agilent Technologies

Chapter 3: Method Development and Optimisation

Ammonium Persulfate (APS)	Fisher Scientific, UK
Biolceanse	Tekon
Chemical / Material	Source / Supplier
Brilliant III Ultra-Fast QPCR Master Mix	Agilent Technologies
Chelex 100	Sigma Aldrich, UK
Copper	Farnell, UK
Copper (Particles)	Sigma Aldrich, UK
Copper(I)oxide (particles)	Sigma Aldrich, UK
Copper(II)oxide (particles)	Sigma Aldrich, UK
Cyclic Olefin Copolymer (COC)	Topas 8007504
Cyclo Olefin Polymer (COP)	Zeonex 690R
Cyclohexane	Sigma Aldrich, UK
Delrin™	Direct Plastics, UK
Dneasy Kit Blood & Tissue	Qiagen, UK
dNTP Mix (10 mM)	New Englad Biolabs, UK
Ethanol 100% (v/v)	Sigma Aldrich, UK
Formaldehyde (36.5-38%)	Sigma Aldrich, UK
Formamide	Sigma Aldrich, UK
Gel Extraction Kit	Qiagen, UK
King B media	Fluka / Sigma-Aldrich,
	UK
Lysozyme	Sigma Aldrich, UK
Magnesium chloride (50mM)	New Englad Biolabs, UK
NulceoSpin Gel and PCR Clean-up Kit	Machery-Nagel, UK
Pico green	Invitrogen, UK
Poly-methyl methacrylate (PMMA)	Direct Plastics, UK
Precast Agarose gel	Sigma Aldrich, UK
Qiaquick PCR clen up Kit	Qiagen, UK
Sodium dodecyl sulphate	Sigma Aldrich, UK
Sodium citrate	Sigma Aldrich, UK
Sodium hydroxide	Sigma Aldrich, UK
Ethylenediaminetetraacetic disodium salt dihydrat (Na-EDTA)	Sigma Aldrich, UK
Stainless steel grade 374	supplied by Daivid
	Walker
Standard Taq Reaction Buffer (10x)	New Englad Biolabs, UK
Swab F150CA plain with polypropylene swab tubes wooden	Fisher Scientific, UK
stick (Sterilin)	
SYBR Gold Nucliec Acid Gel Stain	Invitrogen, UK
SYBR Safe DNA gel Stain	Invirtogen

Chapter 3: Method Development and

Optimisation

	- p
Syto 9	Invitrogen, UK
TAE buffer 50x	Fisher Scientific, UK
Chemical / Material	Source / Supplier
Taq DNA Polymerase	New Englad Biolabs, UK
Temed	Sigma Aldrich, UK
Trisma Hydrochloride	Sigma Aldrich, UK
Triton x-100	Sigma Aldrich, UK
Trizol	Invitrogen, UK
Urea	Fisher Scientific, UK
Whatmann GF/D glass microfiber filter 0.7um pore size	Whatman, UK
Whatmann GF/D glass microfiber filter 3um pore size	Whatman, UK

2.1.2 Solutions

Solutions and their components used are listed in the following tables.

Chelex extraction

Table 2.2: Solutions for DNA extractrion using Chelex

Solution	Reagents
Lysis Buffer:	0.1x TE solution with 10 mg / ml lysozyme
1x TE stock solution	10mM TrisHCl 1mM EDTA
Chelex 100 suspesion	10% Chelex resin in 50mM Tris pH 11
50mM Tris pH 11 (100ml)	605 mg Trisma Base adjust pH with NaOH to 11
Sodium Citrate	0.1 M sodium citrate in 10% ethanol

DNeasy Extraction Kit, Qiagen

Table 2.3: Solutions for DNeasy extraction Kit

Solution	Reagents
Enzymatic Lysis Buffer	20mM Tris-HCl, pH 8
	2mM Na-EDTA
	1.2% Triton®x-100
	Immediately before use add 20mg/ml
	Lysozyme

Solutions for DGGE

Table 2.4: Solutions for DGGE

Solution	Reagents	
8% acrylamide sotuion (total volume 100 ml):	40% Acrylamide/Bis (37.5:1) TAE Buffer (x50%) Rnase/Dnasefree Water	20 ml 2 ml 78 ml
30% denaturing acrylamide solution (total volume 100ml)	40% Acrylamide/Bis (37.5:1) 20 ml TAE Buffer (x50%) 2 ml Rnase/Dnasefree Water 66 ml Foramide 12 ml Urea 12.6 g	
Solution	Reagents	
50% denatuting acrylamide solution (total volume 100ml)	40% Acrylamide/Bis (37.5:1) TAE Buffer (x50%) Rnase/Dnasefree Water Foramide Urea	20 ml 2 ml 58 ml 20 ml 21 g
80% denaturing acrylamide solution (total volume 100ml)	40% Acrylamide/Bis (37.5:1) TAE Buffer (x50%) Rnase/Dnasefree Water Foramide Urea	_

2.2 Microscope Techniques

In this study four different microscopy techniques were used for analysing the samples in order to compensate for artefacts generated by sample preparation and imaging process: EDIC, which allows the microscopic examination of opaque surfaces, epi-fluorescence microscopy, LSCM and environmental SEM.

2.2.1 EDIC/EF Microscopy

To examine the heterogeneity and topography of biofilms on opaque surfaces EDIC microscopy has been proven to be useful (Keevil, 2003). As EDIC does not require the use of a cover slip, the biofilm is not compressed and it allows a detailed study of the surface topography. When used in conjunction with fluorescence DNA stains, this method allows the distinction between microbes and inorganic particles and produces a pseudo-3D image without depth scanning. In this project ethanol fixed samples were stained with the nucleic acid stain SYTO®9 and examined with a Nikon Eclipse ME600 microscope (Best Scientific, Swindon, UK) using 40x long working distance objective. Filters in conjunction with EDIC used were Calcium Crimson (excitation 580/20 nm,

emission 630/ nm), FITC/Bodipy/Fluo3/Di O (excitation 480/40 nm, emission 535/50 nm), and R&B Phycoerythrin (546/11 nm, emission 585/40 nm).

2.2.2 Laser Scanning Confocal Microscopy

LSCM allows the generation of 3D images and the measurement of the thickness of the biofilm developed on the surfaces. The samples were stained with 1 μ g ml⁻¹ DAPI (Invitrogen, UK) and images taken with the LSM 700 (Zeiss) using the following settings: 40x objective, 405nm laser at 2% power level and beam splitter set at 420nm, pinhole size was 50 μ m and z-step size 1 μ m.

2.2.3 Environmental Scanning Electron Microscopy

The samples for the SEM were fixed by incubating in 36.5-38% Formaldehyde (Sigma-Aldrich, UK) for 10 minutes. Afterwards the samples were rinsed carefully with RNase/DNase free water and air-dried. For the examination the Miniscope TM-1000 (Hitachi) was used. As this is an environmental SEM, the samples were not metalised and the following conditions applied: Accelerating voltage: 15000 V, Emission current: 65 mA, low vacuum and working distance: 7250 μ m to 7270 μ m.

2.2.4 Staining Protocol using fluorescent Dyes

For this project of several fluorescent stains, SYTO®9, 4´,6´-diamidin-2-phenylindole dichloride (DAPI), and 5-cyano-2,3-ditolyltetrazolium chloride (CTC) (Invitrogen, UK) were used. These stains were chosen because the staining protocols are quick and easy. Both SYTO®9 and DAPI are nucleic acid stains that fluoresce upon binding to double stranded DNA and are able to penetrate cell membranes. The resulting fluorescence can be used for a count of all attached cells.

CTC is generally used to evaluated respiratory activity as it is reduced through the electron transport of the respiring cells to a red fluorescence and can thus been used as a live cell stain (Wirtanen et al., 2001), M.N. Tsaloglou in communication):

For the microscopic analysis if alive/total cell the sample is first stained with CTC by covering the surface with $5\mu M$ CTC and incubate them overnight at $25^{\circ}C$ and slightly agitated (70 rpm). The next morning sample surface is carefully rinsed with DNase/RNase free water and fixed in formaldehyde. After additional rinsing with DNase/RNase free water the sample is air dried for approximately 30 min, before continuing with the DAPI Staining. Again the sample surface is covered with $1\mu g/ml$ DAPI and incubated at room temperature for 30 min. Before rinsing the sample is carefully rinsed with DNase/RNase free water, air dried and stored at $4^{\circ}C$ in the dark.

For the staining with Syto $^{\circ}$ 9 a concentration of 5 μ M and an incubation time of 30 min at RT in the dark was used as the recommendation of the manufacturer for bacterial cells were 50 nM to 20 μ M with incubation between 1 to 30 min, and 10 nM to 5 μ M and 10 to 120 min incubation for eukaryotic cells.

The staining is stable for several weeks when stored at 4°C and protected from light.

2.2.5 Quantification using fluorescent images

The fluorescence of the stained samples can also be used for the quantification of the biofilms coverage of a surface as an indicator for biomass (Surman et al., 1996, Keevil, 2003, Wirtanen et al., 2001). For the quantification ten images of each material were taken with a fluorescence microscope (EVOSfl AMG, USA), using the GFP filter (470 nm excitation, 525 nm emission) for Syto®9 stained samples, the RFP filter (531 nm excitation, 593 nm emission) and 10x objective. The surface coverage of the biofilm formation was quantified by using a custom MATLAB™ (supplied by Xi Huang; see Appendix I).

2.3 Contamination of surfaces with *Pseudomonas* fluorescens

Pseudomonas fluorescens is biofilm forming organisms used as a model organisms in wide range of laboratory experiments examining biofilm formation and mitigation techniques. Therefore this organism was also used to test DGGE extraction with subsequent sequencing as well as to examine effectiveness of surface modifications as antifouling technique in laboratory experiments.

P. fluorescens was grown in King B media at 23°C and 120 rpm. Before contamination a subculture was grown using 5 ml culture in 150 ml media and grown for 24 hours. This culture was used as inoculum for another subculture which was grown for approximately 7 hours before using it for the contamination of surfaces. The surfaces were incubated overnight at 23°C and 120 rpm. Afterwards the access media was carefully removed and the fluorescent staining protocol using CTC and DAPI was followed.

2.4 Molecular Techniques

As mentioned earlier analysis of the microbial community in the biofilm is an important aspect in the assessment of the severity of the biofouling or rather the effectiveness of any mitigation strategy. This analysis consists of several steps which

need to be optimised. The following schematic gives overview of the flow of methods and possible control mechanisms using PCR, DGGE and sequencing for this purpose:

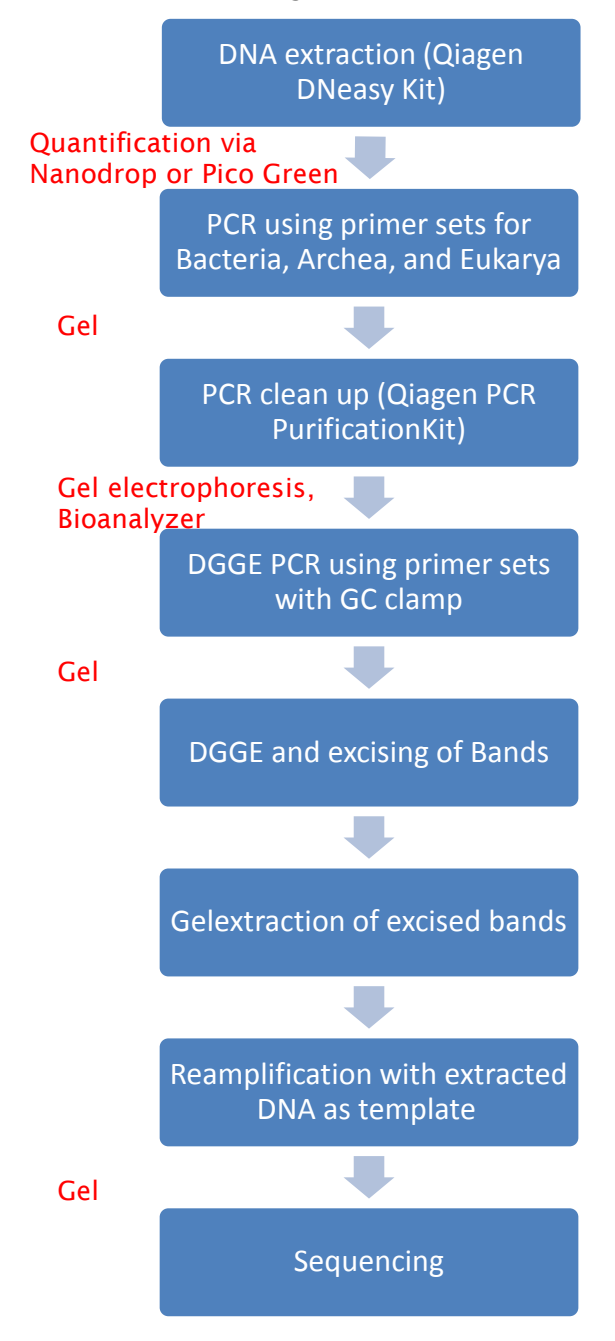


Figure 2.1: Flow Chart of the analysis of microbial community using DGGE and the control mechanisms (red)

2.4.1 Quantification of DNA extracts

DNA extracts were quantified either using the Pico Green Assay (Invitrogen, UK) or by measuring the absorption at 260 nm using the NanoDrop 1000 Spectrophotometer (Thermo Scientific). Using the absorption allows also to control the quality regarding protein and RNA content of the extraction by determining the 260/280 ratio, a ratio of

around 1.8 indicates pure DNA with little or no contamination (Warburg and Christian, 1941).

The Pico Green assay was used according to the manufactures guidelines except that the assay volume was reduced from 200 μ l to 100 μ l as this was the maximal volume the plates could accommodate. All samples were run as duplicates and measured using the same reagents allowing the use of the following standard curve to calculate the concentrations (Figure 2.2):

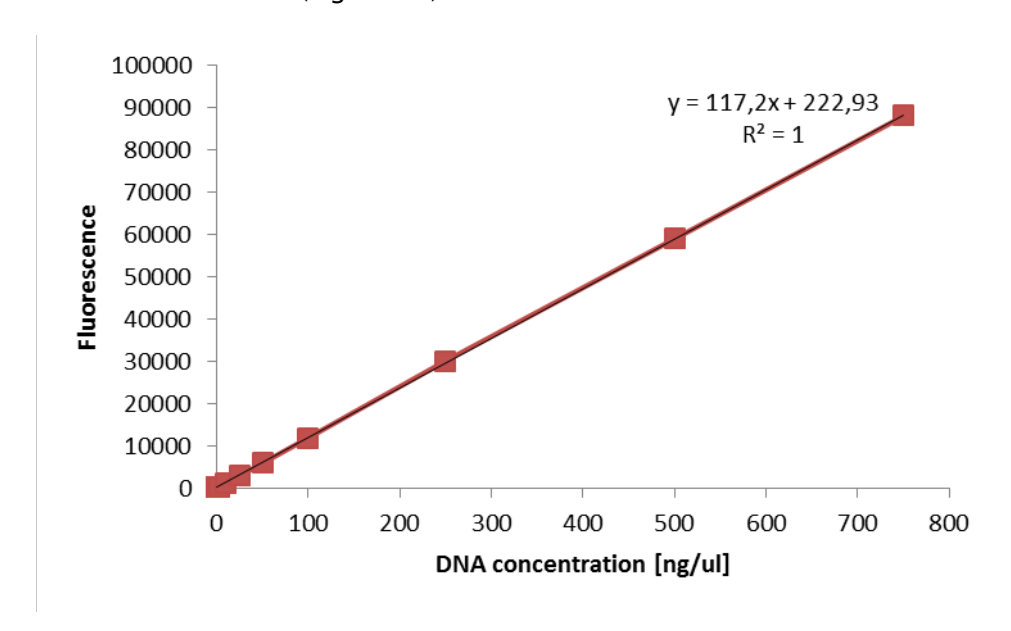


Figure 2.2: Standard curve of Pico Green assay used to calculate DNA concentrations of DNA extracts; n=2

2.4.2 Biofilm Removal and DNA extraction optimisation

Three different techniques for the removal of biofilm from a surface for DNA extraction were tested in order to find the most efficient one, for two of these also different elusions included. The biofilms used were grown microscope slides made out of glass by exposure to the Solent water for 14 days (12th October 2009 – 26th October 2009).

1. Using sterile swabs:

a. Elution with water: the swab tip is cut off into a 2 ml sterile tube. Add 750 μ l water and vortex, centrifuge for 15 min at 13000 rpm, remove supernatant and tip carefully without disturbing the pellet

Add 180 µl lysis buffer and re-suspend pellet and follow the DNeasy Pretreatment and DNA extraction for Gram-Positive Bacteria Protocol.

b. Elution with enzymatic lysis buffer (20 mM TricCl, pH 8; 2 mM Na-EDTA, 1.2 % Triton®X100, 20mg/ml Lysozyme): the swab tip is cut off into a 2 ml sterile tube and 180 µl lysis buffer added and the DNeasy

Pretreatment and DNA extraction for Gram-Positive Bacteria Protocol followed.

2. <u>Glass Beads and Sonification:</u> approx. 2 g sterile glass beads; 0.7 μm diameter (Sigma Aldrich, UK) and 1.5 ml water are added to a 50 ml Flacon Tube with the glass slide. The mixture is sonificated for about 2 min and the water carefully transferred into a 2 ml tube. After centrifugation for 15 min at 13000 rpm the supernatant is carefully removed and the pellet re-suspended in 180 μl enzymatic lysis buffer. The DNA extraction is continued by following the DNeasy Pretreatment and DNA extraction for Gram-Positive Bacteria Protocol.

3. Micropastels

- a. Elution with enzymatic lysis buffer: Micropastels were used on the surface and eluted with 180 µl lysis buffer into a 2 ml cap and the DNA extracted by following the DNeasy Pretreatment and DNA extraction for Gram-Positive Bacteria Protocol.
- b. Elution with water: Micropastels were used on the surface and eluted with 750 µl water into a 2 ml cap and centrifuged for 15 min at 13000rpm. After removal of the supernatant the pellet was resuspended in 180 µl lysis buffer and the DNA extracted by following DNeasy Pretreatment and DNA extraction for Gram-Positive Bacteria Protocol

Results & Conclusions

The quantification of the DNA extracts from the biofilm removal experiment using absorption showed the highest DNA concentration of 6.09 ng/ μ l in the samples where a swab was used and the cell lysis step was performed directly (Figure 2.3A). The additional elution step with water in both the biofilm removal via swabs and micropastels resulted in a lower DNA concentration, 3.08 ng/ μ l ±0.35 and 3.85 ng/ μ l ±0.99 compared to 6.09 ng/ μ l ±1.15 and 4.77 ng/ μ l ±0.78. For the swab samples the DNA concentration was reduced by almost 50 %. The Biofilm removal using glass beads in conjunction with sonification resulted in a similar DNA concentration, 4.71 ng/ μ l ±0.82 as the micro-pastels without the additional elution step. A gel-electrophoresis of a PCR sample using the DNA extract of the swab B samples as template resulted in a product with the expected base pair length (Figure 2.3B).

Chapter 3: Method Development and

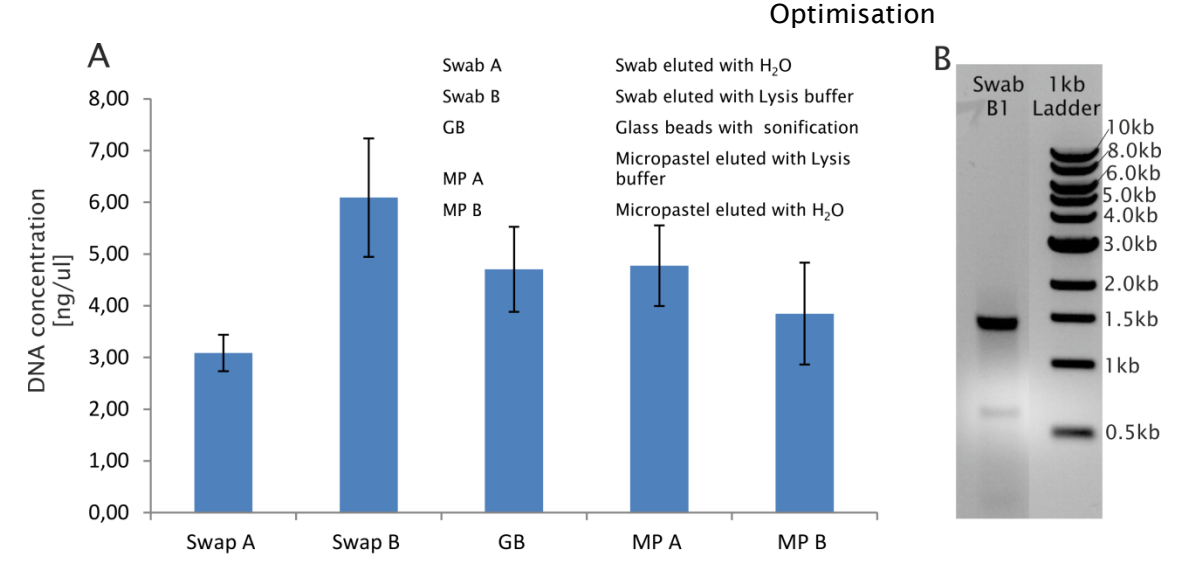


Figure 2.3: Analysis of DNA extracts from biofilm removal experiments; (A)

Quantification of DNA extracts from the biofilm removal experiment using the NanoDrop 1000 Spectrophotometer (Thermo Scientific); n=3. (B) Gel-ectrophoresis image of the PCR amplification product

2.4.3 Testing DNA Extraction Techniques

Three different genomic DNA extraction techniques were compared to determine the most efficient for biofilm removed with sterile swabs: Chelex-100, Qiagen DNeasy Kit, Invitrogen Trizol® Extraction. The biofilms were grown on glass slides exposed in the Solent for 28 days (5th January 2010 – 2nd February 2010) and afterwards removed with cotton swaps.

1. <u>Protocol: Pretreatment and DNA extraction for Gram-Positive Bacteria (DNeasy kit Blood & Tissue Qiagen)</u>

The swab tip is cut off into a 2 ml sterile tube and 180 µl lysis buffer added and incubated for 30 min at 37°C. Then 25 µl proteinase K and 200 µl Buffer AL (without ethanol) are added, the mixture vortexed and incubated at 56°C for 30 min. Afterwards 200 µl ethanol (96-100%) is added and the mixture again vortexed. Everything is transferred into DNeasy Mini spin column in a 2ml collection tube, centrifuge at 8000 rpm for 1 min and both flow-through and collection tube discarded. After placing the spin column into new collection tube, adding 500 µl Buffer AW1, and centrifuging for 1 min at 8000 rpm, the flow-through and collection tube are again discarded. In the next step the spin column is placed into new collection tube, 500µl Buffer AW2 added, and centrifuged for 3 min at 14000 rpm. Flow-through and collection tube were discarded. In the final step the spin column was placed in a clean 2 ml tube, and 200 µl Buffer AE pipetted directly onto the membrane. Everything is incubated at RT for 1 min, and centrifuged for 1 min @ 8000rpm) to elute.

2. Chelex DNA extraction (Martín-Platero et al., 2010)

The swab tip is cut off into a 2 ml sterile tube, 100 μ l lysis buffer (0.1 x TE solution with 10mg/ml lysozyme) are added and the mixture incubated for 45 min at 37°C. Afterwards 1 μ l proteinase K [10mg/ml] and 1 μ l SDS [10%] are added and again incubated at 37°C for 30 min. Then 100 μ l Chelex [10%] is added, everything gently mixed and incubated for 30 min at 56°C.

After vortexing the mixture for 10 sec and incubating for 10 min at 100°C, everything is centrifuged 5 min at 14000 rpm and the supernatant transferred into a new tube.

3. DNA extraction using Trizol LS® reagent (Invitrogen, UK)

The swab tip is cut off into a 2 ml sterile tube and 0.75 ml Trizol added. After an incubation for 5 min at RT, 0.2 ml chloroform are added and the mixture shaken for 15 sec. Incubating again for 15 min at RT before centrifuging everything for 15 min at 1200 g. This step results into three phases, of which the aqueous phase is removed. After adding 0.3 ml of 100 % ethanol to the phenol-chloroform phase and mixing by inversion, the sample is stored for 2-3 min at RT before centrifuged for 5 min at 2000 g. The following steps are repeated: removing the supernatant and re-suspending the pellet with 1 ml 0.1 M sodium citrate in 10 % ethanol, leave for 30min @15-30°C with periodic mixing and centrifuge for 5 min at 2000 g. After removing the supernatant for the pellet is re-dissolved in 1.5-2ml 75% ethanol, stored for 10 to 20 min RT with periodic mixing and centrifuged for 5 min at 2000 g. Discarding the supernatant, the DNA pellet is briefly dried under vacuum before the pellet is dissolved in 0.3 to 0.6 ml of 8 mM NaOH and un-dissolved material is removed by centrifugation for 10 min at 12000 g.

All samples were done in triplicates. The DNA concentration of the biofilm removal and DNA extraction experiments were quantified using the NanoDrop 1000 Spectrophotometer (Thermo Scientific). Additional a PCR was run using the following conditions: the reaction mixture contained five µl of DNA extract as template, 0,25 µM primer of each primer specific for 16S DNA of bacteria (Table 2.1: 27F; 1387R), 0.2 mM of each deoxynucleoside triphosphate (dNTP's), 1.5 mM MgCl₂, and 0.625U Crimson Taq Polymerase (NEB, UK) in a total volume of 25 µl. The thermal cycling used was: Initial denaturation step at 94°C for 3 min, then five cycles with 60 sec at 95°C, 60 sec at 40°C and 90 sec at 72°C, this is followed by 30 cycles with 30 sec at 95°C, 30 sec at 43°C and 30sec 72°C. The final extension step is run for five minutes at 72°C. The expected PCR-product is 1396bp long (Dang and Lovell, 2000).

Results and Conclusion

Following the results from the biofilm removal experiment, swabs were used for the removal of the biofilms in the DNA extraction experiment. The Trizol and chelex extraction showed the highest DNA concentration with 95.57 ng/µl ±3.61 and 98.55 ng/µl ±48.13 (Figure 2.4A). But the chelex extraction also showed a very high standard deviation making this not a very desirable technique. The DNA extraction using the Qiagen Kit showed the lowest DNA concentration with 1.79 ng/µl ±0.57. Unfortunately no PCR amplification could be detected in either the samples using the Trizol or the Chelex-100 technique (Figure 2.4B). This might be due to the absence of DNA or the presence of contaminations interfering with the reaction (Abu Al-Soud and Rådström, 1998). In light of the results from both experiments to analyse the microbial community for this project, genomic DNA was extracted from samples taken with sterile swabs. Genomic DNA was extracted using the DNeasy Kit Blood & Tissue (Qiagen) according to the manufacturer's tissue protocol with an extended cell lysis incubation overnight instead of the 'Pretreatment and DNA extraction for Gram-Positive Bacteria' protocol as the DNA concentration proved to be in a similar range without the additional pre-treatment.

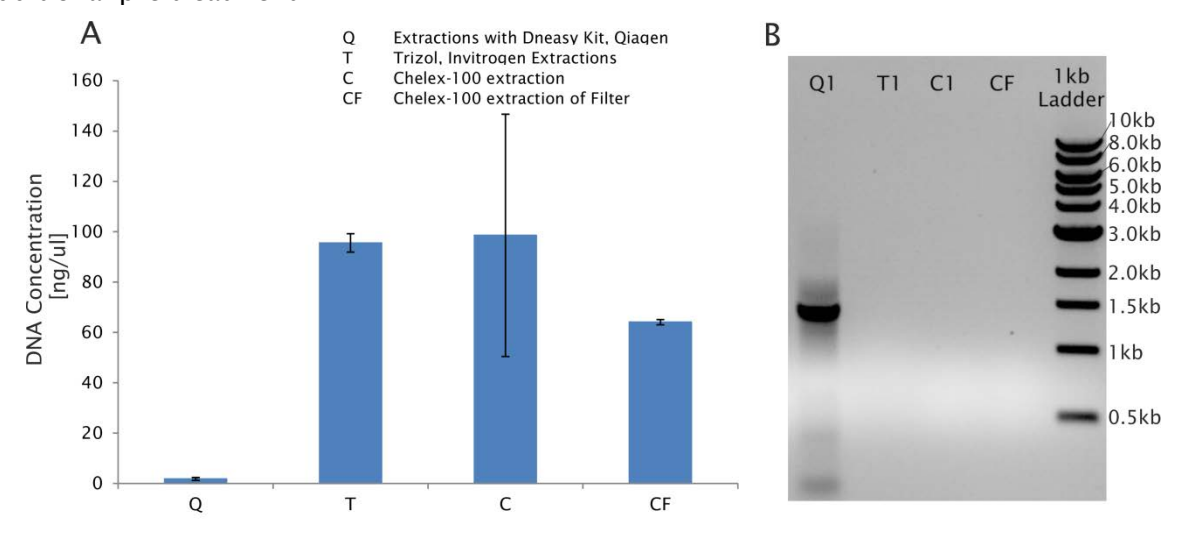


Figure 2.4: Analysis of DNA extracts form DNA extraction experiments; A) Quantification of DNA extracts from the DNA extraction experiment using the NanoDrop 1000 Spectrophotometer (Thermo Scientific); n=3. B) Gel-ectrophoresis image of the PCR amplification product

2.4.4 Polymerase Chain Reaction

Typically five µI of DNA extract were used as template in a Polymerase Chain Reaction (PCR) was performed using a universal primer set specific for 16S DNA of bacteria (Table 2.5: 27F; 1387R) (Dang and Lovell, 2000), specific 16S primers for archea (Table 2.5: A751F; UA1406R) (Baker et al., 2003), and 18S DNA specific primers for Eukarya(Table 2.5: EukF; EukR) (Delong, 1992).

Table 2.5: List of primers used in the project

Domain	Primer Name	Sequence	Reference
Bacteria (universal	27F	AGA GTT TGA TCM TGG CTC	Dang & Lovell
primer set)	1387R	GGG CGG WGT GTA CAA GGC	(2000)
Archea (universal	A751F	CCGA CGG TGA GRG RYG AA	Baker et al.
primer set)	UA1406R	ACG GGC GGT GWG TRC AA	(2003)
Eukarya	EukF	AAC CTG GTT GAT CCT GC CAG T	
(universal primer set)	EukR	TGA TCC TTC TGC AGG TTC ACC TAC	Delong (1992)
	Muy fwd	CCT ACG GGA GGC AGC AG	
Do et e vie	Muy rev ATT ACC GC GG CT GC TGG		Muyzer et al
Bacteria	Muy DGGE	CGC CCG CCG CGC GCG GGC GGG GCG GCA CGG GGG GCC TAC GGG AGG CAG CAG	(1993)
	Cren771F	ACG GTG AGG GAT GAA AGC T	Ochsenreiter et
Archea	Cren957R	CGG CGT TGA CTC CAA TTG	al. (2003)
Archea	nA fwd	AGA CGA TGC AGG CTA GGT GT	
	nA rev	CGG ACA TTT CAC AAC ACG AG	
Eukarya	nE fwd	GTT CCA GGG GAG GTA TGG TT	
Eukaiya	nE rev	TAG CAG GAC GGA GTC TCG TT	

A reaction mixture (final volume: $25~\mu l$) for the PCR amplification containing $5~\mu l$ DNA extract, 1x Standard Buffer (New England Biolabs Inc., UK), each deoxynucleotide triphosphates with a concentration of 0.2~mM and for each primer set a specific amount of DNA Taq polymerase (New England Biolabs Inc., UK) and the relevant primers; $0.25~\mu M$ of the bacteria primers with 0.625~U Taq, $0.5~\mu M$ archea primers and 1~U, and $0.2~\mu M$ of each eukaryotic primer with 2.5~U. The PCR reactions contain additional $1.5~mM~MgCl_2$ for the bacterial and archean amplification reactions and $2~mM~MgCl_2$ for the eukaryotic ones.

The PCR cycling consisted of an initial denaturation step at 94°C for 2 min, 30 cycles with 94°C for 60 sec, 55°C for 60 sec, and 68°C for 60 sec. The final extension step occurred at 68°C for 10 min. The expected PCR products were 1396 bp for the Bacteria specific, 655 bp for the archea specific, and 1817 bp for the Eukarya specific primer set.

2.4.5 Quantitative PCR

To support the microscopic quantification of the biomass qPCR was used in some experiments of this project. For the reaction mixture the Brilliant III Ultra-Fast qPCR Master Mix (Agilent, UK) was used with 0.2 μ M of the Muyzer primer set for Bacteria and nE pirmer set for Eukrya (Table 2.5) and 2 μ l of DNA extract as template. The qPCR cycling consisted of an initial denaturation step lasting 10 min at 95°C, 40 cycles with 95°C for 60 sec, 55°C for 60 sec, and 72°C for 60 sec. The qPCR was run on the Stratagene Mx3005P, (Agilent, UK) and the results were analysed using the MXPro software.

2.4.6 DGGE

The extracted DNA was amplified using the Muyzer primer set (primer sequences see Table 2.5: Muy fwd, Muy rev) or the Archea primer set (primer sequences see Table 2.1: Cren 771F, Cren957R) (Ochsenreiter et al., 2003, Muyzer et al., 1993, Muyzer et al., 1995) The resulting products were cleaned using the Qiagen PCR Purification Kit according to the manufacturers protocol and used as template for the DGGE PCR where the forward primer in the Muyzer PCR products included an additional GC-clamp (Table 2.5: Muy DGGE, Muy rev) (Muyzer et al., 1995, Muyzer et al., 1993). In both cases the reaction mixture (final volume: $25~\mu$ l) for the PCR amplification contained 0.25 μ M of each appropriate primer, 5 μ l DNA extract, 1x Standard Buffer (New England Biolabs Inc., UK), each deoxynucleoside triphosphates with a concentration of 0.2 mM and for each primer set a 1U of DNA Taq polymerase (New England Biolabs Inc., UK).

The PCR cycling consisted of an initial denaturation step at 94°C for 2 min, 30 cycles with 94°C for 60 sec, 55°C for 60 sec, and 68°C for 60 sec. The final extension step occurred at 68°C for 10 min.

The DGGE parameters were the following: 8% Acrylamide/Bis solution (37.5/1) (Biorad, UK) with a denaturant gradient between 30 and 80% were found to be sufficient for the separation of bands with 1600Volt hours (Vhrs) at 60°C. A more detailed protocol can be found in Appendix II.

The DNA fragments of the most prominent bands were extracted, re-amplified and cleaned up (Qiaquick PCR clean up kit, Qiagen, UK). The pure eluent was sequenced using dideoxy chain termination technology (Eurofins MWG Operon, Germany) (Li,

Optimisation

2006). The resulting sequences were identified using the online alignment software BLAST to search the Nucleotide collection (nr/nt) database. The search parameters used in this study were a megaBlast with the 'expect' value set below ten indicating that a random match is unlikely (Altschul, 1997, Altschul et al., 1997, McGinnis and Madden, 2004).

2.5 Problems with the re-amplification of DGGE extracts

After testing was complete and a workflow for analysing microbial community composition was established, samples collected in the field were analysed using the domain specific universal primer sets (Table 2.5) in order to analyse microbial community composition.

Unfortunately most of these sequencing results using Eukarya and Archea specific primers came back as failed. This was unexpected as prior analysis of Mid Cayman samples in a different laboratory with similar set-up and the same primers did lead to some usable preliminary results.

Reasons for this can range from DNA concentrations being too high to allow sufficient separation of the PCR products during DGGE to complete or partial degradation during the extraction process after DGGE. Therefore both possibilities were tested their the following experiments.

2.5.1 Testing DNA concentrations

At first in ordered to determine where the problem with the re-amplification of the DGGE extracts originated, different dilutions (undiluted, 1:5, 1:10, and 1:20) of the gelextract were used as DNA template in conjunction with the normal PCR cycling program, a touchdown PCR cycling program and a step up program. For the DGGE extraction the Qiagen Gel Extraction Kit (Qiagen, UK) was used. For all PCR reaction the bacteria primer set with the relevant PCR mixture was used.

The touchdown cycling program consisted of an initial denaturation step at 94°C for 5 min, 10 cycles with 94°C for 1 min, 1 min of decreasing the annealing temperature from 65°C to 55°C by 1°C per cycle and 94°c for 1 min. this was then followed by30 cycles with 94°C for 60 sec, 55°C for 60 sec, and 68°C for 60 sec. The final extension step occurred at 68°C for 10 min.

The step up cycling program an initial denaturation step at 94°C for 3 min, first 10 cycles with 94°C for 1 min, 1 min of increasing annealing temperature by 1°C per cycle starting from 45°C to 55°C and 68°C for 90 sec. Following this a second loop of 30 cycles with 94°C for 60 sec, 55°C for 60 sec, and 68°C for 60 sec. The final extension step occurred at 68°C for 10 min.

A gel-electrophoresis of the PCR products was run in a 1% agarose gel.

Results & Conclusion

Comparing the images of the gel-electrophoresis run as control before the DGGE with the images of the re-amplification products showed either no PCR product or a smear (Figure 2.5). These results could indicate that the DNA was partially or completely degraded during the extraction step.

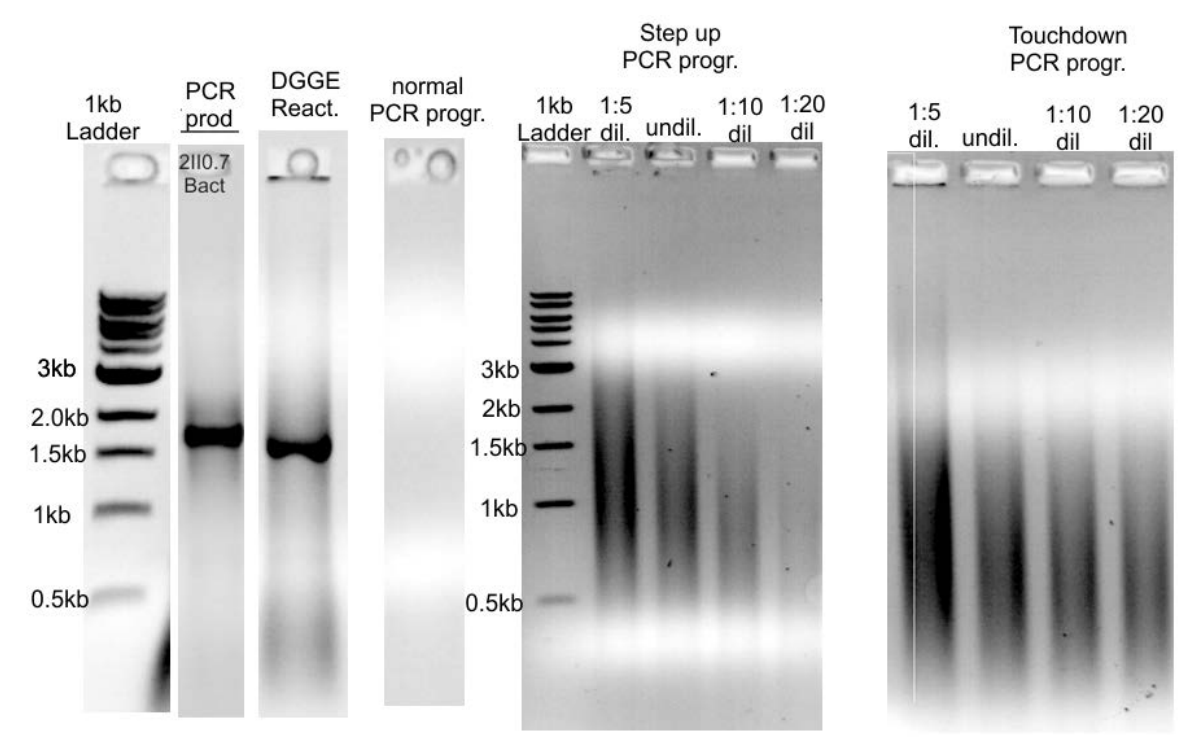


Figure 2.5: Comparison of gel-electrophoresis images of PCR products before DGGE and re-amplification products using different template dilutions in conjunction with the normal PCR cycling, step up, and touchdown cycling program

2.5.2 Test Gel extraction Methods

The next step to confirm that gel-extraction is degrading the DNA positive DGGE PCR products were run on DGGE reactions are run on a horizontal 8 % Acrylamide gel without gradient and bands (Arrows in Figure 2.6) were excised to be used for testing six different extraction techniques:

- A. The gel fragment is air dried for approx. 10 min and crushed using a pipette tip, than the fragments are re-suspended in 20 μ l water and incubated overnight at 4 $^{\circ}$ C.
- B. The gel fragment is briefly vortexed with glass beads and 50 μ l water, than the mixture is incubated at 37 $^{\circ}$ C for 30 min.
- C. The gel fragment is briefly vortexed with glass beads and 50 μ l water, than incubated at 4 $^{\circ}$ C overnight.
- D. Using the Gel extraction Kit, Qiagen UK according to the manufactures instruction
- E. The gel fragment is crushed, re-suspended in 30 μ l TE buffer and incubated at 4 $^{\circ}$ C overnight.
- F. Using the Gel Extraction Kit, Machery-Nagel, UK according to the manufactures instructions

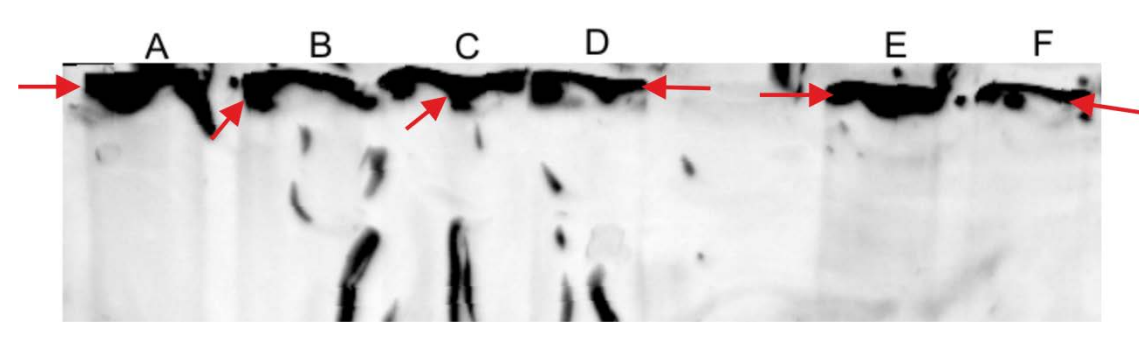


Figure 2.6: Horizontal 8 % acrylamide gel without denaturant gradient; marked bands were excised and used for testing different extraction methods

Each extract was used as DNA template in a PCR using bacterial primer set (Table 2.5: 27F, 1387R) with the appropriate PCR mixture.

Results & Conclusions

Gel-electrophoresis of the gel-extracts in a 1 % agarose gel revealed DNA of the relevant base pair size using technique A and B as described before (Figure 2.7), whereby technique A (air dried for approx. 10 min and crushed using a pipette tip, than the fragments are re-suspended in 20 μ l water and incubated overnight at 4 °C) appears to give a better overall result. No DNA could be detected for any of the other methods.

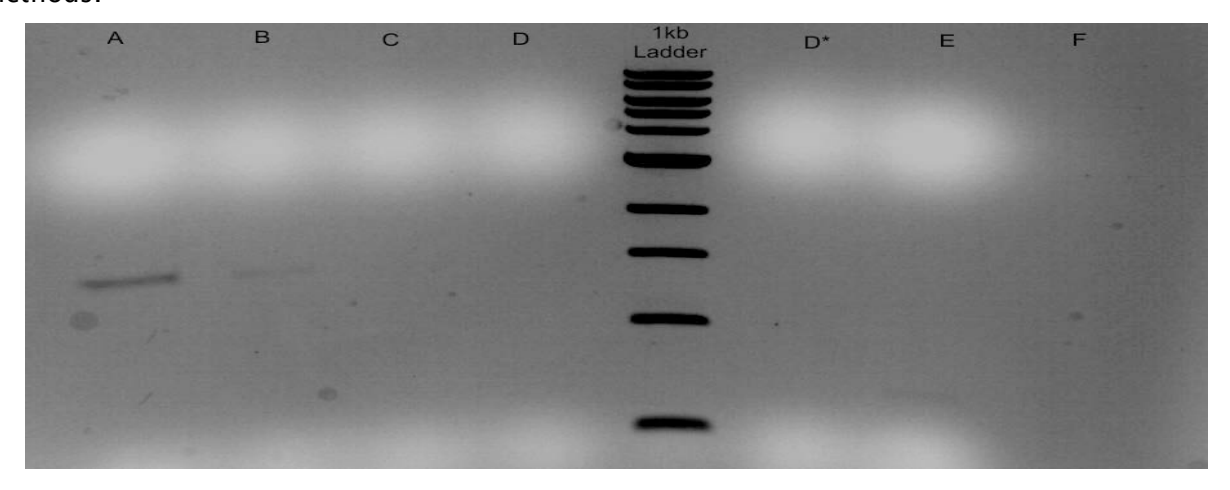


Figure 2.7: Gel-electrophoresis image of the gel-extracts run in a 1 % agarose gel; A: gel fragment is air dried for approx. 10 min and crushed using a pipette tip, than the fragments are re-suspended in 20 μl water and incubated overnight at 4 °C, B: gel fragment is briefly vortexed with glass beads and 50 μl water, than the mixture is incubated at 37 °C for 30 min, C.gel fragment is briefly vortexed with glass beads and 50 μl water, than incubated at 4 °C overnight, D Gel extraction Kit, Qiagen UK according to the manufactures instruction, E: gel fragment is crushed, re-suspended in 30 μl TE buffer and incubated at 4 °C overnight, :. Gel Extraction Kit, Machery-Nagel, UK according to the manufactures instructions

After re-amplification a smear could be detected for all extraction techniques except the last one, suggesting the presence of DNA where the smear occurred (Figure 2.8).

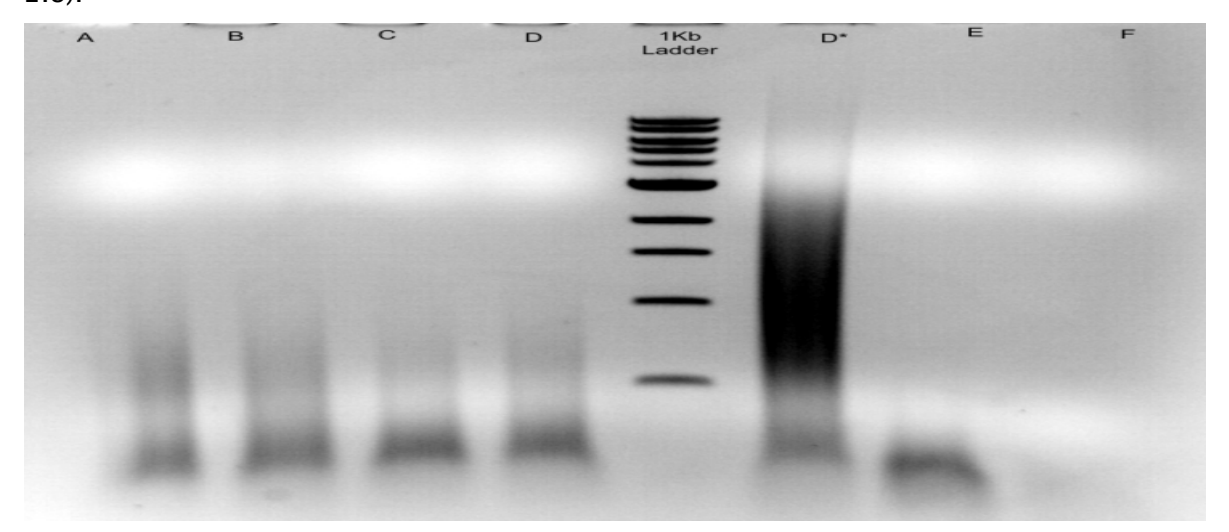


Figure 2.8: Gel-electrophoresis image of re-amplified gel-extracts from the different extraction techniques

This indicates that the extraction methods except F (Gel Extraction Kit, Machery-Nagel), which showed no re-amplification product, might not be the cause of the problem. Other possibilities might be interference of the GC clamp with the annealing of the forward primer during re-amplification or maybe the degradation of just the ends of the PCR product, destroying the primer binding site. This degeneration could be linked with the length of the PCR product as this re-amplification problem did not appear when using the Muyzer primer for DGGE, which result in a much shorter PCR product.

2.5.3 Gel-extraction and re-amplification using Pseudomonas fluorescens

Using nested primers for re-amplification of DGGE gel-extracts might be a solution to the problem. To test this assumption DNA extracts of *Pseudomonas fluorescens*, a biofilm forming spoilage forming bacterium (Sillankorva et al., 2008), were used for PCR using the universal bacterial primer set 27F and 1387R with the relevant conditions (see PCR section) and a primer set specific for *P. fluorescens* 16S rDNA region (Table 2.6). The PCR mixture for the specific primers contained contained 0.2 µM of each primer, 5 µl DNA extract, 1x Standard Buffer (New England Biolabs Inc., UK), each deoxynucleoside triphosphates with a concentration of 0.2 mM and 1U of DNA Taq polymerase (New England Biolabs Inc., UK) in a final volume of 25 µl. The PCR cycling consisted of an initial denaturation step at 94°C for 10 min, 30 cycles with 94°C

for 45 sec, 60°C for 30 sec, and 68°C for 90 sec. The final extension step occurred at 68°C for 10 min. The expected amplicon size is 240 base pair.

Table 2.6: Primer sequences for specific for *P. fluorescens* 16S rDNA (Tsaloglou et al 2012)

Forward primer	CAG CTC GTG TCG TGA GAT GT
Reverse primer	CGG AC TAC GAT CGG TTT TGT

First an aliquot of the PCR products were controlled by running a gelelectrophoresis in a 1% agarose gel (Figure 2.9). After confirming that the PCR worked the remaining PCR products were used for a gel-electrophoresis in 8 % acrylamide gel. The bands were excised and extracted by crushing the gel fragment, adding 100 μ l water, and incubating overnight at 4°C.

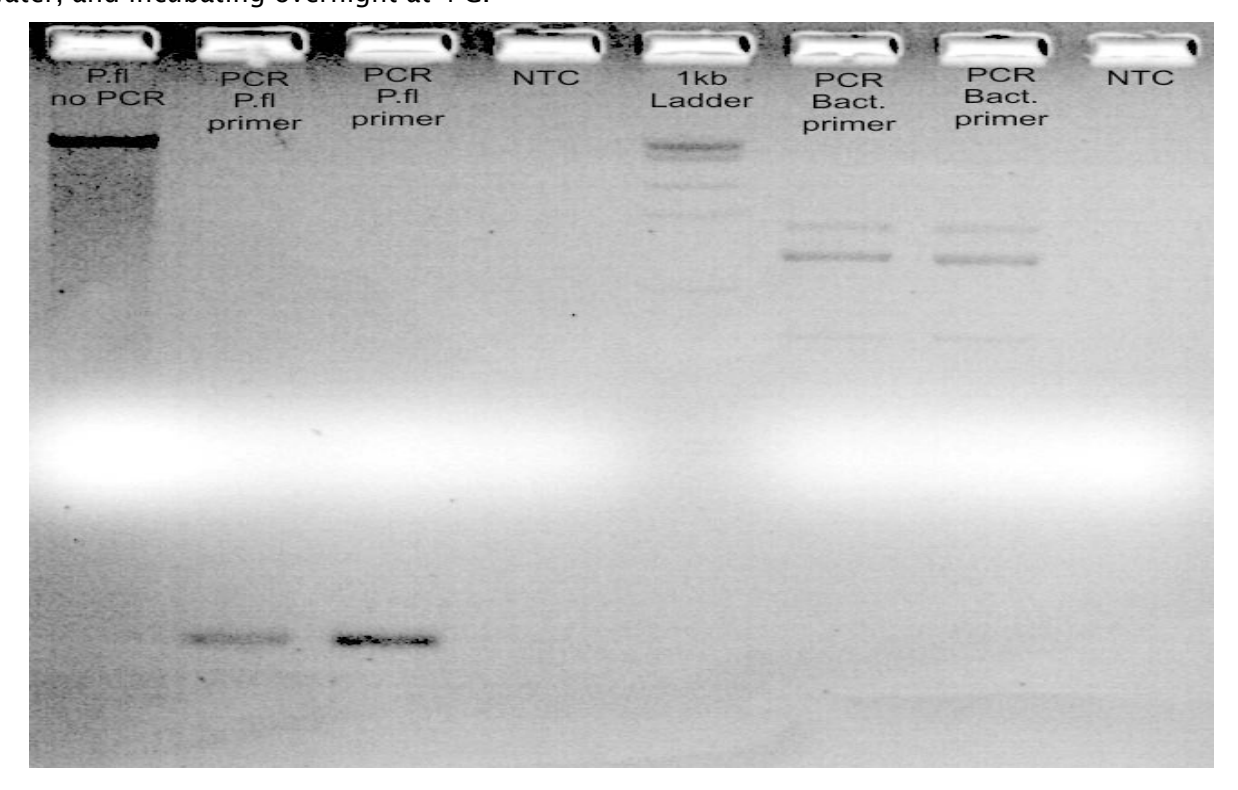


Figure 2.9: Gel-electrophoresis image of initial PCR products run a 1 % agarose gel

Results & Conclusion

Re-amplification was only successful when using *P. fluorescens* specific primers regardless if the gel-extract template was originally amplified using the specific or the universal primer set (Figure 2.9). In case of the template originally being amplified using the universal primers, the *P. fluorescens* primer set was nested inside the

Chapter 3: Method Development and Optimisation

original PCR product for the re-amplification reaction.

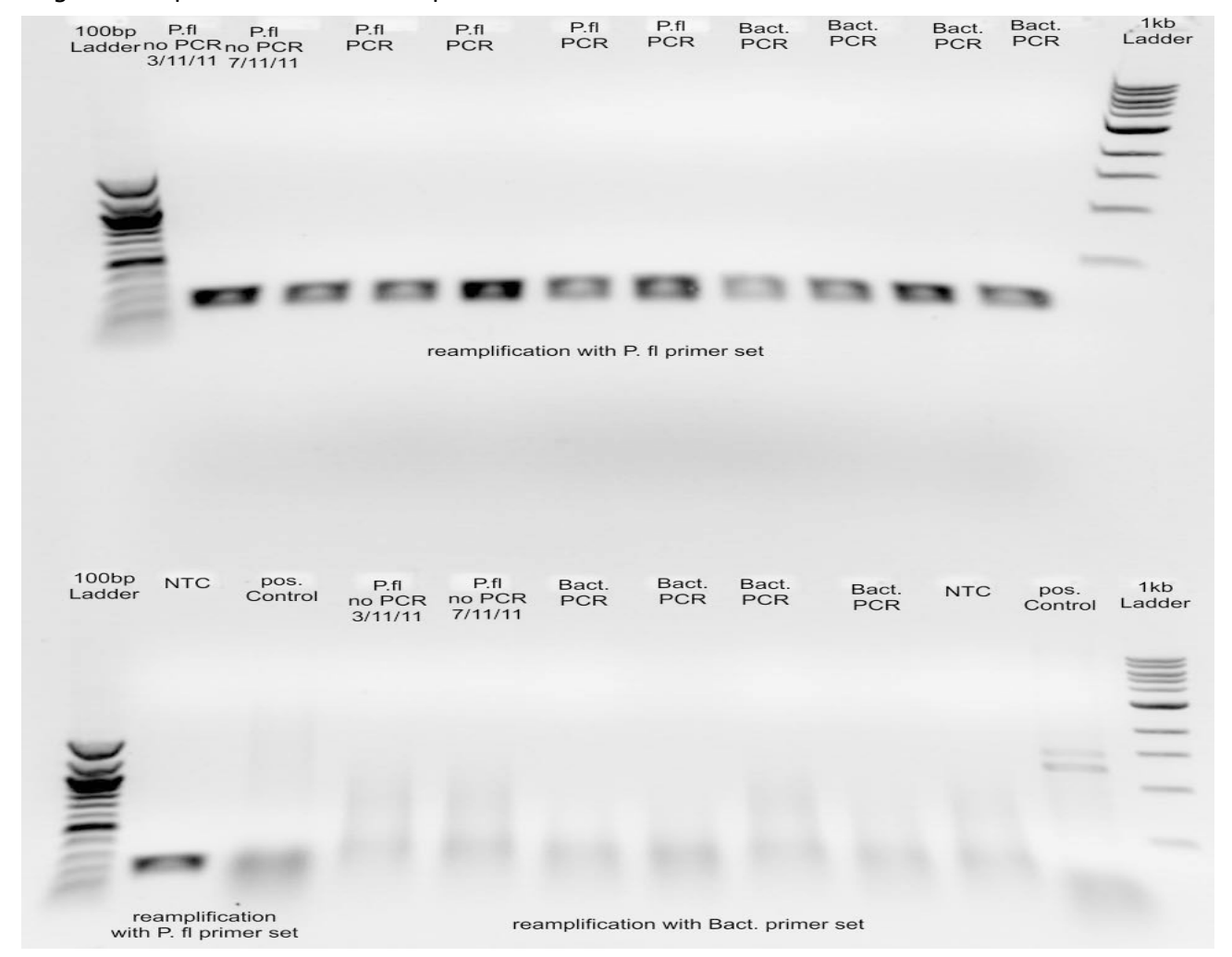


Figure 2.10: Re-amplification results after gel-extraction from 8% acrylamide gel; gelelectrophoresis run in a 1 % agarose gel

When sequenced the samples amplified with the *Pseudomonas fluorescens* specific primers came back a match for the 16S rDNA of *Pseudomonas sp.*, suggesting that the re-amplification problem might in fact be the destruction of the primer binding site in the original PCR product through the degeneration at its ends. Designing a set of nested primers for the kingdoms Archea and Eukarya (see Table 2.5: nA fwd, nA rev, nE fwd, nE rev) solved the sequencing problems, for Bacteria the Muyzer primer sets were used for DGGE and subsequent sequencing.

Chapter 3: Microbial Community Structure of the Mid-Cayman Ridge

3.1 Introduction

Knowledge of in situ microbial community structure both planktonic and sessile of any aquatic environment is an important aspect as the both are the source for any fouling occurring. During development of biofilms the release of cells into the environment and the associated change from surface associated to planktonic life style is vital for the dispersal and propagation of microbes. As such studying the planktonic and established natural biofilm communities can give an important insight into expected biofouling. Therefore both planktonic microbial community structure in regard to depth and biofilm found on natural substrate were examined in an attempt to find a correlation between both and the hyperbaric biofilms found on artificial substrates (Chapter 4).

In an oligotrophic environment such as the open ocean and the deep sea, most planktonic cells occur in a dormant state; these can resume an active physiological state and form biofilms with complex microbial communities on available surfaces in nutrient rich environments (Stoodley et al., 2002). This response to nutrient availability seems to exist in a similar pattern in nearly all ocean regions (Stoodley et al., 2002).

In addition to nutrient availability, Biofilm formation is influenced by a number of factors such as seawater chemistry, turbulence, temperature, light and biota in the water column (Marszalek et al., 1979). Schnetzer and collegues demonstrated that depth also has significant impact on the microbial community structure of plankton (Schnetzer et al., 2011).

During the cruise JC044 to the Mid-Cayman ridge samples were taken for characterisation of the microbial communities in the Cayman Trough and to examine a possible relationship between the planktonic and biofilm microbial community.

3.1.1 The Mid-Cayman Ridge

Geographically the Mid-Cayman rise, lies between two distinct vent biogeographic regions; the East Pacific Rise and the Mid-Atlantic Ridge (Figure 3.7).

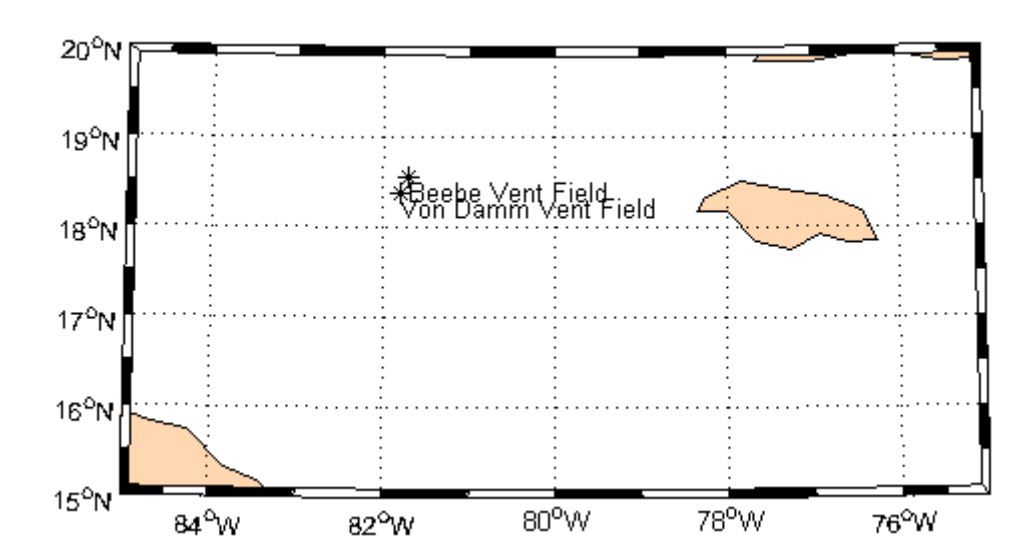


Figure 3.1: geographical positions of the Beebe Vent Field at a depth of 4,960 m, the deepest to date, and Von Damm vent field at a depth of 2,300 m

The East Pacific Rise vent communities are dominated by large tubeworms of the genus Riftia, whereas the Mid-Atlantic Ridge vent systems are dominated by shrimp species of the genera *Rimicaris* and *Chorocharis* (Van Dover, 2000, Van Dover, 1995, Gebruk et al., 1997, Tunnicliffe et al., 1998, Desbruyeres, 1985). These two biogeographic regions are now only connected through the Pacific-Atlantic and Indian Ocean ridge systems at high latitudes (Van Dover, 2002). A dispersal pathway may have existed between the East Pacific Rise-Galapagos rift system and the Mid-Atlantic Ridge though the Isthmus of Panama before its closure approximately 3.1 Ma ago (Van Dover, 2002, German, 2011).

During a cruise in April 2010 to the Mid-Cayman rise, the deepest hydrothermal vent field was discovered, the Beebe vent field at a depth of 4,930 m (Figure 3.1) (Connelly et al., 2012). At the macrofaunal level the vent was dominated by shrimps later to be identified as an alvinocaridia species within the Rimicaris Chorocaris-Opaepele clade, linking this site to the Mid-Atlantic Ridge biogeographic region (Nye et al., 2011).

It is also important to take the geological settings of the ridge system into account as they impact the spacing and longevity of the hydrothermal vents, influences the chemistry of the hydrothermal vent fluids, and the stability of these habitats directly (Van Dover, 2000). The Mid-Cayman ridge is a 110 km long, ultra-slow spreading centre, which is isolated from the continuous Mid-Ocean Ridge system (Connelly et al.,

2012). With depth of the spreading axis ranging from 4,200 m to over 6,000 m, it is the deepest seafloor spreading centre (ten Brink et al., 2002).

3.2 Methods and Materials

3.2.1 Sample Acquisitioning and Treatment

Planktonic microbial community

During CTD dives, including dives where tow-yo'ing the CTD was used to narrow in on hydrothermal vent site (Figure 3.2), seawater samples from different depths were taken using Niskin bottles. CTD's are instruments measuring conductivity, temperature and depth, which in this case were incorporated into a rosette of Niskin sampling bottles.

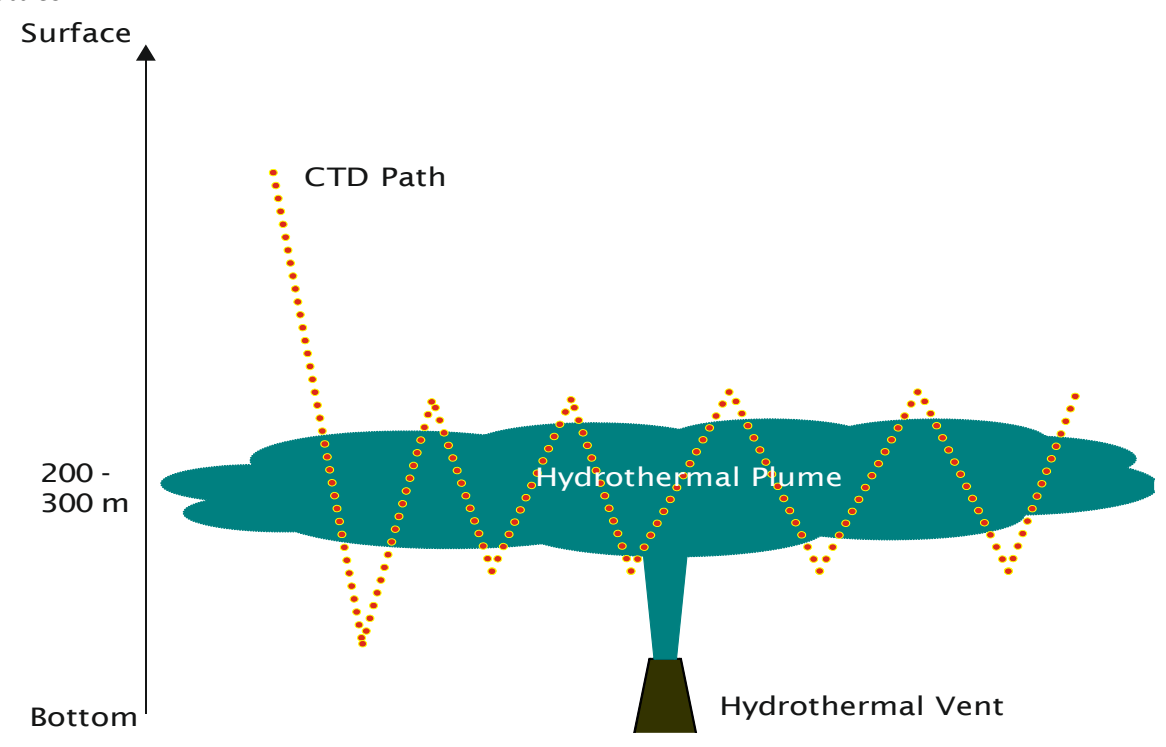


Figure 3.2: Diagram of tow-yo'ing CTD to locate hydrothermal vent sites; metre indication describes approximate height above the seafloor

To analyse the planktonic microbial community approximately 50 I were filtered using glass microfiber filters with 3 µm and 0.7µm pore size in sequence (Whatman GF/D, Ø 47 mm) in conjunction with flow rate of 10 on the Masterflex I/P easyload filtration system (Millipore). The filters were stored at -80°C and later used for DNA extraction. Genomic DNA was extracted from halved filters using the DNeasy Kit Blood & Tissue (Qiagen) according to the manufacturer's tissue protocol with extended cell

lysis incubation overnight. The DNA concentrations were quantified using Pico Green assay. Extracted DNA was used for DGGE as describe before using the primer sets for bacteria (Table 2.5) (Muyzer et al., 1993, Muyzer et al., 1995) and Crenarcheaota (Ochsenreiter et al., 2003).

Natural Biofilm community at hydrothermal vent sites in the Cayman Trough
We collected natural biofilm samples from an old hydrothermal vent chimney
(Figure 3.3) and debris material recovered from Beebe vent field at a depth of
approximately 4962m at the Mid-Cayman Rise (Connelly et al., 2012).



Figure 3.3: Image of the old hydrothermal vent chimney from the Beebe vent field at a depth of 4,960 m used for sampling natural biofilm

Sampling occurred while the piece of chimney was still being held by the grab of the Remote Operated Vehicle (ROV) HYBIS to minimize contamination. Microbial filaments could be seen with the naked eye on the chimney and were targeted for sampling using sterile swabs. Genomic DNA was extracted on board the ship using the DNeasy Kit (Qiagen) according to the manufacturer's tissue protocol. The acquired pure DNA extract was divided into aliquots and stored both at 4°C and at -80°C. The DNA concentrations were quantified later in the laboratory using Pico Green assay.

3.2.2 DGGE

The biofilm samples were amplified using a universal primer set specific for 16S DNA of bacteria (Table 2.5 27F; 1387R) (Dang and Lovell, 2000), and specific 16S primers for archea (Table 2.5: A751F; UA1406R) (Baker et al., 2003) with the relevant conditions (see 2.4.4).

Positive products of these reactions were re-amplified using with a CG clamp (CGC CCG CGC GCG CGG GGG CGG GGG CAC GGG GG) modified forward primer and run on a DGGE

3.2.3 Sequencing

Both planktonic and biofilm DGGE DNA fragments were extracted, re-amplified and cleaned up (Qiaquick PCR clean up kit,Qiagen, UK), sent for sequencing and the results were checked using the online alignment software as describe before.

Using the Molecular Evolutionary Genetics Analysis (MEGA5) software version 5, a phylogenetic tree was generated from the closest matches (Tamura et al., 2011). Using the Minimum Evolution (ME) method to find the optimal tree (Rzhetsky and Nei, 1992) and the Maximum Composite Likelihood (MCL) method to compute the evolutionary distances (Tamura et al., 2004). The ME tree was searched using the Close-Neighbor-Interchange (CNI) algorithm (Nei and Kumar, 2000) at a search level of 0. The Neighbor-joining algorithm (Saitou and Nei, 1987) was used to generate the initial tree. All gaps and missing data in the sequences were eliminated for the computation of the evolutionary history.

In order to identify similarities between sequencing results of bands extracted from the DGGE (Figure 3.4A, Figure 3.5A, Figure 3.6A), the 'expect' value was less than 1 to ensure the exclusion of random matches.

3.3 Results & Discussion

3.3.1 Planktonic DNA concentrations in various depths at the Mid Cayman Rise

The DNA concentration of the extracted filters were generally lower for the 3 µm pore size except for the samples from the background sample at 4000 m and the sample above the hydrothermal plume at 3500 m (Table 3.1). A lower DNA concentration for the 3 µm pore size filter was expected as most bacteria sizes are no larger than 1 µm would be able to pass through these and get caught in the second filter with the 0.7 µm pore size. The unexpected higher DNA concentrations (160.39 ng/µl and 243.66 ng/µl) could be due to marine snow particles, up to several µm size (Azam and Long, 2001), being accidently captured in the collected water samples. Considering just the DNA concentrations of the 0.7µm pore size filters from the background samples, the highest concentrations were found at the lowest depth, 2000 m and the lowest DNA concentrations at the deepest depth of 4550 m (Table 3.1). This aspect reflects the food-limiting character of the non-chemosynthetic deepsea environment as the DNA concentration is linked to the abundance of microorganisms (Van Dover, 2002, Lalli and Parsons, 1997c).

Table 3.1: DNA concentration of filter extracts; direct measurement without re-

Sample ID	DNA	Source
	concentration	
	[ng/µl]*	
depth 4550 m; filtersize 3 µm	22.76	
depth 4550 m; filtersize 0.7 µm	90.00	
depth 4000 m; filtersize 3 µm	160.39	Background sample; position:
depth 4000 m; filtersize 0.7 µm	100.24	17°54.998N 81°46.001W
depth 2000 m; filtersize 3 µm	28.30	
depth 2000 m; filtersize 0.7um	217.11	
depth 4090 m; filtersize 3 µm	18.34	inside hydrothermal plume;
depth 4090 m; filtersize 0.7 µm	99.62	position: 18°32.996N
		81°43.351W
depth 3500 m; filtersize 3 µm	248.66	above hydrothermal plume;
depth 3500 m; filtersize 0.7 µm	57.31	position: 18°32.996N
		81°43.351W

Microbial Community

PCR and DGGE

No PCR amplification could be deteced from sample from inside the hydrothermal plume taken with the filter pore size 3 μ m. This could be due to interference of chemical interference of the PCR reaction of the filter residue from the hydrothermal plume (Thornton and Passen, 2004).

Results of the DGGE of the background seawater samples using the Muyzer primer set show between two and five bands (Figure 3.4A: L1-L5) with only two bands detected in the samples from the 3 µm pore size filters. Most bands were detected at 4000 m depth indicating a higher biodiversity than at 2000 m. No bands could be detected from the 3 µm pore size samples above the hydrothermal plume. The samples from inside and above the hydrothermal plume show seven to nine bands and a very similar band pattern (Figure 3.4A: L6 & L8). The higher number of bands indicate a higher biodiversity in and above the plume than in the background samples. The weaker appearance of the bands in the sample from inside the plume might again be a result of interferance of chemicals from the plume with the PCR reactions.

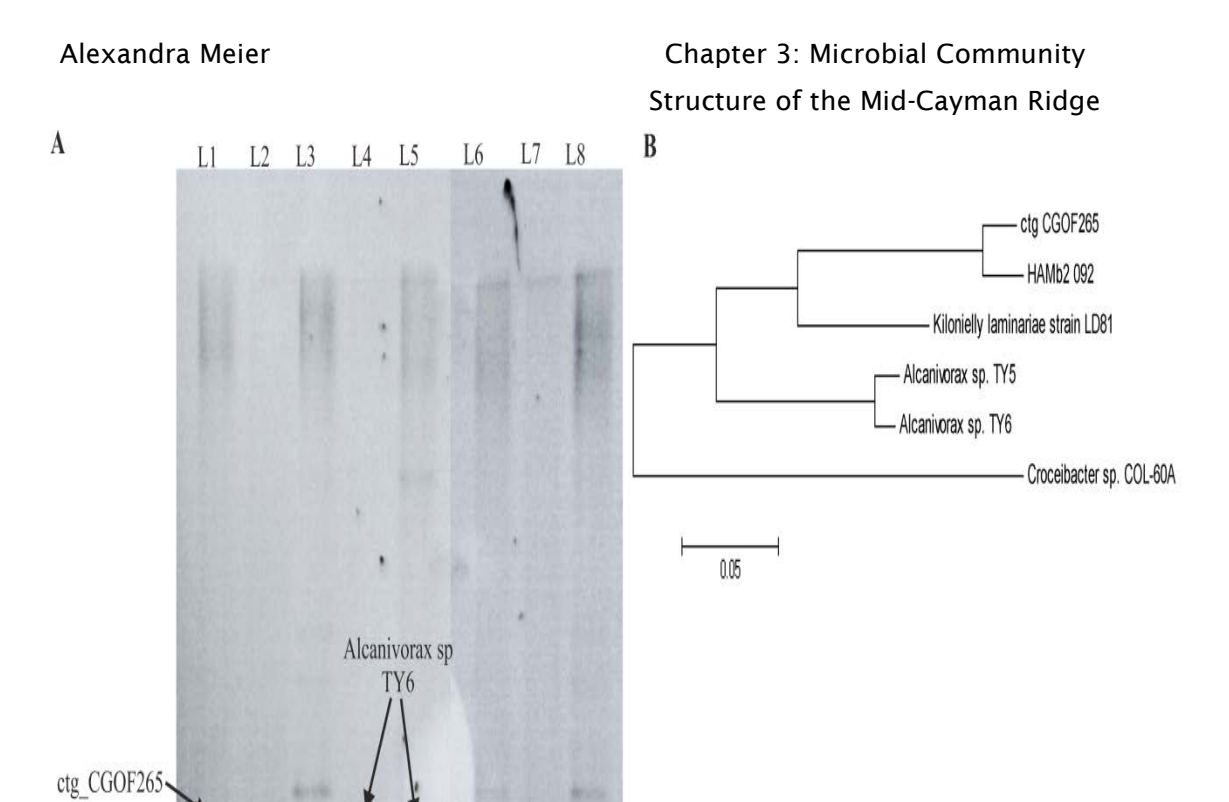


Figure 3.4: Analysis of DNA extracts from seawater filtrates using Muyer primer set; (A) Image of DGGE gel for extracted DNA from seawater filtrates collected at different depths using Muyzer primer set for amplification; (L1) Background sample collection depth 4550 m; filter pore size 0.7 μm; (L2) Background sample collection depth 4000 m; filter pore size 3 μm; (L3) as L2 except filter pore size 0.7 μm; (L4) Background sample collection depth 2000 m; filter pore size 3 μm; (L5) as L4 except filter pore size 0.7 μm; (L6) sample collected inside the hydrothermal plume at a depth 4090 m; filter pore size 0.7 μm; (L7) sample collected above hydrothermal plume at a depth of 3500 m; filter pore size 3 μm; (L8) as L7 except filter pore size 0.7 μm; arrows point to the extracted and sequenced bands with the aliment match found in the online aliment software BLAST; (B) (B) Phylogenetic tree of the 16S DNA sequences from the Mid Cayman Rise and their closest matches alignment matches Table 3.3

Alcanivorax sp

HAMb2 092

Croveibacter sp.

COL-60A

Kilomiella, laminareae

DGGE using Crenarchaeota primer set show even less biodiversity than the Muyzer primer set, with only two and three bands in the background samples and five bands in the samples from inside and above the hydrothermal plume (Figure 3.5A). Plume samples show the same band pattern indicating the same community structure.

The different band patterns seen in the background samples between 2000 m and 4000 m depth using the DGGE with Muyzer primer are in agreement with observations

of Schnetzer and colleagues (2011) that dominant protistan taxa within an assemblage can differ significantly over spatial scales (Schnetzer et al., 2011).

A common community structure pattern of a "rare biosphere" is either characterized by small biodiversity with a large abundance or a large number of taxa in low abundance, (Amaral-Zettler et al., 2009, Caron and Countway, 2009, Sogin et al., 2006, Schnetzer et al., 2011). In this case both bacterial and crenarchean community show a low biodiversity.

Identical position of bands might indicate identical sequences in the fragments, as confirmed by some sequencing results e.g.: Alcanivorax sp. TY5, Alcanivorax sp. TY6 (Figure 3.4A) or JR224_E9_IV-C4 (Figure 3.5A), but not necessarily as separation is a function of the DNA melting behaviour (Muyzer et al., 1993). This can be seen in some of the sequencing results (Figure 3.4A, Figure 3.5A).

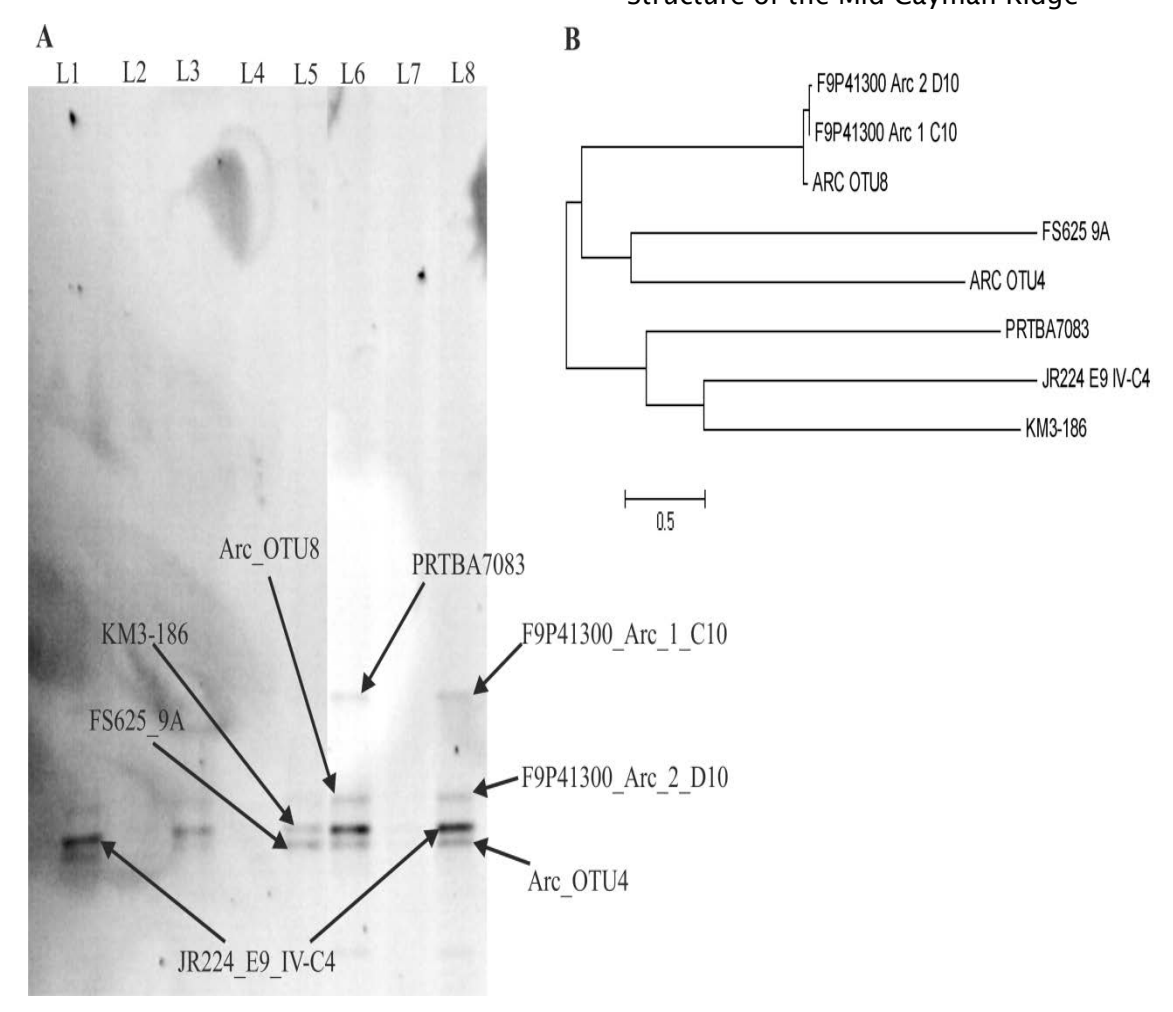


Figure 3.5: DNA extracts using Crenarcheota primer set; (A) Image of DGGE gel for extracted DNA from seawater filtrates collected at different depths using Crenarcheota primer set for amplification; (L1) Background sample collection depth 4550 m; filter pore size 0.7 μm; (L2) Background sample collection depth 4000 m; filter pore size 3 μm; (L3) as L2 except filter pore size 0.7 μm; (L4) Background sample collection depth 2000 m; filter pore size 3 μm; (L5) as L4 except filter pore size 0.7 μm; (L6) sample collected inside the hydrothermal plume at a depth 4090 m; filter pre size 0.7 μm; (L7) sample collected above hydrothermal plume at a depth of 3500 m; filter pore size 3 μm; (L8) as L7 except filter pore size 0.7 μm; arrows point to the extracted and sequenced bands with the aliment match found in the online aliment software BLAST (B) Phylogenetic tree of the 16S DNA sequences from the Mid Cayman Rise and their closest matches alignment matches of Table 3.3

Sequencing

Regarding sequencing results all represented alignment matches were between 97% and 100 %. Most of the found alignment matches found are from uncultured organisms (Table 3.2).

Table 3.2: 16S rDNA sequence similarities to closest alignment match of extracted DGGE bands from seawater filtration

Closest alignment match	Accession number	% Identity	Expect value	Source
Uncultured organism clone ctg_CGOF265	DQ395696	99	4e-80	environmental sample; deep-sea octacoral
Uncultured bacterium clone HAMb2_092	JX984078	100	7e-53	biofilm developed from HAM lagoon water, Magdalen Islands; biofilm sampled after 2 weeks incubation
Kiloniella laminariae strain LD81	NR_042646	97	3e-40	marine macro-alga Laminaria saccharina
Alcanivorax sp. TY5	JX467656	99 98	2e-93 5e-91	Gulf of Mexico
Croceibacter sp. COL- 60A	HQ534336	99	3e-91	Antarctic seawater
Alcanivorax sp. TY6	JX467657	99	2e-93, 4e-92	Gulf of Mexico
Uncultured prokaryote clone JR224_E9_IV-C4	JN562672	100	1e-92, 6e-95	deep-sea hydrothermal vent in the southern ocean
Uncultured crenarchaeote clone KM3-186	EF597693	99	7e-84	3010m depth from Ionian Km3 Station in the Mediterranean Sea
Uncultured archaeon clone FS625_9A	HQ636101	98	2e-90	deep-sea hydrothermal vent Endeavour Segment, Easter Island Vent, depth 2198 meters
Uncultured marine archaeon clone F9P41300_Arc_2_D10	JQ222354	99	9e-83	ocean water marine sample, Northeast subarctic Pacific Ocean, Station P4, 1400m depth
Uncultured marine group I crenarchaeote clone PRTBA7083	HM799679	99	3e-93	ocean water collected from 6,000m depth within the Puerto Rico Trench
Uncultured archaeon clone Arc_OTU4	JX262880	100	3e-55	seawater adjacent to the Southwest Indian Ocean Ridge
Uncultured archaeon clone Arc_OTU8	JX262881	100	4e-92	seawater adjacent to the Southwest Indian Ocean Ridge
Uncultured marine archaeon clone F9P41300_Arc_1_C10	JQ222261	100	2e-85	ocean water marine sample, Northeast subarctic Pacific Ocean, Station P4, 1400m depth

For surface associated microorganisms we found a 97% identity match to the α -proteobacterium *Kiloniella laminariae* strain LD 81 isolated from a macro-algae (Wiese et al., 2009), a 100% match to the uncultured bacterium clone HAMb2_092 isolated from a biofilm grown in the Southern part of the Gulf of Lawrence, Canada (Toupoint et

al., 2012), and a 99% match to an uncultured organisms clone ctg_CGOF265 found on a deep-sea octacoral (Penn et al, unpublished). All these sequences matches were found in background water samples taken at a depth of 4550 m (Figure 3.4A, Figure 3.5A). All of the other alignment match sources were seawater samples.

The sequence matches found from inside the hydrothermal plume sample PTRBA7083, 99% identity match, was first from seawater collected at 6000 m in the Puerto-Rico Trench ((Eloe et al., 2011) and 100% match to Arc_OTU8, found in the proximity of the Southwest Indian Ocean Ridge (He and Li, unpublished).

Above the hydrothermal plume a 99% and 100% identity match to uncultured archean clones F9P4300_Arc_1_ C10 and F9P41300_ Arc2_D10 respectively was found. The source for these two sequences was the Northeast subarctic Pacific at a depth of 1400 m (Wright and Hallam, unpublished). Also a 99% and 100% match to Alcanivorax sp. TY5 and the uncultured prokaryote clone JR224_E9_IV-C4 respectively was found. Alcanivorax sp. TY5 sequence was first found in a deep-sea oil plume in the Gulf of Mexico during the Deepwater Horizon oil spill (Yang et al, unpublished) and JR224_E9_IV-C4 at a deep-sea hydrothermal vent in the Southern Ocean (Rogers et al., 2012). Sequencing matches for these two were also found in the background samples at 4000 m (Figure 3.4A) and 4550 m (figure 3.5A), indicating a more widespread depth distribution. In the background water sample of 400 m depth an 99% match was found to the Flavobacterium Croceibacter sp. Col-60A, originally isolated form Antarctic costal seawater (Lo Giudice et al., 2012). At 2000 m depth sequence matches of 98% and 99% were found to uncultured archean clone FS625_9A, original source deep-sea hydrothermal vent Endeavor segment, Easter Island vent at a depth of 2198 m (Huber et al, unpublished), and uncultured crenarchaeote clone KM3-186, isolated from seawater collected at 3010 m depth in the Mediterranean (Martin-Cuadrado et al., 2007).

Finding species at a lower or higher depth the original sources, F9P4300_Arc_1_ C10 and F9P41300_ Arc2_D10 for example originally found at 1400 m in subarctic and now at 3500 m in tropical waters, or KM3-186 originally found at 3010 m in the Mediterranean sea and now at 2000 m in the Caribbean sea, could indicate a wider geographical distribution than previously known.

3.3.2 Microbial Hydrothermal Vent Community of the Mid-Cayman Rise

DGGE

DGGE results of the natural biofilm samples showed between five and seven distinctly separated bands in our samples (Figure 3.6A), indicating low community diversity.

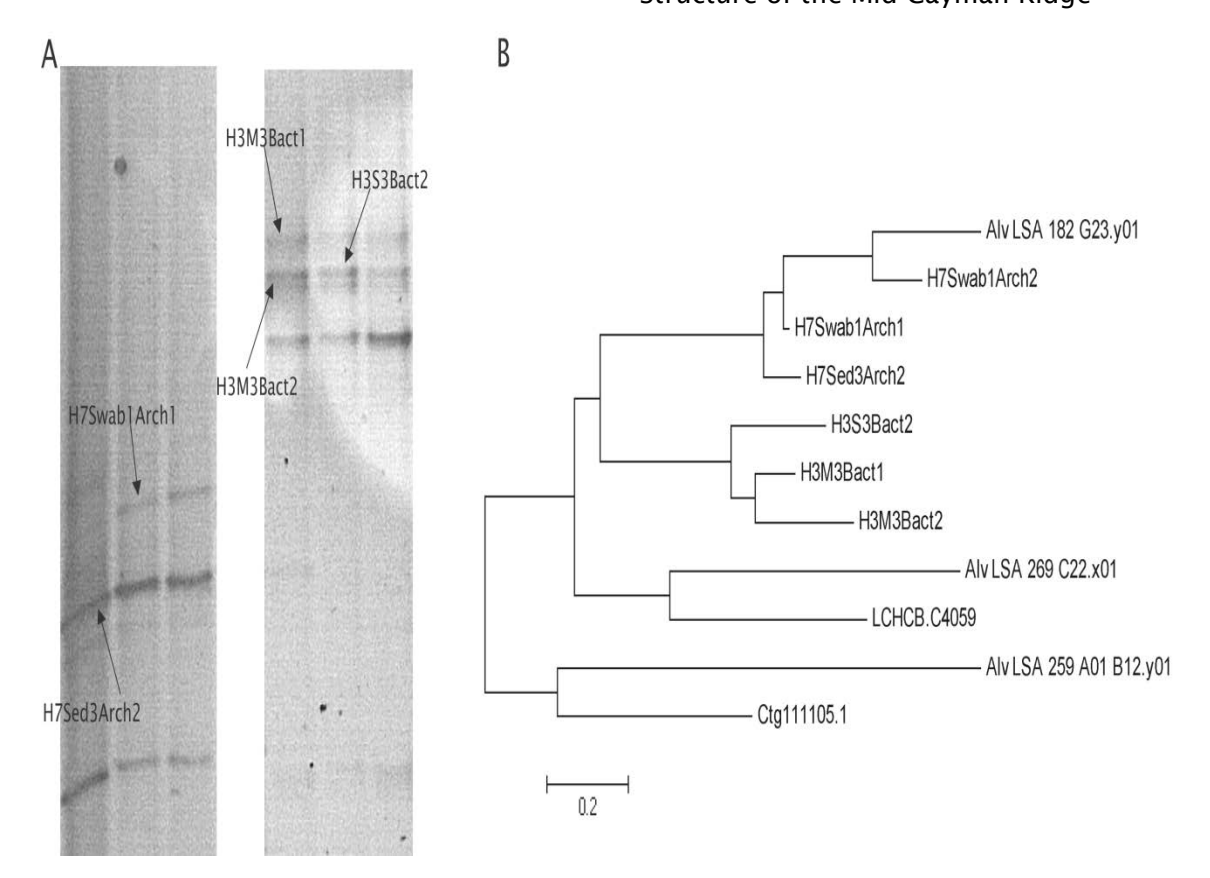


Figure 3.6: Analysis of DNA extracts from natural biofilm samples (A) images of DGGE gel of 16S DNA specific fragments the right DGGE image the bacterial primer set was used and the Archea specific on the left; arrows point to extracted and sequenced bands (B) Phylogenetic tree of the 16S DNA sequences from the Mid Cayman Rise and their closest matches alignment matches.

These findings are in agreement with the observations of Muyzers and colleagues (1993) of between five and ten different bands in biofilm populations isolated from bacterial mats in Wadden Sea sediments and waste water treatment plants (Muyzer et al., 1993). The low community diversity in our samples, in connection with the findings of one phylotype of epsilon-proteobacteria dominating a hydrothermal vent site at the Mid-Atlantic Rigde by Polz and Cavanaugh (1995) (Polz and Cavanaugh, 1995) and a low organism diversity of Lost City biofilms by Brazelton and Baross (2009) (Brazelton, 2009) supports the hypothesis of the microbial community of hydrothermal vents being characterized by low diversities compared to other less extreme habitats (Van Dover, 2000, Tunnicliffe et al., 1998).

Sequencing

As for the planktonic samples all identity similarities of the sequencing results from the DGGE extracted DNA bands (Figure 3.6), presented had an 'expect' value of less than 1 to ensure the exclusion of random matches (Table 3.3).

Table 3.3: 16S rDNA sequence similarities to closest alignment match of extracted DGGE bands from the Beebe Vent Field

Closest alignment	Accession	%	Expect	Carrier
match	number	Identity	value	Source
Epibiont metagenome	AAUQ010	84%	4e-06	Bio9 vent, 9-N
Alv_LSA_182_G23.y01	53748			hydrothermal vent field,
				East Pacific Rise
Epibiont metagenome	AAUQ011	88%	7e-10	Bio9 vent, 9-N
Ctg11105.1	00930			hydrothermal vent field,
				East Pacific Rise
Epibiont metagenome	AAUQ010	86%	0.70	Bio9 vent, 9-N
Alv_LSA_269_C22.x01	18274			hydrothermal vent field,
				East Pacific Rise
Hydrothermal vent	ACQI0100	86%	0.70	Lost City Vent Field, Mid-
metagenome	4059			Atlantic Ridge system
LCHCB.C4059				
Epibiont metagenome	AAUQ011	93%	0.86	Bio9 vent, 9-N
Alv_LSA_259_A01_B12.y	28726			hydrothermal vent field,
01				East Pacific Rise

We found 86% identity similarity in the sequences of the samples from the Beebe vent field to the hydrothermal vent metagenome LCHCB.C4059 (Table 3.3), isolated from carbonate chimneys at the Lost City Hydrothermal Field on the Mid-Atlantic Ridge (Brazelton, 2009). These findings support the theory of a possible link between the Mid-Cayman Rise hydrothermal vent site to the biogeographic province of the Mid-Atlantic Ridge. At the hydrothermal vents of the Mid-Atlantic Ridge system filamentous bacteria have been reported with one specific phylotype of the epibiontic bacteria being associated with the alvinocaridid shrimp, *Rimicaris exoculata*. These epibiontic bacteria were also found to be the dominant component of the remaining surface associated microbial community at these sites (Polz and Cavanaugh, 1995).

We also discovered from the same Mid-Cayman vent field between 84% to 93% identity similarity to four different epibiont metagenome sequences, Alv_LSA_182_G23.y01, Ctg11105.1, Alv_LSA_269_C22.x01, and Alv_LSA_259_A01_B12.y01, (Table 3.3). All metagenome sequences were isolated from

the Bio9 vent at the 9-N hydrothermal vent field on the East Pacific Rise (Grzymski, 2008). These epibiont metagenome sequences are associated with *Alvinella pompejana*, characterised by a filamentous microflora on its back (Desbruyeres, 1985). This polychaete species and its filamentous epibionts are endemic to vents 21 °N to 33 °S on the East Pacific Rise (Hurtado et al., 2004). These relationships indicate a possible link of at least part of the Mid-Cayman Rise vent fauna to the East Pacific Rise biogeographic region.

The filamentous epibionts found on the alvinellid polychaetes, *Alvinella pompejana*, at East Pacific Rise hydrothermal vents and on the alvinocaridid shrimp, *Rimicaris exoculata* at the Mid-Atlantic Ridge belong to the epsilon subdivision of the Proteobacteria (Polz and Cavanaugh, 1995, Haddad et al., 1995).

From the sequence results and the closest matches a phylogenetic tree (Figure 3.6B) was generated using the Molecular Evolutionary Genetics Analysis software version 5 (MEGA5) (Tamura et al., 2011). In this tree all samples from the Mid Cayman Rise (labelled H3 and H7) cluster close together and show the closest relationship to Alv_LSA_182_G23.y01, for which the BLAST found an 84% identity match (Table 3.3). The second and third closest relations were Alv_LSA_269_C22.x01 and LCHCB.C4059. The highest identity match Alv_LSA_259_A01_B12.y01 with 93% was less closely related. This mismatch between the relationships indicated by BLAST and the MEGA5 software is most likely a result of the elimination of gaps and missing data when MEGA5 is computing the evolutionary history. It might also be influenced by the relative low percentage of the identity matches. The low percentage matches might be due to not using nested primers for the re-amplification of the extracted DGGE bands before sequencing. Despite this both analyses showed a relationship of the biofilm organisms found at the Mid Cayman Rise to microbes sampled at vent sites on the Mid-Atlantic Ridge and the East Pacific Rise.

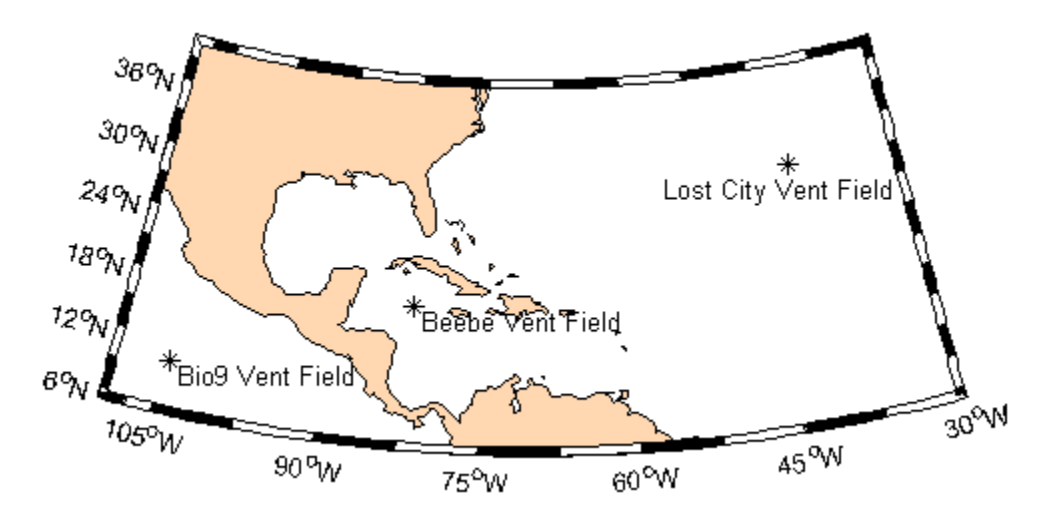


Figure 3.7: Overview of geographical positions of sample site and sources of closest found alignment match; the vent fields of the closest alignment matches are located in two

different biogeographic regions, on the East Pacific Rise, Bio9 Vent of the 9N vent field, and the Lost City Vent Field on the Mid-Atlantic Ridge system

A genetic relationship between microbes of a biofilm community and epibionts has been shown as a single bacterial epibiontic phylotype isolated from the surface of *Rimicaris exoculata* was found not to be restricted to their host surfaces. But this specific strain was also found being a major constituent of the free-living microbial community (Polz and Cavanaugh, 1995). Also single symbiont strains are not necessarily restricted to a single host, in such cases they can be generally found over a wide range of hosts (Van Dover, 2000). Grzymski and colleagues (Grzymski, 2008) found genetic characteristics in epibionts similar to pathogens and biofilm microorganisms that facilitate their success. It is hypothesized that mobile DNA, a segment of DNA able to move between sites within or even between other DNA molecules, might possess an important role in the microbial evolution and the adaption to extreme environment of vent ecosystems (Grzymski, 2008). This mechanism would increase the likelihood of a gene flow between different epibionts and other surface associated micro-organisms.

Chapter 4: Development of biofilms on artificial surfaces

4.1 General Introduction

In marine environments all surfaces, natural and artificial, are subject to fouling from organisms ranging from Bacteria, algae, and Protozoans to metazoan larvae (Cowling et al., 2000).

Environmental factors like nutrient availability as well as biological, physical and chemical stress play an important role on the development of biofilms after the initial attachment (Bar-Or, 1990). Therefore first the biofouling found on a seaglider deployed in the North-Atlantic for 110 days is examined before the biofilm formation on a variety of artificial, 'off-the-shelf' materials deployed on moorings in the Cayman Trough at a depth of approximately 4700 m is examined.

4.2 Biofouling on Seaglider after 110 day deployment in the North Atlantic

During this project the opportunity arose to acquire biofouling samples form a deployed seaglider as real life example of the problem.

Seagliders are autonomous underwater vehicles that were developed as instrument platforms to expand monitoring of ocean processes (Eriksen et al., 2001). In recent years gliders have been used in a number of applications such as the study of physical oceanographic parameters (Hatun et al., 2007, Janzen and Creed, 2011) and biological parameters such as phytoplankton and algal blooms (Frajka-Williams et al., 2009, Perry et al., 2008). Because they are designed for long-term deployment, up to several months, and can cover distances of several thousand kilometres, the need of antifouling strategies is essential as can be clearly seen in Figure 4.1.

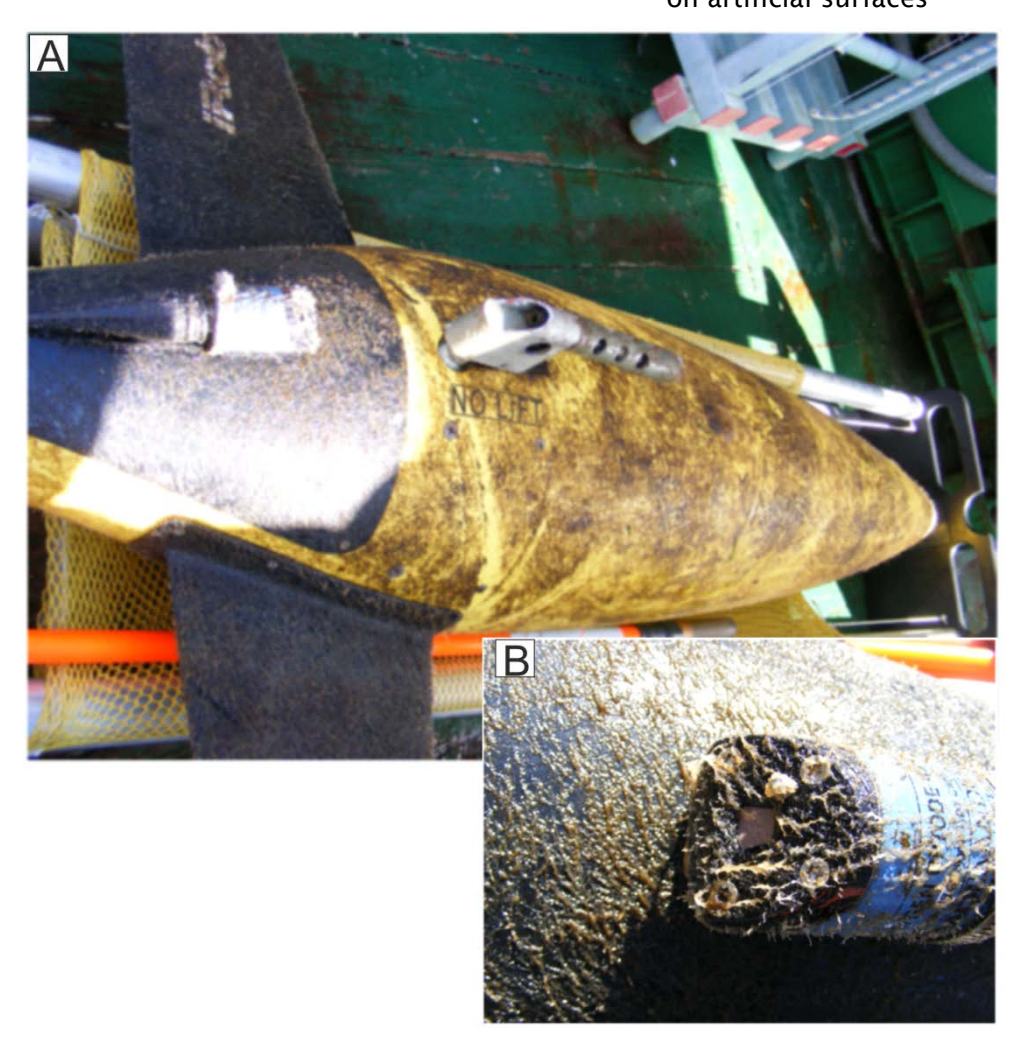


Figure 4.1: Photographs of the seaglider on recovery after 110 day deployment in the North Atlantic

4.2.1 Methods and material

Sample Acquisition

Samples were collected by Chris Brown from a seaglider of the East Anglia University that was deployed for \sim 110 days in the North Atlantic and 1411 dives.

Samples #1 and #2 were from two `No Lift´ stickers, Sample #3 a growth that could be peeled off with some tweezers and sample #4 the plastic covering plate of the optode sensor. These samples were treated the same way as the samples from the cruise. For DNA analysis the sensor face of the seaglider was scrubbed with a brush labelled sample #5.

Microscopic Analysis

For microscopic analysis with the EVOSfl (AMG, USA) the remaining sample were stained with SYTO®9. Images of the SYTO®9 stained samples were taken with three different fluorescent filters: GFP for SYTO®9 fluorescence (excitation 470 nm,

emission 525 nm; green colour), RFP (excitation 530 nm, emission 593 nm; red colour), and DAPI (excitation 360 nm, emission 447 nm; blue colour), and a 4x magnification. The images were overlaid using the inbuilt microscope software. The samples were also examined using a Laser Scanning Confocal Microscope (LSM 700, Zeiss).

Molecular Analysis

Filaments from the brush were removed in the lab and DNA extracted using DNeasy Kit and the Tissue protocol from Qiagen. Three small pieces of each of the stickers and the peeled off growth were cut off using sterile scissors and three swabs of the edge of the sensor cover, where it would not interfere with the microscopy, were taken and used for DNA extraction. The DNA extracts were amplified via PCR and DGGE run using the Muyzer primer asset according to the parameters. Afterwards the most prominent bands were extracted, re-amplified, sequenced, and identified as describe before in Chapter 2.

4.2.2 Results and Discussion

Microscopic Analysis

After recovery the seaglider was covered by a significant amount of macro-fouling. In these images most structures were fluorescent in all filters, indicated by the red and yellow colouration in the composites. The auto-fluorescence in the red filter is most likely a result of the presence of photosynthetic pigments like phycoerythrocyanin which has fluorescence emissions at 575 nm and 595 nm (Saga and Tamiaki, 2004).

On the peeled of growth (Figure 4.2C) green fluorescent features, probably of the staining, can be seen that seem to lie on top of the growth. This could indicate the presence of a bacterial biofilm growing on the other organism. Small filaments that also fluoresce only green can be seen on the sensor cover (Figure 4.2D). In both cases the green coloration in the overlaid images shows there is no chlorophyll present, which means these are not algae. In Figure 4.2D a polyp can be clearly distinguished (red arrow). Polyps are the sessile part of the two stage reproduction cycle of Cnidaria (Wintzer et al., 2011, Fernandez-Leborans and Gabilondo, 2005).

Chapter 4: Development of biofilms on artificial surfaces

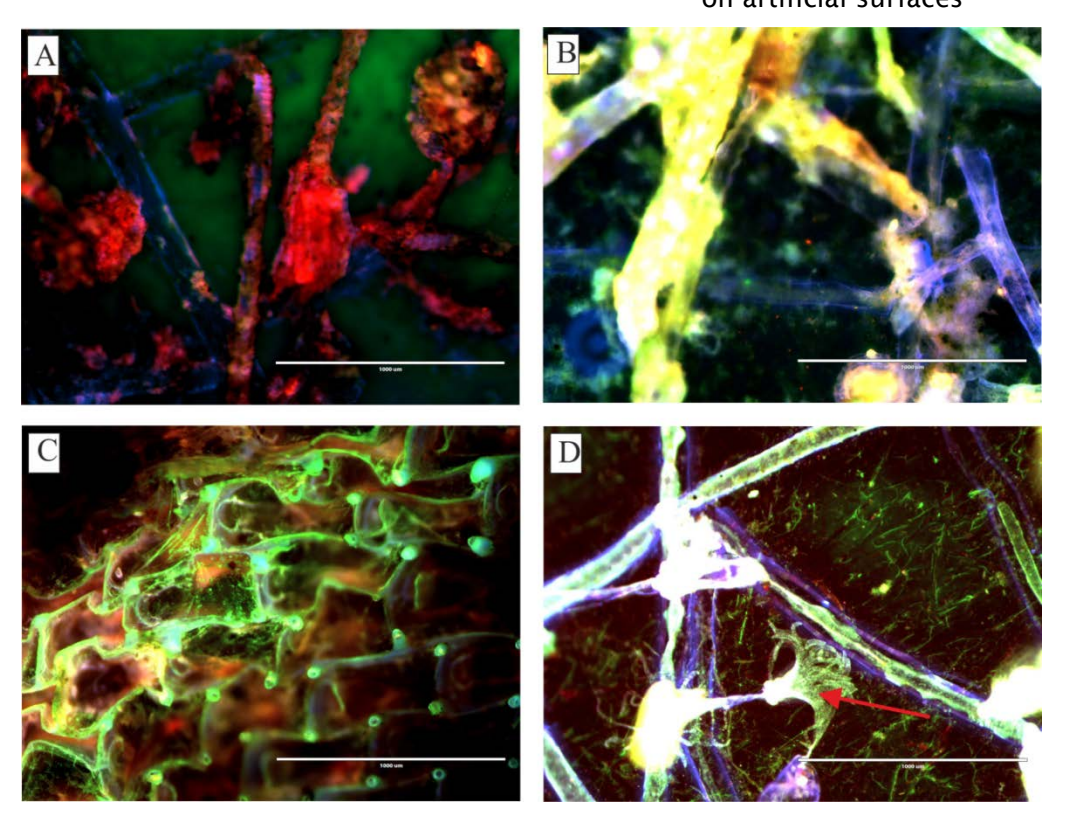


Figure 4.2: Overlay images of SYTO©9 stained seaglider samples taken with EVOS_fl microscope in three different fluorescent filters; GFP (excitation 470 nm, emission 525 nm; green colour), RFP (excitation 530 nm, emission 593 nm; red colour), and DAPI (excitation 360 nm, emission 447 nm; blue colour), and a 4x magnification, scale bar: 1000µm; (A) Seaglider sample #1 `No Lift´ sticker, (B) Seaglider sample #2 `No Lift´ sticker, (C) Sample #3: growth that could be peeled off with tweezers, (D) sample #4 plastic covering plate of the optode sensor

A blue fluorescence was seen in the DAPI filter, despite the samples not being stained with DAPI. This seems to indicate the presence of another undetermined fluorescent pigment.

Using the laser scanning confocal microscope (LSCM) a 3D image of a section of the biofouling was generated (Figure 4.3A). Microbial biofouling, small structures such as microcolonies, and macro-fouling, large structures, could be identified in the 3D image.

Using the depth range colouring a maximal biofouling thickness of 120 μ m was determined (Figure 4.3B).Both fluorescence microscopic and LSCM images show a very large heterogeneity in the biofouling. The biofilm coverage was not quantified in these samples as the 3D structures made it unfeasible.

Chapter 4: Development of biofilms on artificial surfaces

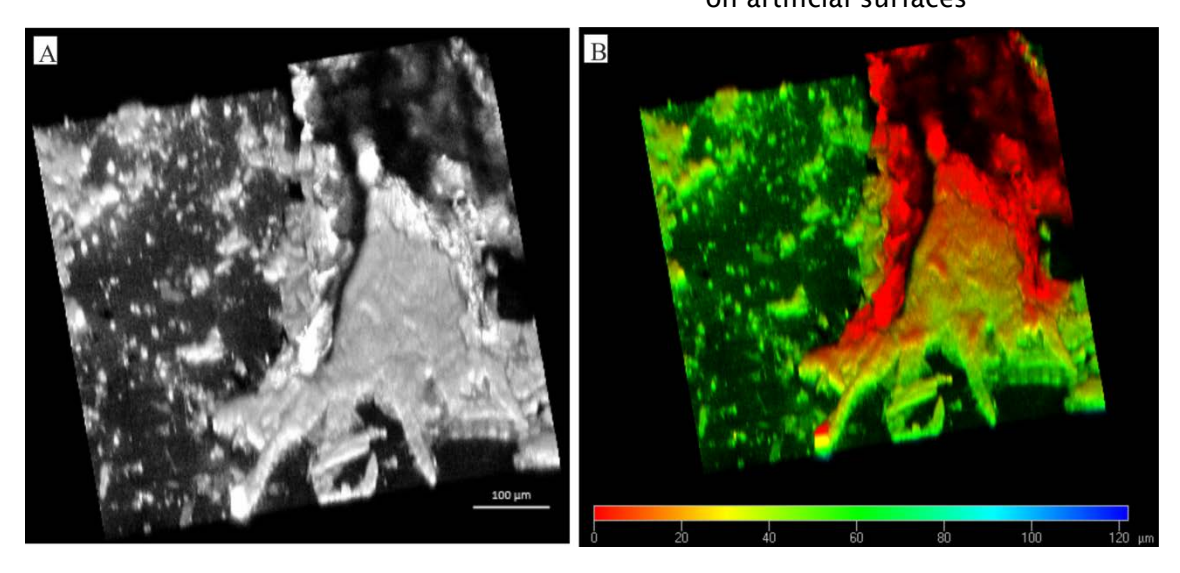


Figure 4.3: Laser Scanning Confocal Microscopy image of biofouling section on seaglider after 110 day deployment in the North Atlantic; (A) 3D image project, scale bar 100 μ m, (B) 3D image with depth range colouring

The photographs and microscopic images clearly show the later stages of fouling with the presence of multicellular organisms, e.g.: polyps, being present (Abarzua and Jakubowski, 1995).

Molecular Analysis DGGE

All samples show more than 15 clearly distinguishable bands indicating a high biodiversity of the microbial community (Figure 4.4).

The DGGE image of the glider samples #1 and #2 show a very similar band pattern, which is to be expected since they both have the same surface, 'No Lift' sticker.

In the sample of the peeled off growth (sample #3; Figure 4.4: L3) a very prominent band could be seen at the bottom of the gel, which did not occur in any of the other samples. In sample #5 the lowest number of bands was detected with most of the bottom bands seen in the other samples missing (Figure 4.4: L5). This indicates an influence of the sampling method on the biodiversity detected in the DGGE.

Most of the bands seem to occur in all samples with just different intensities. This seems to indicate that the same microbes occur regardless of the location on the glider and just the abundance varies. But since identical band position does not necessarily correspond to the same sequence as the melting behaviour of the DNA determines the separation (Muyzer et al., 1993), this assumption needs to be confirmed by sequencing. Unfortunately no successful sequencing results were

archived from bands in the same position. Failure of sequencing can have a number of reasons: no re-amplification could be achieved due to interference in the PCR reaction or degradation of the DNA template, DNA concentration was not high enough for the sequencing reaction, or an incomplete separation was achieved during DGGE and resulted in multiple sequences in the same DGGE band.

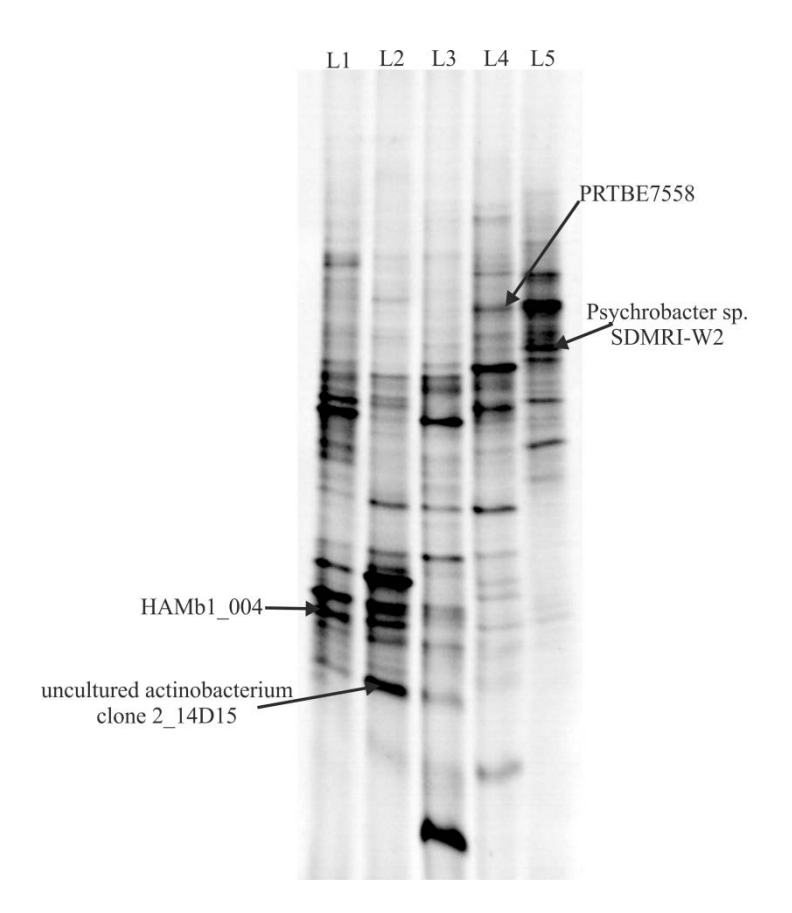


Figure 4.4: Image of DGGE gel of DNA extracts; (L1) `No Lift´ sticker; (L2) second `No Lift´ sticker; (L3) growth that could be peeled off with some tweezers (L4) plastic covering plate of the optode sensor; (L5) scrubbing of the sensor face of the seaglider; arrows point to the extracted and sequenced bands with the aliment match found in the online aliment software BLAST

Sequencing

For the identity similarities of the sequencing results from the DGGE extracted DNA bands (Figure 4.4), presented the 'expect' value was less than 1 to ensure the exclusion of random matches (Table 4.1). All four alignment matches represented lied between 97% and 100 %. All found alignment matches found are from uncultured organisms.

A 97% identity match was identified to an uncultured actinobacterium clone 2_14D15 isolated from a biofilm found in a heat exchange system (Taracido et al, unpublished). Another 100% identity match to the γ -proteobacterium *Psychrobacter*

sp. SMRI-W2, a bacterium isolated that is associated with coral disease (Thinesh and Edward, unpublished). The ubiquitous distributed *Psychrobacter* are characterized as being psychrotolerant or psychrophilic and halotolerant (Bowman et al., 1996), meaning they can at least tolerate low temperatures and high salinity. The other two sequence alignment matches found were to HAMb_1004 (99%) and PRTBE7558 (98%). HAMb_1104 is surface-associated uncultured bacterium clone that was isolated from a biofilm grown in the Southern part of the Gulf of Lawrence, Canada (Toupoint et al., 2012). PRTBE7558 was first from seawater collected at 6000 m in the Puerto-Rico Trench (Eloe et al., 2011).

Table 4.1: Closest alignment match to 16SrDNA sequence of extracted DGGE bands of the seaglider samples

Closest	Accessio	%	Expect	Source
alignment	n	Identity	value	
match	number			
HAMb1_004	JX984073	99	2e-41	biofilm developed from HAM
				lagoon water, Magdalen Islands;
				biofilm sampled after 1 week
				incubation
uncultured	GQ27412	97	8e-41	marine biofouling in heat
actinobacterium	3			exchangers
clone 2_14D15				
PRTBE7558	HM80011	98	3e-46	ocean water collected from
	3			6,000m depth within the Puerto
				Rico Trench
Psychrobacter sp. SDMRI-W2	JF268251	100	1e-38	diseased coral

Both of which were originally isolated from the same sources as two sequence matches found in the seawater samples collected in the Mid-Cayman Ridge (Chapter 3).

4.3 Development of hyper-baric biofilms on engineering surfaces in the Deep-Sea

At present research into biofouling has concentrated on the eutrophic and euphotic zone of the oceans, neglecting the deep sea because of the difficulties in experimental setup due to limited accessibility and the minor importance of the environment for most operations. While barophilic bacteria have been cultured from a depth greater the 4,000 m, these mostly originated from specific nutrient-rich environments (Deming et al., 1984, Jannasch and Wirsen, 1984). This led to the assumption that biofouling in the oligotrophic regions could be regarded as insignificant (Railkin, 2004). As a result very little is known about biofilm formation in the deep sea. But culture-independent methods have revealed significant microbial diversity even in surface sediments of the Mariana Trench (11,000m) (Kato et al., 1997). This means that the previous assumption of biofouling being only a minor factor in this environment needs to be re-examined. With the recent necessity to monitor deep sea processes to assess e.g. the environmental impact of deep-sea mining (Hoagland et al., 2010), the question arises if biofouling is an issue in these areas and whether we need to intensify our studies of deep-sea biofilms.

4.3.1 Methods and Materials

Sample acquisition

During the cruise 44 of the RRS James Cook (24 March99 to 21 April 2010) several materials were deployed on moorings for 10 days (Mooring I) and for 23 months (Mooring II & III), in a depth of around 4700m (Figure 4.5). The Moorings II and III were recovered during the cruise 374 on the RRS Discovery in March 2012. Mooring II was placed in the same position as Mooring I, the short-term mooring, and Mooring III was located in the vicinity of the Beebe vent filed (Figure 4.5).

Chapter 4: Development of biofilms on artificial surfaces

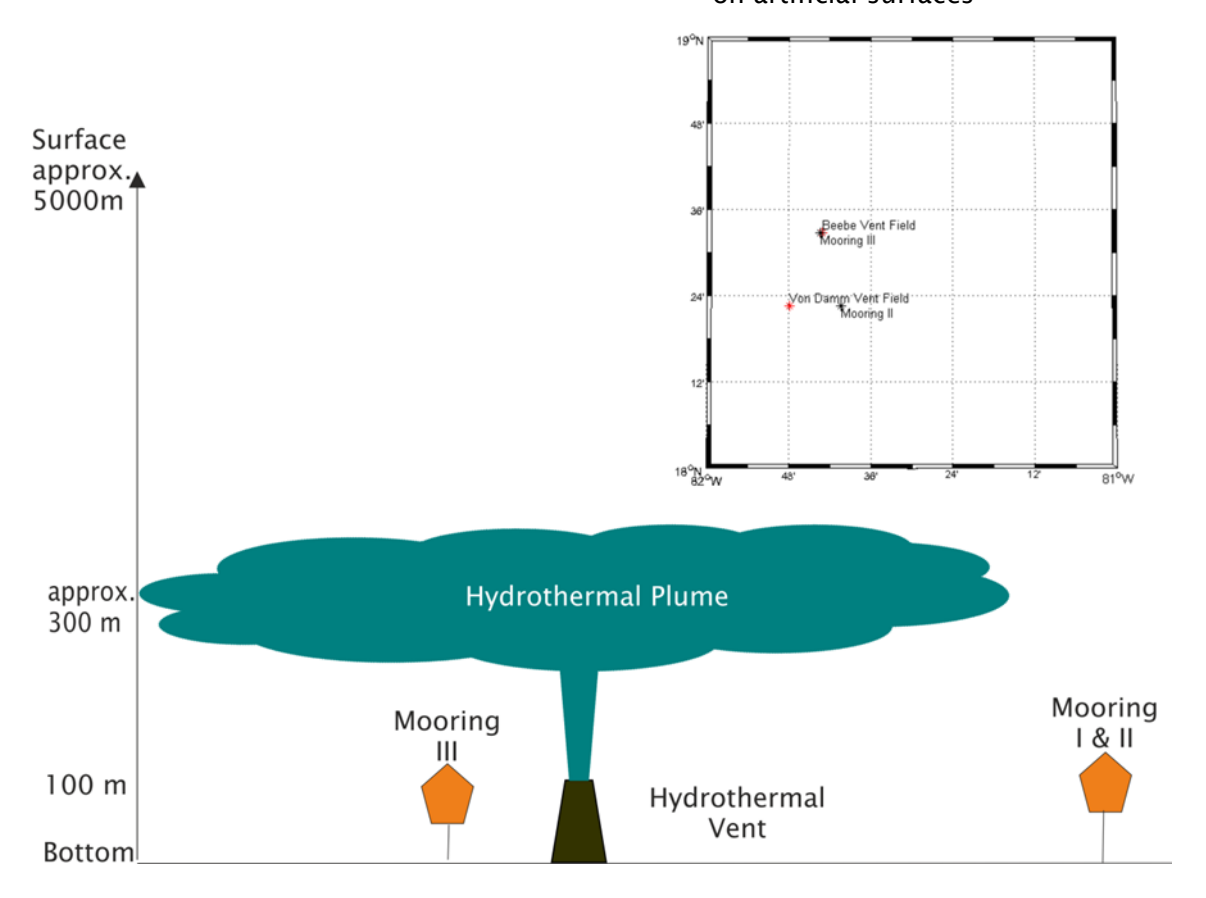


Figure 4.5: Scheme of the position of the moorings in relation to the Hydrothermal Vents and geographical positions

The setup of the experiment on Mooring I and II consisted of a biofouling tube, simulating the inside of a microfluidic sensor by filtering the water through a 50um nylon mesh, and a biofouling box simulating the outside (Figure 4.6: A and B). The position of the setup on the mooring was a 100m of the bottom in the Cayman Trough (Figure 4.5). The material deployed on Mooring I were copper, for its known antifouling properties, several polymers used in sensor manufacturing such as DelrinTM, Poly-methyl methacrylate (PMMA), and plain glass, as it is known to be a good substrate for biofilm attachment. On Mooring II additionally stainless steel Grade 374, Cyclic Olefin Copolymer (COC, Topas 8007 504) and Cyclo Olefin Polymer (COP, Zeonex 690R) were deployed. For Mooring III copper, glass and Delrin™ were deployed in a holder simulating sensor exterior (Figure 4.6: C & D).

All materials were "off the shelf" and the only treatment provided before deployment was cleaning with Biocleanse™ (Teknon). After recovery of the mooring one part of the sample was used for DNA extraction, while the other was fixed for microscopy using 100% ethanol or formaldehyde.

Chapter 4: Development of biofilms on artificial surfaces

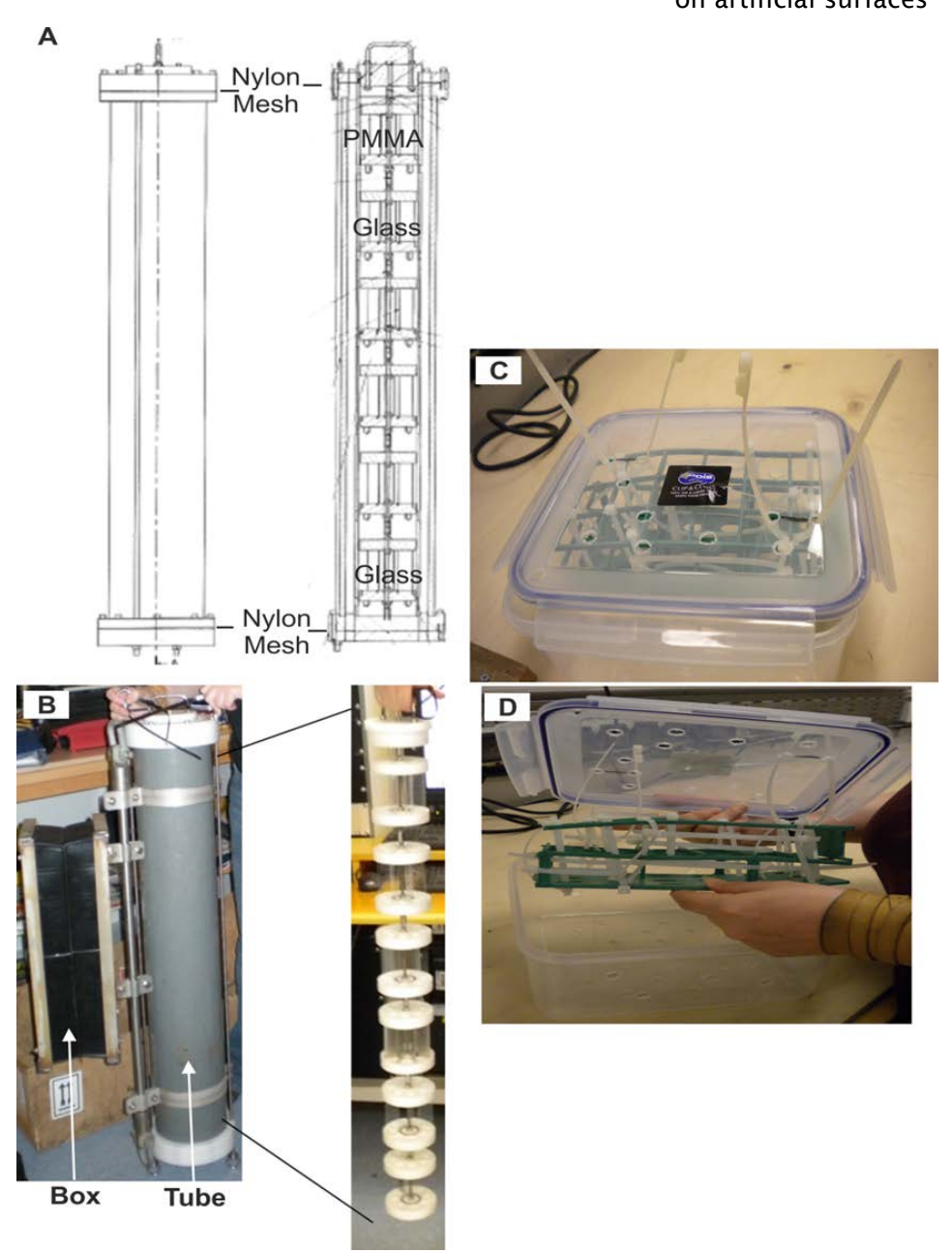


Figure 4.6: Mooring setup of the biofouling experiment; (A) diagram of the biofouling tube simulating a sensor interior by filtering the seawater through a nylon mesh with a pore size of 50 μ m; and position of the engineering surfaces inside the tube (B) picture of the actual mooring setup with the biofouling tube and biofouling box simulating the outside of a sensor used for Mooring I and II (C & D) pictures of the actual setup for Mooring III

Microscopy

All four available microscopy techniques were used for analysing the samples. The surface coverage of the biofilm formation was quantified by using the epifluorescence microscopy images in conjunction with the custom MATLAB™ (supplied by Xi Huang; see Apendix I).

Molecular Techniques

To analyse the microbial community for this project genomic DNA was extracted from samples taken with sterile swabs. The DNA extraction was performed directly on board using the DNeasy Kit in conjunction with the Tissue protocol provided from Qiagen. One half of the DNA extracts were stored at 4°C and the other half at -80°C. The extracted DNA was quantified using the NanoDrop 1000 Spectrophotometer (Thermo Scientific). Five µl of each DNA extract were used as template in a Polymerase Chain Reaction (PCR) that was performed using a universal primer set specific for 16S DNA of bacteria (Table 2.5: 27F; 1387R) (Dang and Lovell, 2000), specific 16S primers for archea (Table 2.5: A751F; UA1406R) (Baker et al., 2003), and 18S DNA specific primers for Eukarya (Table 2.5: EukF; EukR) (Delong, 1992) and the previously described reaction parameters.

DGGE

The extracted DNA was amplified and prepared according to the protocol from Muyzer (Table 2.5: Muy fwd, Muy rev, and Muy DGGE) (Muyzer et al., 1995, Muyzer et al., 1993). The DGGE parameters were the following: 8% Acrylamide/Bis solution (37.5/1) (Biorad, UK) with a denaturant gradient between 30 and 80% were found to be sufficient for the separation of bands with 1600Volt hours (Vhrs) at 60°C.

The DNA fragments of the most prominent bands were extracted, re-amplified, cleaned up and sequenced.

4.3.2 Results for Mooring I: Biofouling after 10 day deployment in the deep-sea

Microscopy

Microscopic analysis using EDIC and Epifluorescence showed early stages of biofouling on the surface of all deployed material; ranging from microcolonies to the beginning of biofilm formation (Figure 4.7: glass as an example).

Chapter 4: Development of biofilms on artificial surfaces

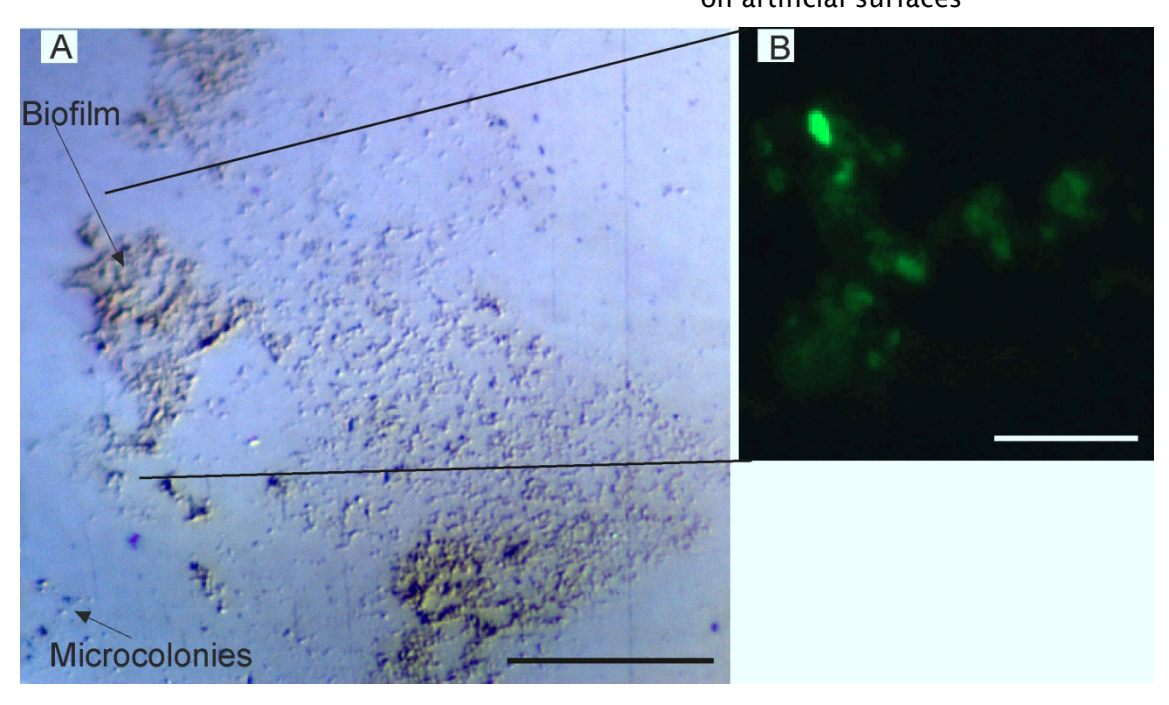


Figure 4.7: Microscope images of Biofilm formation on plain glass slide deployed at 4,700 m for 10 days; (A) Enhanced Differential Interference microscopy; (B) Epifluorescence microscopy, sample was stained with the nucleic acid stain SYTO9, used Filter:

FITC/Bodipy/Fluo3/Di O (excitation: 480/40 emission: 535/50; both images were taken with the Nikon Eclipse ME600 microscope (Best Scientific, Swindon, UK) using 40x long working distance objective

In the LSCM images (Figure 4.8) microcolonies and biofilm formation could also be observed on all materials.

The overlay of the fluorescence microscope image with the EDIC image shows a clear correlation of between the severity of biofouling and imperfections in the material surfaces. The fluorescence of the stained biofilms (green colour observed in the overlays Figure 4.8: A, D, G, J, M) is clearly associated with depressions in the material surfaces. In the EDIC/Fluorescence overlays of the copper and Delrin surfaces this was especially clear (Fig.4.8: J and M). The SEM images (Figure 4.9) do confirm this observation. The arrows point to cells in imperfections of the copper surface. On the glass from the Biofouling Tube additionally filamentous microorganisms could be found in the SEM images.

Using a depth range colouring on the 3D images taken with the LSCM (Figure 4.8: C, F, I, L, and O), the thickness of the biofilms was estimated. On both glass samples from the biofouling box and tube, single biofilm structures were estimated to be up to 16 μ m with an average thickness of around 10 μ m. On the Delrin surface the micro-colonies/biofilm was up to 5 μ m and on the PMMA between 4 to 6 μ m thick. On the copper surface the biofilm appears to be up the 30 μ m thick.

Chapter 4: Development of biofilms on artificial surfaces

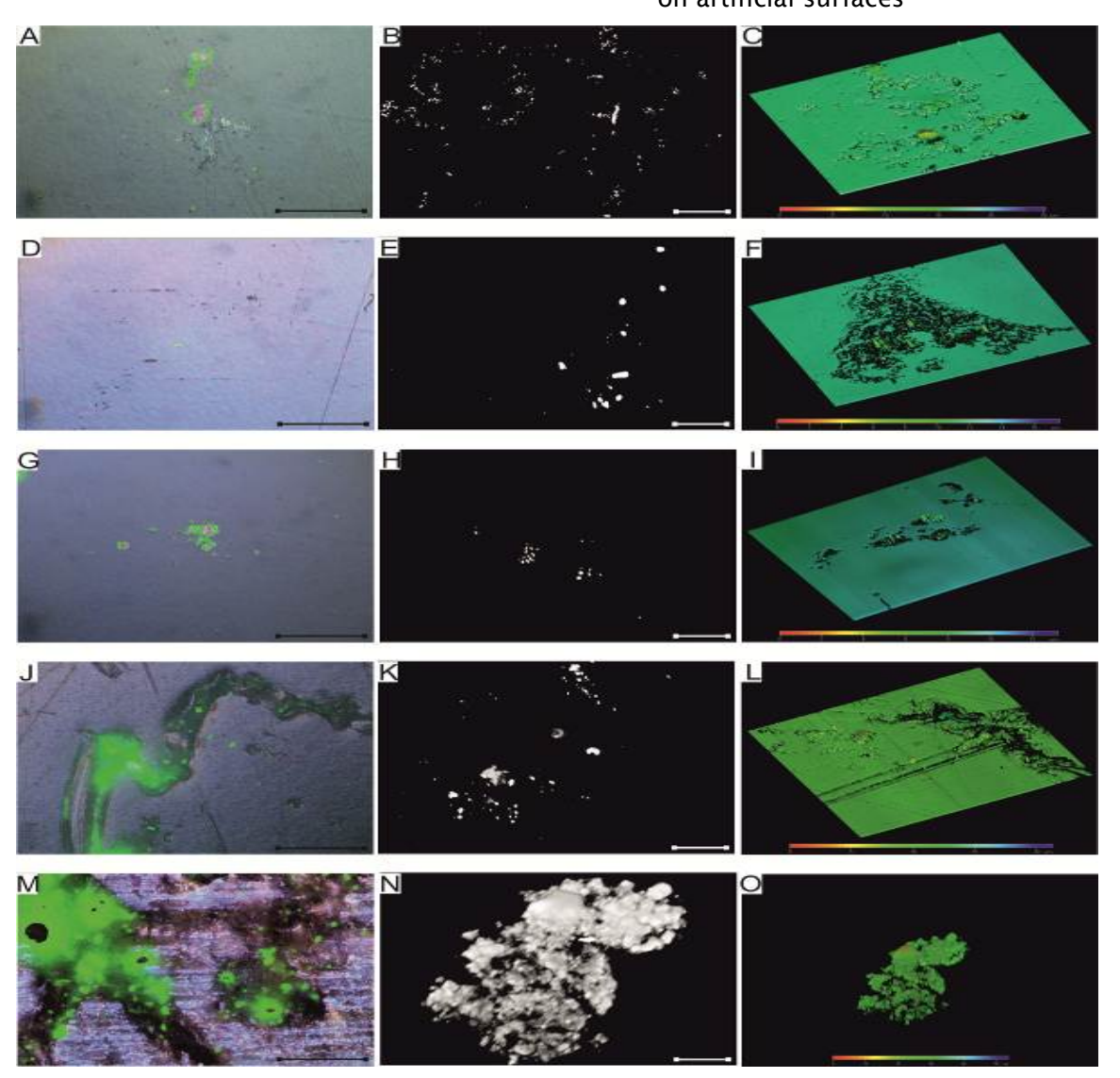


Figure 4.8: Microscopic images of biofouling on artificial surfaces after 10 day deployment at 4,700 m; (A) glass without pre-filtering of seawater simulating exterior of sensors; overlay of EDIC and epifluorescence images; (B) as A; Laser Scanning Confocal Microscopy image; (C) as A; Laser Scanning Confocal Microscopy image with depth range colouring; (D) copper without pre-filtering of seawater simulating exterior of sensors; overlay of EDIC and epifluorescence images; (E) as D; Laser Scanning Confocal Microscopy image; (F) as D; Laser Scanning Confocal Microscopy image with depth range colouring; (G) Delrin without pre-filtering of seawater simulating exterior of sensors; overlay of EDIC and epifluorescence images; (H) as G; Laser Scanning Confocal Microscopy image; (I) as G; Laser Scanning Confocal Microscopy image with depth range colouring; (J) glass simulating interior of sensor by pre-filtering the seawater through a 50 µm nylon mesh; overlay of EDIC and epifluorescence images; (K) as J; Laser Scanning Confocal Microscopy image; (L) as J; Laser Scanning Confocal Microscopy image with depth range colouring; (M) PMMA glass simulating interior of sensor by pre-filtering the seawater through a 50 µm nylon mesh; overlay of EDIC and epifluorescence images; (N) as M; Laser Scanning Confocal Microscopy image; (O) as M; Laser Scanning Confocal Microscopy image with depth range colouring; A D G J M: scale bar 100 μ m; B, E, H, K, N scale bar 20 μ m

Chapter 4: Development of biofilms on artificial surfaces

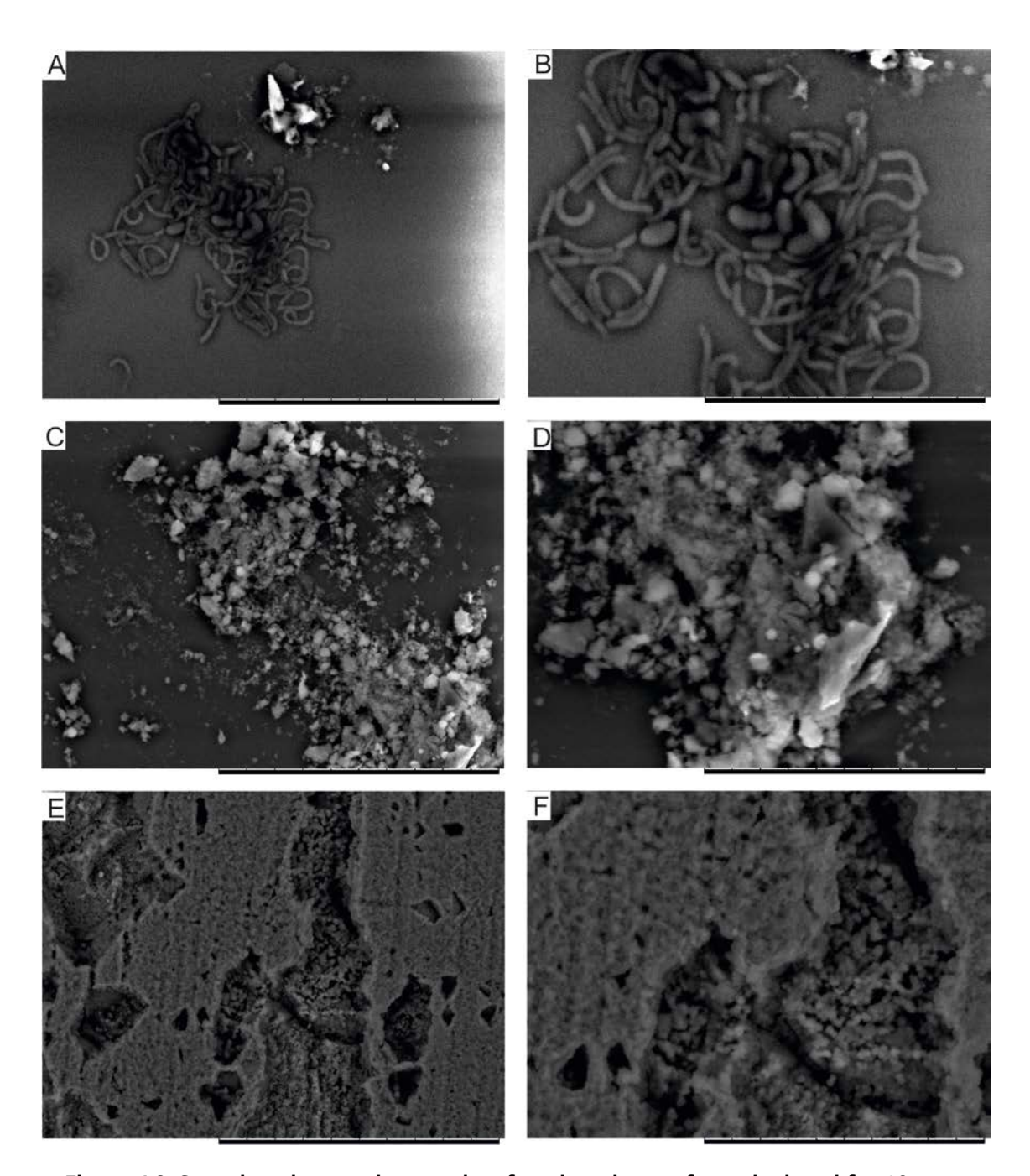


Figure 4.9: Scanning electro-micrographs of engineering surfaces deployed for 10 days at 4,700 m; (A) glass simulating the interior of sensors by pre-filtering water through a 50 μm nylon mesh, magnification 5,000x (B) as A with 10,000x magnification (C) Glass simulation of sensor exteriors; magnification 5,000x (D) as C with 10,000x magnification (E) copper simulating the exterior of sensors; magnification 5,000x (F) as E with 10,000x magnification. Scalebar at 20 μm or 10 μm for 5,000x and 10,000x magnification respectively

Quantification using fluorescent images

Using biofilm coverage as an indicator for biomass showed cooper and PMMA to be the most resistant to biofouling. The biofilm coverage on copper $(3.62 \% \pm 1.24)$ and PMMA $(4.65 \% \pm 3.3)$ was a third of that found on DelrinTM, $(12.62 \% \pm 4.42)$. About 10% of the glass slide surfaces were covered by biofilm independent of their position (inside the biofouling tube or box). This coverage is more than double that found on copper and PMMA (Figure 4.10).

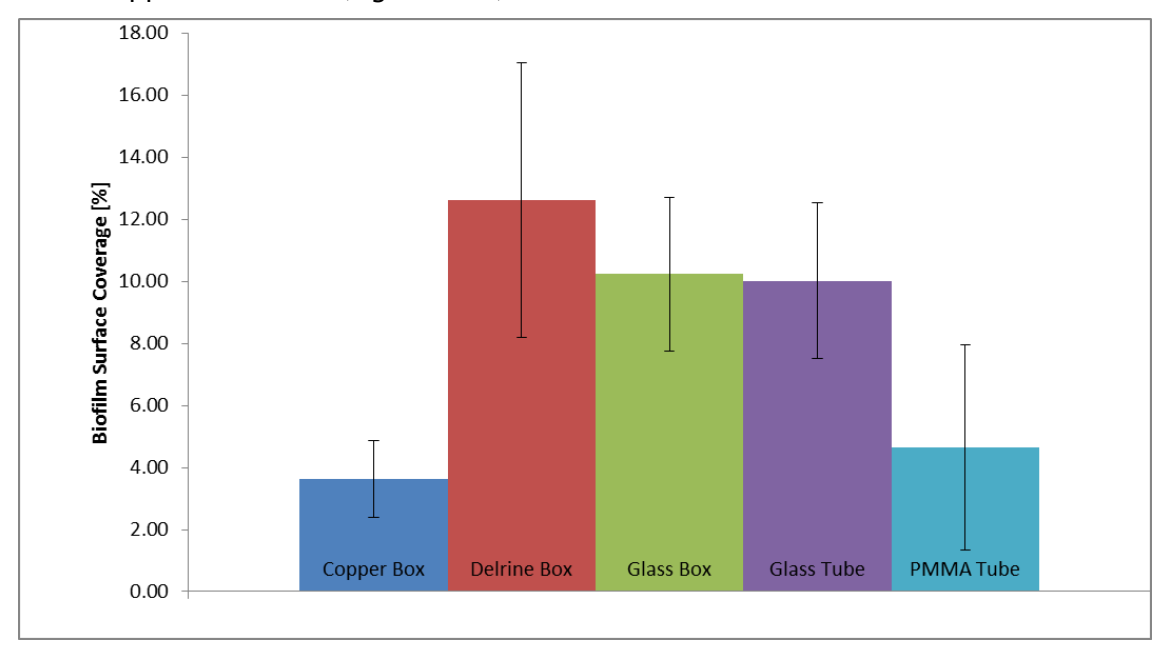


Figure 4.10: Biofilm surface coverage as indicator for biomass on engineering surface deployed for 10 days at 4,700 m (Mooring I); copper box, Delrin box and glass box simulating the exterior of sensors; glass tube and PMMA tube simulating the interior of sensors by pre-filtering water through a 50 µm nylon mesh

The large standard deviation is the result of the heterogeneity in the biofilm coverage of the surfaces which can be seen on the microscopy images (Figure 4.8).

Single factor ANOVA analysis with subsequent Post-Hoc comparison showed that the differences between most materials were statistically significant (Table 4.2). No significant difference between the biofouling of the glass from the Biofouling Tube and the Biofouling Box was found. This means the biofilm coverage of the copper and PMMA could be directly compared without any adjustments despite their different locations the box and the tube on the mooring and was found to be not significantly different. Also no significant difference existed in the biofilm coverage between the DelrinTM and the glass surfaces.

Table 4.2: Single-factor ANOVA with subsequent post-hoc comparison results of the biofilm coverage determined by the quantification of the fluorescence microscopy images

	Duralina	P(T<=t)	E aule	-!: :: !
	P-value	two tailed	F crit	significance
ANOVA including all	4.48E-		2.45821	significant
samples	13		2.43021	Significant
copper vs Delrin		1.42E-		significant
copper vs Denni		08		signineant
copper vs glass box		9.36E-		significant
copper vs glass box		07		signineant
copper vs glass tube		7.38E-		significant
copper vs glass tube		08		signineant
copper vs PMMA		0.8151		not
copper vs riving		39		significant
Delrin vs glass box		0.0135		not
Dell'III vs glass box		28		significant
Delrin vs glass tube		0.0132		not
Delilli va glasa tube		65		significant
Delrin vs PMMA		2.55E-		significant
Dell'III V3 I WIWA		07		Significant
glass box vs glass tube		0.9056		not
glass box vs glass tube	,	08		significant
PMMA vs glass box		4.87E-		significant
T WIMA V3 glass box		05		Significant
PMMA vs glass tube		1.22E-		significant
rivilina vs glass tube		05		Significant

Molecular Analysis

The quantification of the DNA extracts measured via nanodrop showed a concentration range between 5.4 and 14.4 ng/µl with an average 260/280 ratio of 1.87 indicating pure DNA with little or no contamination of proteins and RNA (Warburg and Christian, 1941, Glasel, 1995). Comparing the PCR product size using the High Sensitivity Assay of the Agilent Bioanalyzer shows a good correlation for the archean primer set between the expected size (655 bp) and the measured ones (642 bp -666 bp). The PCR product sizes results for the Bacterial and Eukaryotic primer sets are in general 100 bp to 200 bp larger than the expected product size (Table 4.3).

Table 4.3: Results for PCR amplification using High Sensitive DNA Assay (Bioanalyser, Agilent)

	Bacteria		Ar	chea	Eukarya		
Material	Peak	Conc.	Peak	Conc	Peak	Conc	
	Size [bp]	[pg/ul]	Size [bp]	. [pg/ul]	Size [bp]	. [pg/ul]	
PMMA Box	1547	46.2	648	248.	1871	64.8	
FIMINIA BOX	1347	1547 40.2		54	1071	3	
PMMA Tube	1569	409.4	661	127.	1854	26.4	
FINIMA TUBE	1309	1309 409.4		55		1	
Glass Box	1593	27.17	661	174.	1922	604.	
GIASS BUX	1393	27.17		86		04	
Glass Tube	1568 61.45	61.45	666	372.	1918	127.	
Glass Tube	1300	01.43		02		75	
Delrin	1575	221.65	321.65 653	82.9	82.9	1887	183.
Dell'III	1373	321.03		6	1007	52	
Copper	1598	1500 22.70	654	11.0			
	1598 32.78	4					

The bioanalyzer results can also be used for quantification of the PCR products (area of the peaks in the electrogramms; (Figure 4.11B).

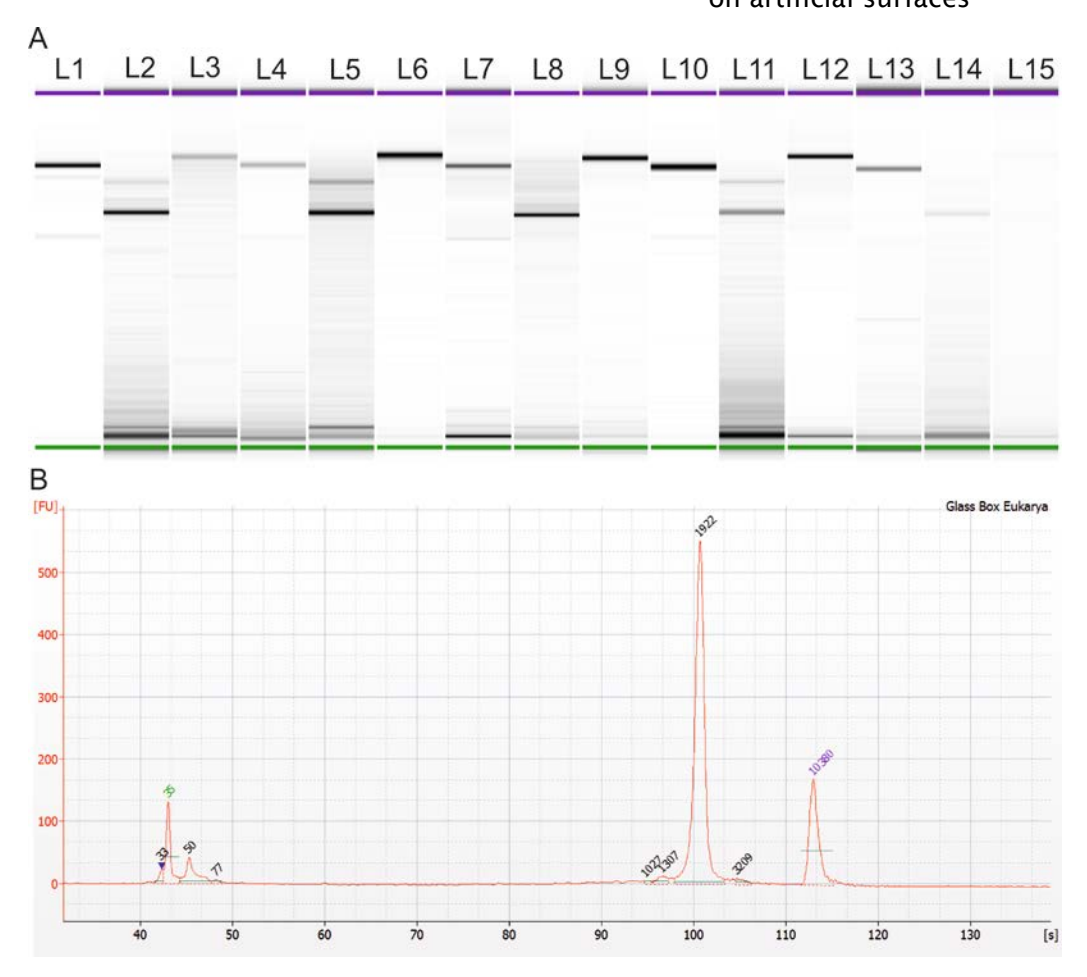


Figure 4.11: Bioanalyzer results for PCR products of extracted DNA from different engineering surfaces after 10 day deployment at 4,700 m; (A) image of gel simulation; L1 – L3: PMMA simulating interior of sensors, bacterial, archeal and eukaryotic PCR product respectively; L4-L6: glass simulating the exterior of sensors, bacterial, archeal and eukaryotic PCR product respectively; L7-L9: glass simulating interior of sensors, bacterial, archeal and eukaryotic PCR product respectively; L10-L12: Delrin simulating the exterior of sensors, bacterial, archeal and eukaryotic PCR product respectively L 13-L15: copper simulating the exterior of sensors, bacterial, archeal and eukaryotic PCR product respectively (B) example of electrogram

These can be used as an indicator for the initial DNA concentration amplified in the PCR reaction. The amounts of PCR products for the bacterial primer set lie between 27.17 ng μl^{-1} and 409.9 ng μl^{-1} , for the archean primers between 82.96 ng μl^{-1} and 248.54 ng μl^{-1} , and for the eukaryotic between 26.41 ng μl^{-1} and 183.52 ng μl^{-1} (Table 4.3).

PCR products showed that Archea and Bacteria (Figure 4.12: light grey and cross pattern in the pie charts) were present in the biofilm of all materials. Eukaryotic DNA (dark grey) could be amplified in all samples except in biofilms found on the copper surfaces this could be due to metal interference with the eukaryotic PCR reactions (Thornton and Passen, 2004), degradation of the DNA by copper ions (Warnes and

on artificial surfaces

Keevil, 2011) or the simple absence of Eukaryote in the biofilm community. On the Copper, Delrin™, and PMMA surfaces Bacteria seemed to be the dominant kingdom of the attached microbes with 75 %; 55 %; and 73 % respectively. The glass samples from the Biofouling Tube and Box varied drastically in their community composition regarding the Kingdoms. Archea represented the dominant kingdom (66 %) on the glass surface from the Tube, whereas Eukarya had the highest percentage (75 %) on the glass located in the Box.

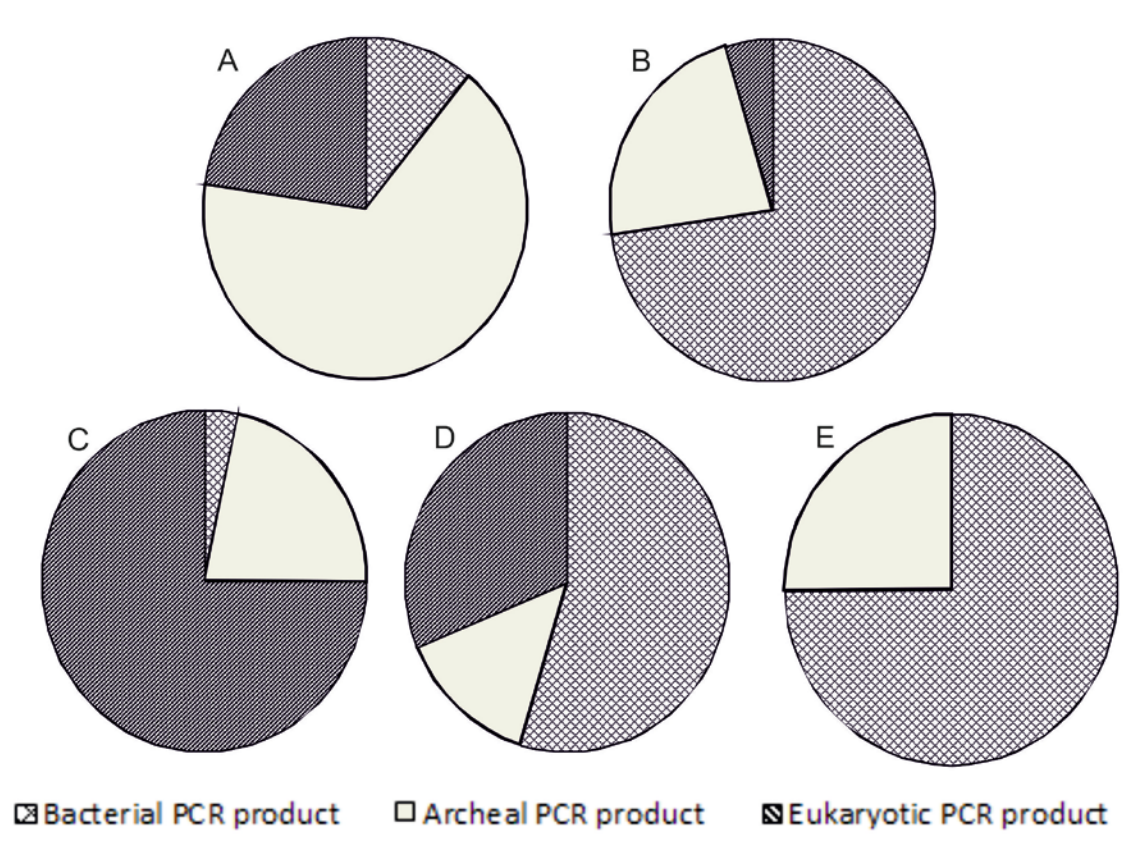


Figure 4.12: Pie Charts of PCR product quantification using a Bioanalyzer; (A) glass simulating interior of sensors by pre-filtering water through a 50 µm nylon mesh; (B) PMMA simulating interior of sensors by pre-filtering water through a 50 μm nylon mesh (C) glass simulating outside of sensors (D) Delrin simulating outside of sensors (E) copper simulating ouside of sensors

DGGE

On the DGGE (Figure 4.13) seven to ten clearly separated bands could be detected. The intensity of some bands varies between different materials. But a shift could also be found between the glass from the Tube and the Box indicating the influence of excluding larger particles in the water column by the $50 \mu m$ nylon mesh.

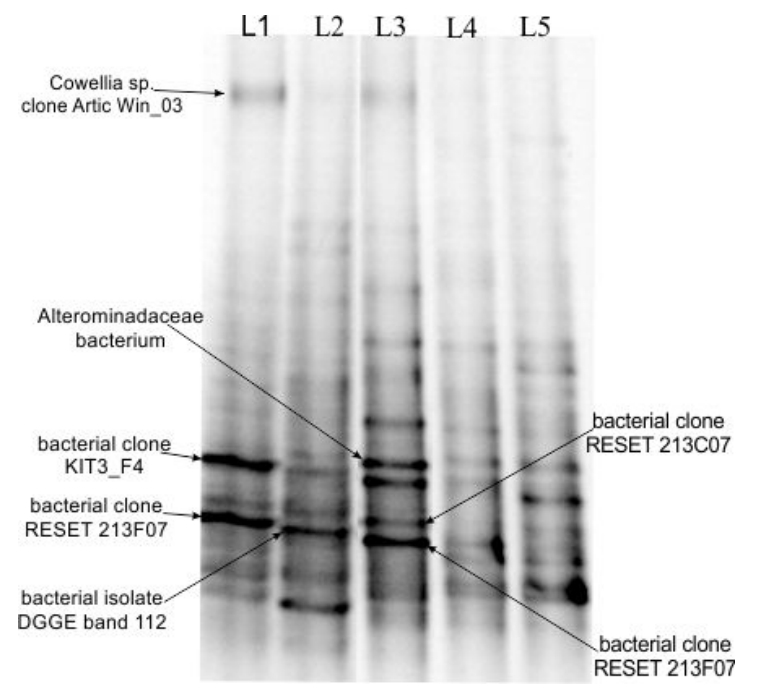


Figure 4.13: Image of DGGE gel for extracted DNA from different engineering surface after 10 day deployment at 4,700 m; (L1) glass simulating the interior of sensors by prefiltering water through a 50 µm nylon mesh; (L2) glass simulating the exterior of sensors; (L3) PMMA simulating the interior of sensors; (L4) Delrin simulating the exterior of sensors; (L5) copper simulating the exterior of sensors; arrows point to the extracted and sequenced bands with the aliment match found in the online aliment software BLAST

For the identity similarities of the sequencing results from the DGGE extracted DNA bands (Figure 4.13), presented in this study the 'expect' value was less than 1 to ensure the exclusion of random matches (Table 4.4).

on artificial surfaces

Table 4.4: closest alignment match to 16S rDNA sequence of extracted DGGE bands from short-term mooring

Material	Closest alignment match	Accession number	% Identity	Expect value	Source
Glass Tube	Uncultured Colwellia sp. clone ArcticWin_03	JN399062	100	4e-55	Environmental sample; Arctic Ocean, Beaufort Sea, Canada
	Uncultured bacterium clone KIT3_F4	JN621686	100	3e-61	Marine sediments; Ulleung Basin, Southa Korea
	Uncultured bacterium clone RESET_213C07	JN874334	99	3e-72	TrapR2 115 m southwest of Ty/lo vents, East Pacific Rise, 9°50´N
Glass Box	Uncultured bacterium isolate DGGE gel band 112	GQ924739	100	3e-27	Coral associated microbial community; Great Barrier Reef
PMMA	Uncultured Alteromonadacea e bacterium	AJ567604	98	2e-35	Deep-sea sediment; Middle Pacific, China
	Uncultured bacterium clone RESET_213C07	JN874363	98	2e-68	TrapR2 115 m southwest of Ty/Io vents, East Pacific Rise, 9°50 ´N
	Uncultured bacterium clone RESET_213C07	JN874334	97	4e-66	TrapR2 115 m southwest of Ty/Io vents, East Pacific Rise, 9°50´N

100% identity matches to a *Colwellia sp.* isolated from an environmental sample from the Arctic Ocean (Galand et al, unpublished), an uncultured bacterium clone KIT_F4 (Vandieken et al., 2012) from marine sediment in the Ulleung Basin, and to a DGGE gel band of an uncultured bacterium of a Coral associated microbial community from the Great Barrier Reef (Kvennefors et al, unpublished) were found. We also found a 99 % and 98 % match to two uncultured bacterial clones, RESET_213F07 and RESET_C07, with the same source: TrapR2, 11 m southwest of vent sites on the East Pacific Rise (9°50´N) (Sylvan et al, unpublished). The last alignment we found was a 98 % match to an uncultured *Alteromonadaceae* bacterium isolated forma deep-sea sediment in the Middle Pacific (Xu et al., 2005).

4.3.3 Results for mooring II and III: Biofouling after 23 month deployment in the deep-sea

Microscopic Analysis
Auto-fluorescence

During initial microscopic examination of the glass samples from Moo II simulating sensor exterior and Moo III the biofouling showed a pattern of nodes that were linked with each other (Figure 4.14).

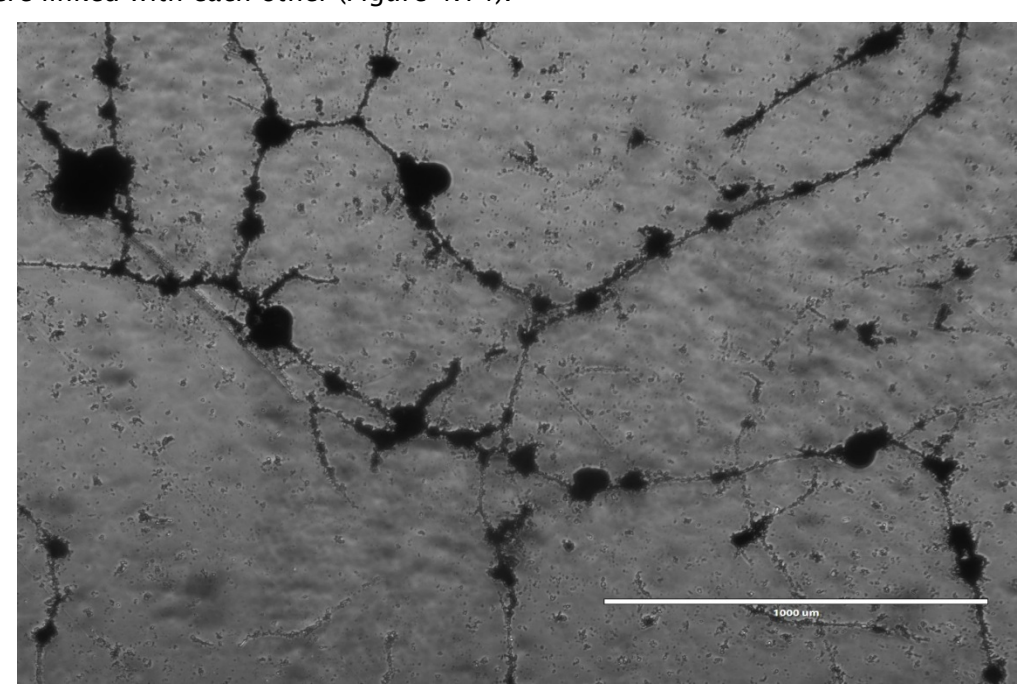


Figure 4.14: Brightfield microscopic image of glass surface deployed on mooring II for 23 months using the EVOSfI (AMG, USA), scale bar 1000 µm

In these samples auto-fluorescence was also detected. Auto-fluorescence has been detected before in autotrophic biofilms containing algae, but those are generally confined to the phototrophic regions of the marine environment (Barranguet et al., 2004). Closer examination using the EDIC microscopy (Best Scientific, Swindon, UK) with different fluorescence filters Calcium Crimson (excitation 580/20 nm, emission 630/ nm) and R&B Phycoerythrin (546/11 nm, emission 585/40 nm) showed the auto-fluorescence (Figure 4.15: B, C, E, and F). This is a surprising finding since photosynthesis is restricted to surface waters.

Chapter 4: Development of biofilms on artificial surfaces

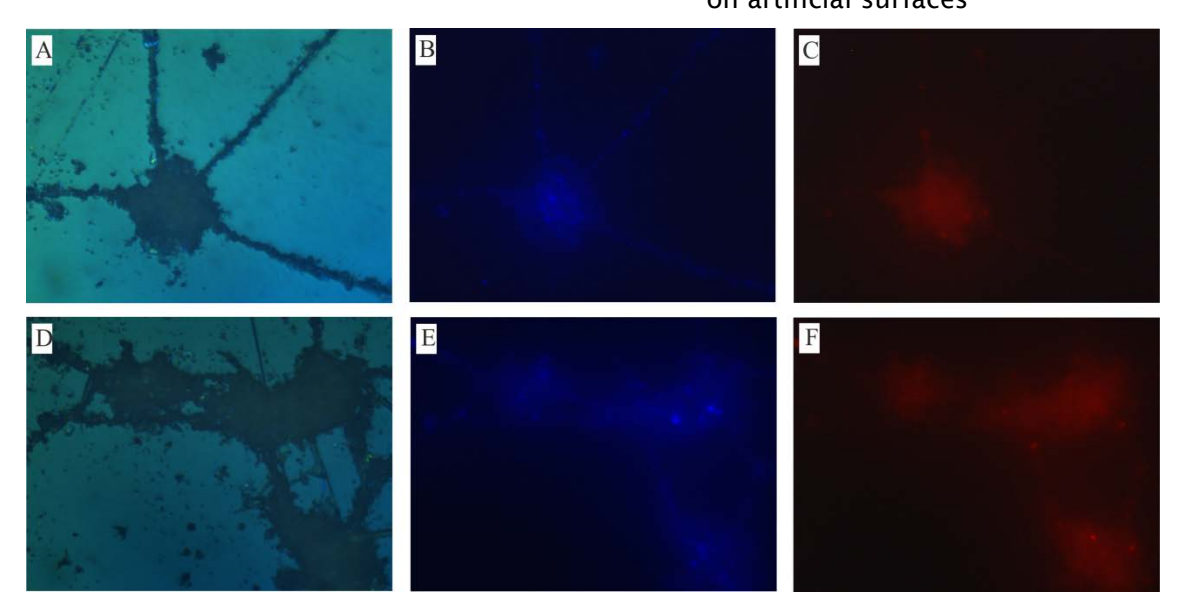


Figure 4.15: Microscopic images of unstained glass surface simulating sensor exterior after 23 month at 4,700 m; (A) glass on mooring II; EDIC image (B) as A; epifluorescence image using Calcium Crimson filter (C) as A; epifluorescence image using R&B Phycoerythrin filter (D) glass on mooring III in the vicinity of the Beebe bent field (E) as D; epifluorescence image using Calcium Crimson filter (F) as D; epifluorescence image using R&B Phycoerythrin filter

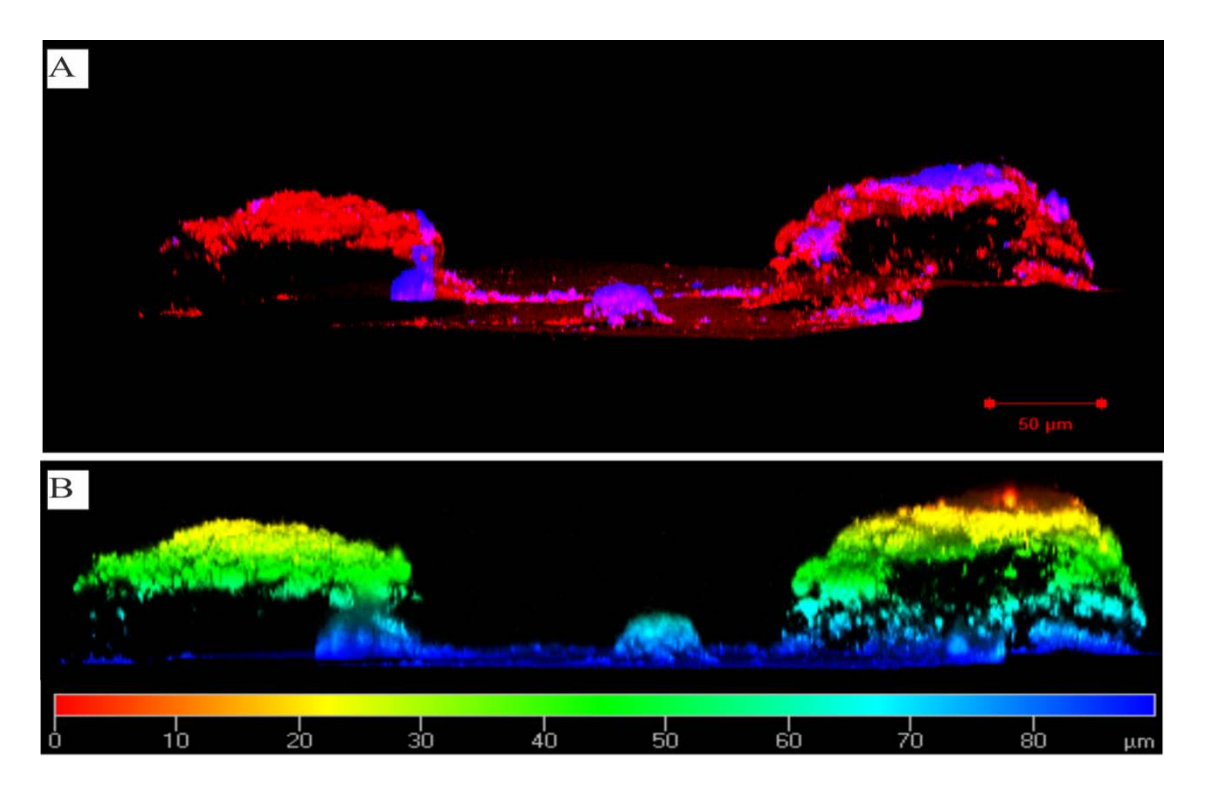


Figure 4.16: 3D image of auto-fluorescence detected on glass surface deployed on mooring III for 23 months in the vicinity of the Beebe vent field; (A) Laser Scanning Confocal Microscopy image; scalebar 50 µm (B) as A; Laser Scanning Confocal Microscopy image with depth range colouring

The LSCM was used to create a 3D image of a section of the biofouling found on the glass surface deployed in the vicinity of the Beebe vent field. This scan showed that the fluorescence originated from the surface of the fouling structures (Figure 4.16A). Using the depth range colouring a maximal thickness of the node structures of over $80~\mu m$ was determined.

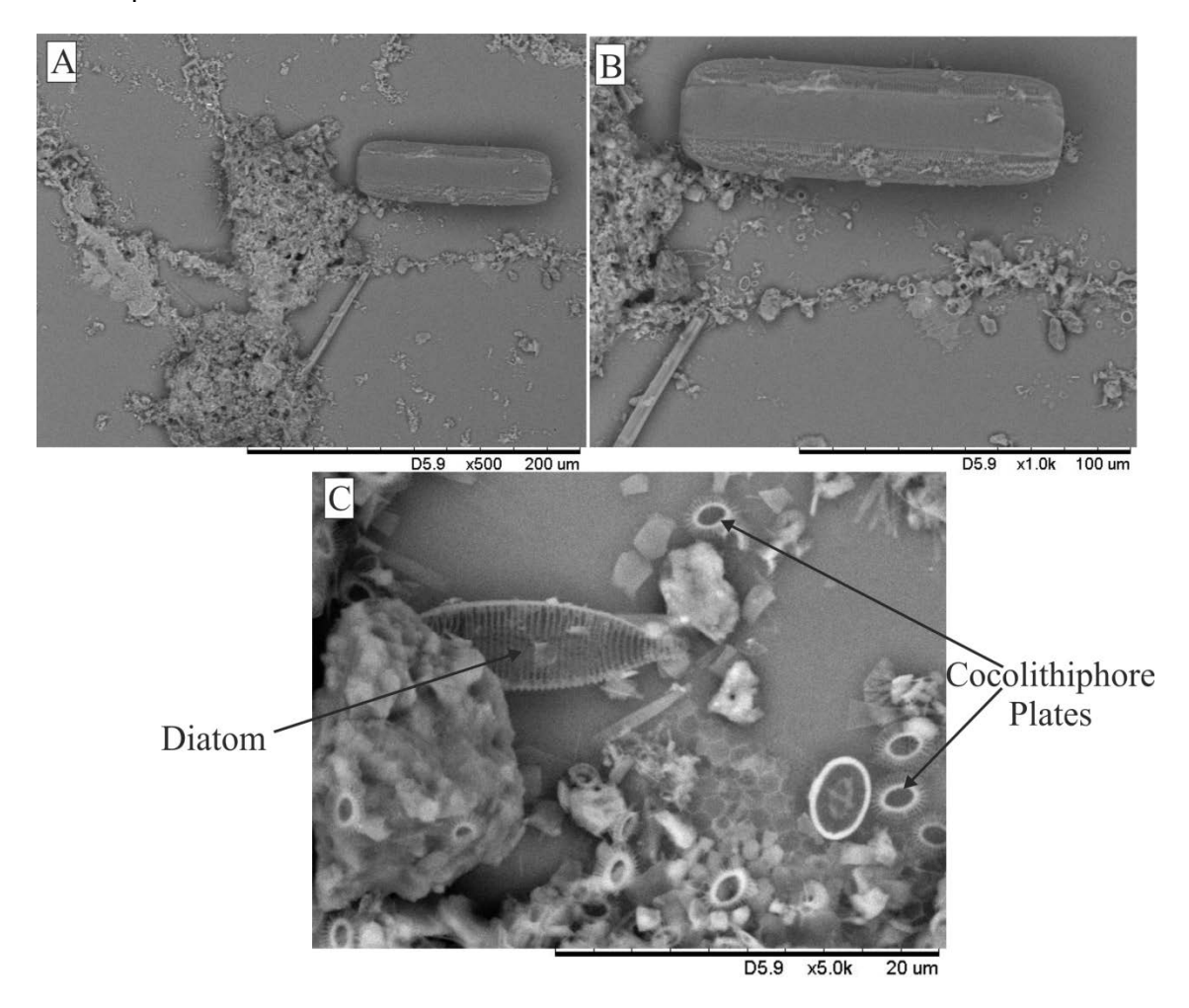


Figure 4.17: SEM images of glass surface deployed on mooring III for 23 months in the vicinity of the Beebe vent field; (A) 500x magnification (B) 1000x magnification (C) 5000x magnification

Examination with the SEM enabling higher magnification of the biofouling identified possible sources for the auto-fluorescence. In these images especially at 5000x magnification diatoms and plates of cocolithiphores could be identified (Figure 4.17). The presents of both algae might explain the detection of auto-fluorescence pointing to the presence of photosynthetic pigments. These findings seem to indicate that the remains of photo-plankton organisms which sank to the bottom were incorporated into the biofilm structures.

Biofouling

As to be expected the biofouling on the long-term moorings appears to be more extensive than on the short-term mooring in the microscopic images. As observed on the short-term mooring samples the overlay of fluorescence and EDIC microscopic images show a correlation between the severity of fouling and surface imperfections (Figure 4.18, Figure 4.19, Figure 4.20). Especially clear can this correlation been seen in the PMMA and Delrin™ samples (Figure 4.18G, Figure 4.19: A & B, Figure 4.20A). On the SEM images of the metal samples a similar trend could be seen (Figure 4.21: A, B, and G, Figure 4.22: C and D).

As mentioned before the glass surfaces, simulating a sensor exterior surface, the biofouling on both long-term moorings showed a pattern of nodes being linked with each other, which could clearly identified in the EDIC images (Figure 4.19G and Figure 4.20D). On the PMMA sample of mooring II structures could be found which might be the initial stage of this growth pattern (Figure 4.19D).

The thickness of the biofouling was estimated using depth range colouring on 3D images generated with the LSCM Figure 4.18: C, F, I, L, and O, Figure 4.19: C, F, I, L, and O, Figure 4.20: C, F, and I). On mooring II, outside the influence of the Beebe hydrothermal vent field, the thickness of the biofilm was generally thinner on the samples simulating the interior of sensors than on the ones simulating the exterior. On the glass slides the biofilm thickness simulating the interior was 25 μ m and simulating the outside of sensors the nodes were approximately 45 μ m and the links around 20 μ m. On the glass slides deployed in the vicinity of the Beebe vent field the thickness of the nodes reached up to 80 μ m (Figure 4.16B). On the stainless steel surface the biofilm averaged a thickness between 10 and 15 μ m, whereas on the copper it varied between 30 and 35 μ m. All plastics showed average 20 μ m thick biofilm.

Comparing the of the materials from the Biofouling Box on mooring II and mooring III, in the vicinity of the Beebe a similar biofilm thickness was found for the same materials.

Chapter 4: Development of biofilms on artificial surfaces

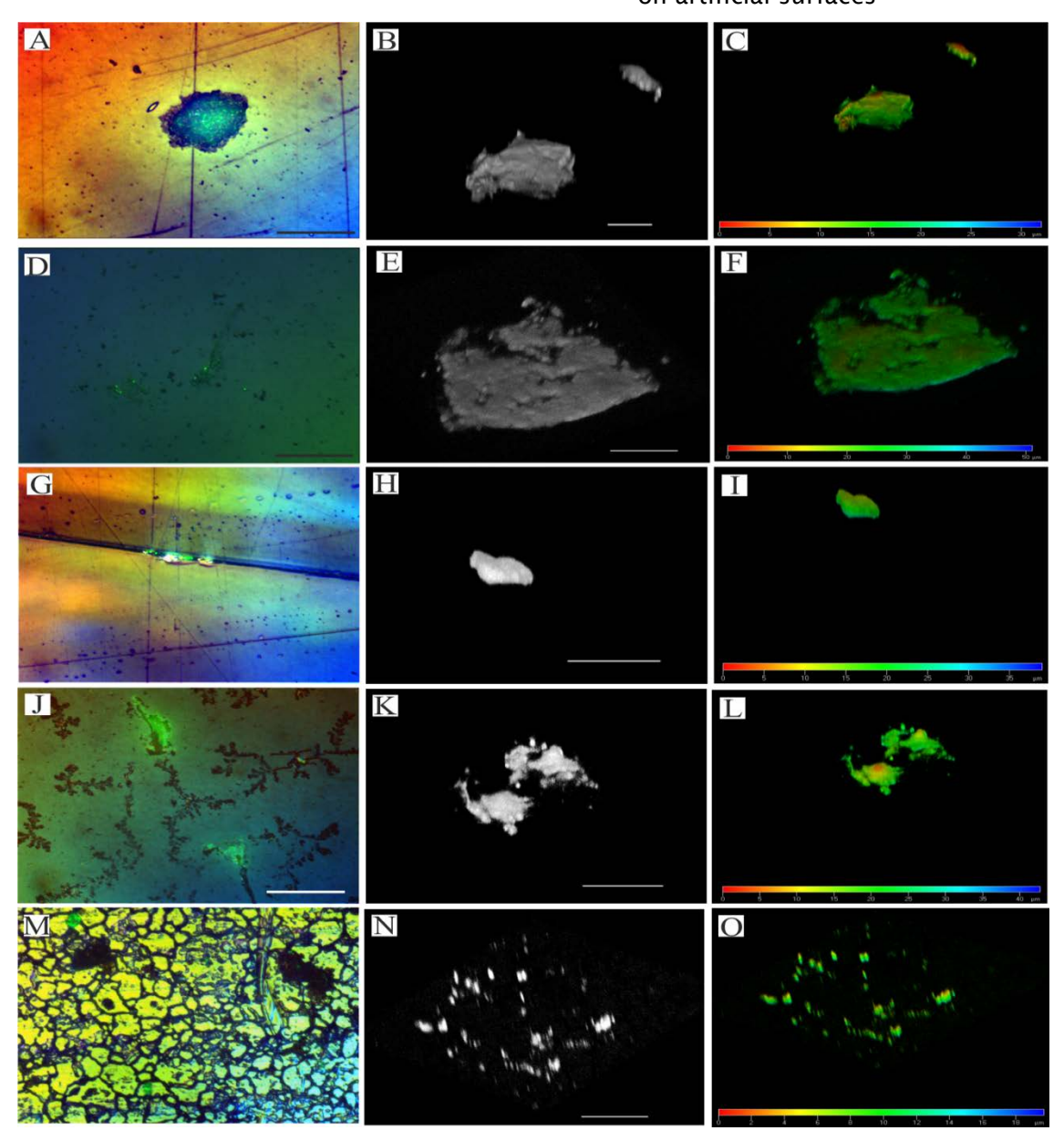


Figure 4.18: Microscopic images of biofouling on artificial surfaces after 23 month deployment on mooring II at 4,700 m in the biofouling tube simulating interior of sensor by pre-filtering the seawater through a 50 μm nylon mesh; (A) COC; overlay of EDIC and epifluorescence images; (B) as A; Laser Scanning Confocal Microscopy image; (C) as A; Laser Scanning Confocal Microscopy image with depth range colouring; (D) COP; overlay of EDIC and epifluorescence images; (E) as D; Laser Scanning Confocal Microscopy image with depth range colouring; (G) PMMA; overlay of EDIC and epifluorescence images; (H) as G; Laser Scanning Confocal Microscopy image; (I) as G; Laser Scanning Confocal Microscopy image with depth range colouring; (J) glass; overlay of EDIC and epifluorescence images; (K) as J; Laser Scanning Confocal Microscopy image; (L) as J; Laser Scanning Confocal Microscopy image with depth range colouring; (M) steel; overlay of EDIC and epifluorescence images; (N) as M; Laser Scanning Confocal Microscopy image; (O) as M; Laser Scanning Confocal Microscopy image with depth range colouring; A D G J M: scale bar 100 μm; B, E, H, K, N scale bar 20 μm

Chapter 4: Development of biofilms on artificial surfaces

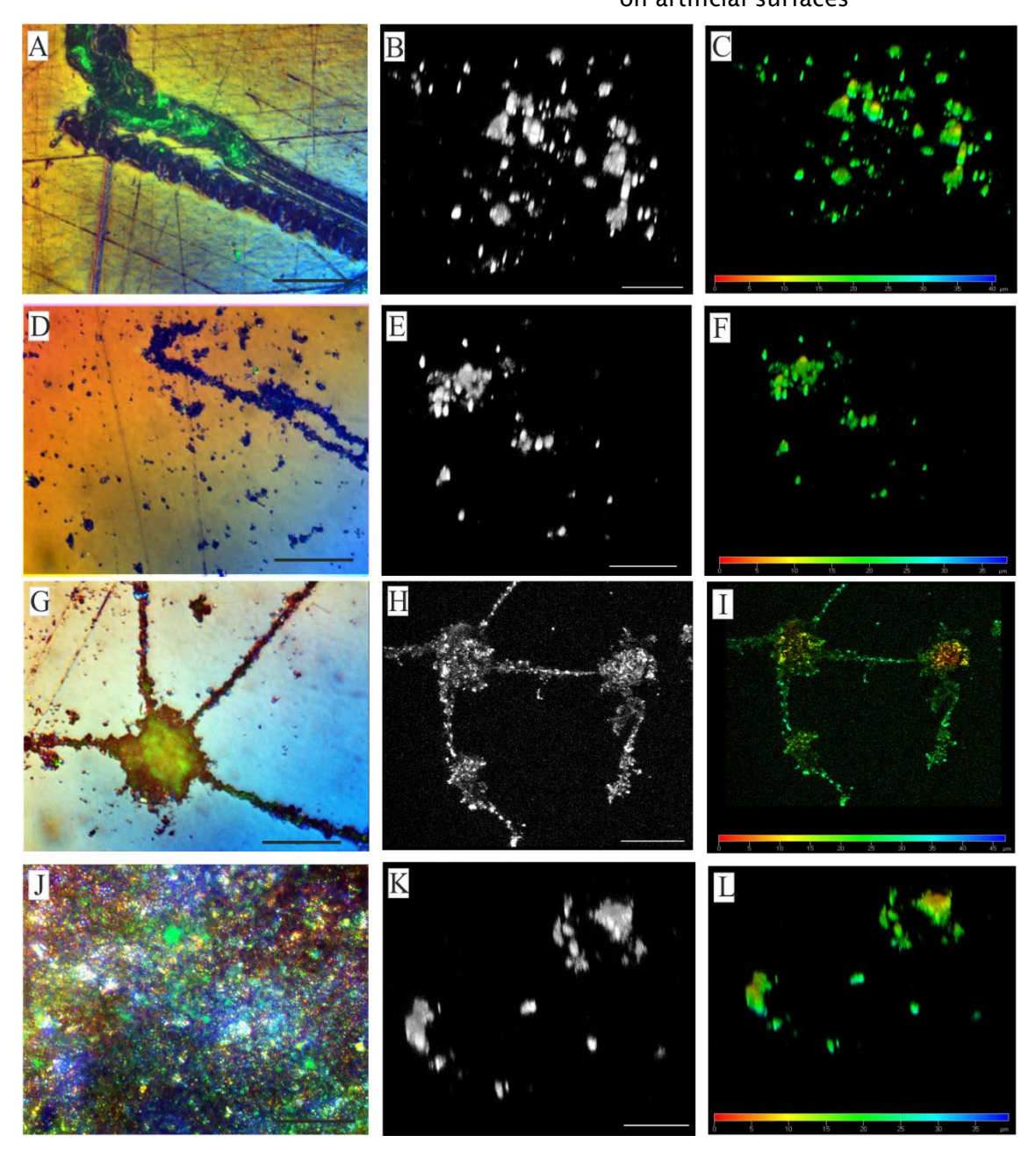


Figure 4.19: Microscopic images of biofouling on artificial surfaces after 23 month deployment on mooring II at 4,700 m in the biofouling box simulating exterior of sensor;

(A) Delrin; overlay of EDIC and epifluorescence images; (B) as A; Laser Scanning Confocal Microscopy image; (C) as A; Laser Scanning Confocal Microscopy image with depth range colouring; (D) PMMA; overlay of EDIC and epifluorescence images; (E) as D; Laser Scanning Confocal Microscopy image with depth range colouring; (G) glass; overlay of EDIC and epifluorescence images; (H) as G; Laser Scanning Confocal Microscopy image with depth range colouring; (J) copper; overlay of EDIC and epifluorescence images; (K) as J; Laser Scanning Confocal Microscopy image with depth range colouring; A D G J scale bar 100 μm; B, E, H, scale bar 20 μm

Chapter 4: Development of biofilms on artificial surfaces

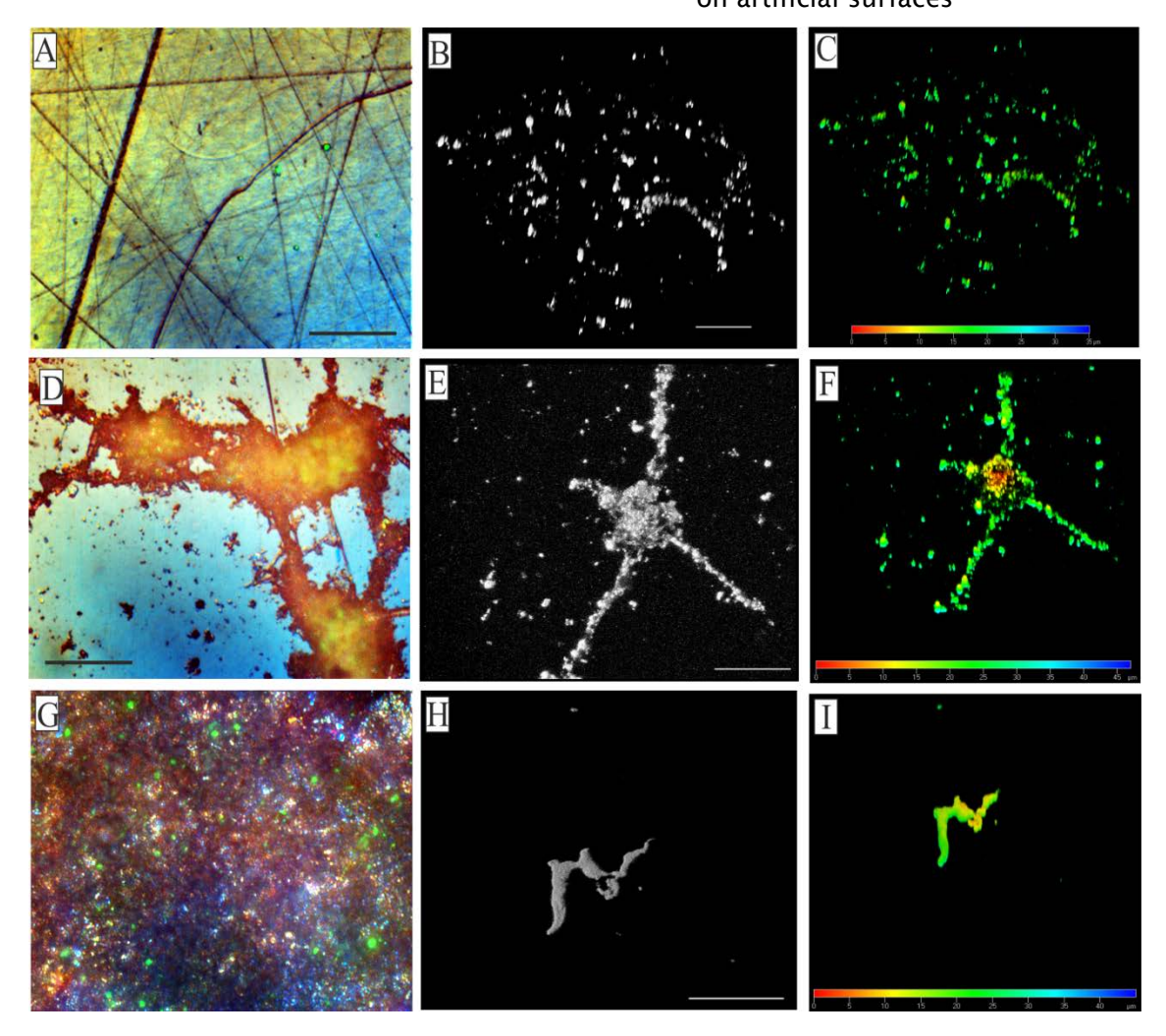


Figure 4.20: Microscopic images of biofouling on artificial surfaces after 23 month deployment on mooring III at 4,700 m in the in the vicinity of the BeeBe vent field; (A)

Delrin; overlay of EDIC and epifluorescence images; (B) as A; Laser Scanning Confocal Microscopy image; (C) as A; Laser Scanning Confocal Microscopy image with depth range colouring; (D) glass; overlay of EDIC and epifluorescence images; (E) as D; Laser Scanning Confocal Microscopy image with depth range colouring; (G) copper; overlay of EDIC and epifluorescence images; (H) as G; Laser Scanning Confocal Microscopy image with depth range colouring; A D G scale bar 100 μm; B, E, H, scale bar 20 μm

Chapter 4: Development of biofilms on artificial surfaces

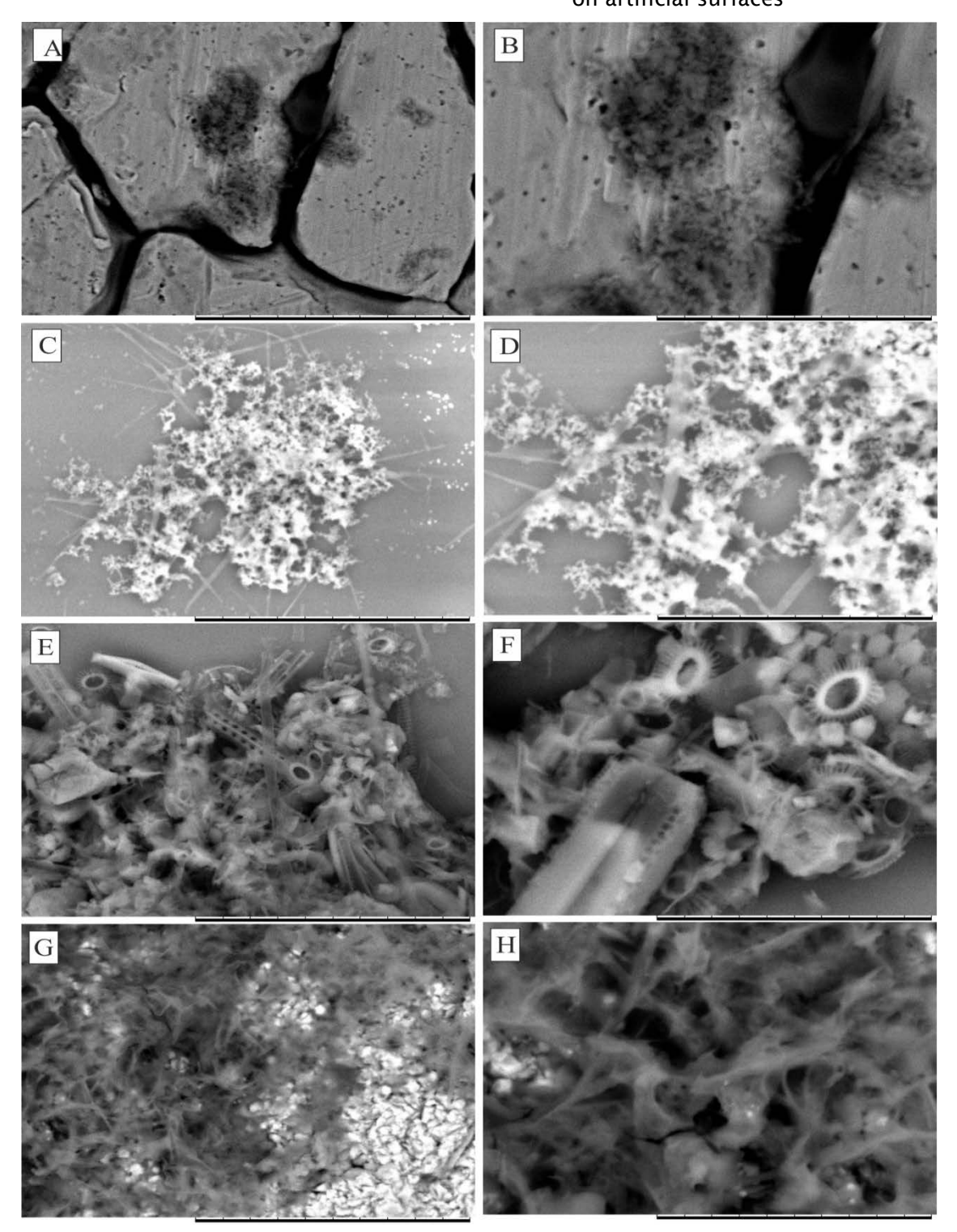


Figure 4.21: Scanning electro-micrographs of engineering surfaces deployed on mooring II for 23 month at 4,700 m; (A) steel simulating the interior of sensors by prefiltering water through a 50 μm nylon mesh, magnification 5,000x (B) as A with 10,000x magnification (C) glass simulating the interior of sensors by pre-filtering water through a 50 μm nylon mesh, magnification 5,000x (D) as C with 10,000x magnification (E) Glass simulation of sensor exteriors; magnification 5,000x (F) as E with 10,000x magnification (G) copper simulating the exterior of sensors; magnification 5,000x (H) as G with 10,000x magnification. Scalebar at 20 μm or 10 μm for 5,000x and 10,000x magnification respectively

Chapter 4: Development of biofilms on artificial surfaces

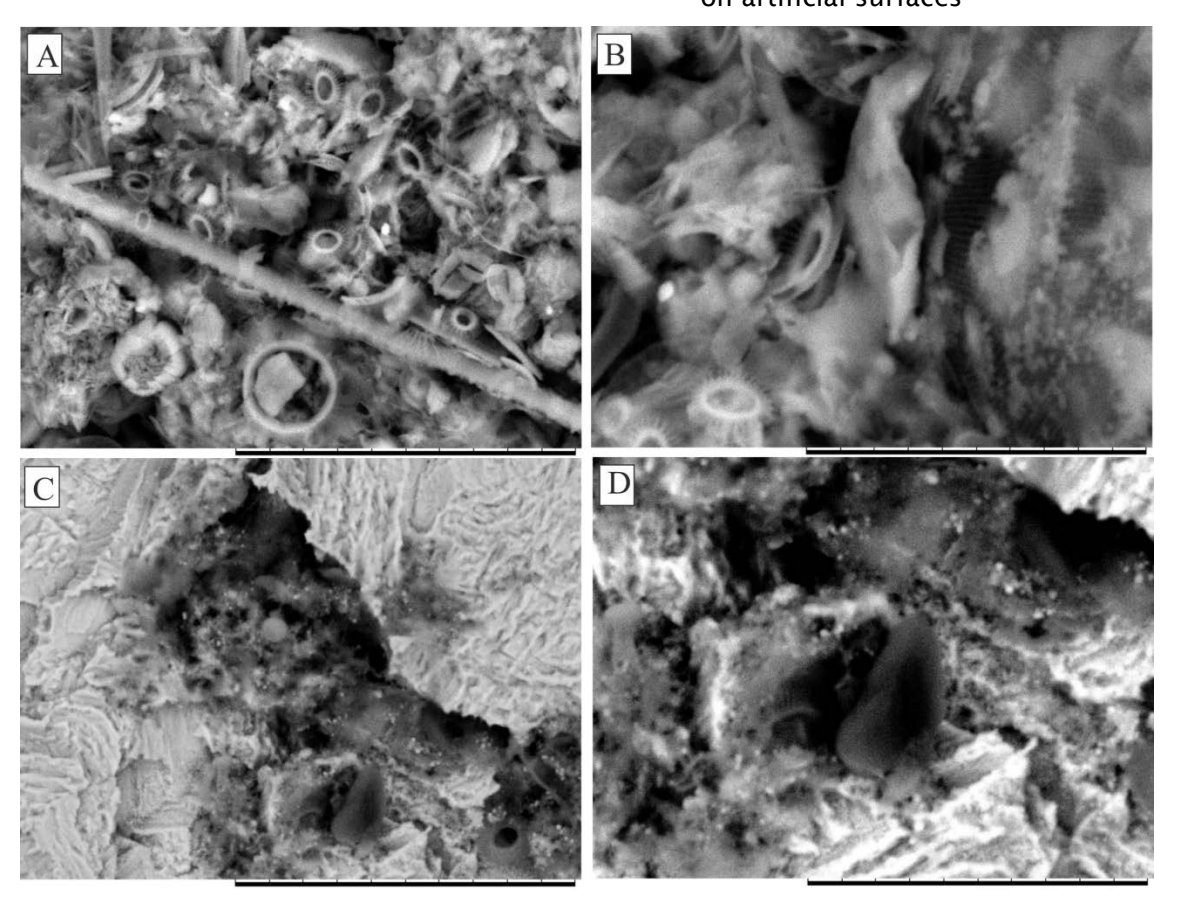


Figure 4.22: Scanning electro-micrographs of engineering surfaces deployed on mooring III for 23 month at 4,700 m within the vicinity of the BeeBe vent field; (A) Glass simulation of sensor exteriors; magnification 5,000x (B) as A with 10,000x magnification (C) copper simulating the exterior of sensors; magnification 5,000x (D) as C with 10,000x magnification. Scalebar at 20 μ m or 10 μ m for 5,000x and 10,000x magnification respectively

The SEM images showed a clear structural difference between the biofilm on the glass substrates simulating the interior and the exterior (Figure 4.21: C, D, E, and F, Figure 4.22: A and B). As mentioned before on the glass slides simulating the exterior diatoms, Cocolithiphore plates and other planktonic debris was incorporated into the biofouling matrix. On the steel substrate biofilm structures seem to be associated with pitting of the metal surface.

Quantification using fluorescence images

The biofouling surface coverage on all of the substrates of mooring II ranged between 4 and 5% except for DelrinTM and copper which were $12.7\% \pm 2.7$ and $18.2\% \pm 4.4$ respectively (Figure 4.23). Again Single ANOVA factor with subsequent post hoc comparison showed no significant difference between the fouling coverage of the substrates from inside the Biofouling Tube and Box (Table 4.5.). The only exception found to show significant differences included the DelrinTM and copper samples.

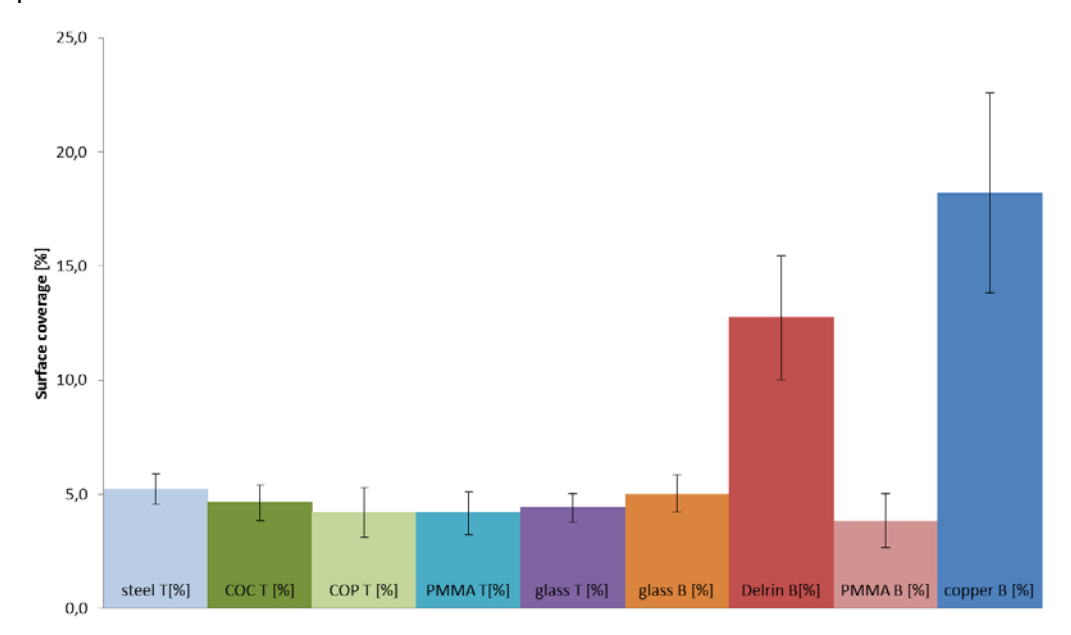


Figure 4.23: Biofilm surface coverage as indicator for biomass on engineering surface deployed for 23 months at 4,700 m (Mooring II); copper B, Delrin B, PMMA B and glass B simulating the exterior of sensors; steel T, COC T, COP T, PMMA T and glass T simulating the interior of sensors

The mooring under the influence of the hydrothermal vent field showed a different surface coverage of the materials compared to the mooring outside. Here the coverage of the glass $(9.6\% \pm 2.2)$ was approximately twice of that found on mooring II (5.0 ± 0.8) . The opposite trend could be found for the DelrinTM and copper surface coverage; $4.6\% \pm 0.9$ compared to 12.7 ± 2.7 and 12.3 ± 4.5 compare to 18.2 ± 4.4 (Figure 4.24).

Chapter 4: Development of biofilms on artificial surfaces

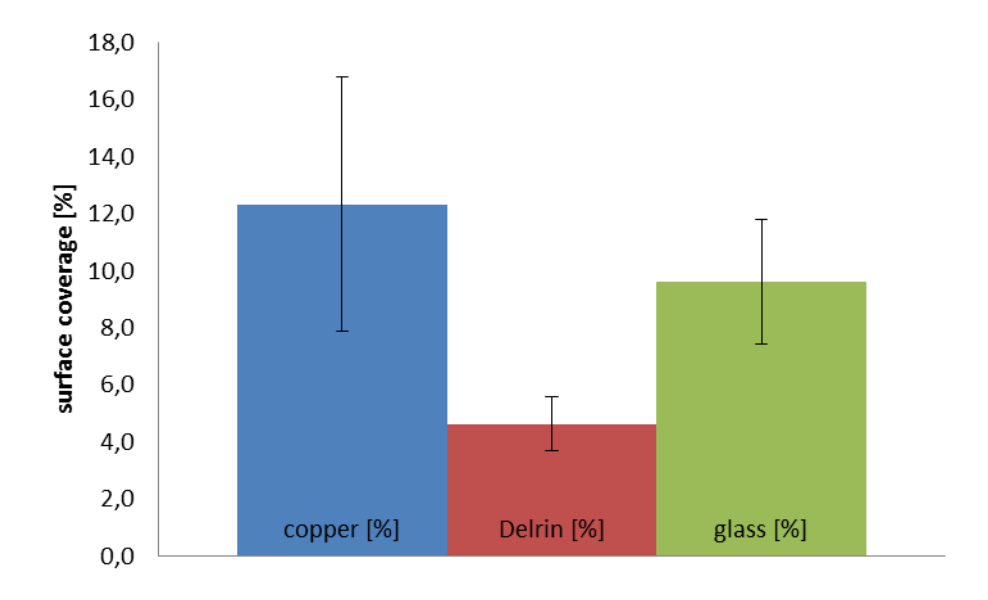


Figure 4.24: Biofilm surface coverage as indicator for biomass on engineering surface deployed for 23 months at 4,700 m in the vicinity of the Beebe bent field (Mooring III); materials deployed copper, Delrin, and glassin a holder simulating the exterior of sensors

Single factor ANOVA analysis with subsequent post hoc comparison showed significant difference in the surface coverage between all substrate on mooring III (Table 4.5).

Table 4.5: Single factor ANOVA with subsequent post hoc comparison results of the biofilm coverage determined by the quantification of fluorescence images of surfaces

	P-value	P (T ≤ t)	F crit	Significance
		two tailed		
ANOVA including all	1.7711E-		2.05488	
samples mooring II	33			
Steel vs. COC		0.082559		Not
				significant
Steel vs. COP		0.106358		Not
				significant
Steel vs. PMMA tube		0.077522		Not
				significant
Steel vs. PMMA box		0.015831		Not
				significant
Steel vs. glass tube		0.056867		Not
				significant
Steel vs. glass box		0.20144		Not
				significant
Steel vs. copper		0.003537		Significant
Steel vs. Delrin		6.95E-10		Significant

Chapter 4: Development of biofilms on artificial surfaces

	P-value P(T ≤ t)	F crit	Significanc
	two tailed		
COC vs. COP	0.712341		Not
			significant
COC vs. PMMA box	0.666095		Not
			significant
COC vs. glass tube	0.731429		Not
			significant
COC vs. glass box	0.550864		Not
			significant
COC vs. copper	0.000857		Significar
COP vs. PMMA tube	0.740656		Not
			significant
COC vs. Delrin	2.59E-11		Significar
COP vs. PMMA box	0.328368		Not
			significant
COP vs. glass tube	0.480799		Not
			significant
COP vs. glass box	0.770197		Not
			significant
COP vs. copper	0.001018		Significa
COP vs. Delrin	1.44E-11		Significar
PMMA tube vs. PMMA box	0.599834		Not
			significant
PMMA tube vs. glass tube	0.686021		Not
			significant
PMMA tube vs. glass box	0.566906		Not
			significant
PMMA tube vs. copper	0.000861		Significar
PMMA tube vs. Delrin	1.8E-11		Significar
PMMA box vs. glass tube	0.990097		Not
			significant
PMMA box vs. glass box	0.235925		Not
_			significant
PMMA box vs. copper	0.000562		Significar
PMMA box vs. Derlin	3.02E-12		Significar
Glass tube vs. glass box	0.371819		Not
-			significant
Glass tube vs. copper	0.000689		Significar
Glass tube vs. Delrin	3.71E-11		Significar
Glass box vs. copper	0.001288		Significar
Glass box vs. Delrin	3.91E-11		Significar

Chapter 4: Development of biofilms on artificial surfaces

	P-value	$P(T \le t)$ two tailed	F crit	Significance
Delrin vs. copper		0.524934		Not
				significant
ANOVA including all samples mooring III	3.8913E- 07		3.35413	
Copper vs. Delrin		2.74E-09		significant
Copper vs. glass		0.12051 9		significant
Delrin vs. glass		5.9E-06		significant

After combining the surface coverage with the estimated biofilm thickness and then comparing it with the short-term mooring samples, either the coverage of the surface (copper sample) or the thickness increased on the long-term mooring samples (Table 4.6).

Table 4.6: Comparison of surface coverage and biofilm thickness of short-term and long-term mooring samples

Material _	surface coverage [%]		Biofilm thickness [µm]	
materiai <u> </u>	Mooring I	Mooring II	Mooring I	Mooring II
glass	~10	4.4 & 5	10	25
PMMA	4.65	4.2	4-6	20
Delrin™	12.62	12.7	5	20
copper	3.62	18.2	30	30-35

This confirms the initial visual impression of the microscopic analysis of an increase of the biofouling on the long-term samples.

Molecular Analysis

Using the Pico Green assay the DNA concentration of the extracts of all substrate deployed in the Deep-Sea lied between 7.66 and 17.18 $ng/\mu l$ (Table 4.7), showing surprisingly no large variation between the short-term and the long-term moorings.

Table 4.7: Concentrations [ng/µl] of DNA extracts using Pico Green Assay

	Mooring I	Mooring II	Moring III
PMMA	11.22	8.14	
Tube	11.22	0.14	
СОР	9.07	9.02	
COC	9.14	8.42	
Glass	9.01	8.84	
Tube	9.01	0.04	
steel	8.70	8.44	
PMMA Box	8.32	8.73	
Delrin		8.10	8.31
Glass Box	9.31	15.53	17.18
copper	8.49	7.75	7.66

In most samples the concentrations of PCR products were below detection limit of the Bioanalyzer (Table 4.8), so that using the quantification as indicator for the initial DNA concentration was not feasible. But when above the detection limit the concentrations of the PCR products were higher than for the short-term mooring samples.

Table 4.8: Results for PCR amplification using DNA 7500 Assay (Bioanalyzer, Agilent)

	Ва	cteria	Ai	rchea	Eu	karya
Material	Peak	Conc	Peak	Conc	Peak	Conc
	Size [bp]	. [pg/µl]	Size [bp]	. [pg/µl]	Size [bp]	. [pg/µl]
PMMA Box	n/a	n/a	n/a	n/a	n/a	n/a
MooII	,	,	,	,	,	.,
PMMA	n/a	n/a	n/a	n/a	n/a	n/a
Tube Mooll	, \	, \	, a	, &	, a	, u
Glass Box	n/a	n/a	n/a	n/a	n/a	n/a
MooII	11/ α					
Glass	1567	640	665	970	n/a	n/a
Tube Mooll	1307	040	003	370	11/ α	11/ α
COP MooII	497	4600	666	610	n/a	n/a
COC Mooll	1406	400	666	740	n/a	n/a
Delrin	n/a	n/a	663	680	n/a	n/a
MooII	11/α	11/α	003	080	11/α	11/α
Copper	378	690	n/a	n/a	n/a	n/a
MooII	370	090	11/α	11/α	11/α	11/α
Steel	1396	850	648	460	n/a	n/a
MooII	1544	1350	665	1630	n/a	n/a
Glass	n /a	n /a	n/2	n / 2	n/2	n /a
MooIII	n/a	n/a	n/a	n/a	n/a	n/a
Copper	275	920	n /s	n / c	n /s	n /s
MooIII	375	820	n/a	n/a	n/a	n/a
Delrin	375	670	657	650	n/a	n/a
MooIII	1438	610	n/a	n/a	n/a	n/a

DGGE

Between 15 and 25 clearly separated bands could be distinguished on the DGGE gel for the samples deployed on mooring II (Figure 4.25). Samples deployed on mooring III in the vicinity of the Beebe hydrothermal vent field 12 to 20 separated bands could be identified (Figure 4.25). The different band pattern observed between Moo II and Moo III indicating different community structure; Moo II with more bands than Moo III indicates lower diversity in biofilm community at the vent field. Unfortunately no bands could be detected for both cooper samples.

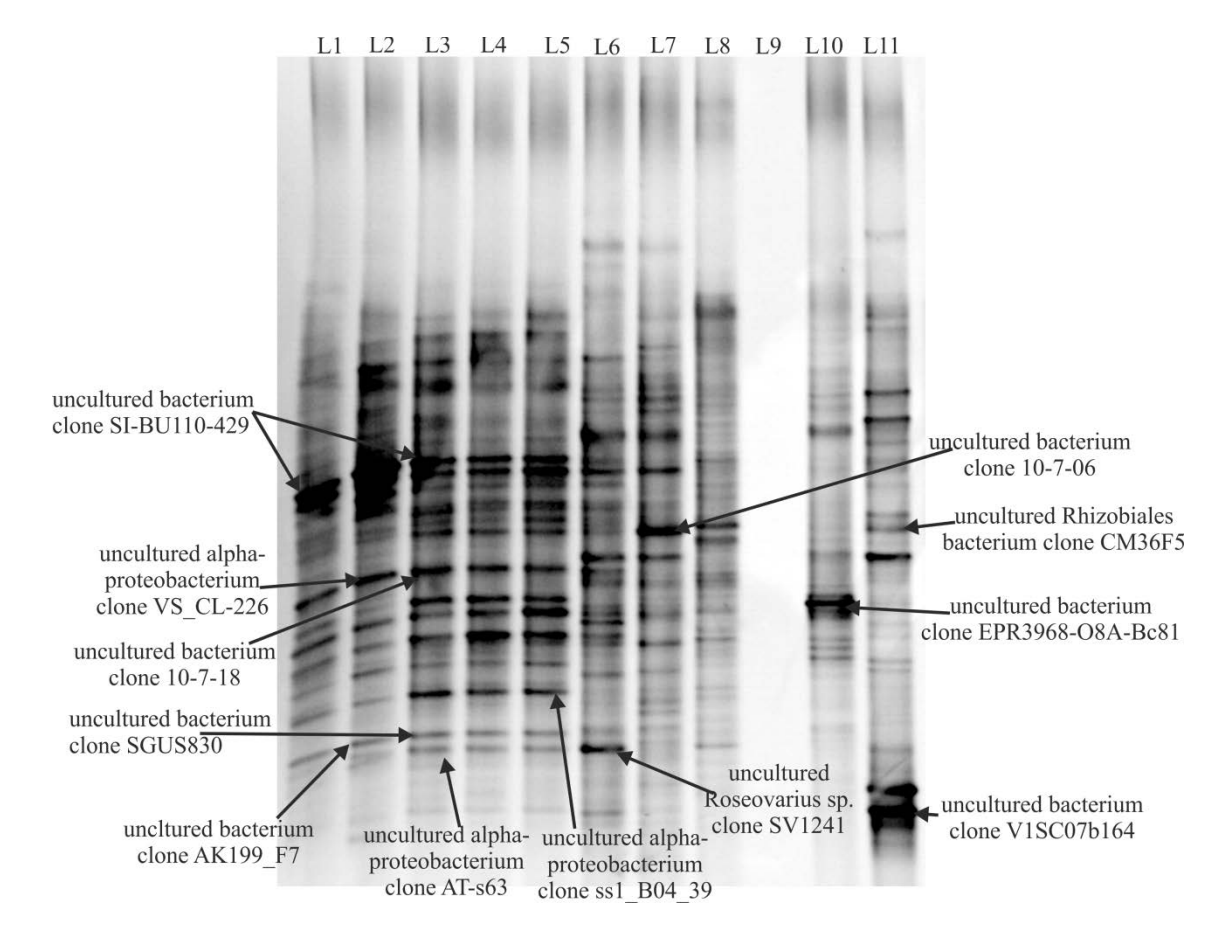


Figure 4.25: Image of DGGE gel from extracted DNA from different engineering surface 23 month deployment at 4,700 m; (L1) glass; (L2) PMMA; (L3) COP; (L4) COC; (L5) steel; (L6) glass simulating the exterior of sensors; (L7) PMMA; (L8) Delrin; (L9) copper; L1-L5 simulating the interior of sensors by pre-filtering water through a 50 µm nylon mesh; L6-L9 simulating the exterior of sensors; (L10) glass in the vicinity of BeeBe vent field; (L11) Delrin in the vicinity of BeeBe vent field; arrows point to the extracted and sequenced bands with the aliment match found in the online aliment software BLAST

As before for the presented alignment matches of the sequencing results (Figure 4.25) the 'expect' value was less than 1 to ensure the exclusion of random matches (Table 4.9).

Chapter 4: Development of biofilms on artificial surfaces

Table 4.9: Closest alignment match to 16S rDNA sequence of extracted DGGE bands from long-term moorings

Material	Closest	Accession	%	Expect	Source
	alignment	number	Identity	value	
	match				
Glass	uncultured	JN172482	100	4e-60	methanotrophic
Tube/COP	bacterium clone		98	1e-55	communites of
MOOII	SI-BU110-429				Saanich
PMMA	uncultured α -	FJ497475	99	3e-50	Vailulu'u
Tube	proteobacterium				Seamount,
MOOII	clone VS_CL226				American Samoa,
					South Pacific
	uncultured	JQ256816	99	2e-42	tidal surface
	bacterium clone				sediment,
	AK199_F7				Germany
COP	uncultured	JN18512	99	2e-52	Gulf of Mexico
MOOII	bacterium clone				stable isotope
	10-7-18				probing
					incubations
	uncultured	FJ202722	100	4e-44	coral
	bacterium clone				Montastraea
	SGUS830				faveolata kept in
					aquarium for 23
					days
	uncultured α -	AY225602	99	8e-46	Mid-Atlantic
	proteobacterium				Ridge
	clone AT-s63				hydrothermal
					sediment
Steel	uncultured α -	EU050748	99	2e-47	sediment from
MOOII	proteobacterium				the Kings Bay,
	clone ss1_B04_39				Svalbard, Arctic
Glass Box	uncultured	JG859027	96	4e-44	marine sample
MOOII	Roseovaruis sp.				
	clone SV1241				
PMMA Box	uncultured	JN018510	100	5e-54	Gulf of Mexico
MOOII	bacterium clone				stable isotope
	10-7-06				probing
					incubations

Chapter 4: Development of biofilms on artificial surfaces

Material	Closest	Accession	%	Expect	Source
	alignment	number	Identity	value	
	match				
Glass	uncultured	EU491749	98	9e-57	seafloor lavas
MOOIII	bacterium clone				from the East
	EPR3968-O8A-				Pacific Rise
	Bc81				
Delrin	uncultured	AM936321	98	3e-40	pilot-scale
MOOIII	Rhizobiales				bioremediation
	bacterium clone				process of a
	CM36F5				hydrocarbon-
					contaminated
					soil
	uncultured	HQ153987	98	4e-50	white
	bacterium clone				filamentous
	V1SC7b164				microbial mat in
					the photic zone
					of a shallow
					hydrothermal
					vent, Volcano 1,
					South Tonga Arc
					at a depth of
					115.3 m

100% identity matches were found to the uncultured bacterium clones SI-BU110-429 original source the methanotrophic community of Saanich Inlet, British Columbia, Canada (Sauter et al., 2012), SGUS830, found on the Caribbean coral *Montastraea faveolata* (Sunagawa et al., 2009), and 10-07-06, with the gulf of Mexico as origin (Redmond and Valentine, 2012).

Also found were 99% sequence similarities to the uncultured α -proteobacteria clones VS_CL226, originating on the Vailulu seamount (Sudek et al, unpublished), AT-s63, found in the Rainbow hydrothermal sediment, Mid-Atlantic Ridge (Lopez-Garcia et al., 2003) and ss1_B04_39, from the Kings Bay sediment, Svalbard, Artic (Tian et al., 2009); as well as to the uncultured bacterium clones Akk199_F7, isolated from a tidal surface sediment, and 10-7-18, gulf of Mexico ((Redmond and Valentine, 2012).

The uncultured bacteria clones ERP 3968-O8A-Bc81, seafloor lavas from the East Pacific Rise ((Santelli et al., 2008) and V1SC7b164, microbial mat of a shallow hydrothermal vent, South Tonga Arc (Murdock et al, unpublished), and to the

uncultured Rhizobales bacterium clone CM36F5 (Militon et al., 2010) showed a 98% match to sequences isolated from DGGE gel.

Additionally a 96% match was found to the uncultured Roseovarius sp. clone SV1241 (Pinhassi & Fahlgren, unpublished).

Rhizobiales as Roseovarius are also subgroups of the α -proteobacteria.

4.4 Discussion Biofouling in the Deep-Sea

4.4.1 Microscopic Analysis

The combination of multiple microscopic techniques for the structural analysis of biofilms gives a more comprehensive insight as they complement each other and increase the recognition of artefacts (Surman et al., 1996).

In this study all microscopic analysis showed significant biofouling of all material surfaces, including copper, even after 10 day deployment in the Cayman Trough at a depth of 4,700 m (mooring I). Finding biofilm formation on the copper surface was surprising as an earlier study Guezennec and colleagues found no bacterial settlement after 9 days in the deep-sea on their copper and aluminium samples outside the influence of the hydrothermal vent fluids of the Snake Pit site, Mid-Atlantic Ridge (Guezennec et al., 1998). This could either mean that our mooring site was somehow under the influence of hydrothermal fluids or that the Cayman Rise deep-sea environment contains microbes more resilient to copper.

After 23 month in the deep-sea the corrosion of the steel surface showed a similar pattern in the SEM images as Cu-Ni alloys after the removal of a 42 day old biofilm. Yuan and colleagues concluded bacterial clusters and discrete biofilm being the cause for the severe pitting of the surface of 70/30 Cu/Ni alloys (Yuan et al., 2007). The SEM images of the copper substrate deployed on mooring II demonstrated a similarity to ESEM images of bacteria within sulphide corrosion layers on commercially pure copper foil in a four month old biofilm examined by Little and colleagues (Little et al., 1991). This observation is in agreement with the statement of a typical biofilm morphology of all copper-containing materials colonized by sulphate-reducing bacteria (SRB) (Little et al., 1991), and leads to the conclusion that the biofilms examined in this project might also contain SRB.

Also while copper alloys prevent or delay the settlement of macrofoulers, microfoulers, such as bacteria, microalgae and protozoa were found to form a slime layer on copper containing surfaces in marine environments to a certain extent (Little et al., 1991, Little and Mansfeld, 1991, Yuan et al., 2007).

Considering the results from the <u>quantification of biofilm coverage</u> after 10 days copper still appears to be the most resistant to biofilm formation even in this extreme environment. PMMA seems to have a similar fouling resistance, whereas

Delrin™ to have the least resistance to fouling. PMMA showing less fouling than glass has been demonstrated before and might be a result of an increased solubility of PMMA in seawater than glass (Kerr, 1998). This increased solubility might lead to a constant renewal of the surface and as such constant removal of the biofilm. But it is surprising that the fouling resistant appears to be similar to copper, which is a toxic metal. The inhibitory effect of copper on microorganisms has been demonstrated in various studies and is currently being studied for its application for surfaces in hospital environments (Wilks et al., 2005, Domek et al., 1984, Rogers et al., 1994a, Rogers et al., 1994b). Several copper alloys have been tested for their antifouling properties, especially in hospital environments due to the emergence of antibiotic resistant pathogens and might also be applicable as mitigation techniques in marine environments (Casey et al., 2009, Weaver et al., 2008, Wilks et al., 2005, Wilks et al., 2006, Pichette et al., 2007, Valcarce et al., 2002).

Finding no significant biofouling difference after a 23 month deployment on the glass and steel samples might indicate a similar fouling rate of these two materials especially since Kielemoes showed no significant difference in the amount of microorganisms after an eight week growth period (Kielemoes, 2001).

The production of EPS (organic slime) in biofilms is significantly increased in the presence of toxic metals, e.g. copper, (Marszalek et al., 1979, Fang et al., 2002). An increased EPS production might explain the bright fluorescence on copper after a 10 days (Figure 4: M) as the extracellular matrix contains eDNA for stabilization of its structure (Flemming, 2008). It also explains finding the thickest biofilm features on the copper surface. The differences in the biofilm thickness and the surface coverage between glass and copper indicate a change in the 3D spatial organisation of biofilm between these two substrates. The increased thickness of the biofilm found on copper might be a protective mechanism to evade the toxicity of the substrate surface.

The increased EPS production might also allow a continuous spreading of the biofilm and thus explain the increased surface coverage after 23 month on the copper sample on mooring II compared to the other substrate except Delrin™.

Apparent differences in the severity of biofouling seem to be related to the smoothness of the surface. Finding a correlation between the surface roughness and the severity biofilm formation is in accordance with the findings of Kerr and colleagues that smoother materials support less fouling (Kerr et al., 2001, Fang et al., 2000, Fang et al., 2002). Dürr showed that on stainless steel not only the surface roughness but also the contact angle as a measurement for the hydrophobicity of the material influences bacterial adhesion (Dürr, 2007). This might also account partly for the apparent similarity of the fouling resistance of copper and PMMA in the early biofilm development, as the contact angle of flat PMMA of $67.8 \pm 1.4^{\circ}$ (Ma et al.,

2007) lies within the range of the contact angle reported for copper 39 to 77° (Hong et al., 1994). The variation in the reported angle measurements could be due to difference in the surface roughness as both are not completely independent of each other (Hong et al., 1994, Dürr, 2007).

In the 23 month biofilm the similarities in the biofilm coverage between the various plastics, with the exception of Delrin™, glass and steel might be a result of the evolution of the biofouling which might cover up the initial differences in the surface characteristics. The average surface coverage of Delrin did not change between 10 day and 23 month deployment at the same location, the biofilm grew only thicker. But in the vicinity of the hydrothermal vent the coverage of Delrin™ was more similar to that of the other plastics on mooring II. This reduction might be a result of chemical reactions of the material with the hydrothermal vent fluids changing the surface characteristic to be less favourable for biofouling. Such a reaction would also explain the difference in the fouling coverage of glass and copper on mooring II and III.

4.4.2 Molecular Analysis

The range of the extracted DNA between 5.4 and 17.18 ng μ l⁻¹ lies within the similar range that has been reported by Bellou and colleagues (3 to 16 ng μ l⁻¹), who performed a similar experiment in the eastern Mediterranean (Bellou et al., 2011).

Marszalek and colleagues found that whereas the predominant members on glass and steel changed over time, bacteria were found to be the dominant members of the fouling community in copper samples (Marszalek et al., 1979). This might indicate that the differences in the main kingdom found in the PCR products represent different stages in the early development of biofilms on the different surfaces.

DGGE

DGGE is a useful technique for the detection of changes in the predominant organisms of a microbial community (Cleary et al., 2012, Muyzer et al., 1993). The finding of only seven to ten distinctly separated bands in the short-term deployment samples are in in agreement with the observations of Muyzers and colleagues (1993) of between five and ten different bands in biofilm populations isolated from bacterial mats in Wadden Sea sediments and waste water treatment plants (Muyzer et al., 1993). The increase in the number of separated bands in the long-term deployment samples is not surprising as later stages in the fouling process with changes in and additions to the community is expected (Railkin, 2004, Yebra, 2004, Yebra, 2006).

Changes in the relative intensity of single bands and the DGGE band pattern indicate an influence of the material characteristic and the location (inside the Tube or Box) on the predominant species in the biofilm (Muyzer and Smalla, 1998). In conjunction with the PCR results for the short-term mooring samples these results indicate changes in the dominant microorganisms the results might point to different stages in the biofilm development (Characklis, 2009, Dang and Lovell, 2000) on the materials after 10 days. Unfortunately such a comparison was not possible for the long-term samples. But the samples simulating the sensor interior showed almost identical band patterns with the same intensities, indicating the same predominant microbes and a similar community composition. For the exterior samples a slight shift in the pattern and in some bands in the intensity could be detected, indicating a significant influence of the pre-filtering of the seawater on the biofilm community. But the most pronounced shift could be found between the 23 month biofouling deployed outside and inside of the hydrothermal vent field. The identification of less separated bands in the DGGE gel of the materials deployed under the influence of the hydrothermal vent field in comparison to the other materials deployed supports the hypothesis of hydrothermal vent communities to be characterized by lower microbial diversity than other less extreme environments, in this case the deep-sea (Van Dover, 2000, Tunnicliffe et al., 1998).

Bands at identical positions in the DGGE gel might represent fragments of identical sequence (Figure 4.13: bacterial clone RESET 213F07; Figure 4.25: uncultured bacterium clone SI-BUI110-429), but there might be exceptions as the separation is dependent on the melting behaviour of the DNA (Figure 4.13: bacterial isolate DGGE band 112; Figure 4.25) (Muyzer et al., 1993). The lack of detectable bands in the extracts of the copper substrates after 23 months could be explained by the DNA being degraded in the presence of copper (Warnes and Keevil, 2011).

All alignment matches of the sequencing results belong to uncultured microorganisms, most of which are not further classified. One extracted sequence of the 10 day biofilm could be associated with *Cowellia sp.*, while another with an *Alterominidaceae* bacterium. Both belong to the y-proteobacteria group.

All except for the coral associated bacteria were found in the extreme environment of the deep-sea. Finding a *Colwellia sp.* among the predominant organisms agrees with the discovery of fatty acids common to many psychrophilic species e.g.: *Pseudomonas sp.* and some *Colwellia/Vibrio sp.* in surface associated cells on the Mid-Atlantic Ridge (Guezennec et al., 1998).

In contrast most of the alignment matches found after 23 months belonged to the α -proteobacteria and none of the 10 day sequence matches were found. The original sources of the sequences found were either surface-associated (SGUS830) (Sunagawa et al., 2009), a white filamentous microbial mat (Murdock et al,

Chapter 4: Development of biofilms on artificial surfaces

unpublished), sediment samples; AT-s63 (Lopez-Garcia et al., 2003), EPR3968-O8A-Bc81 (Santelli et al., 2008), ss1_B04_39 (Tian et al., 2009) or soil sample *Rhizobiales sp.* (Militon et al., 2010).

Rhizobiales sp. was originally found in a soil with a high copper condense 9600 mg kg⁻¹, since this sequence match was found in the vicinity of the hydrothermal vent field it might indicate a link to a high tolerance to copper in this microbe.

The wide geographical spread of the alignment matches might indicate a global distribution of these organisms and a special adaptation to this extreme environment.

Chapter 5: Antifouling strategies

The aim of this project is to find a practical and effective strategy to prevent the biofilm formation on sensors, especially in the marine environment.

Most existing research (Chambers et al., 2006, Cowling, 2000, Kerr, 1998, Kerr et al., 2001, Hellio, 2001, Whelan and Regan, 2006, Yebra, 2006, Yebra, 2004) in the development of antifouling strategies is done with regard to commercial applications, such as in the shipping (Champ, 2001) or oil industries. Some of these existing methods might also be applicable or adaptable for sensors.

In this chapter an overview of the different existing strategies and their mode of operation are given in combination with a possible approach of which methods might be adaptable for the use in remote sensor technologies. In addition the results of several experiments in regard of the application of such mitigation strategies are described and discussed.

Antifouling strategies involve mechanical cleaning e.g. scrubbing the organisms off, the production of gas bubbles, self-polishing coatings, biocide releasing paints non-sticking materials, ultrasonic methods and the electrolysis of seawater (Railkin, 2004). Some of these strategies consume energy, these are categorised as active antifouling methods, others do not (e.g. paints and coatings) and these are passive methods. Both strategies are discussed in more detail below.

5.1 Passive Antifouling Strategies

The problem of fouling ship hulls and as such the development and application of antifouling techniques is as old as the history of shipping. One of the oldest known examples is the lead-sheathed timber from a Phoenician galley dated around 700 BC (Yebra, 2004, Dafforn et al., 2011). The ancient cultures used tar, wax, asphalt as well as copper sheathing and pitch to protect ship hulls. In the 5th century BC oil coatings containing arsenic and sulphur were developed. The Greeks and Romans protected their ships with lead sheaths with copper nails. Later variations of these ancient methods e.g.: various paint mixtures containing tar, grease sulphur, pitch and brimstone or lead, iron and copper either as sheaths or nails were used (Yebra, 2004). But all of these methods could solve the problem of biofouling only for a short period if at all.

In modern times the most successful and widespread antifouling method is the use of tributyltin self-polishing copolymer paints (TBT-SPC paints). Over 70% of the world's shipping fleet in 2006 was estimated to use these paints (Yebra, 2006, Chambers et al., 2006). In TBT-SPC paints TBT, which is a biocide, slowly leaches into the

environment by a controlled hydrolysis of the compound from the copolymer in the paint matrix (Yebra, 2004). These paints also have a self-polishing effect which means that over time the exposed layer is eroded by the movement of the water. This effect provides a low hull roughness in addition to exposing a new layer and thus replenishing the TBT available to leach into the water (Yebra, 2004). But severe adverse effects on the marine ecosystem have led the International Maritime Organisation to ban the use of TBT on ships (Champ, 2001). The global ban started in 2003 with the aim that the paints would be phased out in 2008 (Kristensen, 2008).

Antifouling paints use biocides or include metals like tin or copper, unfortunately most of them have been proven to show or are suspected to have similar adverse environmental impacts as TBT (Kristensen, 2008). One alternative studied is the use of enzymes, but here the preservation of the activity is the major concern. On the other hand copper-containing materials have been shown to foul at a slower rate than stainless steel surfaces; the composition of the micro-flora on copper surfaces was also found to be less diverse than on steel and glass surfaces (Mansfeld et al., 1994). The inhibitory effect of copper on microorganisms was demonstrated in various studies and is currently being studied for its application for surfaces in hospital environments (Wilks et al., 2005, Domek et al., 1984, Rogers et al., 1994c, Rogers et al., 1994d). Several copper alloys have been tested for their antifouling properties, especially in hospital environments due to the emergence of antibiotic resistant pathogens (Li et al., Casey et al., Weaver et al., 2008, Wilks et al., 2005, Wilks et al., 2006, Pichette et al., 2007, Valcarce et al., 2002). Wilks et al. found that copper nickels and copper nickel zinc alloys, so called copper silvers have a greater corrosion resistance, as well as showing a greater antibacterial activity in comparison to stainless steel (Wilks et al., 2005).

A new field of research is to identify natural antifouling methods and find analogues. A number of marine organisms are free of fouling, or have reduced fouling (Cowling, 2000) and it has been determined that the secondary metabolites of marine animals and seaweed are able to control fouling (Whelan and Regan, 2006, Webb et al., 2003). Some of these organisms use chemical defences, such as repellents or toxins, where others have modified surfaces to reduce fouling (Cowling, 2000, Gardella, 1997); over 160 natural antifouling substances have been identified (Chambers et al., 2006).

Natural chemical defences can include short-lived biocides, inhibitors of the Quorum Sensing capability of the bacteria, repellent compounds and enzymes (Kristensen, 2008). The screening of antifouling metabolites has shown that furanones are especially effective as they are thought to inhibit part of the quorum sensing pathway which in turn is thought to prevent the formation of biofilms (Whelan and

Regan, 2006). But the practical application of most of these substances is still not within reach.

It has been found that marine bacteria preferentially attach to surfaces with a hydrophobic low energy (Loeb and Neihof, 1975, Mueller et al., 1992), so surface modification of polymers are investigated as a possible means of antifouling (Kerr et al., 2001) In modifying the surface to be positively charged and high energy might result in the reduction of fouling (Loeb and Neihof, 1975). This assumption led to the development of hydrophilic polymer films mimicking natural occurring fouling resistant surfaces (Cowling, 2000). These films showed a lower level of fouling and are possible materials for providing a protective coating e.g. for the sensor casing.

5.2 Surface Modification

Initial adhesion of bacteria is crucial in the biofilm formation (Razatos et al., 1998). This step is mainly determined by the surface characteristics such as hydrophobicity, roughness, free energy, and electrostatic charge and the interactions are described by the Derjaguin-Landau-Verwey-Overbeek (DLVO) theory of colloidal stability (Norde and Lyklema, 1989, Mueller et al., 1992).

One approach to increase the fouling resistance of materials is to change their surface characteristics, since this plays a major role in its fouling resistance. In this section the influence of changed surface characteristics on the fouling resistance is examined on the example of COC. First surface modification by embedding copper compounds in the surface were examined. Secondly the fouling resistance of micro/nano-structured and plasma treated COC were analysed.

5.2.1 COC with embedded Copper, Copper(I) oxide, and Copper(II) oxide

As mentioned before materials containing copper have a higher fouling resistance and have a lower microbial biofilm diversity compared to glass or stainless steel (Mansfeld et al., 1994, Little et al., 1991). The growth inhibition of copper on microorganisms has been demonstrate in in several studies (Domek et al., 1984, Rogers et al., 1994b, Rogers et al., 1994d, Wilks et al., 2005). Copper surfaces exposed to the marine environment form a Cu₂(OH)₃Cl layer (North and Macleod, 1987). This and the dissolution of copper in seawater delays and/or prevents biofouling (Yebra, 2004, Little et al., 1991). The Cu²⁺ ion released by copper interfere with enzymes located on the cell membranes and transporter molecules interfering with the normal cell functions (Delauney and Ieee, 2009, Gillan, 2004, Delauney, 2009). It was also demonstrated that the presence of an oxide layer has a major influence on the attachment of microbes to metal surfaces (Valcarce et al., 2002).

Taking these studies into account the antifouling effectiveness of copper, copper(I) oxide, and copper(II) oxide embedded into COC samples was examined. These materials were deployed in the Solent for 14 days using a biofouling tube simulating the inside of a sensor.

Methods and Material

COC and COC embedded with copper, copper(I)oxide, and copper(II)oxide (manufacturing see Appendix) were deployed in the Solent for 14 days using a biofouling tube simulating sensor interior by pre-filtering water through a 50 µm Nylon mesh (Figure 4.6: A and B)

After retrieval samples were stained with CTC and DAPI. Visual inspection of the samples and fluorescent microscope showed a very high background for the DAPI stain on the COC sample (Figure 5.1: DAPI). To reduce the background all samples were additionally stained with SYTO©9.

The DNA was extracted, amplified using the Muy primer set, and run on a DGGE with subsequent sequencing as described afore in Chapter 2.

Results and Discussion

Microscopic Analysis

Visual inspection of the microscopic images seemed to indicate a difference in the biofilm formation, especially in the live cell stain of the copper embedded COC (Figure 5.1: CTC).

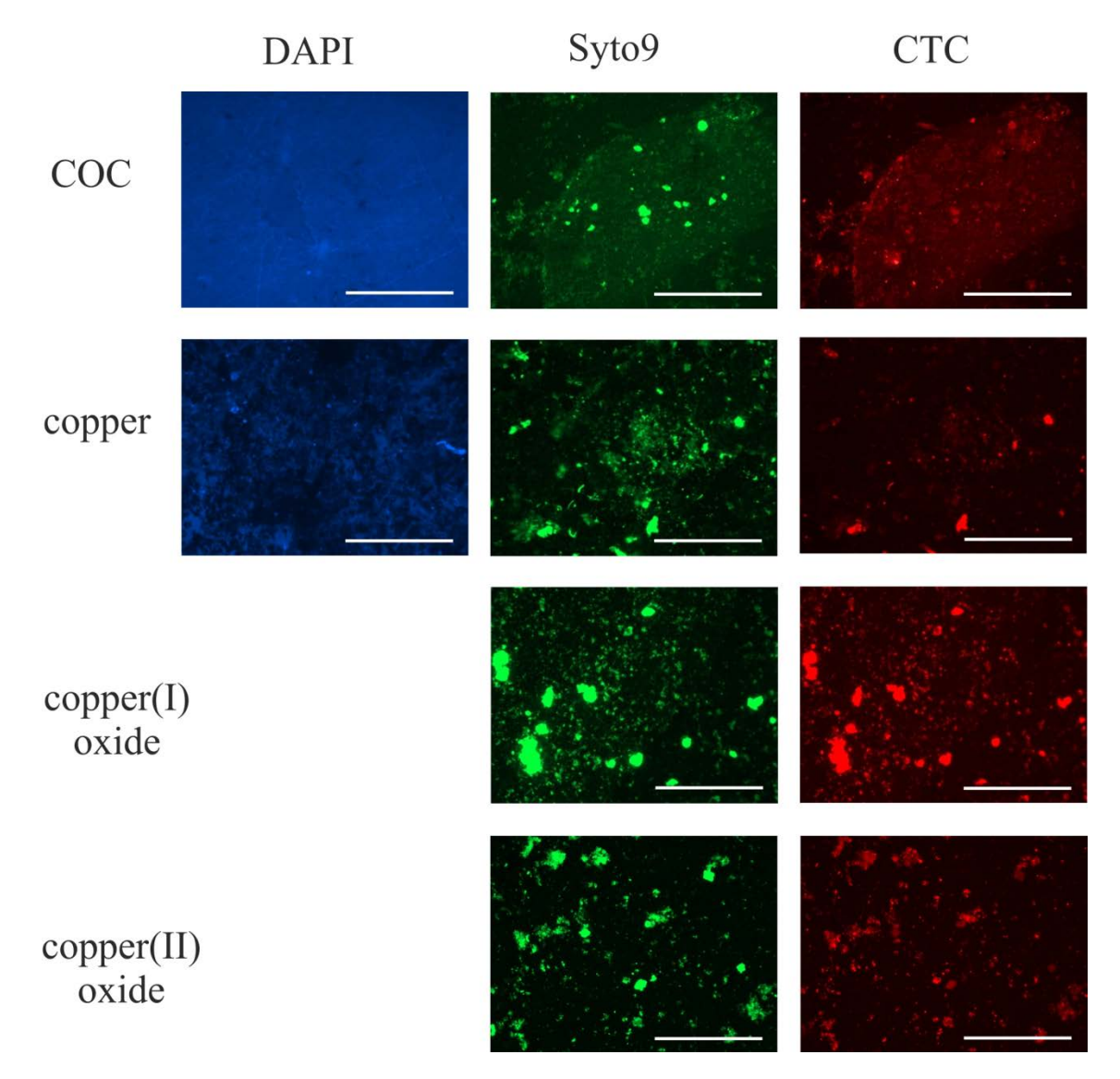


Figure 5.1: Images of COC, copper coated COC; COC coated with a layer of copper, COC coated with a layer of copper(I) oxide, and COC coated with a layer of copper(II) oxide after exposure of 14 days in the Solent and stained with CTC (red), DAPI (blue), and Syto©9(green); images were taken using the EVOSfI microscope with three different fluorescent filters, GFP, RFP, and DAPI and 10x magnification; scale bar 400 μm

Quantification of fluorescent images

Quantification of ten CTC fluorescent images showed the live cell coverage of the COC, Cu, and Cu₂O lied between 17.68 ± 8.78 , $16.18\pm5.53\%$, and $17.68\pm3.05\%$ respectively (Figure 5.2) with no significant difference (Table 5.1). The CuO embedded COC surface showed the lowest alive cell coverage $14.67\pm3.43\%$. This finding is in agreement with Cu²⁺ ions being responsible for the toxicity of copper (Delauney, 2009, Gillan, 2004).

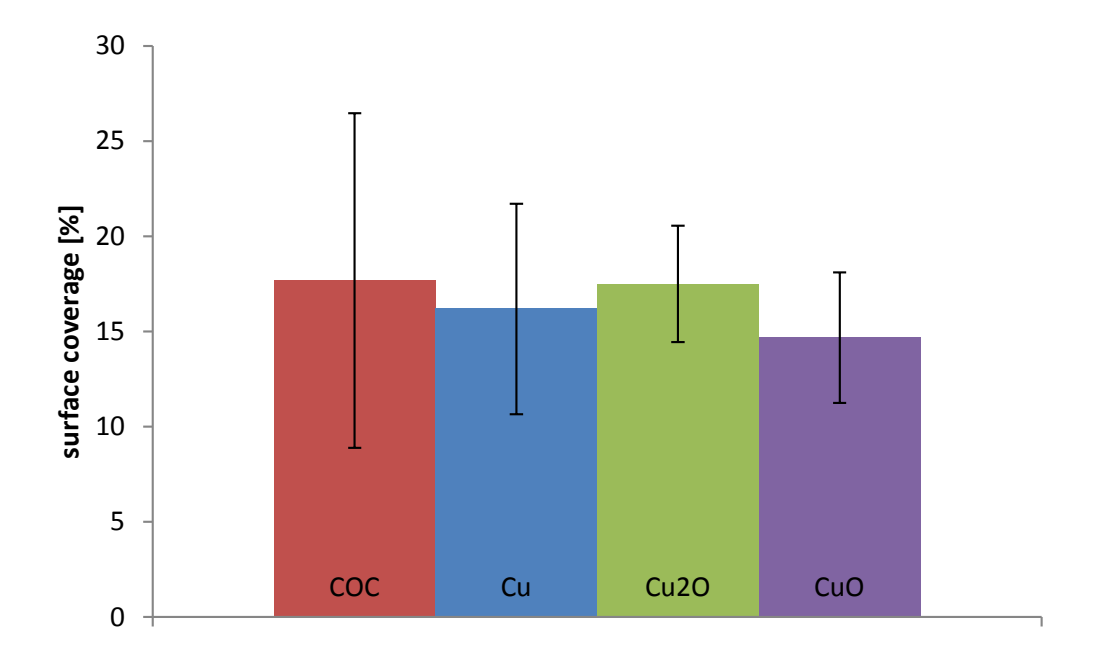


Figure 5.2: Average surface coverage of CTC stained COC and copper coated COC; COC coated with a layer of copper; COC coated with a layer of copper(I) oxide, and COC coated with a layer of copper(II) oxide after exposure of 14 days in the Solent; n=10

CuO also had the lowest total biofilm coverage, $24.13\pm6.6\%$ and copper the highest with $40.9\pm7.17\%$ (Figure 5.3). The COC surface coverage was the second lowest, $28.16\pm7.7\%$ and the Cu₂O the second highest, $37.72\pm10.35\%$. The high total biofilm coverage of the copper and Cu2O embedded COC might be due to an increased EPS production by the microbes. As the syto9 stain would also react with the eDNA contained in the extracellular matrix (Flemming, 2008), such an accumulation would be detected as an increased biofilm surface coverage. Biofilms have been shown to increase their production of EPS in the presence of toxic metals like copper (Fang et al., 2002, Marszalek et al., 1979).

The quantification of the microscope images could not confirm the visual inspection. This shows the importance of including a quantitative measurement of microscopic images.

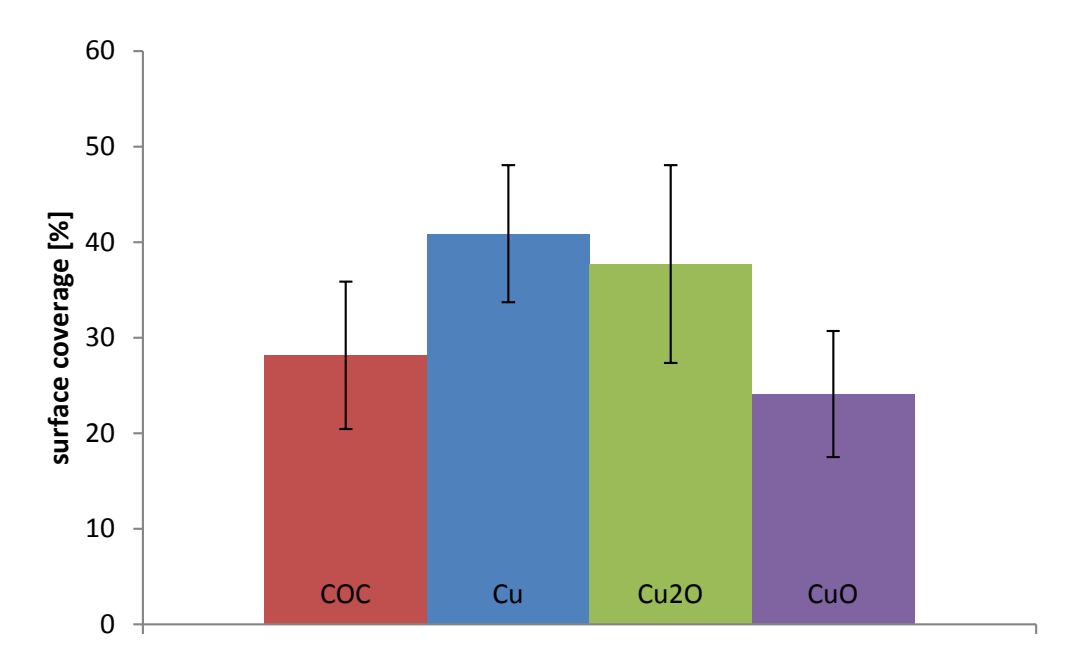


Figure 5.3: Average surface coverage of SYTO $^{\circ}$ 9 stained COC and copper coated COC; COC coated with a layer of copper, COC coated with a layer of copper(I) oxide, and COC coated with a layer of copper(II) oxide after exposure of 14 days in the Solent shows a significant variance (p=9,12E-05) between the materials; n = 10

When the ratio of alive cell coverage to total biofilm coverage was taken into account biofilms on COC and copper(I) oxide / COC composite contain about 40 of live cells where copper and copper(II) oxide / COC composites only have 46 and 61% respectively (Table 5.1). The lower percentage of live cells in the copper and copper(I)oxide embedded COC also indicates a higher EPS production of the microbes on these surfaces.

All samples demonstrated a statistical relevant change in the total biofilm coverage. The subsequent post hoc comparison showed significance differences in the coverage between all samples except between COC and copper(II)oxide and between copper and copper(I)oxide. The statistical analysis showed no significant reduction in the live cell coverage between the samples (Table 5.2).

Table 5.1: Alive cell to total biofilm coverage ratio of the biofilm coverage determined by the quantification of the fluorescence microscopy images and

Embedded	Ratio
material	alive/total
	surface coverage
COC	0.63
copper	0.4
copper(I) oxide	0.46
copper(II)	0.61
oxide	

Table 5.2: Single-factor ANOVA with subsequent post hoc comparison results of the biofilm coverage determined by the quantification of the fluorescence microscopy images

	P- value	$P (T \le t) two$	F crit.	Significance
		tailed		
ANOVA				
including all	9,12E-05		2,866266	
samples total	3,122 03		2,000200	
DNA coverage				
COC vs.		0,001227		Significant
copper		0,001227		Significant
COC vs.		0,030842		Significant
copper(I)oxide		0,030012		Significant
COC vs.		0,224318		Not
copper(II)oxide		0,22 13 10		significant
Copper vs.		0,433954		Not
copper(I)oxide		3, 12222 1		significant
Copper vs.		3,58E-05		Significant
copper(II)oxide		3,502 33		0.9
Copper(I)ox				
ide vs.		0,002547		Significant
copper(II)oxide				
ANOVA				
including all	0,616805		2,866266	Not
samples live	2,2.223		_,	significant
cell coverage				

The copper(II)oxide embedded COC showed an approximate biofouling reduction of 6.8%, whereas the other showed an increased biofouling due to the increased EPS

production. The reason for this might be that the biological active Cu²⁺ions are already available in the CuO embedded COC, but need to be first generated through reactions with the seawater in the other two copper containing materials.

Molecular analysis

The concentrations measured using the Pico Green assay of the initial DNA extracts were COC 3.20 ng/ μ l, copper 48.98 ng/ μ l, copper(l)oxide 59.03 ng/ μ l, and copper(ll)oxide 44.22 ng/ μ l. The high DNA concentrations of the copper containing surfaces might be a result of some interference of copper ions with the assay reagents.

The DGGE gel showed a difference in the band patterns for the COC and the COC surfaces containing copper compounds (Figure 5.4: L2, L3 and L4). It appears that few bands are clearly separated, especially on the copper embedded COC surfaces, indicating lower microbial diversity.

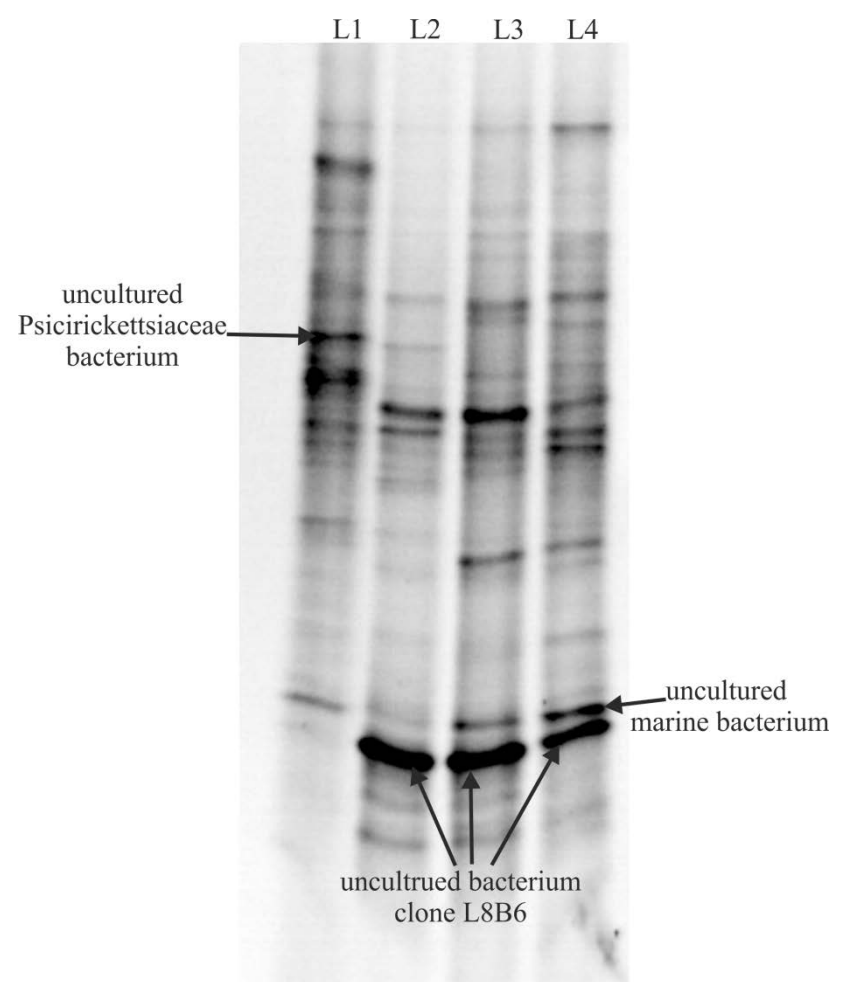


Figure 5.4: Image of DGGE gel of DNA extracts of COC surfaces exposed to the Solent for 14 days; (L1) COC; (L2) COC coated with copper; (L3) COC coated with copper(I)oxide; (L4) COC coated with copper(II)oxide; arrows point to the extracted and sequenced bands with the aliment match found in the online aliment software BLAST

One band in particular could only be detected in the copper containing surfaces. Subsequent sequencing identified a 97 to 98% identity match to the uncultured bacterium clone L8B6 (Table 5.3) isolated from the Logatchev hydrothermal vent field on the Mid-Atlantic Ridge (Voordeckers et al., 2008). It might be that in the extreme environment of hydrothermal vent field this species evolved a high copper tolerance which gave it an advantage on the copper containing substrates.

The sequencing result of another band of interest, only to be clearly detected in the COC substrate (Figure 5.4: L1) showed the closest alignment match to be to the uncultured Psicrickettsiaceae bacterium found in the Lagoon sediment in Venice, Italy (Borin et al., 2009). This bacterium belongs to the γ -proteobacteria.

The third and last match found was 99% to an uncultured marine bacterium originally found in an environmental sample from the Mediterranean, France (Landa et al, unpublished). Unfortunately no further information could be found on this specific sequence.

Table 5.3: closest alignment matches to 16S rDNA sequence of extracted DGGE bands from COC surfaces exposed to the Solent

Closest alignment match	Accession number	% Identity	Expect value	Source
unculured Psicirickettsiaceae bacterium	AM501644	98	8e-58	Lagoon sediment; Venice, Italy
uncultured	EF644808	98	6e-53	MAR
bacterium clone L8B6		97	2e-52	Logatchev hydrothermal vent system, 3000m water depth, sulfide sample
uncultured marine bacterium clone 1209 CS5.3.T8_3271	HE980658	99	2e-52	environmen tal sample Mediterranean Sea, France

5.2.2 Surface modification via plasma treatment and micro-/nanostructuring

As mentioned before hydrophobicity, also known as wettability of surfaces, as well as surface roughness plays a major role in the initial attachment of microorganisms to substrates (Dürr, 2007, Davies, 2002). The wettability of materials is influenced by both chemistry and topography of any given surface (Cortese and Morgan, 2012). A prominent example for the influence of the topography in nature is the self-cleaning lotus leaf whose hierarchical structured surface leaves it extremely water repellent (Koch et al., 2009).

Chemical modification via O₂ and CF₄ plasma treatment and nano-texturing created hydrophobic to super-hydrophilic surfaces with property stability of up to six months (Cortese and Morgan, 2012). Plasma treatment has been used in a wide range of studies regarding chemical surface modification (Wolf and Sparavigna, 2010, Cortese and Morgan, 2012, Zhu et al., 2009). Plasma is an ionized gas which when applied to polymers causes ablation, crosslinking and activation on the surface. Thus changing the chemical property of the polymer surface (Wolf and Sparavigna, 2010).

Methods and Materials

Cortese and Morgan manufactured (Cortese and Morgan, 2012) and provided plasma treated COC samples along with contact angle measurements as indicator for the hydrophobicity and hydrophilicity (Figure 5.5). For the examination of the fouling resistance the samples were contaminated with Pseudomonas fluorescens and incubated overnight at 23 $^{\circ}$ C and 120 rpm to ensure biofilm formation. The biofilm was fixed with formaldehyde and stained using the fluorescence DNA stain Syto9TM (2.5 μ M). For examination with the LSCM the surfaces were additionally stained with DAPI.

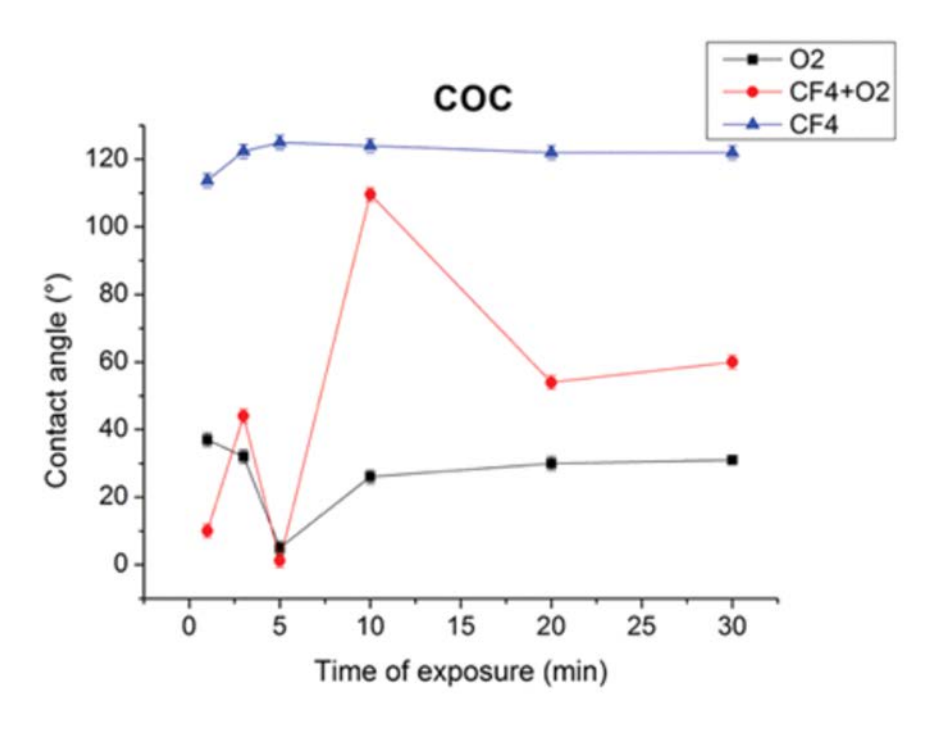


Figure 5.5: Variation in the contact angle of COC dependent on the plasma treatment and time (Cortese and Morgan, 2012)

Results and Discussion

The *P. fluoresens* surface coverage of CF_4 plasma treated COC lied between 13 and 14% regardless of the time of exposure, except for the 1 minute sample where the surface coverage reached 17±5% (Figure 5.6). This corresponds with the contact angle measured for these samples which did stabilize after the initial exposure at a contact angle of approximately 122° (Figure 5.5).

The highest coverage of all samples, $26\pm7\%$, was detected after 1 minute exposure to CF4O2 plasma treatment. After the initially high coverage the remaining samples treated with this plasma mixture trend to a reduction in biofilm coverage the longer the exposure time, until finally the lowest was found on the surface treated with CF_4O_2 plasma for 30 minutes, $7\pm3\%$ (Figure 5.6).

For the O_2 treated samples an increase of the biofilm up to $19\pm4\%$ was detected in the first two samples, one and five minutes plasma exposure, after which the coverage decreased down to $10\pm3\%$ (Figure 5.6Error! Reference source not found.).

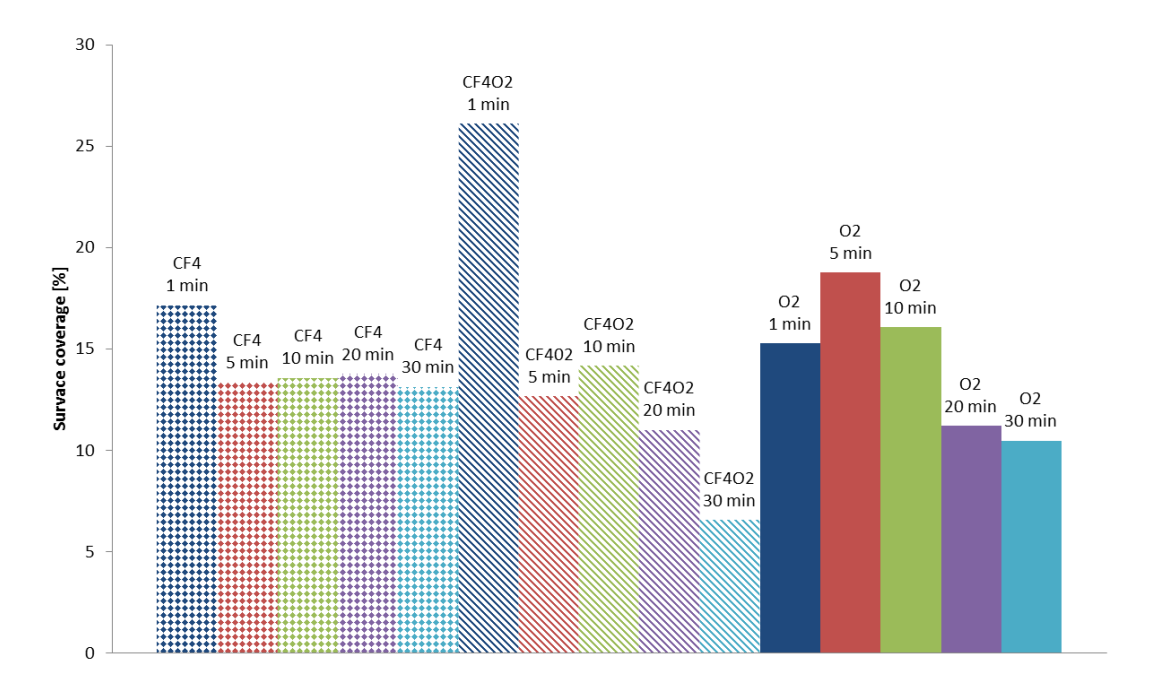


Figure 5.6: *P. fluorescens b*iofilm surface coverage as indicator for biomass on plasma treated COC; plasma CF_4 , O_2 , and CF_4O^2 were applied for 1 minute, 5 minutes, 10 minutes, 20 minutes, and 30 minutes

A correlation between the biofilm surface coverage with the contact angle of the surfaces could be detected in the CF_4 treated samples. In the other samples this correlation was not as obvious. The lowest biomass found corresponded to a contact angle of ~60°, which lies within the range of reported angle for copper, 39° to 77° (Hong et al., 1994), a known antifouling agent. These findings indicate that an intermediate wettability, neither hydrophobic nor hydrophilic might prove to be most resistant to fouling.

The microscopic examination of the structured surfaces showed the pillar to be very delicate and prone to break of the surface (Figure 5.7B). Examination via the LSCM revealed the bacteria to attach to both the pillar surface and the surface between the pillars (Figure 5.7: C and D).

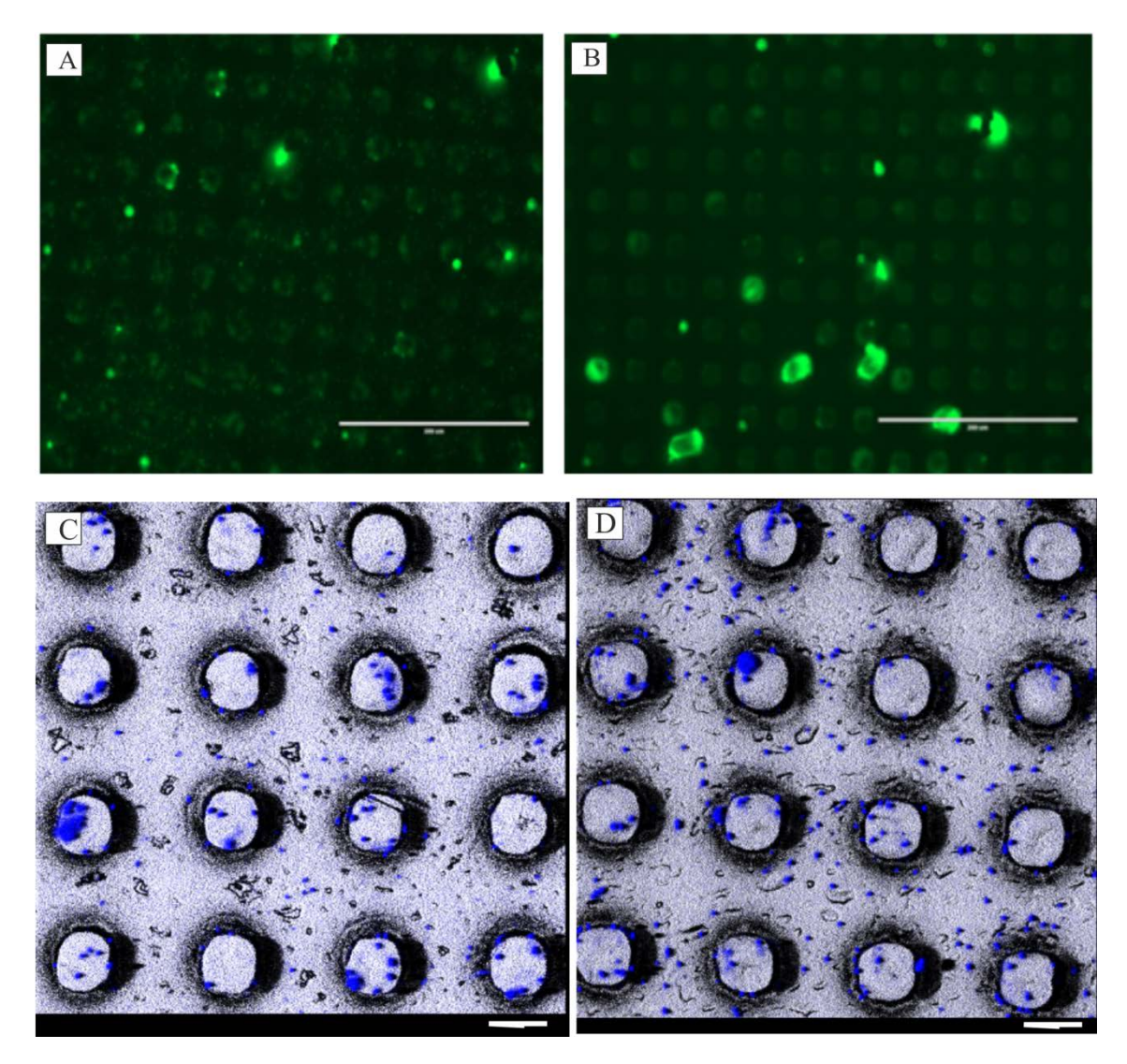


Figure 5.7: Example of fluorescent microscope and laser scanning confocal microscope images of *P. fluorescens* contaminated surface; Pillar size 15 μm spacing 20 μm (A) fluorescent microscope image CF4 treated (B) O2 treated surface (C) LSM image of CF4 treated and (D) O2 treated surface; (A) and (B) scalebar 200 μm, (C) and (D) scalebar 20 μm

When quantifying the fluorescent microscope images the O_2 plasma treated microstructes genrally had a lower surface coverage, between 4% and 9%, than the CF_4 , 9% and 36% treated smaples (Figure 5.8).

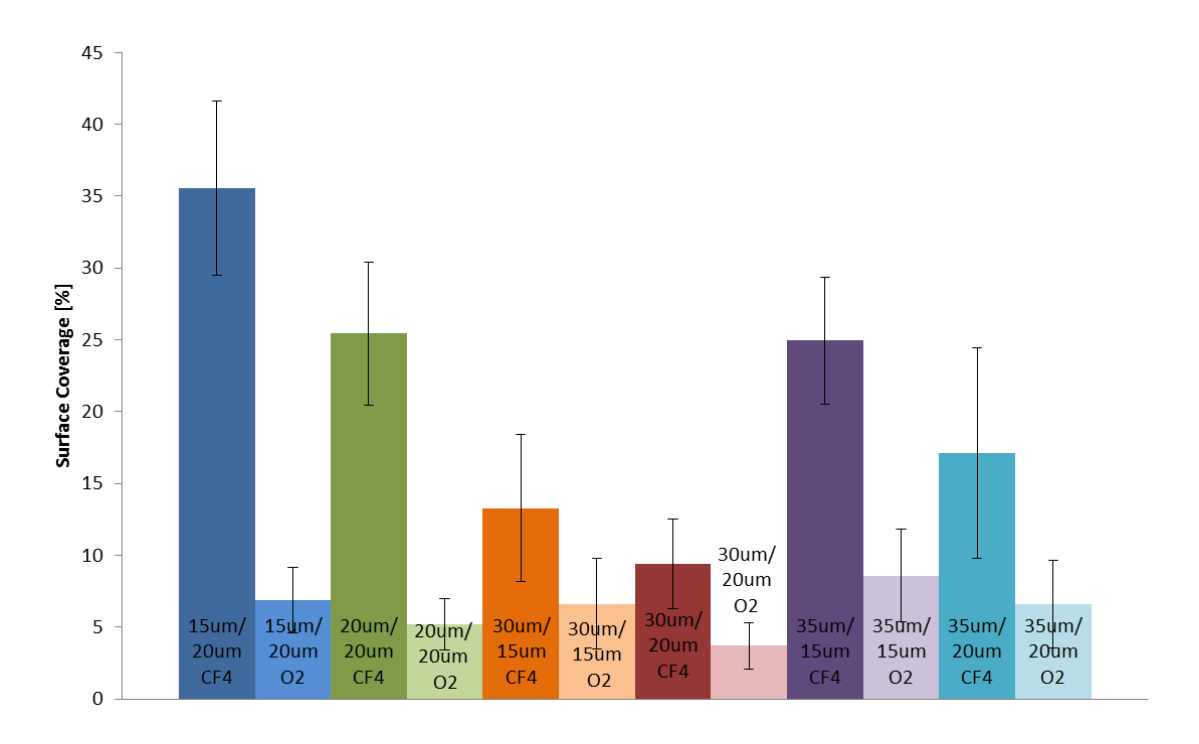


Figure 5.8: *P. fluorecsens* Biofilm surface coverage as indicator for biomass for micro-/nanostructured and plasma treated COC

At first mo correlation between pillar size and/or pillar spacing could be detected. But when taken the ratio of the pillar size to their spacing into account, the lowest biofilm coverage (CF_4 : 9±3%; O_2 : 4±2%) was associated with a ratio of 1.5. Ratios higher or lower showed a higher biomass for both treatments (Table 5.4) indicating an optimal ratio for an increased fouling resistance.

Table 5.4: Biofilm surface coverage in regard to structure ration and plasma treatment

			•	
pillar	Ratio	Biofilm coverage	Biofilm coverage	
size/spacing	pillar	CF₄ [%]	O, [%]	
	size/spacing			
15 μm/20 μm	0.75	36	7	
20 μm/20 μm	1	25	5	
30 μm/15 μm	2	13	7	
30 μm/20 μm	1.5	9	4	
35 µm/15 µm	2.33	25	9	
35 μm/20 μm	1.75	17	7	

5.3 Active Antifouling Strategies

Mechanical cleaning, such as scrubbing the organisms off the ship hull, is the oldest known method of biofouling control and is still sometimes used as a supplementary measure today regardless of what other methods have been applied (Yebra, 2004).

The use of wipers or high pressure water jets on a continuous basis are not practical on ship hulls, neither is the use of gas bubbles (Railkin, 2004), but these methods might be adaptable for use on sensors platforms or the casing of the sensors, if used at intervals. Caron and Sieburth (1981) recommended that mechanical removal of microfoulers should be repeated under marine conditions at least every third day in order for it to be effective(Caron and Sieburth, 1981).

The University of California Santa Barbara Ocean Physics Lab under the auspices of the National Ocean Partnership Programs' (NOPP) Ocean-Systems for Chemical, Optical, and Physical Experiments (O-SCOPE) project in cooperation with Satlantic has developed a shutter device for optical instruments. The shutter protects the sensor between measurements. For measurements the shutter is opened and the sensor is exposed to the surrounding media. The cooper of the shutter has also a biocidal effect reducing fouling (Saltlantic, 2010).

The temporary disruption of the marine communities cannot permanently prevent the general trend of the fouling succession to a climax and does not solve the problem of protection from biofouling, as disrupted communities recover after some time or continue their development in another direction (Railkin, 2004). This leads to the conclusion that the effectiveness of these kinds of antifouling methods depends on the frequency of disruption exceeding the speed of accumulation of the organisms (Railkin, 2004).

The US Navy has developed an oceanographic sensor using a piezoelectric material which removes the biofilm through the use of sonic vibration. The usage of sonic frequencies between 10Khz and those close to the resonance frequency of organic matter produce cavitation forces which are forces created by the pressure at the surface of the sensor and its reduction to the point of water boiling (Edgerton, 1978). But this method has a rather high power requirement which makes it rather impractical for battery powered remote sensors (Whelan and Regan, 2006).

Another widespread method to kill bacteria, especially pathogens is the use of irradiation. The use of ultraviolet light as an antifouling method has been investigated in regard to its application on filtration membranes, sensors etc., but due to the relatively high power requirement it proved impractical in remote sensors (Whelan and Regan, 2006). However, recent developments in the development of UV LEDs may lead to a re-examination of the applicability of this strategy in this area (Whelan and Regan, 2006). Other irradiation methods including the photolysis of water in the presence of

zinc oxide photoactive material to produce hydrogen peroxide, a very effective biocide, has been proposed, but since this reaction needs visible light a light source needs to be supplied in greater depths (Whelan and Regan, 2006)

5.4 Antifouling for a sensor electrode via electrolysis of seawater

Another example for an active antifouling technique is the electrolysis of seawater which produces chlorine (Equation 5.1 (1)) and which in turn reacts with the surrounding water to form hydrochloric acid and hypochloric acid (Equation 5.1 (2)), both of which are potent biocides (Railkin, 2004):

Equation 5.1: Electrolysis of seawater

$$2NaCl + 2H2O \rightarrow Cl2 + 2NaOH + H2$$
 (1)

$$Cl2 + H2O \rightarrow HClO + HCl$$
 (2)

The principle of the reaction of chlorine with water is used in some drinking water treatment plants as a disinfectant (Delauney et al., 2010). There are also some monitoring stations using this system (Woerther, 2002, Woerther and Grouhel, 1998)

Further electrochemical approach uses a tin or graphite-silicone electrode to directly transfer electrons to the fouling organisms and killing them in the process rather than to produce a biocide agent.(Nakayama et al., 1998, Nakasono and Matsunaga, 1993)

Electrical pulse have also been found to be effective to keep cooling water systems free of macro-organisms (Abou-Ghazala and Schoenbach, 2000). As part of this project this method was tested as in incorporated mitigation strategy for a miniature conductivity, temperature and Dissolved Oxygen sensor developed at the University of Southampton.

5.4.1 Method and Materials

The electrodes were deployed from the 25th March 2011 to the 14th April 2011, 20 days, in the Solent estuary, Southampton, UK, without previous treatment. During the deployment a cleaning waveform with the following parameters (Error! Reference source not found.) was applied every 2 sec: 2.24V for chlorine generation -1.36V for oxygen generation, and a resting voltage of 0.44V. The square waveform period was 120ms. After the deployment the samples were fixed with Ethanol and stained with SYTO©9, a fluorescent DNA stain for microscopic analysis. The surface coverage the electrodes was determined using fluorescent microscope image and a custom MATLABTM (supplied by Xi Huang; see Appendix I).

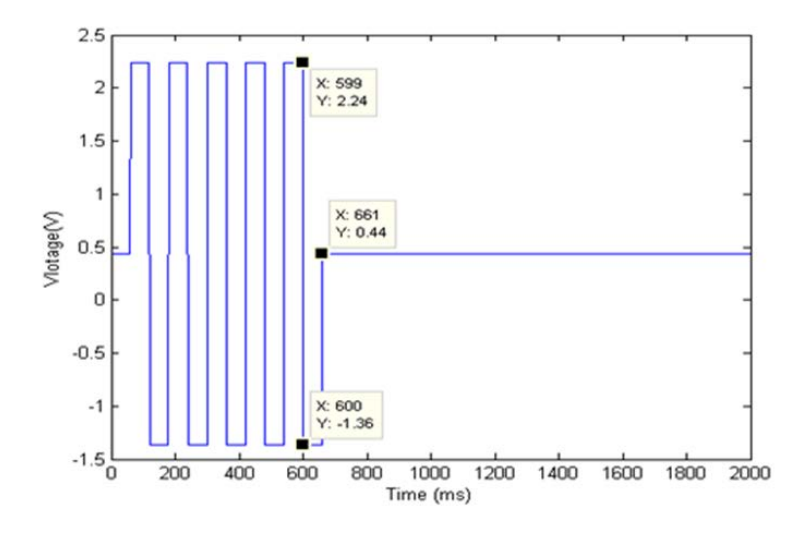


Figure 5.9: Cleaning waveform applied to the electrode during deployment; Chlorine generation: 2.24V, Oxygen generation: -1.36V, Resting: 0.44V, Waveform applied every 2 sec

DGGE

After microscopic analysis the electrode surfaces were swabbed and the swabs used for molecular analysis. DNA extraction performed the DNeasy Kit Blood & Tissue (Qiagen) according to the manufacturer's tissue protocol with extended cell lysis incubation overnight. For the DGGE the DNA was amplified using the Eukarya specific primer set (Delong, 1992) with the in 0 described parameters. The extracted DGGE bands were re-amplified using the nested primer set nE (Table 2.6) and dideoxy chain termination technology (Eurofins MWG Operon, Germany) (Li, 2006) used for sequencing. The resulting sequences were identified using the online alignment software BLAST to search the Nucleotide collection (nr/nt) database. The search parameters used in this study were a megaBlast with the 'expect' value set below ten indicating that a random match is unlikely (Altschul, 1997, Altschul et al., 1997, McGinnis and Madden, 2004).

aPCR

DNA extracts were used for qPCR as described before.

5.4.2 Results and Discussion

The visual inspection of the electrodes after a 20 day deployment demonstrated a clear difference in the fouling between application of the cleaning waform for the electrolysis of seawater and the reference electrode (Figure 5.10).

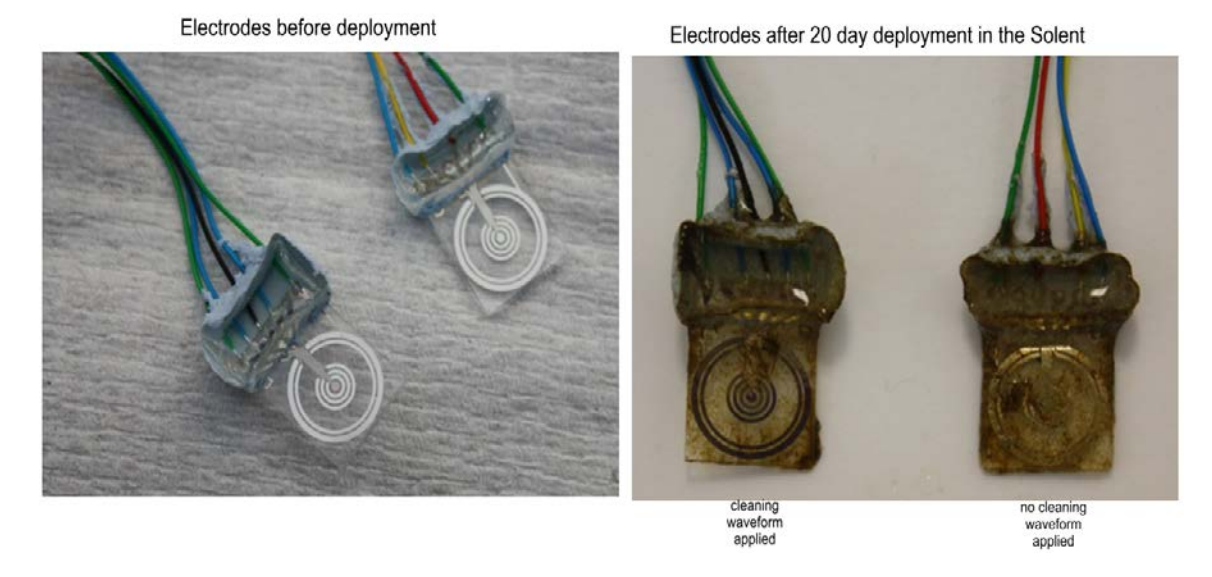


Figure 5.10: Electrodes before and after 20 day deployment showing clear difference in the severity of the biofouling

Microscopic Analysis

The EDIC microscope images also showed a significant difference in the composition of the biofouling at the centre (Figure 5.11). The electrode with the applied waveform showed less diatoms and a more homogenous bacterial biofilm (Figure 5.11A) when compared to the reference electrode.

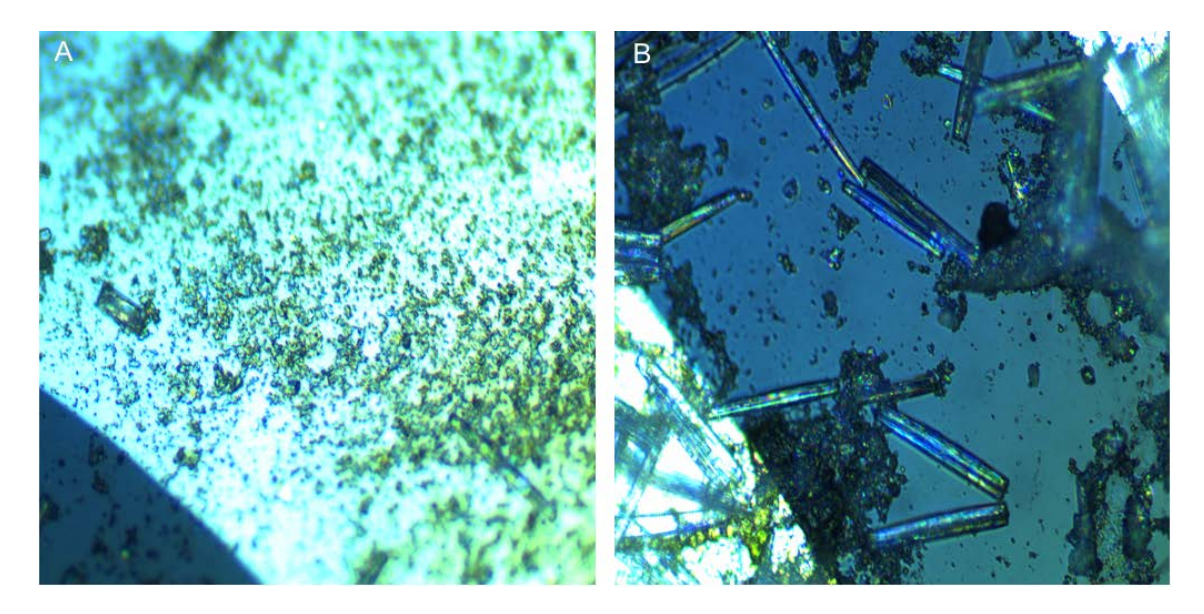


Figure 5.11: Episcopic differential interference contrast (EDIC) microscope images after 20 days deployment showing a significant difference in the composition of the biofouling at the centre. (A) electrode with cleaning waveform, (B) reference-electrode:

Using Brightfield microscopy various diatoms could be identified (Figure 5.12). On both sensor electrodes *Nitzschia sp.* and *Grammatophora sp* could be found. Additionally the diatoms *Catacombes sp.* and *Brachysira sp* could be identified on the reference electrode. On the sensor with the cleaning waveform *Licmophora sp* could be clearly seen, it is probable that this diatom would also be present on the reference and could just not be identified because it was overgrown by other micro-algae. This is a cosmopolitan species found mostly in coastal sea, always attached to an substrate such as seaweeds, shell, stones, and even whales and copepods (Round et al., 2007).

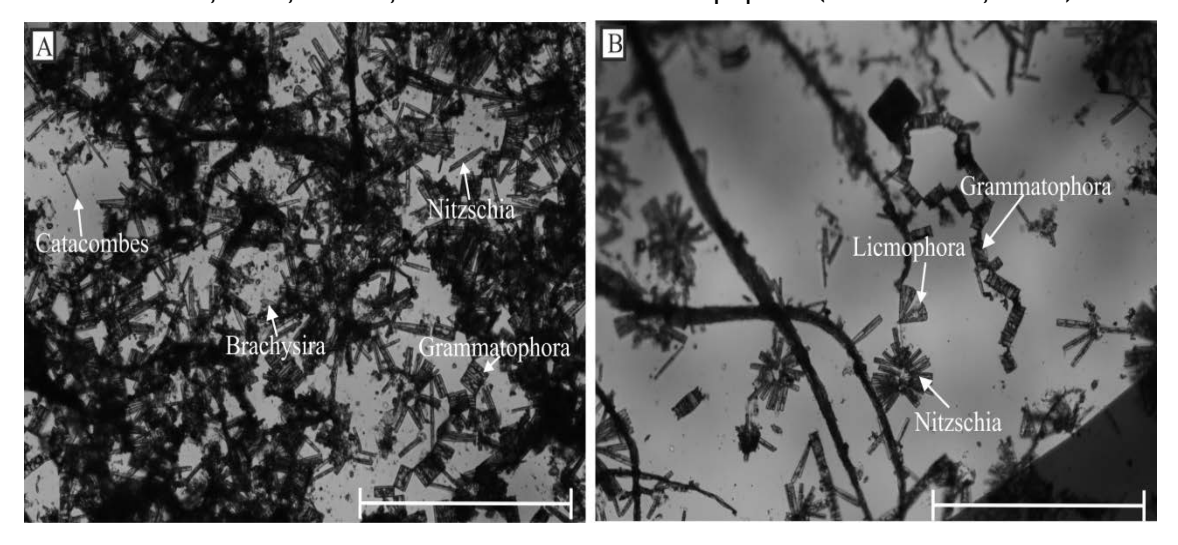


Figure 5.12: Brightfield image of electrodes deployed for 20 days in the Solent; (A) reference electrode; (B) electrode with the cleaning waveform applied; arrows point to microscopic identified diatoms; scalebar 400 µm

Grammatophora sp. and Catacombas sp. are also surface associated diatoms, whereas Nitschia are usually found in epipelic or planktonic environments (Round et al., 2007, Huber et al., 1995).

Finding a large amount of diatoms on the reference electrode was to be expected since up to 99.9% of the micro-fouling biomass can consist of diatoms and bacteria (Railkin, 2004)

The generation of mosaic-composites of transmission and fluorescence microscope images after 20 day deployment showed differences in the distribution of the biofouling between the two sensors (Figure 5.13). On the reference electrodes the distribution of the organisms is more or less equally over the whole surface (Figure 5.13: C and D). In contrast on the electrode with the waveform applied not only less biofouling could be detected it also concentrated on the rim of the sensor surface (Figure 5.13: A and B).



Figure 5.13:: Mosaic of transmission and fluorescence microscope images after 20 day deployment showing distribution of the biofouling; (A) Transmission microscope images of electrode with cleaning waveform applied, (B) Fluorescence microscope images of electrode with cleaning waveform applied (C) Transmission microscope images of electrode without cleaning waveform applied; (D) Fluorescence microscope images of electrode without cleaning waveform applied; samples were stained with SYTO©9, magnification used 10x

The quantification of the fluorescence microscope images used for the creation of the composites (n = 64) revealed and average surface coverage on the reference electrode of $49\%\pm14$ and on the sensor electrode with cleaning waveform of only $22\%\pm12$. This equals a total biofouling reduction of 55.1%.

Molecular Analysis

DNA concentration of the extracts were 28.31 ng/ μ l for the reference electrode and 12.19 ng/ μ l for the electrode with the cleaning waveform applied, agreeing with the microscopic analysis of less fouling/organisms being detected on the sensor with the waveform application.

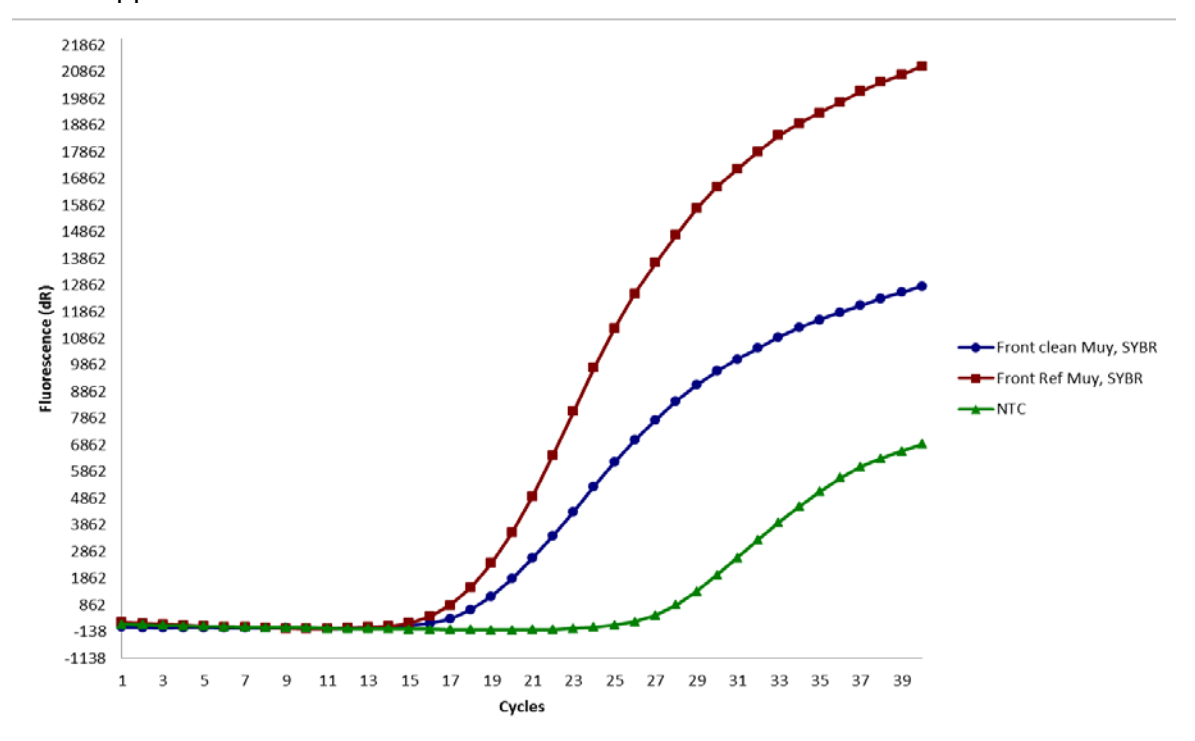


Figure 5.14: qPCR amplification plot of bacterial DNA after 20 day deployment in the Solent using Muy primer set (Muyzer et al., 1993);

Both qPCR amplification plots for bacterial and eukaryotic DNA (Figure 5.14 and Figure 5.15) showed an earlier fluorescence rise for the reference electrode than for the one with the applied waveform. This means that both bacterial and eukaryotic DNA was present in a higher concentration in the initial extracts.

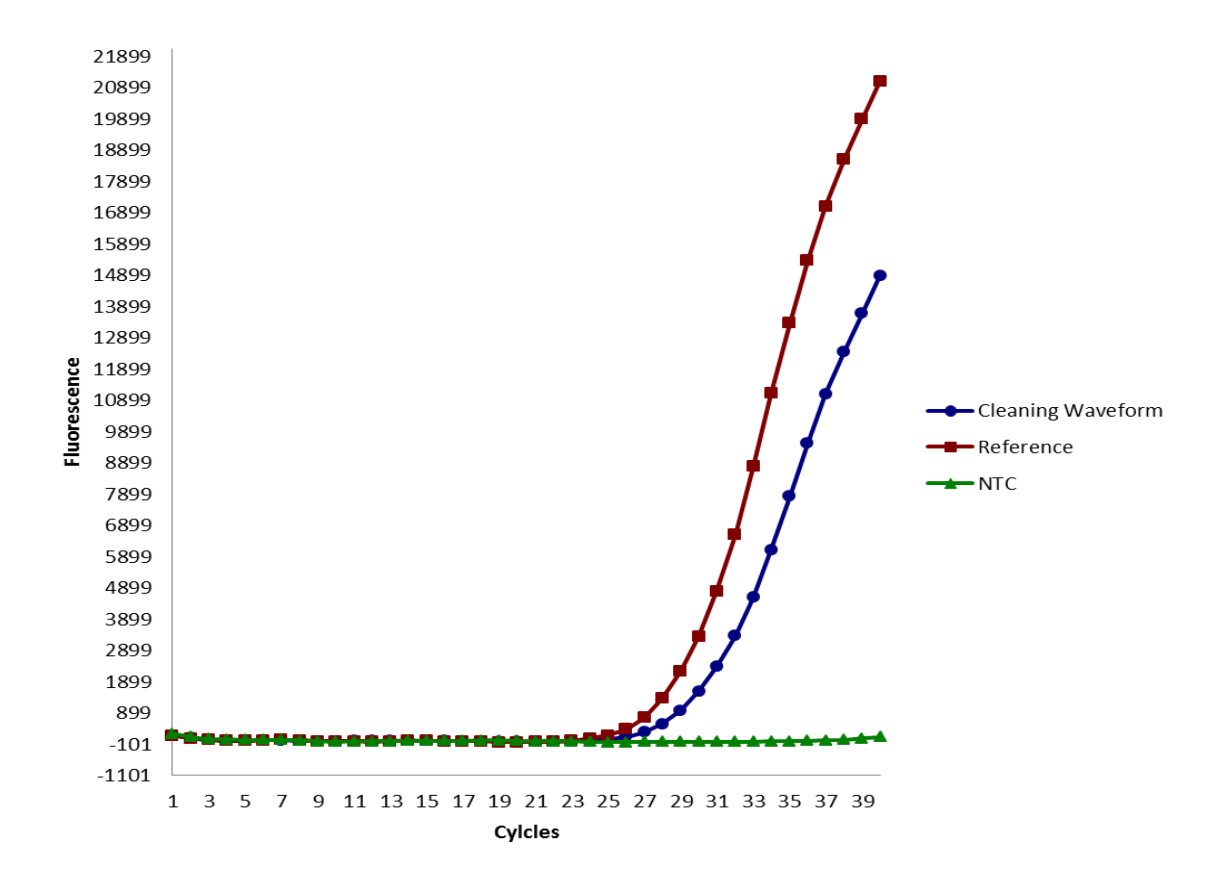


Figure 5.15: qPCR amplification plot of eukaryotic DNA after 20 day deployment in the Solent using nE primer set

The lower CT values of the bacterial DNA in both electrode samples (Reference: 20.53 and Waveform: 19.45) compared to the eukaryotic (Reference: 30.48 and Waveform: 28.71), seems to indicate that Eukarya are less abundant than Bacteria in the biofilm formed.

On the DGGE image no obvious difference could be seen in the band pattern between both sensor electrodes (Figure 5.16). This in conjunction with the other findings seems to indicate that the seawater electrolysis reduced the abundance of microorganisms without changing the community composition of the dominant Eukaryotes.

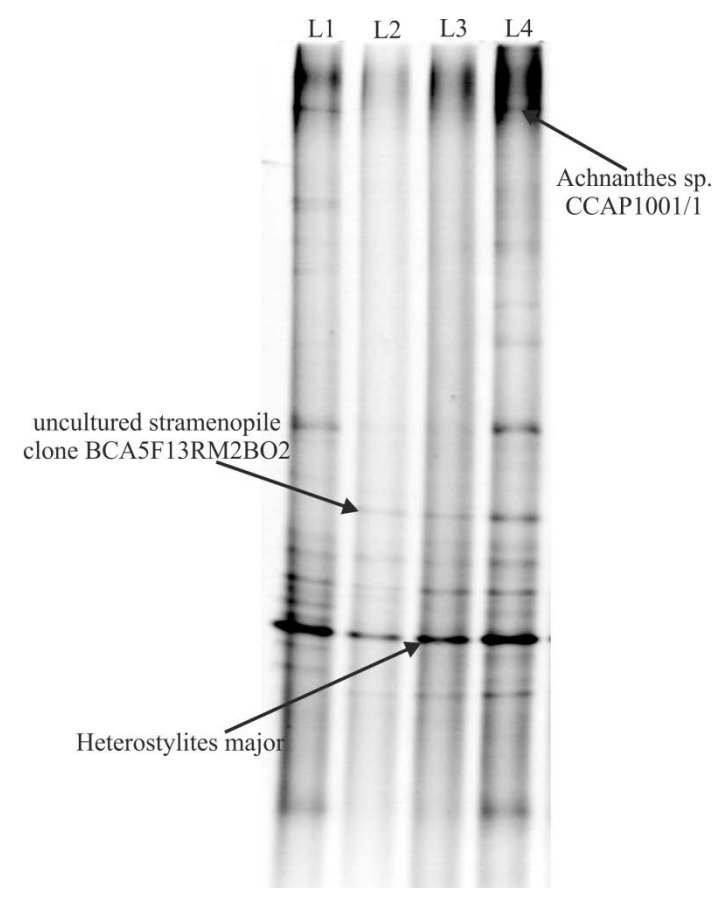


Figure 5.16: Image of DGGE gel of DNA extracts; (L1) Electrode front with cleaning waveform applied; (L2) back of electrode with cleaning waveform applied; (L3) front of reference-electrode; (L4) back of reference-electrode; arrows point to the extracted and sequenced bands with the aliment match found in the online aliment software BLAST

The sequencing results showed three close alignment matches (Table 5.5). Two 98% identity matches to an uncultured stramenopile, isolated from a water column sample in the Caribbean Sea (Edgcomb et al., 2011) and to *Achnantes sp.* (Damste et al., 2004). Also a 99% match was found to *Heterostylites major*, found in Japan (Takenaka et al., 2012).

Table 5.5: Closest alignment match to 18S rDNA of extracted DGGE bands from sensor electrodes deployed in the Solent

Closest alignment match	Accession number	% identity	Expect value	Source
uncultured stramenopile clone BCA5F13RM2BO2	GU823191	98	6e-90	oxygenated water column sample, Cariaco Basin, Caribbean Sea
Heterostylites major	AB625968	99	4e-92	Hokkaido, hakodate, Japan
Achnantes sp. CCAP1001/1	AY485496	98	8e-89	·

Both the uncultured stramenopile and *Achnantes sp.* are diatoms. Unfortunately no diatom sequences could be detected for the microscopic identified diatoms. The third sequence match belongs to a copepod species, this DNA might have been transferred by *Licmophora sp.* which can be found living as epibionts on copepods (Round et al., 2007).

In general, the application of the cleaning waveform as mitigation strategy through the electrolysis of seawater was successful. It significantly reduced the biofouling significant during a 20 day deployment in a eutrophic environment, the Solent. Further optimization of the waveform might improve the efficiency.

Alexandra Meier

Over the last decades requirement of long-term monitoring of the environment by *in situ* sensor technology has increased, in order to asses long-term changes and global processes, e.g. global warming. As biofouling is a general problem limiting the lifetime of environmental sensors severely and is not restricted to one region or a specific environment, development of effective *in situ* antifouling techniques is

necessary. In order to develop such techniques detailed knowledge of biofouling such as initial development, influence of substrates and microbial community structure, is essential.

Experiments of this study demonstrate the need to combine several assessment techniques for a successful analysis of biofilms and the efficiency of mitigations strategies. Most experiments benefited from the application of both microscopic and molecular methods as they complimented and supported one another (e.g.: SEM microscopy and EDIC/microscopy in Chapter 4.2 or microscopy and molecular techniques in chapter 5.3). By relying on only one analysis method important aspects biofilm development might be missed. The possible methods or combinations of them must be examined with regard to their effectiveness as well as their possible interference with the workings of the sensors.

Therefore after developing and optimising assessment methods this study first examined planktonic and biofilm microbial community structure of the Mid Cayman Ridge in order to be able to determine its influence on biofouling of different artificial surfaces, which were deployed for 10 days and 23 months at 4,700 m in the Cayman Trough. This material deployment's main objective was to determine if there is biofouling in the deep sea and in case of biofouling to assess the severity.

The optimal antifouling strategy for sensors would need to be effective, environmental friendly, low cost, low power requirement and easy to use (Whelan and Regan, 2006). Also the type of sensor and the future application of the sensor need to be considered in the development, since different sensors are influenced in different ways by the fouling and the possible impact on the measurement. With regard to different environments, they have a significant impact on the biofouling. Strategies developed for one type of environment might not necessarily be effective in another.

6.1 Microbial Community Structure of the Mid-Cayman Ridge

As mentioned afore the microbial community structure of the Mid-Cayman Ridge was examined in order to determine possible influence of artificial substrates on the biofilm community. As the planktonic community is the source of any biofilm formation (see 1.3.3), the microbial community structure at different depth was examined as well as naturally occurring biofilm attached to an old hydrothermal vent chimney.

Results regarding the samples from inside and above the hydrothermal plume indicate a higher biodiversity of these in comparison to background samples. Differences in the microbial community structure were expected across relative small spatial scales as this was already demonstrated in other studies (Tarasov et al., 2005, Schnetzer et al., 2011, Briand et al., 2012).

Both bacterial and crenarchean community results of the DGGE demonstrate low biodiversity corresponding to the common community structure pattern of a "rare biosphere" (Amaral-Zettler et al., 2009, Caron and Countway, 2009, Sogin et al., 2006, Schnetzer et al., 2011)

Unfortunately no common organisms in the planktonic and the biofilm samples could be detected. This might be because the sensitivity of the method used is not high enough or more likely because different primer sets were used in the examination of the seawater and the hydrothermal vent samples due to problems with the initial primer set that developed during the course (please refer to 2.5). Application of a more sensitive method like pyrosequencing might be able to detect some common microorganisms and give a more detailed image of the microbial community structure of the Mid-Cayman Ridge.

The origin of the alignment matches found in both the planktonic and the natural biofilm samples are geographical widely spread. But the environments these organism sequences originated seem to have similar properties to the environment where the respected samples were taken. This agrees with the general view that geographic distribution of species is influenced by a factor of physical properties and adaptations (Lalli and Parsons, 1997b).

These findings hint that microorganisms of both planktonic and benthic origin are not as constraint to individual biogeographic regions as invertebrates and there might have a more ubiquitous distribution.

6.2 Development of biofilms on artificial surfaces

The majority of biofouling research has concentrated on the eutrophic and euphotic zone of the oceans, the deep sea having been because of the difficulties in experimental setup due to limited accessibility. The general assumption was that biofouling in oligotrophic regions could be regarded as insignificant (Railkin, 2004). Consequently, little is known about biofilm formation in the deep sea. However, culture-independent methods have revealed significant microbial diversity even in surface sediments of the Mariana Trench (11,000m) (Kato et al., 1997). Recent studies in the oligotrophic environment of the Eastern Mediterranean deep sea have demonstrated that biofilms composed of bacteria, cocolithiphores, diatoms and dinoflaggelates form after 155 days on both natural and artificial substrates (Bellou et al., 2011, Bellou et al., 2012). Thus, the previous assumption that biofouling is minor in such environments needs to be re-examined with regard to the question whether biofouling is an issue in such areas.

In comparison to the biofouling on the seaglider deployed for 110 day in the North Atlantic the samples recovered from the Cayman Trough after 23 months showed distinctly less biofouling. This indicates a slower biofouling development in the deepsea. But even this in comparison small amount of biofouling can be potentially destructive for observation platforms especially when using microfluidic devices.

All close matches except for the coral-associated bacteria were originally found in the extreme environment of the deep sea. Finding a *Colwellia* sp. among the predominant organisms agrees with the discovery of fatty acids common to many psychrophilic species, eg *Pseudomonas* sp. and some *Colwellial/Vibrio* sp. in surface-associated cells on the Mid-Atlantic Ridge (Guezennec et al. 1998). This and the wide geographical spread of the alignment matches might indicate a global distribution of these organisms and a special adaptation to the extreme environment.

The results of chapter 4 showed that significant biofilm formation occurred on surfaces deployed in the deep-sea in accordance with studies performed by (Bellou et al., 2012) even after the relative short period of 10 days. As the biofouling in the eutrophic regions of the oceans becomes more severe the longer the exposure of any surface, the same could be demonstrated in the deep sea with the long-term

deployment of 23 months. Therefore, microfouling might turn out to be a major problem for long-term deployment in this type of extreme environment.

The indication of the global distribution of the predominant biofilm species as well as planktonic microorganisms has been demonstrated in the results regarding the microbial community structure of the Mid-Cayman Ridge. This requires further investigation and has to be further addressed by development in the deep sea in different biogeographic regions.

6.3 Antifouling Strategies

The most promising of mitigation strategy tested in the framework of this project was the protection of a sensor electrode via seawater electrolysis with a biofouling reduction of over 50% during a 20 day deployment. Naturally further optimizations to see if the energy consumption could be further reduced and to determine the effective range of this method are still needed.

Regarding the incorporation of biocidal reagents as surface modification, copper and copper oxides were embedded into COC surface as a mitigation technique. Copper(II)oxide embedded COC showed an approximate biofouling reduction of 6.8%, whereas the other showed an increased biofouling due to the increased EPS production. The reason for this might be that the biological active Cu²+ions are already available in the CuO embedded COC, but need to be first generated through reactions with the seawater in the other two copper containing materials. Unfortunately this method might lead to undesired environmental effects as copper might be slowly released into the seawater. As such this method is not applicable without further investigation, which might not be worth pursuing as the mitigation effect is not very large.

But the surface modifications with plasma treatment show that there might be an optimal surface hydrophobicity/hydrophilicity to reduce biofouling. Results indicated that this optimal ratio lies somewhere in the intermediate range of wettability. This technique might warrant further investigation as it does not involve the risk of an undesired release of a biocide into the environment.

Possible combination of different surface modifications and/or with seawater electrolysis might further increase fouling resistance and might be worth further investigation.

Another aspect that needs to be considered is the location of the antifouling strategy on the sensor, because the outside or casing of the sensor is more robust, whereas the inside is more delicate, which will require different approaches.

The casing for example might withstand a high pressure water jet, but the membrane inside of a sensor is most likely destroyed by this.

In order to determine the effectiveness of any antifouling strategy the development of a biofilm and its composition needs to be understood and analysed. For this propose, a combination of assays need to be chosen and properly adapted that give an insight into the biofilm formation, composition and biomass production. The combination of assays with the most potential for this is the combination of DGGE, EDIC/EF, and crystal violet staining. But other methods are also considered and examined in this respect.

The development of a sensible antifouling strategy is a complicated problem with widespread implications.

At last it should be noted that viewing globally meteorological events in the atmosphere and climate change in the ocean and on land are connected over vast distances. Thus human impacts on the sea can and need to be measured on a global scale. With an increasing impact of humans on the ocean, for example the environmental impact of deep-sea mining (Hoagland et al., 2010), and the processes within, the expansion of knowledge about the ecology of the seas becomes essential to (Lalli and Parsons, 1997a). These issues are currently addressed by the development of new environmental sensors and monitoring platforms such as the ARGO floats (globally) and Neptune in Canada. Consequentially, microfouling might turn out to be a major problem for long-term deployment in this type of extreme environment (Bellou et al., 2011, Bellou et al., 2012, Meier et al., 2013). This makes the study of biofouling and the development of effective mitigation strategies essential for the continued operation of any instrument and platform independent of their location on the surface of the oceans or in the deep sea.

Chapter 7 References

- ABARZUA, S. & JAKUBOWSKI, S. 1995. Biotechnological Investigation for the Prevention of Biofouling .1. Biological and Biochemical Principles for the Prevention of Biofouling. *Marine Ecology Progress Series*, 123, 301-312.
- ABOU-GHAZALA, A. & SCHOENBACH, K. H. 2000. Biofouling prevention with pulsed electric fields. *Ieee Transactions on Plasma Science*, 28, 115-121.
- ABU AL-SOUD, W. & RÅDSTRÖM, P. 1998. Capacity of Nine Thermostable DNA Polymerases To Mediate DNA Amplification in the Presence of PCR-Inhibiting Samples. *Applied and Environmental Microbiology*, 64, 3748-3753.
- ALONGI, D. M. 1990. Bacterial-growth rates, production and estimates of detrital carbon utilization in deep-sea sediments of the solomon and coral Seas. *Deep-Sea Research Part a-Oceanographic Research Papers*, 37, 731-746.
- ALTSCHUL, S. E. 1997. Evaluating the statistical significance of multiple distinct local alignments. Theoretical and Computational Methods in Genome Research, 1-14.
- ALTSCHUL, S. F., MADDEN, T. L., SCHAFFER, A. A., ZHANG, J. H., ZHANG, Z., MILLER, W. & LIPMAN, D. J. 1997. Gapped BLAST and PSI-BLAST: a new generation of protein database search programs. *Nucleic Acids Research*, 25, 3389-3402.
- AMANN, R. I., LUDWIG, W. & SCHLEIFER, K. H. 1995. Phylogenetic identification and insitu detection of individual microbial-cells without cultivation. *Microbiological Reviews*, 59, 143-169.
- AMARAL-ZETTLER, L. A., MCCLIMENT, E. A., DUCKLOW, H. W. & HUSE, S. M. 2009. A Method for Studying Protistan Diversity Using Massively Parallel Sequencing of V9 Hypervariable Regions of Small-Subunit Ribosomal RNA Genes. *Plos One*, 4.
- AUGUET, J.-C., BARBERAN, A. & CASAMAYOR, E. O. 2009. Global ecological patterns in uncultured Archaea. *ISME J*, 4, 182-190.
- AZAM, F. & LONG, R. A. 2001. Oceanography Sea snow microcosms. *Nature*, 414, 495-+.
- BAHATTAB, M. A., BASS, J. D., PETERSEN, B., GLEIXNER, S., BAGABAS, A. A. & KIM, H. C. 2011. Controlled hydrothermal growth of TiO(2) nanowires on transparent conductive substrates. *Abstracts of Papers of the American Chemical Society*, 241.
- BAKER, G. C., SMITH, J. J. & COWAN, D. A. 2003. Review and re-analysis of domain-specific 16S primers. *Journal of Microbiological Methods*, 55, 541-555.
- BAKER, J. S., DUDLEY, L.Y. 1998. Biofouling in membrane systems A review. *Desalination*, 118, 9.
- BAKKE, R., KOMMEDAL, R., KALVENES, S. 2001. Quantification of biofilm accumulation by an optical approach. *Journal of Microbiological Methods*, 44, 14.
- BAR-OR, Y. 1990. Hydrophobicity in the aquatic environment. *In:* DOYLE, R. J. & RODSENBERG, M. (eds.) *Microbial cell surface hydrophobicity.* Washington, DC; USA: American Society for Microbiology.
- BARRANGUET, C., VAN BEUSEKOM, S. A. M., VEUGER, B., NEU, T. R., MANDERS, E. M. M., SINKE, J. J. & ADMIRAAL, W. 2004. Studying undisturbed autotrophic biofilms: still a technical challenge. *Aquatic Microbial Ecology*, 34, 1-9.
- BASSLER, B. L. 1999. How bacteria talk to each other: regulation of gene expression by quorum sensing. *Current Opinion in Microbiology*, 2, 582-587.
- BASSLER, B. L. 2002. Small Talk: Cell-to-Cell Communication in Bacteria. *Cell*, 109, 421-424
- BEECH, I. B. 2004. Corrosion of technical materials in the presence of biofilms current understanding and state-of-the art methods of study. *International Biodeterioration & Biodegradation*, 53, 177-183.
- BEECH, W. B. & SUNNER, J. 2004. Biocorrosion: towards understanding interactions between biofilms and metals. *Current Opinion in Biotechnology*, 15, 181-186.
- BELLOU, N., COLIJN, F. & PAPATHANASSIOU, E. 2011. Experimental settlement study in the Eastern Mediterranean deep sea (Ionian Sea). *Nuclear Instruments and*

- Methods in Physics Research Section A: Accelerators, Spectrometers, Detectors and Associated Equipment, 626-627, \$102-\$105.
- BELLOU, N., PAPATHANASSIOU, E., DOBRETSOV, S., LYKOUSIS, V. & COLIJN, F. 2012. The effect of substratum type, orientation and depth on the development of bacterial deep-sea biofilm communities grown on artificial substrata deployed in the Eastern Mediterranean. *Biofouling*, 28, 199-213.
- BIDDLE, J. F., LIPP, J. S., LEVER, M. A., LLOYD, K. G., SORENSEN, K. B., ANDERSON, R., FREDRICKS, H. F., ELVERT, M., KELLY, T. J., SCHRAG, D. P., SOGIN, M. L., BRENCHLEY, J. E., TESKE, A., HOUSE, C. H. & HINRICHS, K. U. 2006. Heterotrophic Archaea dominate sedimentary subsurface ecosystems off Peru. *Proceedings of the National Academy of Sciences of the United States of America*, 103, 3846-3851.
- BLACK, M. B., HALANYCH, K. M., MAAS, P. A. Y., HOEH, W. R., HASHIMOTO, J., DESBRUYERES, D., LUTZ, R. A. & VRIJENHOEK, R. C. 1997. Molecular systematics of vestimentiferan tubeworms from hydrothermal vents and cold-water seeps. *Marine Biology*, 130, 141-149.
- BLACK, M. B., TRIVEDI, A., MAAS, P. A. Y., LUTZ, R. A. & VRIJENHOEK, R. C. 1998.

 Population genetics and biogeography of vestimentiferan tube worms. *Deep-Sea Research Part Ii-Topical Studies in Oceanography*, 45, 365-382.
- BLOOMFIELD, S. F., STEWART, G. S. A. B., DODD, C. E. R., BOOTH, I. R. & POWER, E. G. M. 1998. The viable but non-culturable phenomenon explained? *Microbiology*, 144, 1-3.
- BOOM, R., SOL, C.J.A., SALIMANS, M.M.M., JANSEN, C.L., WERTHEIM-VAN DILLEN, P.M.E., VAN DER NOORDAA, J. 1990. Rapid and simple method for purification of nucleic acids. *Journal of Clinical Microbiology*, 28, 9.
- BORIN, S., BRUSETTI, L., DAFFONCHIO, D., DELANEY, E. & BALDI, F. 2009. Biodiversity of prokaryotic communities in sediments of different sub-basins of the Venice lagoon. *Research in Microbiology*, 160, 307-314.
- BOWMAN, J. P., CAVANAGH, J., AUSTIN, J. J. & SANDERSON, K. 1996. Novel Psychrobacter Species from Antarctic Ornithogenic Soils. *International Journal of Systematic Bacteriology*, 46, 841-848.
- BOYER, S. L., FLECHTNER, V. R. & JOHANSEN, J. R. 2001. Is the 16S-23S rRNA internal transcribed spacer region a good tool for use in molecular systematics and population genetics? A case study in cyanobacteria. *Molecular Biology and Evolution*, 18, 1057-1069.
- BRACKMAN, G., HILLAERT, U., VAN CALENBERG, S., NELIS, H.N., COENYE, T. 2009. Use of quorum sensing inhibitors to interfere with biofilm formation and development in Burkholderia multivorans and Burkholderia cenocepacia. *Research in Microbiology*, 160, 8.
- BRAZELTON, W. J., BAROSS, J.A. 2009. Abundant transposases encoded by the metagenome of a hydrothermal chimney biofilm. *ISME J*, 3, 1420-1424.
- BRIAND, J. F., DJERIDI, I., JAMET, D., COUPE, S., BRESSY, C., MOLMERET, M., LE BERRE, B., RIMET, F., BOUCHEZ, A. & BLACHE, Y. 2012. Pioneer marine biofilms on artificial surfaces including antifouling coatings immersed in two contrasting French Mediterranean coast sites. *Biofouling*, 28, 453-463.
- BROCK, T. D. 1987. The study of microorganisms *in-situ*: Progress and problems. *Fletcher, M., T. R. G. Gray and J. G. Jones.*
- BROCK, T. D., MADIGAN, M.T., MARTINKO, J.M., PARKER, J. 1994. *Biology of Microorganisms*, Prentice-Hall International, Inc.
- BROWN, D. A., BEVERIDGE, T.J., KEEVIL, C.W., SHERIFF, B.L. 1998. Evaluation of microscopic techniques to observe precipitation in a natural microbial biofilm. *FEMS Microbiology Ecology*, 26, 14.
- CANGANELLA, F. & KATO, C. 2001. Deep Ocean Ecosystems. *eLS.* John Wiley & Sons,
- CARON, D. A. & COUNTWAY, P. D. 2009. Hypotheses on the role of the protistan rare biosphere in a changing world. *Aquatic Microbial Ecology*, 57, 227-238.

- CARON, D. A. & SIEBURTH, J. M. 1981. Disruption of the primary fouling sequence on fiber glass-reinforced plastic submerged in the marine-environment. *Applied and Environmental Microbiology*, 41, 268-273.
- CASEY, A. L., ADAMS, D., KARPANEN, T. J., LAMBERT, P. A., COOKSON, B. D., NIGHTINGALE, P., MIRUSZENKO, L., SHILLAM, R., CHRISTIAN, P. & ELLIOTT, T. S. J. Role of copper in reducing hospital environment contamination. *Journal of Hospital Infection*, 74, 72-77.
- CASEY, A. L., ADAMS, D., KARPANEN, T. J., LAMBERT, P. A., COOKSON, B. D., NIGHTINGALE, P., MIRUSZENKO, L., SHILLAM, R., CHRISTIAN, P. & ELLIOTT, T. S. J. 2009. Role of copper in reducing hospital environment contamination. Journal of Hospital Infection, 74, 72-77.
- CAVANAUGH, C. M. 1983. Symbiotic chemoautotrophic Bacteria in marine-invertebrates from sulfide-rich habitats. *Nature*, 302, 58-61.
- CHAMBERS, L. D., STOKES, K. R., WALSH, F. C. & WOOD, R. J. K. 2006. Modern approaches to marine antifouling coatings. *Surface and Coatings Technology*, 201, 3642-3652.
- CHAMP, M. A. 2001. New IMO convention to control anti-fouling systems on ships. *Sea Technology*, 42, 48-50.
- CHARACKLIS, W. G. 2009. Fouling biofilm development: A process analysis. Biotechnology and Bioengineering, 102, 310-347.
- CHARACKLIS, W. G., MARSHALL, K.C. 1990. Biofilms, New York, John Wiley & Sons.
- CHRISTENSEN, G. D., SIMPSON, W. A., YOUNGER, J. J., BADDOUR, L. M., BARRETT, F. F., MELTON, D. M. & BEACHEY, E. H. 1985. Adherence of coagulase-negative Staphylococci to plastic tissue-culture plates a quantitative model for the adherence of Staphylococci to medical devices. *Journal of Clinical Microbiology*, 22, 996-1006.
- CLEARY, D. F. R., SMALLA, K., MENDONÇA-HAGLER, L. C. S. & GOMES, N. C. M. 2012.

 Assessment of variation in bacterial composition among microhabitats in a mangrove environment using DGGE fingerprints and barcoded pyrosequencing. *Plos One*, 7, e29380.
- CONNELLY, D. P., COPLEY, J. T., MURTON, B. J., STANSFIELD, K., TYLER, P. A., GERMAN, C. R., VAN DOVER, C. L., AMON, D., FURLONG, M., GRINDLAY, N., HAYMAN, N., HUHNERBACH, V., JUDGE, M., LE BAS, T., MCPHAIL, S., MEIER, A., NAKAMURA, K.-I., NYE, V., PEBODY, M., PEDERSEN, R. B., PLOUVIEZ, S., SANDS, C., SEARLE, R. C., STEVENSON, P., TAWS, S. & WILCOX, S. 2012. Hydrothermal vent fields and chemosynthetic biota on the world's deepest seafloor spreading centre. *Nat Commun*, 3, 620.
- COOKSEY, B. & COOKSEY, K. E. 1988. Chemical Signal-Response in Diatoms of the Genus Amphora. *Journal of Cell Science*, 91, 523-529.
- COOKSEY, R. C., CRAWFORD, J. T., JACOBS, W. R., JR & SHINNICK, T. M. 1993. A rapid method for screening antimicrobial agents for activities against a strain of Mycobacterium tuberculosis expressing firefly luciferase. *Antimicrob. Agents Chemother.*, 37, 1348-1352.
- CORLISS, J. B., DYMOND, J., GORDON, L. I., EDMOND, J. M., HERZEN, R. P. V., BALLARD, R. D., GREEN, K., WILLIAMS, D., BAINBRIDGE, A., CRANE, K. & VANANDEL, T. H. 1979. Submarine thermal springs on the Galapagos Rift. *Science*, 203, 1073-1083.
- CORTESE, B. & MORGAN, H. 2012. Controlling the wettability of hierarchically structured thermoplastics. *Langmuir*, 28, 896-904.
- COSTERTON, J. W. 1995. Overview of microbial biofilms. *Journal of Industrial Microbiology*, 15, 137-140.
- COWLING, M. J., HODGKIESS, T., PARR, A. C. S., SMITH, M. J. & MARRS, S. J. 2000. An alternative approach to antifouling based on analogues of natural processes. *The Science of The Total Environment*, 258, 129-137.
- COWLING, M. J., HODGKIESS, T., PARR, A. C. S., SMITH, M. J., MARRS, S. J. 2000. An alternative approach to antifouling based on analogues of natural processes. *The Science of The Total Environment*, 258, 129-137.

- DAFFORN, K. A., LEWIS, J. A. & JOHNSTON, E. L. 2011. Antifouling strategies: History and regulation, ecological impacts and mitigation. *Marine Pollution Bulletin*, 62, 453-465.
- DAMSTE, J. S. S., MUYZER, G., ABBAS, B., RAMPEN, S. W., MASSE, G., ALLARD, W. G., BELT, S. T., ROBERT, J. M., ROWLAND, S. J., MOLDOWAN, J. M., BARBANTI, S. M., FAGO, F. J., DENISEVICH, P., DAHL, J., TRINDADE, L. A. F. & SCHOUTEN, S. 2004. The rise of the rhizosolenid diatoms. *Science*, 304, 584-587.
- DANG, H. Y. & LOVELL, C. R. 2000. Bacterial primary colonization and early succession on surfaces in marine waters as determined by amplified rRNA gene restriction analysis and sequence analysis of 16S rRNA genes. *Applied and Environmental Microbiology*, 66, 467-475.
- DAVIES, D. G. 2002. Regulatory Events in Biofilm Development. *In:* MCCLAIN, R. J. C., DECHO. A.W. (ed.) *Molecular Ecology of Biofilms.* Norfolk: Horizon Scientific Press
- DECHO, A. W. & LOPEZ, G. R. 1993. Exopolymer microenvironments of microbial-flora multiple and interactive effects on trophic relationships. *Limnology and Oceanography*, 38, 1633-1645.
- DELAUNEY, L. 2009. Biofouling protection for marine underwater observatories sensors. *Oceans* 2009 Europe, Vols 1 and 2.
- DELAUNEY, L., COMPÈRE, C. & LEHAITRE, M. 2010. Biofouling protection for marine environmental sensors. *Ocean Sci.*, 6, 503-511.
- DELAUNEY, L. & IEEE 2009. Biofouling protection for marine underwater observatories sensors. *Oceans 2009 Europe, Vols 1 and 2.*
- DELONG, E. F. 1992. Archaea in coastal marine environments. *Proceedings of the National Academy of Sciences of the United States of America*, 89, 5685-5689.
- DEMING, J. W. 1998. Deep ocean environmental biotechnology. *Current Opinion in Biotechnology*, 9, 283-287.
- DEMING, J. W. & COLWELL, R. R. 1985. Observations of barophilic microbial activity in samples of sediment and intercepted particulates from the Demerara Abyssal-Plain. *Applied and Environmental Microbiology*, 50, 1002-1006.
- DEMING, J. W., HADA, H., COLWELL, R. R., LUEHRSEN, K. R. & FOX, G. E. 1984. The Ribonucleotide Sequence of 5s Ribosomal-Rna from 2 Strains of Deep-Sea Barophilic Bacteria. *Journal of General Microbiology*, 130, 1911-1920.
- DESBRUYERES, D., GAILL F., LAUBIER, L., FOUQUET, Y. 1985. Polychaetous annelids from hydrothermal vent ecosytems: An ecological overview. *Bulletin of the Biological Society of Washington*, 6, 103-116.
- DOBRETSOV, S., DAHMS, H. U. & QIAN, P. Y. 2006. Inhibition of biofouling by marine microorganisms and their metabolites. *Biofouling*, 22, 43-54.
- DOIRON, K., LINOSSIER, I., FAY, F., YONG, J., ABD WAHID, E., HADJIEV, D. & BOURGOUGNON, N. 2012. Dynamic approaches of mixed species biofilm formation using modern technologies. *Marine Environmental Research*, 78, 40-47.
- DOMEK, M. J., LECHEVALLIER, M. W., CAMERON, S. C. & MCFETERS, G. A. 1984. Evidence for the Role of Copper in the Injury Process of Coliform Bacteria in Drinking-Water. *Applied and Environmental Microbiology*, 48, 289-293.
- DÜRR, H. 2007. Influence of Surface Roughness and Wettability of Stainless Steel on Soil Adhesion, Cleanability and Microbial Inactivation. *Food and Bioproducts Processing*, 85, 49-56.
- EDGCOMB, V., ORSI, W., BUNGE, J., JEON, S., CHRISTEN, R., LESLIN, C., HOLDER, M., TAYLOR, G. T., SUAREZ, P., VARELA, R. & EPSTEIN, S. 2011. Protistan microbial observatory in the Cariaco Basin, Caribbean. I. Pyrosequencing vs Sanger insights into species richness. *Isme Journal*, 5, 1344-1356.
- EDGERTON, G. A. V., CA). 1978. Oceanographic sensor with in-situ cleaning and biofouling prevention system. United States patent application 4092858.
- EIGENBRODE, J., BENNING, L. G., MAULE, J., WAINWRIGHT, N., STEELE, A., AMUNDSEN, H. E. F. & TEAM, A. 2009. A field-based cleaning protocol for sampling devices used in life-detection studies. *Astrobiology*, 9, 455-465.

- ELLWOOD, D. C., KEEVIL, C. W., MARSH, P. D., BROWN, C. M. & WARDELL, J. N. 1982. Surface-associated growth. *Philosophical Transactions of the Royal Society of London Series B-Biological Sciences*, 297, 517-532.
- ELOE, E. A., SHULSE, C. N., FADROSH, D. W., WILLIAMSON, S. J., ALLEN, E. E. & BARTLETT, D. H. 2011. Compositional differences in particle-associated and free-living microbial assemblages from an extreme deep-ocean environment. *Environmental Microbiology Reports*, 3, 449-458.
- ERIKSEN, C. C., OSSE, T. J., LIGHT, R. D., WEN, T., LEHMAN, T. W., SABIN, P. L., BALLARD, J. W. & CHIODI, A. M. 2001. Seaglider: A long-range autonomous underwater vehicle for oceanographic research. *leee Journal of Oceanic Engineering*, 26, 424-436.
- FANG, H. H. P., CHAN, K. Y. & XU, L. C. 2000. Quantification of bacterial adhesion forces using atomic force microscopy (AFM). *Journal of Microbiological Methods*, 40, 89-97.
- FANG, H. H. P., XU, L.-C. & CHAN, K.-Y. 2002. Effects of toxic metals and chemicals on biofilm and biocorrosion. *Water Research*, 36, 4709-4716.
- FERNANDEZ-LEBORANS, G. & GABILONDO, R. 2005. Hydrozoan and protozoan epibionts on two decapod species, Liocarcinus depurator (Linnaeus, 1758) and Pilumnus hirtellus (Linnaeus, 1761), from Scotland. *Zoologischer Anzeiger A Journal of Comparative Zoology*, 244, 59-72.
- FLEMMING, H. C. 2008. Biofilms. *In:* SONS, J. W. (ed.) *Encyclopedia of Life @Sciences.* John Wiley & Sons.
- FLORES, G. E., CAMPBELL, J. H., KIRSHTEIN, J. D., MENEGHIN, J., PODAR, M., STEINBERG, J. I., SEEWALD, J. S., TIVEY, M. K., VOYTEK, M. A., YANG, Z. K. & REYSENBACH, A.-L. 2011. Microbial community structure of hydrothermal deposits from geochemically different vent fields along the Mid-Atlantic Ridge. *Environmental Microbiology*, 13, 2158-2171.
- FRAJKA-WILLIAMS, E., RHINES, P. B. & ERIKSEN, C. C. 2009. Physical controls and mesoscale variability in the Labrador Sea spring phytoplankton bloom observed by Seaglider. *Deep-Sea Research Part I-Oceanographic Research Papers*, 56, 2144-2161.
- GAGE J.D., T. P. A. 1991. *Deep-Sea Biology: A natural history of organisms at the deep-sea floor*, Cambridge, United Kingdom, Cambridge University Press.
- GARDELLA, J. A., JR., WYNNE, K.J., MCCARTHY, T.J., RABOLT, J.F, BELFORD, G. 1997. New technologies for surface analysis to assess biofouling resistance. *Naval Research Reviews*, Four/1997, 16.
- GARRETT, T. R., BHAKOO, M. & ZHANG, Z. B. 2008. Bacterial adhesion and biofilms on surfaces. *Progress in Natural Science-Materials International*, 18, 1049-1056.
- GEBRUK, A. V., GALKIN, S. V., VERESHCHAKA, A. L., MOSKALEV, L. I. & SOUTHWARD, A. J. 1997. Ecology and biogeography of the hydrothermal vent fauna of the Mid-Atlantic Ridge. *Advances in Marine Biology, Vol 32*, 32, 93-144.
- GERMAN, C. R., RAMIREZ-LLODRA, E., BAKER, M.C., TYLER, P.A., THE CHESS SCIENTIFIC STEERING, COMMITTEE 2011. Deep-water chemosynthetic ecosystem research during the Census of Marine Life decade and beyond: A proposed deep-ocean road map. *Plos One*, 6, e23259.
- GIAO, M. S., WILKS, S. A., AZEVEDO, N. F., VIEIRA, M. J. & KEEVIL, C. W. 2009. Comparison between standard culture and peptide nucleic acid 16S rRNA hybridization quantification to study the influence of physico-chemical parameters on Legionella pneumophila survival in drinking water biofilms. *Biofouling*, 25, 335-343.
- GILLAN, D. C. 2004. The effect of an acute copper exposure on the diversity of a microbial community in North Sea sediments as revealed by DGGE analysis--the importance of the protocol. *Marine Pollution Bulletin*, 49, 504-513.
- GLASEL, J. A. 1995. Validity of nucleic acid purities monitored by 260nm/280nm absorbance ratios. *Biotechniques*, 18, 62-3.
- GODWIN WESLEY, S., SATHEESH, S. 2009. Temporal variability of nutrient concentration in marine biofilm developed on acrylic panels. *Journal of Experimental Marine Biology and Ecology*, 379, 7.

- GRZYMSKI, J. J., MURRAY, A.E., CAMPBELL, B.J., KAPLAREVIC, M., GAO, G.R., LEE, C., DANIEL, R., GHADIRI, A., FELDMAN, R. A., CARY, S.C. 2008. Metagenome analysis of an extreme microbial symbiosis reveals eurythermal adaptation and metabolic flexibility. *Proceedings of the National Academy of Sciences*, 105, 17516-17521.
- GU, J. D., ROMAN, M., ESSELMAN, T. & MITCHELL, R. 1998. The role of microbial biofilms in deterioration of space station candidate materials. *International Biodeterioration & Biodegradation*, 41, 25-33.
- GUEZENNEC, J., ORTEGA-MORALES, O., RAGUENES, G. & GEESEY, G. 1998. Bacterial colonization of artificial substrate in the vicinity of deep-sea hydrothermal vents. *FEMS Microbiology Ecology*, 26, 89-99.
- HADDAD, A., CAMACHO, F., DURAND, P. & CARY, S. C. 1995. Phylogenetic characterization of the epibiotic bacteria associated with the hydrothermal vent polychaete Alvinella-Pompejana. *Applied and Environmental Microbiology*, 61, 1679-1687.
- HAIMOV-KOCHMAN, R., FISHER, S. J. & WINN, V. D. 2006. Modification of the Standard Trizol-Based Technique Improves the Integrity of RNA Isolated from RNase-Rich Placental Tissue. *Clin Chem*, 52, 159-160.
- HATUN, H., ERIKSEN, C. C. & RHINES, P. B. 2007. Buoyant eddies entering the Labrador Sea observed with gliders and altimetry. *Journal of Physical Oceanography*, 37, 2838-2854.
- HELLIO, C., DE LA BROISE, D., DUFOSSE, L., LE GAL, Y., BOURGOUGNON, N. 2001. Inhibition of marine bacteria by extracts of macroalgae: potential use for environmentally friendly antifouling paints. *Marine Environmental Research*, 52, 17.
- HERMANSSON, M. 1999. The DLVO theory in microbial adhesion. *Colloids and Surfaces B-Biointerfaces*, 14, 105-119.
- HIROMOTO, S., ONODERA, E., CHIBA, A., ASAMI, K. & HANAWA, T. 2005. Microstructure and corrosion behaviour in biological environments of the new forged low-Ni Co-Cr-Mo alloys. *Biomaterials*, 26, 4912-4923.
- HOAGLAND, P., BEAULIEU, S., TIVEY, M. A., EGGERT, R. G., GERMAN, C., GLOWKA, L. & LIN, J. 2010. Deep-sea mining of seafloor massive sulfides. *Marine Policy*, 34, 728-732.
- HOLDEN, M. T. G., DIGGLE, S.P., WILLIAMS, P. 2007. Quorum sensing. *In:* WILEY & SONS, L. (ed.) *Encyclopedia of Life Sciences.* Wiley & Sons, Ltd.
- HOLMSTROM, C., EGAN, S., FRANKS, A., MCCLOY, S., KJELLEBERG, S. 2002. Antifouling activities expressed by marine surface associated Pseudoalteromonas species. *FEMS Microbiology Ecology*, 41, 12.
- HONG, K. T., IMADOJEMU, H. & WEBB, R. L. 1994. Effects of oxidation and surface roughness on contact angle. *Experimental Thermal and Fluid Science*, 8, 279-285.
- HONRAET, K., NELIS, H.J. 2006. Use of modified robbins device and fluorescent staining to screen plant extracts for the inhibition of S. mutans biofilm formation. *Journal of Microbiological Methods*, 64, 8.
- HUBER, I., SPANGGAARD, B., APPEL, K. F., ROSSEN, L., NIELSEN, T. & GRAM, L. 2004. Phylogenetic analysis and in situ identification of the intestinal microbial community of rainbow trout (Oncorhynchus mykiss, Walbaum). *Journal of Applied Microbiology*, 96, 117-132.
- HUBER, J. A., MARK WELCH, D., MORRISON, H. G., HUSE, S. M., NEAL, P. R., BUTTERFIELD, D. A. & SOGIN, M. L. 2007. Microbial population structures in the deep marine biosphere. *Science*, 318, 97-100.
- HUBER, R., STOHR, J., HOHENHAUS, S., RACHEL, R., BURGGRAF, S., JANNASCH, H. W. & STETTER, K. O. 1995. Thermococcus chitonophagus Sp-Nov, a novel, chitin-degrading, hyperthermophillic Archaeum from a deep-sea hydrothermal vent environment. *Archives of Microbiology*, 164, 255-264.
- HUNG, O. S., GOSSELIN, L. A., THIYAGARAJAN, V., WU, R. S. S. & QIAN, P. Y. 2005a. Do effects of ultraviolet radiation on microbial films have indirect effects on larval

- attachment of the barnacle Balanus amphitrite? *Journal of Experimental Marine Biology and Ecology*, 323, 16-26.
- HUNG, O. S., THIYAGARAJAN, V., WU, R. S. S. & QIAN, P. Y. 2005b. Effect of ultraviolet radiation on biofilms and subsequent larval settlement of Hydroides elegans. *Marine Ecology-Progress Series*, 304, 155-166.
- HURTADO, L. A., LUTZ, R. A. & VRIJENHOEK, R. C. 2004. Distinct patterns of genetic differentiation among annelids of eastern Pacific hydrothermal vents. *Molecular Ecology*, 13, 2603-2615.
- HUSE, S. M., DETHLEFSEN, L., HUBER, J. A., WELCH, D. M., RELMAN, D. A. & SOGIN, M. L. 2008. Exploring microbial diversity and taxonomy using SSU rRNA hypervariable tag sequencing. *PLoS Genet*, 4, e1000255.
- ISHII, K., MUßMANN, M., MACGREGOR, B. J. & AMANN, R. 2004. An improved fluorescence in situ hybridization protocol for the identification of bacteria and archaea in marine sediments. *FEMS Microbiology Ecology*, 50, 203-212.
- J.D., G. & P.A., T. 1991. Deep-Sea Biology: A natural history of organisms at the deep-sea floor. Cambridge, United Kingdom: Cambridge University Press.
- JANNASCH, H. W. 1995. Microbial interactions with hydrothermal fluids. *In:* HUMPHRIS (ed.) *Seafloor hydrothermal systems: physical, chemical, biological, and geological interactions.* American Geophysical Union.
- JANNASCH, H. W. & TAYLOR, C. D. 1984. Deep-Sea Microbiology. *Annual Review of Microbiology*, 38, 487-514.
- JANNASCH, H. W. & WIRSEN, C. O. 1984. Variability of Pressure Adaptation in Deep-Sea Bacteria. *Archives of Microbiology*, 139, 281-288.
- JANZEN, C. D. & CREED, E. L. 2011. Physical Oceanographic Data from Seaglider Trials in Stratified Coastal Waters Using a New Pumped Payload CTD. *Oceans* 2011.
- JENKINSON, H. F., LAPPIN-SCOTT, H.M. 2001. Biofilms adhere to stay. *Trends in Microbiology*, 9, 2.
- JOHNSON, K. S., CHILDRESS, J. J. & BEEHLER, C. L. 1988a. Short-Term Temperature Variability in the Rose Garden Hydrothermal Vent Field an Unstable Deep-Sea Environment. *Deep-Sea Research Part a-Oceanographic Research Papers*, 35, 1711-&.
- JOHNSON, K. S., CHILDRESS, J. J., HESSLER, R. R., SAKAMOTOARNOLD, C. M. & BEEHLER, C. L. 1988b. Chemical and Biological Interactions in the Rose Garden Hydrothermal Vent Field, Galapagos Spreading Center. *Deep-Sea Research Part a-Oceanographic Research Papers*, 35, 1723-1744.
- KARL, D. M. 1995. Ecology of free-living, hydrothermal vent microbial communities. *In:* KARL, D. M. (ed.) *The Microbiology of Deep-Sea Hydrothermal Vents.* New York: CRC Press.
- KATO, C., LI, L. N., TAMAOKA, J. & HORIKOSHI, K. 1997. Molecular analyses of the sediment of the 11000-m deep Mariana Trench. Extremophiles, 1, 117-123.
- KEEVIL, C. W. 2002. Pathogens in environmental biofilms. *In:* BITTON (ed.) *Encyclopedia of Environmental Microbiology*. New York: Wiley.
- KEEVIL, C. W. 2003. Rapid detection of biofilms and adherent pathogens using scanning confocal laser microscopy and episcopic differential interference contrast microscopy. *Water Science and Technology*, 47, 105-116.
- KERR, A., COWLING, M.J.., BEVERIGDE, C.M., SMITH, M.J., PARR, A.C.S. 1998. The early stages of marine biofouling and its effect on two types of optical sensors. *Environmental International*, 24, 13.
- KERR, A., SMITH, M. J., COWLING, M. J. & HODGKIESS, T. 2001. The biofouling resistant properties of six transparent polymers with and without pre-treatment by two antimicrobial solutions. *Materials & Design*, 22, 383-392.
- KIELEMOES, J., BULTINCK, I., STORMS, H., BOON, N., VERTRAETE, W. 2001. Occurence of manganese-oxidizing microorganisms and manganese deposition during biofilm formation on stainless steel in a brackish surface water. *FEMS Microbiology Ecology*, 39, 14.
- KLEVENZ, V., BACH, W., SCHMIDT, K., HENTSCHER, M., KOSCHINSKY, A. & PETERSEN, S. 2011. Geochemistry of vent fluid particles formed during initial hydrothermal

- fluid-seawater mixing along the Mid-Atlantic Ridge. *Geochemistry Geophysics Geosystems*, 12.
- KOCH, K., BHUSHAN, B. & BARTHLOTT, W. 2009. Multifunctional surface structures of plants: An inspiration for biomimetics. *Progress in Materials Science*, 54, 137-178.
- KRISTENSEN, J. B., MEYER, R.L., LAURSEN, B.S., SHIPOVSKOV, S., BESENBACHER, F., POULSEN, C.H. 2008. Antifouling enzymes and the biochemistry of marine settlement. *Biotechnology Advances*, 26, 11.
- LALLI, C. M. & PARSONS, T. R. 1997a. Chapter 1 Introduction. *Biological Oceanography: An Introduction (Second Edition)*. Oxford: Butterworth-Heinemann.
- LALLI, C. M. & PARSONS, T. R. 1997b. Chapter 2 The abiotic environment. *Biological Oceanography: An Introduction (Second Edition)*. Oxford: Butterworth-Heinemann.
- LALLI, C. M. & PARSONS, T. R. 1997c. Chapter 8 Benthic communities. *Biological Oceanography: An Introduction (Second Edition)*. Oxford: Butterworth-Heinemann.
- LANDOULSI, J., COOKSEY, K. E. & DUPRES, V. 2011. Review Interactions between diatoms and stainless steel: focus on biofouling and biocorrosion. *Biofouling*, 27, 1105-1124.
- LAWRENCE, J. R., NEU, T.R., SWERHONE, G.D.W. 1998. Application of multiple parameter imaging for the quantification of algal, bacterial and exopolymer components of microbial biofilms. *Journal of Microbiological Methods*, 32, 9.
- LENK, S., ARNDS, J., ZERJATKE, K., MUSAT, N., AMANN, R. & MUßMANN, M. 2011. Novel groups of Gammaproteobacteria catalyse sulfur oxidation and carbon fixation in a coastal, intertidal sediment. *Environmental Microbiology*, 13, 758-774.
- LI, J., LI, J., YUAN, W. & DU, Y. Biocorrosion characteristics of the copper alloys BFe30-1-1 and HSn70-1AB by SRB using Atomic Force Microscopy and Scanning Electron Microscopy. *International Biodeterioration & Biodegradation,* In Press, Corrected Proof.
- LI, J., YUAN, W. & DU, Y. 2010. Biocorrosion characteristics of the copper alloys BFe30-1-1 and HSn70-1AB by SRB using Atomic Force Microscopy and Scanning Electron Microscopy. *International Biodeterioration & Biodegradation,* In Press, Corrected Proof.
- LI, Z.-Y., HE, L.-M., WU, J., JIANG, Q. 2006. Bacterial community diversity associated with four marine sponges from the South China Sea based on 16S rDNA-DGGE fingerprinting. *Journal of Experimental Marine Biology and Ecology*, 329, 75-85.
- LIGHTFOOT, R. H., TYLER, P. A. & GAGE, J. D. 1979. Seasonal reproduction in deep-sea bivalves and brittlestars. *Deep Sea Research Part A. Oceanographic Research Papers*, 26, 967-973.
- LITTLE, B., WAGNER, P., RAY, R., POPE, R. & SCHEETZ, R. 1991. Biofilms an Esem evaluation of artifacts introduced during SEM preparation. *Journal of Industrial Microbiology*, 8, 213-221.
- LITTLE, B. J. & MANSFELD, F. B. 1991. The corrosion behavior of stainless-steels and copper-alloys exposed to natural seawater. *Werkstoffe Und Korrosion-Materials and Corrosion*, 42, 331-340.
- LIU, W. T., MARSH, T. L., CHENG, H. & FORNEY, L. J. 1997. Characterization of microbial diversity by determining terminal restriction fragment length polymorphisms of genes encoding 16S rRNA. *Applied and Environmental Microbiology*, 63, 4516-4522.
- LO GIUDICE, A., CARUSO, C., MANGANO, S., BRUNI, V., DE DOMENICO, M. & MICHAUD, L. 2012. Marine Bacterioplankton Diversity and Community Composition in an Antarctic Coastal Environment. *Microbial Ecology*, 63, 210-223.
- LOEB, G. I. & NEIHOF, R. A. 1975. Marine conditioning films. *Advances in Chemistry Series*, 319-335.
- LONSDALE, P. 1977. Clustering of suspension-feeding macrobenthos near abyssal hydrothermal vents at Oceanic Spreading Centers. *Deep-Sea Research*, 24, 857-&.

- LOPEZ-GARCIA, P., DUPERRON, S., PHILIPPOT, P., FORIEL, J., SUSINI, J. & MOREIRA, D. 2003. Bacterial diversity in hydrothermal sediment and epsilon proteobacterial dominance in experimental microcolonizers at the Mid-Atlantic Ridge. *Environmental Microbiology*, 5, 961-976.
- LUNA, G. M., STUMM, K., PUSCEDDU, A. & DANOVARO, R. 2009. Archaeal diversity in deep-sea sediments estimated by means of different Terminal-Restriction Fragment Length Polymorphisms (T-RFLP) protocols. *Current Microbiology*, 59, 356-361.
- MA, Y., CAO, X., FENG, X., MA, Y. & ZOU, H. 2007. Fabrication of super-hydrophobic film from PMMA with intrinsic water contact angle below 90°. *Polymer*, 48, 7455-7460.
- MANSFELD, F., LIU, G., XIAO, H., TSAI, C. H. & LITTLE, B. J. 1994. The corrosion behavior of copper alloys, stainless steels and titanium in seawater. *Corrosion Science*, 36, 2063-2095.
- MARSZALEK, D. S., GERCHAKOV, S. M. & UDEY, L. R. 1979. Influence of substrate composition on marine microfouling. *Applied and Environmental Microbiology*, 38, 987-995.
- MARTIN-CUADRADO, A. B., LOPEZ-GARCIA, P., ALBA, J. C., MOREIRA, D., MONTICELLI, L., STRITTMATTER, A., GOTTSCHALK, G. & RODRIGUEZ-VALERA, F. 2007.

 Metagenomics of the Deep Mediterranean, a Warm Bathypelagic Habitat. *Plos One.* 2.
- MARTÍN-PLATERO, A. M., PERALTA-SÁNCHEZ, J. M., SOLER, J. J. & MARTÍNEZ-BUENO, M. Chelex-based DNA isolation procedure for the identification of microbial communities of eggshell surfaces. *Analytical Biochemistry*, 397, 253-255.
- MARTÍN-PLATERO, A. M., PERALTA-SÁNCHEZ, J. M., SOLER, J. J. & MARTÍNEZ-BUENO, M. 2010. Chelex-based DNA isolation procedure for the identification of microbial communities of eggshell surfaces. *Analytical Biochemistry*, 397, 253-255.
- MATHEE, K., KHARAZMI, A., HOBY, N. 2002. Rile of exopolysaccharides in biofilm matrix formation: The Alginate paradigm. *In:* MCCLAIN, R. J. C., DECHO. A.W. (ed.) *Molecular Ecology of Biofilms*. Norfolk: Horizon Scientific Press.
- MAUKONEN, J., MATTILA-SANDHOLM, T. & WIRTANEN, G. 2000. Metabolic indicators for assessing bacterial viability in hygiene sampling using cells in suspension and swabbed biofilm. *Lebensmittel-Wissenschaft und-Technologie*, 33, 225-233.
- MCGINNIS, S. & MADDEN, T. L. 2004. BLAST: at the core of a powerful and diverse set of sequence analysis tools. *Nucleic Acids Research*, 32, W20-W25.
- MCLEAN, R. J. C. 2002. An overview of biofilm molecular ecology. *In:* MCLEAN, R. J. C., DECHO, A.W. (ed.) *Molecular Ecology of Biofilms.* 1 ed. Norfolk: Horizon Sientific Press
- MEIER, A., TSALOGLOU, N.-M., MOWLEM, M. C., KEEVIL, C. W. & CONNELLY, D. P. 2013. Hyperbaric biofilms on engineering surfaces formed in the deep sea. *Biofouling*, 29, 1029-1042.
- MELZAK, K. A., SHERWOOD, C. S., TURNER, R. F. B. & HAYNES, C. A. 1996. Driving forces for DNA adsorption to silica in perchlorate solutions. *Journal of Colloid and Interface Science*, 181, 635-644.
- MILITON, C., BOUCHER, D., VACHELARD, C., PERCHET, G., BARRA, V., TROQUET, J., PEYRETAILLADE, E. & PEYRET, P. 2010. Bacterial community changes during bioremediation of aliphatic hydrocarbon-contaminated soil. *Fems Microbiology Ecology*, 74, 669-681.
- MITCHELL, S. B., LAWLER, D. M., WEST, J. R. & COUPERTHWAITE, J. S. 2003. Use of continuous turbidity sensor in the prediction of fine sediment transport in the turbidity maximum of the Trent Estuary, UK. *Estuarine Coastal and Shelf Science*, 58, 645-652.
- MOALIC, Y., DESBRUYÈRES, D., DUARTE, C. M., ROZENFELD, A. F., BACHRATY, C. & ARNAUD-HAOND, S. 2011. Biogeography revisited with Network Theory: Retracing the history of hydrothermal vent communities. *Systematic Biology*.
- MOESENEDER, M. M., WINTER, C., ARRIETA, J. M. & HERNDL, G. J. 2001a. Terminal-restriction fragment length polymorphism (T-RFLP) screening of a marine

- archaeal clone library to determine the different phylotypes. *Journal of Microbiological Methods*, 44, 159-172.
- MOESENEDER, M. M., WINTER, C. & HERNDL, G. J. 2001b. Horizontal and vertical complexity of attached and free-living bacteria of the eastern Mediterranean Sea, determined by 16S rDNA and 16S rRNA fingerprints. *Limnology and Oceanography*, 46, 95-107.
- MUELLER, R. F., CHARACKLIS, W. G., JONES, W. L. & SEARS, J. T. 1992. Characterization of initial events in bacterial surface colonization by 2 Pseudomonas species using Image-Analysis. *Biotechnology and Bioengineering*, 39, 1161-1170.
- MUYZER, G., DEWAAL, E. C. & UITTERLINDEN, A. G. 1993. Profiling of complex microbial-populations by Denaturing Gradient Gel-Electrophoresis analysis of Polymerase Chain Reaction-amplified genes-coding for 16s ribosomal-RNA. *Applied and Environmental Microbiology*, 59, 695-700.
- MUYZER, G. & SMALLA, K. 1998. Application of denaturing gradient gel electrophoresis (DGGE) and temperature gradient gel electrophoresis (TGGE) in microbial ecology. Antonie Van Leeuwenhoek International Journal of General and Molecular Microbiology, 73, 127-141.
- MUYZER, G., TESKE, A., WIRSEN, C. O. & JANNASCH, H. W. 1995. Phylogenetic-relationships of Thiomicrospira species and their identification in deep-sea hydrothermal vent samples by Denaturing Gradient Gel-Electrophoresis of 16s rDNA fragments. *Archives of Microbiology*, 164, 165-172.
- NAKASONO, S. & MATSUNAGA, T. 1993. Electrochemical sterilization of marine-bacteria adsorbed onto a graphite-silicone electrode by application of an alternating potential. *Denki Kagaku*, 61, 899-902.
- NAKAYAMA, T., WAKE, H., OZAWA, K., KODAMA, H., NAKAMURA, N. & MATSUNAGA, T. 1998. Use of a titanium nitride for electrochemical inactivation of marine bacteria. *Environmental Science & Technology*, 32, 798-801.
- NEI, M. & KUMAR, S. 2000. *Molecular evolution and phylogenetics,* New York, Oxford University Press.
- NORDE, W. & LYKLEMA, J. 1989. Protein adsorption and bacterial adhesion to solidsurfaces - a colloid-chemical approach. *Colloids and Surfaces*, 38, 1-13.
- NORTH, N. A. & MACLEOD, I. D. 1987. *Corrosion of metals,* London, United Kingdom, Buttersworths.
- NYE, V., COPLEY, J. & PLOUVIEZ, S. 2011. A new species of Rimicaris (Crustacea: Decapoda: Caridea: Alvinocarididae) from hydrothermal vent fields on the Mid-Cayman Spreading Centre, Caribbean. *Journal of the Marine Biological Association of the United Kingdom*, FirstView, 1-16.
- OCHSENREITER, T., SELEZI, D., QUAISER, A., BONCH-OSMOLOVSKAYA, L. & SCHLEPER, C. 2003. Diversity and abundance of Crenarchaeota in terrestrial habitats studied by 16S RNA surveys and real time PCR. *Environmental Microbiology*, 5, 787-797.
- PEETERS, E., NELIS, H.J., COENYE, T. 2008. Comparison of multiple methods for quantification of microbial biofilms grown in microtiter plates. *Journal of Microbiological Methods*, 72, 9.
- PERRY, M. J., SACKMANN, B. S., ERIKSEN, C. C. & LEE, C. M. 2008. Seaglider observations of blooms and subsurface chlorophyll maxima off the Washington coast. *Limnology and Oceanography*, 53, 2169-2179.
- PETERSEN, J. M., ZIELINSKI, F. U., PAPE, T., SEIFERT, R., MORARU, C., AMANN, R., HOURDEZ, S., GIRGUIS, P. R., WANKEL, S. D., BARBE, V., PELLETIER, E., FINK, D., BOROWSKI, C., BACH, W. & DUBILIER, N. 2011. Hydrogen is an energy source for hydrothermal vent symbioses. *Nature*, 476, 176-180.
- PICHETTE, C., ZHANG, H., DAVISON, W. & SAUVÉ, S. 2007. Preventing biofilm development on DGT devices using metals and antibiotics. *Talanta*, 72, 716-722.
- POLZ, M. F. & CAVANAUGH, C. M. 1995. Dominance of one bacterial phylotype at a Mid-Atlantic Ridge hydrothermal vent site. *Proceedings of the National Academy of Sciences of the United States of America*, 92, 7232-7236.

- POZOS, N., SCOW, K., WUERTZ, S. & DARBY, J. 2004. UV disinfection in a model distribution system: biofilm growth and microbial community. *Water Research*, 38, 3083-3091.
- PRICE, C. W., LESLIE, D.C., LANDERS, J.P. 2009. Nucleic acid extraction techniques and application to the microchip. *Lab Chip*.
- PRIEN, R. D. 2007. The future of chemical in situ sensors. *Marine Chemistry*, 107, 422-432.
- RAILKIN, A. I. 2004. Marine Biofouling: colonisation processes and defences, CRC Press. RAZATOS, A., ONG, Y. L., SHARMA, M. M. & GEORGIOU, G. 1998. Molecular determinants of bacterial adhesion monitored by atomic force microscopy. Proceedings of the National Academy of Sciences of the United States of America, 95, 11059-11064.
- REDMOND, M. C. & VALENTINE, D. L. 2012. Natural gas and temperature structured a microbial community response to the Deepwater Horizon oil spill. *Proceedings of the National Academy of Sciences of the United States of America*, 109, 20292-20297.
- ROBINSON, P. J., WALKER, J. T., KEEVIL, C. W. & COLE, J. 1995. Reporter genes and fluorescent probes for studying the colonisation of biofilms in a drinking water supply line by enteric bacteria. *FEMS Microbiology Letters*, 129, 183-188.
- ROBINSON, P. J., WALKER, J.T., KEEVIL, C.W., COLE, C. 1995. Reporter genes and flourescent probes for studying the colonisation of biofilms in a drinking water supply line by enteric bacteria. *FEMS Microbiology Letters*, 129, 6.
- RODRIGUEZ, G. G., PHIPPS, D., ISHIGURO, K. & RIDGWAY, H. F. 1992. Use of a fluorescent redox probe for direct visualization of actively respiring Bacteria. Applied and Environmental Microbiology, 58, 1801-1808.
- ROGERS, A. D., TYLER, P. A., CONNELLY, D. P., COPLEY, J. T., JAMES, R., LARTER, R. D., LINSE, K., MILLS, R. A., GARABATO, A. N., PANCOST, R. D., PEARCE, D. A., POLUNIN, N. V. C., GERMAN, C. R., SHANK, T., BOERSCH-SUPAN, P. H., ALKER, B. J., AQUILINA, A., BENNETT, S. A., CLARKE, A., DINLEY, R. J. J., GRAHAM, A. G. C., GREEN, D. R. H., HAWKES, J. A., HEPBURN, L., HILARIO, A., HUVENNE, V. A. I., MARSH, L., RAMIREZ-LLODRA, E., REID, W. D. K., ROTERMAN, C. N., SWEETING, C. J., THATJE, S. & ZWIRGLMAIER, K. 2012. The Discovery of New Deep-Sea Hydrothermal Vent Communities in the Southern Ocean and Implications for Biogeography. *Plos Biology*, 10.
- ROGERS, C. E., BENNETT, J. G. & KESSEL, S. L. 1994a. Corrosivity Test Methods for Polymeric Materials .2. Cnet Test Method. *Journal of Fire Sciences*, 12, 134-154.
- ROGERS, J., DOWSETT, A. B., DENNIS, P. J., LEE, J. V. & KEEVIL, C. W. 1994b. Influence of plumbing materials on biofilm formation and growth of Legionella-Pneumophila in portable water-systems. *Applied and Environmental Microbiology*, 60, 1842-1851.
- ROGERS, J., DOWSETT, A. B., DENNIS, P. J., LEE, J. V. & KEEVIL, C. W. 1994c. Influence of Plumbing Materials on Biofilm Formation and Growth of Legionella-Pneumophila in Potable Water-Systems. *Applied and Environmental Microbiology*, 60, 1842-1851.
- ROGERS, J., DOWSETT, A. B., DENNIS, P. J., LEE, J. V. & KEEVIL, C. W. 1994d. Influence of temperature and plumbing material selection on biofilm formation and growth of Legionella-Pneumophila in a model potable water-system containing complex microbial-flora. *Applied and Environmental Microbiology*, 60, 1585-1592.
- ROUND, F. E., CRAWFORD, R. M. & MANN, D. G. 2007. *The Diatoms Biology and Morphology of the Genera*, Cambridge University Press.
- RZHETSKY, A. & NEI, M. 1992. A simple method for estimating and testing Minimum-Evolution trees. *Molecular Biology and Evolution*, 9, 945-967.
- SAGA, Y. & TAMIAKI, H. 2004. Fluorescence spectroscopy of single photosynthetic light-harvesting supramolecular systems. *Cell Biochemistry and Biophysics*, 40, 149-165.
- SAITOU, N. & NEI, M. 1987. The Neighbor-Joining Method a New Method for Reconstructing Phylogenetic Trees. *Molecular Biology and Evolution,* 4, 406-425.

- SALTLANTIC. 2010. *BioShutter* [Online]. Available: http://www.planet-ocean.co.uk/satlantic/.
- SANDERS, H. 1968. Marine Benthic Diversity: A Comparative Study. *The American Naturalist*, 102, 243-282.
- SANDERS, H. L., HESSLER, R. R. & HAMPSON, G. R. 1965. An introduction to the study of deep-sea benthic faunal assemblages along the Gay Head-Bermuda transect. Deep Sea Research and Oceanographic Abstracts, 12, 845-867.
- SANTELLI, C. M., ORCUTT, B. N., BANNING, E., BACH, W., MOYER, C. L., SOGIN, M. L., STAUDIGEL, H. & EDWARDS, K. J. 2008. Abundance and diversity of microbial life in ocean crust. *Nature*, 453, 653-U7.
- SAUER, K., CAMPER, A. K., EHRLICH, G. D., COSTERTON, J. W. & DAVIES, D. G. 2002. Pseudomonas aeruginosa displays multiple phenotypes during development as a biofilm. *Journal of Bacteriology*, 184, 1140-1154.
- SAUTER, L. M., LATYPOVA, E., SMALLEY, N. E., LIDSTROM, M. E., HALLAM, S. & KALYUZHNAYA, M. G. 2012. Methanotrophic communities of Saanich Inlet: A microcosm perspective. *Systematic and Applied Microbiology*, 35, 198-203.
- SCHNETZER, A., MOORTHI, S. D., COUNTWAY, P. D., GAST, R. J., GILG, I. C. & CARON, D. A. 2011. Depth matters: Microbial eukaryote diversity and community structure in the eastern North Pacific revealed through environmental gene libraries. Deep-Sea Research Part I-Oceanographic Research Papers, 58, 16-26.
- SILLANKORVA, S., NEUBAUER, P. & AZEREDO, J. 2008. Pseudomonas fluorescens biofilms subjected to phage philBB-PF7A. *BMC Biotechnology*, 8, 79.
- SNELGROVE, P. 2001. Marine Communities. eLS. John Wiley & Sons, Ltd.
- SOGIN, M. L., MORRISON, H. G., HUBER, J. A., MARK WELCH, D., HUSE, S. M., NEAL, P. R., ARRIETA, J. M. & HERNDL, G. J. 2006. Microbial diversity in the deep sea and the underexplored "rare biosphere". *Proceedings of the National Academy of Sciences of the United States of America*, 103, 12115-12120.
- SOMERO, G. N., SIEBENALLER, J. F. & P.W., H. 1983. Biochemical and Physiological Adaptations of Deep-Sea Animals. *In:* ROWE, G. T. (ed.) *The Sea.* New York: Wiley-Interscience.
- STOODLEY, P., SAUER, K., DAVIES, D. G. & COSTERTON, J. W. 2002. Biofilms as complex differentiated communities. *Annual Review of Microbiology*, 56, 187-209.
- STRAMMA, L., JOHNSON, G. C., SPRINTALL, J. & MOHRHOLZ, V. 2008. Expanding oxygen-minimum zones in the tropical oceans. *Science*, 320, 655-658.
- STRAMMA, L., PRINCE, E. D., SCHMIDTKO, S., LUO, J. G., HOOLIHAN, J. P., VISBECK, M., WALLACE, D. W. R., BRANDT, P. & KORTZINGER, A. 2012. Expansion of oxygen minimum zones may reduce available habitat for tropical pelagic fishes. *Nature Climate Change*, 2, 33-37.
- SUNAGAWA, S., DESANTIS, T. Z., PICENO, Y. M., BRODIE, E. L., DESALVO, M. K., VOOLSTRA, C. R., WEIL, E., ANDERSEN, G. L. & MEDINA, M. 2009. Bacterial diversity and White Plague Disease-associated community changes in the Caribbean coral Montastraea faveolata. *Isme Journal*, 3, 512-521.
- SURMAN, S. B., WALKER, J. T., GODDARD, D. T., MORTON, L. H. G., KEEVIL, C. W., WEAVER, W., SKINNER, A., HANSON, K., CALDWELL, D. & KURTZ, J. 1996. Comparison of microscope techniques for examination of biofilms. *Journal of Microbiological Methods*, 25, 14.
- SVEDRUP, H. U., JOHNSON, M. W. & FLEMING, R. H. 1942. The oceans, their physics, cemistry, and general biology, New York, Prentice-Hall, Inc.
- TAKENAKA, Y., YAMAGUCHI, A., TSURUOKA, N., TORIMURA, M., GOJOBORI, T. & SHIGERI, Y. 2012. Evolution of Bioluminescence in Marine Planktonic Copepods. *Molecular Biology and Evolution*, 29, 1669-1681.
- TAMURA, K., NEI, M. & KUMAR, S. 2004. Prospects for inferring very large phylogenies by using the neighbor-joining method. *Proceedings of the National Academy of Sciences of the United States of America*, 101, 11030-11035.
- TAMURA, K., PETERSON, D., PETERSON, N., STECHER, G., NEI, M. & KUMAR, S. 2011. MEGA5: Molecular Evolutionary Genetics Analysis Using Maximum Likelihood, Evolutionary Distance, and Maximum Parsimony Methods. *Molecular Biology and Evolution*, 28, 2731-2739.

- TARASOV, V. G., GEBRUK, A. V., MIRONOV, A. N. & MOSKALEV, L. I. 2005. Deep-sea and shallow-water hydrothermal vent communities: Two different phenomena? *Chemical Geology*, 224, 5-39.
- TEN BRINK, U. S., COLEMAN, D. F. & DILLON, W. P. 2002. The nature of the crust under Cayman Trough from gravity. *Marine and Petroleum Geology*, 19, 971-987.
- THOMPSON, J. R., PACOCHA, S., PHARINO, C., KLEPAC-CERAJ, V., HUNT, D. E., BENOIT, J., SARMA-RUPAVTARM, R., DISTEL, D. L. & POLZ, M. F. 2005. Genotypic diversity within a natural coastal bacterioplankton population. *Science*, 307, 1311-1313.
- THOMPSON, J. R., RANDA, M. A., MARCELINO, L. A., TOMITA-MITCHELL, A., LIM, E. & POLZ, M. F. 2004. Diversity and dynamics of a north Atlantic coastal Vibrio community. *Applied and Environmental Microbiology*, 70, 4103-4110.
- THORNTON, C. G. & PASSEN, S. 2004. Inhibition of PCR amplification by phytic acid, and treatment of bovine fecal specimens with phytase to reduce inhibition. *Journal of Microbiological Methods*, 59, 43-52.
- TIAN, F., YU, Y., CHEN, B., LI, H. R., YAO, Y. F. & GUO, X. K. 2009. Bacterial, archaeal and eukaryotic diversity in Arctic sediment as revealed by 16S rRNA and 18S rRNA gene clone libraries analysis. *Polar Biology*, 32, 93-103.
- TOUPOINT, N., MOHIT, V., LINOSSIER, I., BOURGOUGNON, N., MYRAND, B., OLIVIER, F., LOVEJOY, C. & TREMBLAY, R. 2012. Effect of biofilm age on settlement of Mytilus edulis. *Biofouling*, 28, 985-1001.
- TUNNICLIFFE, V., MCARTHUR, A. G. & MCHUGH, D. 1998. A biogeographical perspective of the deep-sea hydrothermal vent fauna. *Advances in Marine Biology, Vol 34*, 34, 353-442.
- TURLEY, C. M., LOCHTE, K. & PATTERSON, D. J. 1988. A barophilic flagellate isolated from 4500 m in the Mid-North Atlantic. *Deep-Sea Research Part a-Oceanographic Research Papers*, 35, 1079-1092.
- TYLER, P. A. & GAGE, J. D. 1984. Seasonal reproduction of Echinus affinis (Echinodermata: Echinoidea) in the Rockall trough, northeast Atlantic Ocean. Deep Sea Research Part A. Oceanographic Research Papers, 31, 387-402.
- VALCARCE, M. B., BUSALMEN, J. P. & DE SÁNCHEZ, S. R. 2002. The influence of the surface condition on the adhesion of Pseudomonas fluorescens (ATCC 17552) to copper and aluminium brass. *International Biodeterioration & Biodegradation*, 50, 61-66.
- VAN DOVER, C. L. 1995. Ecology of Mid-Atlantic Ridge Hydrothermal Vents. *J. Geol. Soc. London Spec. Publ.*, 87, 257-294.
- VAN DOVER, C. L. 2000. *The Ecology of Deep-Sea Hydrothermal Vents,* Princeton, NJ, Princeton University Press.
- VAN DOVER, C. L., GERMAN, C. R., SPEER, K. G., PARSON, L. M., VRIJENHOEK, R. C. 2002. Evolution and Biogeography of Deep-Sea Vent and Seep Invertebrates. *Science*, 295, 1253-1257.
- VANDIEKEN, V., PESTER, M., FINKE, N., HYUN, J.-H., FRIEDRICH, M. W., LOY, A. & THAMDRUP, B. 2012. Three manganese oxide-rich marine sediments harbor similar communities of acetate-oxidizing manganese-reducing bacteria. *ISME J.*
- VENKATESWARAN, K., HATTORI, N., LA DUC, M. T. & KERN, R. 2003. ATP as a biomarker of viable microorganisms in clean-room facilities. *Journal of Microbiological Methods*, 52, 367-377.
- VOORDECKERS, J. W., DO, M. H., HUGLER, M., KO, V., SIEVERT, S. M. & VETRIANI, C. 2008. Culture dependent and independent analyses of 16S rRNA and ATP citrate lyase genes: a comparison of microbial communities from different black smoker chimneys on the Mid-Atlantic Ridge. *Extremophiles*, 12, 627-640.
- VRIJENHOEK, R. C. 1997. Gene flow and genetic diversity in naturally fragmented metapopulations of deep-sea hydrothermal vent animals. *Journal of Heredity*, 88, 285-293.
- WALKER, J. T., HANSON, K., CALDWELL, D. & KEEVIL, C. W. 1998. Scanning confocal laser microscopy study of biofilm induced corrosion on copper plumbing tubes. *Biofouling*, 12, 333-+.
- WARBURG, O. & CHRISTIAN, W. 1941. Isolierung und Kristallisation des Gärungsferments Enolase. *Naturwissenschaften*, 29, 589-590.

- WARNES, S. L. & KEEVIL, C. W. 2011. Mechanism of Copper Surface Toxicity in Vancomycin-Resistant Enterococci following Wet or Dry Surface Contact. *Applied and Environmental Microbiology*, 77, 6049-6059.
- WEAVER, L., MICHELS, H. T. & KEEVIL, C. W. 2008. Survival of Clostridium difficile on copper and steel: futuristic options for hospital hygiene. *Journal of Hospital Infection*, 68, 145-151.
- WEBB, J. S., GIVSKOV, M. & KJELLEBERG, S. 2003. Bacterial biofilms: prokaryotic adventures in multicellularity. *Current Opinion in Microbiology*, 6, 578-585.
- WEN, J., ZHAO, K. L., GU, T. Y. & RAAD, I. I. 2009. A green biocide enhancer for the treatment of sulfate-reducing bacteria (SRB) biofilms on carbon steel surfaces using glutaraldehyde. *International Biodeterioration & Biodegradation*, 63, 1102-1106.
- WHELAN, A. & REGAN, F. 2006. Antifouling strategies for marine and riverine sensors. Journal of Environmental Monitoring, 8, 880-886.
- WILKS, S. A., MICHELS, H. & KEEVIL, C. W. 2005. The survival of Escherichia coli O157 on a range of metal surfaces. *International Journal of Food Microbiology*, 105, 445-454.
- WILKS, S. A., MICHELS, H. T. & KEEVIL, C. W. 2006. Survival of Listeria monocytogenes Scott A on metal surfaces: Implications for cross-contamination. *International Journal of Food Microbiology*, 111, 93-98.
- WILSON, G. S., RAFTOS, D.A., CORRIGAN, L., NAIR, S.V. 2009. Diversity and antimicrobial activities of surface-attached marine bacteria from Sydney Harbour, Australia. *Microbiological Research*.
- WINTZER, A. P., MEEK, M. H. & MOYLE, P. B. 2011. Life history and population dynamics of Moerisia sp., a non-native hydrozoan, in the upper San Francisco Estuary (U.S.A.). Estuarine, Coastal and Shelf Science, 94, 48-55.
- WIRTANEN, G., SALO, S., HELANDER, I. M. & MATTILA-SANDHOLM, T. 2001.

 Microbiological methods for testing disinfectant efficiency on Pseudomonas biofilm. *Colloids and Surfaces B-Biointerfaces*, 20, 37-50.
- WOERTHER, P. 2002. Coastal environment of the Seine Bay area monitored by a new French system of automated measurement stations. *Operational Oceanography*, 66, 255-264
- 555.
 WOERTHER, P. & GROUHEL, A. 1998. MAREL: Automated measurement network for the coastal environment. *Oceans'98 Conference Proceedings, Vols 1-3*, 1149-1154 1853.
- WOLF, R. & SPARAVIGNA, A. C. 2010. Role of plasma surface treatments on wetting and adhesion. *Engineering*, 2, 397.
- XU, M. X., WANG, P., WANG, F. P. & XIAO, X. 2005. Microbial diversity at a deep-sea station of the Pacific nodule province. *Biodiversity and Conservation*, 14, 3363-3380.
- YEBRA, D. M., KIIL, S., DAM-JOHANSEN, K. 2004. Antifouling technology past, present and future steps towards efficient and environmentally friendly antifouling coatings. *Progress in Organic Coatings*, 50, 30.
- YEBRA, D. M., KIIL, S., WEINELL, C.E., DAM-JOHANSEN, K. 2006. Effects of marine microbial biofilms on the biocide release rate from ntifouling paints A model-based analysis. *Progress in Organic Coatings*, 57, 11.
- YI, J. L., ZHANG, X. M., CHEN, M. A., GU, R. & DENG, Y. L. 2009. Corrosion resistance of cerium conversion film electrodeposited on Mg-Gd-Y-Zr magnesium alloy. Journal of Central South University of Technology, 16, 38-42.
- YUAN, S. J., CHOONG, A. M. F. & PEHKONEN, S. O. 2007. The influence of the marine aerobic Pseudomonas strain on the corrosion of 70/30 Cu-Ni alloy. *Corrosion Science*, 49, 4352-4385.
- ZHU, X. L., YAO, Z. J., GU, X. D., CONG, W. & ZHANG, P. Z. 2009. Microstructure and corrosion resistance of Fe-Al intermetallic coating on 45 steel synthesized by double glow plasma surface alloying technology. *Transactions of Nonferrous Metals Society of China*, 19, 143-148.

- ZOBELL, C. E. 1943. The effect of solid surfaces upon bacterial activity. *Journal of bacteriology*, 46, 39.
- ZOBELL, C. E. & ALLEN, E. C. 1935. The significance of marine bacteria in the fouling of submerged surfaces. *Journal of bacteriology*, 29, 239.
- ZOBELL, C. E. & ANDERSON, D. Q. 1936. Observations on the multiplication of bacteria in different volumes of stored sea water and the influence of oxygen tension and solid surfaces. *The Biological Bulletin*, 71, 324-342.

Appendix I: Code of Matlab program for pixel counter

Written by Xi Huang

```
%PIXELCOUNTER M-file for pixelcounter.fig
   응
          PIXELCOUNTER, by itself, creates a new PIXELCOUNTER or raises the
existing
   9
          singleton*.
   응
          H = PIXELCOUNTER returns the handle to a new PIXELCOUNTER or the handle
to
   응
          the existing singleton*.
         PIXELCOUNTER('Property','Value',...) creates a new PIXELCOUNTER using the
         given property value pairs. Unrecognized properties are passed via
   응
         varargin to pixelcounter_OpeningFcn. This calling syntax produces a
         warning when there is an existing singleton*.
   응
         PIXELCOUNTER('CALLBACK') and PIXELCOUNTER('CALLBACK', hObject,...) call
the
   응
         local function named CALLBACK in PIXELCOUNTER.M with the given input
   응
          arguments.
   응
   2
          *See GUI Options on GUIDE's Tools menu. Choose "GUI allows only one
   응
          instance to run (singleton)".
   % See also: GUIDE, GUIDATA, GUIHANDLES
   % Edit the above text to modify the response to help pixelcounter
   % Last Modified by GUIDE v2.5 02-Jun-2011 12:16:49
   % Begin initialization code - DO NOT EDIT
   gui_Singleton = 1;
   gui_State = struct('gui_Name',
                                        mfilename,
                       'gui_Singleton', gui_Singleton, ...
                      'gui_OpeningFcn', @pixelcounter_OpeningFcn, ...
                      'gui_OutputFcn', @pixelcounter_OutputFcn, ...
                       'gui_LayoutFcn', [], ...
                       'gui_Callback',
   if nargin && ischar(varargin{1})
      gui_State.gui_Callback = str2func(varargin{1});
   end
   if nargout
      [varargout{1:nargout}] = gui_mainfcn(gui_State, varargin{:});
       gui_mainfcn(gui_State, varargin{:});
   % End initialization code - DO NOT EDIT
   % --- Executes just before pixelcounter is made visible.
   function pixelcounter_OpeningFcn(hObject, eventdata, handles, varargin)
   \mbox{\ensuremath{\mbox{\$}}} This function has no output args, see OutputFcn.
   % hObject
               handle to figure
   % eventdata reserved - to be defined in a future version of MATLAB
   % handles
               structure with handles and user data (see GUIDATA)
   % varargin unrecognized PropertyName/PropertyValue pairs from the
               command line (see VARARGIN)
   % Choose default command line output for pixelcounter
```

Appendix I: Code of Matlab program for pixel counter

```
handles.output = hObject;

% Update handles structure
guidata(hObject, handles);

% UIWAIT makes pixelcounter wait for user response (see UIRESUME)
% uiwait(handles.figure1);

% --- Outputs from this function are returned to the command line.
```

```
% --- Outputs from this function are returned to the command line.
function varargout = pixelcounter_OutputFcn(hObject, eventdata, handles)
% varargout cell array for returning output args (see VARARGOUT);
% hObject handle to figure
% eventdata reserved - to be defined in a future version of MATLAB
             structure with handles and user data (see GUIDATA)
% Get default command line output from handles structure
varargout{1} = handles.output;
% --- Executes on button press in pushbutton4.
function pushbutton4_Callback(hObject, eventdata, handles)
% hObject handle to pushbutton4 (see GCBO)
% eventdata reserved - to be defined in a future version of MATLAB
% handles structure with handles and user data (see GUIDATA)
global filename;
global img0;
global img1;
global msg0;
global msg1;
[FileName, PathName] = uigetfile('*.jpg', 'Select the image data file');
filename=[PathName,FileName];
img0=importdata(filename);
[a,b,c]=size(img0);
for i=1:a
   for j=1:b
        if sum(img0(i,j,:)) >= 700
            img0(i,j,:)=[0 0 0];
        end
    end
end
axes(handles.axes1);
image(img0);
imq1=imq0;
msg0='Image loaded.';
set(handles.t_msg,'String',msg0);
% --- Executes on button press in p_select.
function p_select_Callback(hObject, eventdata, handles)
% hObject handle to p_select (see GCBO)
% eventdata reserved - to be defined in a future version of MATLAB
% handles structure with handles and user data (see GUIDATA)
global filename;
global img0;
global img1;
global msg0;
global msg1;
axes(handles.axes1);
[y,x] = ginput(1);
x=round(x)
y=round(y)
img0(x,y,:)
r=5; %radix of selected area
[a,b,c]=size(img0);
bx=x-r;
by=y-r;
ex=x+5i
```

```
ey=y+5;
if bx <1
    bx=1;
end
if by <1
   by=1;
end
if ex >a
   ex=a;
end
if ey >b
   by=b;
pbias=mean(img0(bx:ex,by:ey,:));
pbias=mean(pbias);
pbias=sum(pbias);
 img1=img0;
 count=0;
 for i=1:a
    for j=1:b
         if sum(img0(i,j,:)) >= pbias
             img0(i,j,:)=[255 255 255];
             count=count+1;
         end
     end
 end
 axes(handles.axes1);
 image(img0);
 msq1=msq0;
 msg0=sprintf('%d pixels are selected, in %.4f%%', count,count*100/a/b);
 set(handles.t_msg,'String',msg0);
% --- Executes on button press in p_back.
function p_back_Callback(hObject, eventdata, handles)
% hObject handle to p_back (see GCBO)
% eventdata reserved - to be defined in a future version of MATLAB
% handles
            structure with handles and user data (see GUIDATA)
global filename;
global img0;
global img1;
global msg0;
global msg1;
img0=img1;
msg0=msg1;
axes(handles.axes1);
image(img0);
set(handles.t_msg,'String',msg0);
```

Published with MATLAB® R2012b

Appendix II: Denaturing Gradient Gel Electrophoresis (DGGE) Protocol

Solutions & Chemicals

- Temed
- 10%Ammonium Persulfate (APS)
- 40%Acrylamide/Bis solution (37.5:1)
- Formamide
- Urea
- 8% acrylamide sotuion for top & bottom of the gel (total volume 100ml):

Reagent		Amoun
	t	
40% Acrylamide/Bis (37.5:1)		20 ml
TAE Buffer (x50%)		2ml
Rnase/Dnasefree Water		78ml

• 30% denaturing acrylamide solution (total volume 100ml):

Reagent		Amoun
	t	
40% Acrylamide/Bis (37.5:1)		20 ml
TAE Buffer (x50%)		2ml
Rnase/Dnasefree Water		78ml
Foramide		12ml
Urea		12.6g

• 50% denatuting acrylamide solution (total volume 100ml):

Reagent	Amount 20 ml	
40% Acrylamide/Bis (37.5:1)		
TAE Buffer (x50%)	2ml	
Rnase/Dnasefree Water	78ml	
Foramide	20ml	
Urea	21g	

• 80% denaturing acrylamide solution (total volume 100ml):

Reagent	Amount
40% Acrylamide/Bis	20 ml
(37.5:1)	
TAE Buffer (x50%)	2ml
Rnase/Dnasefree	78ml
Water	
Foramide	32ml
Urea	33.6g

Electrophoresis (DGGE) Protocol

Preparation of the Denaturing Gradient Gel

Gel Plate Preparation & Assembly

- Clean glass plates, spacers, and combs with a mild detergent, rinse with water and wipe with 70% Ethanol
- Loosen the clamping plates on the gel-running module and slide the glass plates divided by spacers into the module with the notched glass plates facing the centre. Align the spacers and glass plates carefully using the aligner and the bench top. Tighten the screws to hold glass plates and spacers in position (Figure 0.1).

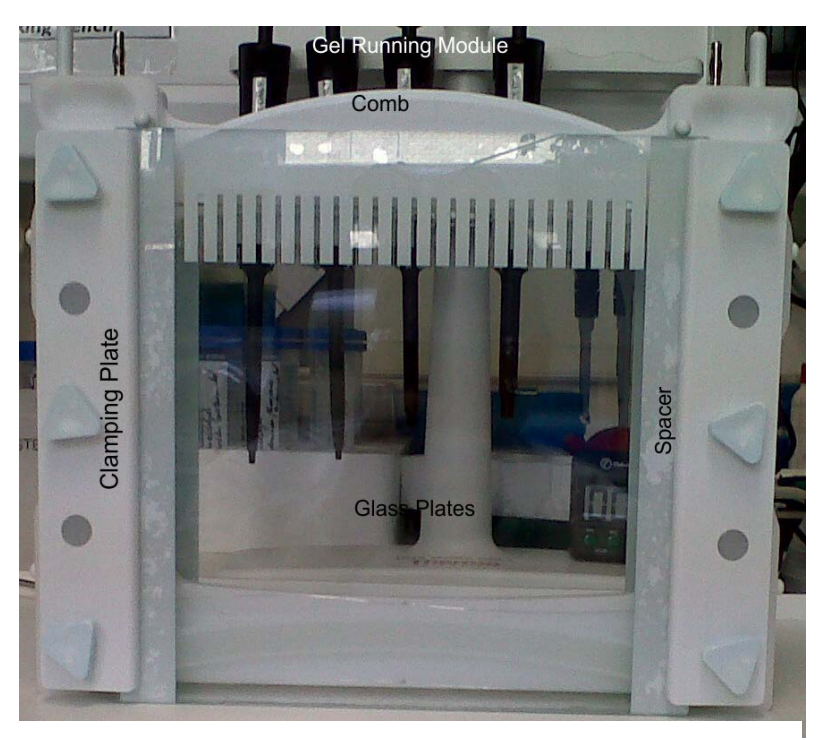


Figure 0.1: Assemblage of gel plates

 Place the gel running module onto the casting base (Figure 0.2) with the cam-pin levers pointing to the bench surface. Slot pins into position, turning clockwise so that the gel cassettes are drawn onto the silicone seals. (maybe check for leaks with 2ml of water)

Electrophoresis (DGGE) Protocol

Gel Pouring

- Prepare 15ml of a 8% acrylamide solution. Pipette 5ml of this into a disposable tube and add Temed (5µl) and 10% APS (50µl). Mix well and pipette 1ml between the glass plates and ensure that it spreads in an equal layer at the bottom of the plates. Use about 1ml to seal the sides of the the glass plates. Allow the Acrylamide to polymerise.
- Setup the Gradient Mixer, Pump, and the Gel Casting Frame as shown in Figure 0.2.



Figure 0.2: Setup for pouring gel gradient

- Make two solutions of 15ml each; a "low" denaturing concentration solution, and a "high" denaturing solution. 30% and 50% for the separation of Eukaryon PCR products or 30% and 80% for separation of archean and bacterial PCR products.
- Add Temed (7.5µl) and 10% APS(75µl) to each solution and mix well. Transfer 13ml of low denaturant concentration solution to the left side of the gradient mixer (Figure 0.3) and slowly open stop cock to allow the solution to fill the gap between the mixer sides. Close the cock again.



Figure 0.3: Gradient mixer

- Transfer 13ml of the high denaturant solution to the right hand side of the mixer and place a small magnetic follower inside. Switch on the magnetic stirrer and ensure the follower is rotating freely.
- Switch on the pump and open both valves simultaneously or first the valve closes to the pump. A flow rate of 5ml per min (22rpm, cw) is sufficient for pouring the gel.
- Run the acrylamide denaturing gel mix slowly down the inside edge of the gel cassette. Avoid aeration and airbubbles. (Formation of bubbles can be prevented through gentle tapping of the glass plates.
- Allow all solution in the mixing chamber to empty before turning off the peristaltic pump. If more than one gel is cast rinse mixer and tubing with water immediately.
- Pipette 2ml of 1x TAE buffer to prevent the gel setting in a smile.
- Allow gel to set for at least 1hour.
- Remove the delivery tube from the top of the plates and clean through with warm water.
- Remove 1x TAE buffer.
- Pipette 6ml of 8% acrylamide solution into a disposable tube and add Temed (6µl) and 10% APS (60µl). Mix well and pipette aprox.3ml between the glass plates. Carefully place the comb between the plates (Figure 0.1). Allow the gel to set.

Running the Gel

- Prepare 5I of 1x TAE buffer and fill the Tank; put aside about 0.7I for later use and preheat the buffer in the DGGE apparatus to 65°C; setup see Figure 0.4; this will take about 2 hours.
- When temperature is about 50° interrupt heating and fill the inner reservoir of the Gel Running Moduel with buffer.
- Flush each well with buffer and load 10-20µl of PCR product containing loading dye (note: Crimson Taq buffer already contains loading dye). Load into unused wells the same amount of 1x loading dye as used for PCR products to ensure straight running of the samples.
- Place Gel Running Module into the DGGE apparatus and adjust temperature to 60°C and run at 50V for 20min, then run at 100V for 16hrs (1600V.hrs). Important: Do not place plates in to buffer that is above 55°C! plates might crack
- On completion switch of electrophoresis unit, stirrer, and heater.



Figure 0.4: Setup for running the DGGE

Developing and Viewing the Gel

- Add 25µl of Sybr Gold stain to 250ml TAE buffer and transfer mixture to developing tank.
- Remove the Gel Running Module from DGGE Tank and remove glass plates.

Electrophoresis (DGGE) Protocol

- Carefully remove spacers from between the glass plates and apply gentle pressure to move the glass plates apart. The gel should stick to one of the plates.
- Gently remove the gel and transfer it into the developing tank.
- Incubate for about 45 minutes in the dark at room temperature. Drain staining solution from the tank (note: staining solution can be reused several times; store in the fridge and protect from light) and place the gel gently onto a UV transluminator to take an image. Afterwards transfer gel back into developing tank. (note: arranging the gel on the transluminator is easier with a little bit of water on it.)

Excising DNA bands

- Use image of the gel to identify bands to be excised. Prepare sufficient amount of 1.5ml tubes and label them.
- Place gel back onto the transluminator and wearing the appropriate PPE excise bands using a sterile scalpel and transfer the band into the tubes.
- Extract DNA from excised bands using Qiaquick Gel Extraction Kit.

Appendix III: Creation of copper embedded COC samples

(D. Walker in communication)

The following standard operating procedure is for the creation of Cyclic Olefin Copolymer (COC) wafers coated with copper or copper oxide particles, for tests for the anti-fouling effects of copper.

Creation of COC/cyclohexane solution

- Cut 20g of COC (8007) into small pieces (to aid dissolving)
- Add 200g (256.9ml) of cyclohexane
- Allow the COC to dissolve. This will take several hours and is probably best to leave it over night.

Creation of copper/COC mixtures

- Transfer 3g of COC/cyclohexane solution to a lidded glass vial.
- Add 1g of either copper particles, copper (I) oxide or copper (II) oxide.
- Stir with a glass rod to mix thoroughly.

Coating COC wafers

- Place a wafer of high melting temperature COC onto a spinner.
- Switch on the vacuum pump to stop the wafer from moving.
- Put approximately 3g of the COC/cyclohexane/copper mixture onto the wafer, covering as much of the surface as possible. Note 1: This must be done quickly before the cyclohexane evaporates. Note 2: The more the mixture is spread out on the wafer surface, the smoother the final coating will be.
- Spin the coated wafer for 1 minute at 1000rpm, with an initial ramp of 25 and a final ramp of 50.
- Repeat the coating process.
- Allow all cyclohexane to evaporate.
- Coat the other side of the wafer as above.

Flattening the coated wafer surfaces

- Prepare a non-stick laminating surface by cutting a laminating pouch into two pieces (2 A4 sized pieces).
- Use these pieces of laminate to laminate 1 side of two pieces of card.
- Set the temperature of the laminator to 110°C. at speed 2.
- Sandwich the coated wafers between the two laminated pieces of card, with the laminated side facing inwards.
- Feed this thorough the laminator several times, changing the orientation of the wafer frequently, to achieve a uniform, flat surface.

Exposing the copper particles

• Using low grit sized lapping paper, remove a small amount of the coating to expose the copper particles.